

TI-PMLK BUCK

Würth Elektronik Edition

TI Power Management Laboratory Kit
Experiment Book

TI-PMLK BUCK-WE

by Nicola Femia



Technology by

**TEXAS
INSTRUMENTS**

Name

University/Company name

Address

Phone

E-mail

TI-PMLK Würth Elektronik Edition Foreword

Why did we make the TI-PMLK Würth Elektronik Edition?

At Würth Elektronik, we take pride in making every design better, by providing the best components and making sure that our customers choose the best parts for their design. Our qualified employees on the front line provide hundreds of seminars worldwide to share our expertise. Unfortunately, we are not able to reach everyone! We are hopeful that our complete hands-on learning kit will bridge that gap by having quality training accessible at everyone's reach.

Most universities don't have the resources to provide specific courses in the area of power management, especially those that address the challenges associated with design and optimization of the magnetics in a power supply, which is a key component in any electronic system. The TI-PMLK Würth Elektronik Edition has been designed by Prof. Nicola Femia, from University of Salerno, who has been teaching board design for the past 25 years. This experiment book makes the learning kit accessible for autonomous learning to most students, while offering a wide range of experiments thanks to the board flexible design.

Why are magnetics important?

The inductors and transformers are key components of any DC-DC converters that are widely used in power management application. From electric car, to microwave, or data center, any electric product requires a power supply. As the technology evolves, so do the magnetics, the components get smaller, more efficient, new material are introduced. At a time of "everything electric and everything efficient", the importance of magnetics has never been greater.

Happy learning!

This learning kit is directed to all levels of electrical engineers, no matter what level of skills. Our hope is that engineering students will be excited to learn about magnetics fundamental with this very accessible learning kit. A senior hardware design engineer will develop a deep understanding of magnetic trade-off in a converter, and how it impacts his design.

Because we believe, that learning by doing is worth any theoretical class, this learning kit will require you to physically conduct experiments on the board, while understanding the theory behind it. Have fun!



Alexander Gerfer

CEO of Würth Elektronik eiSos GmbH & Co. KG

CTO of Würth Elektronik eiSos Group

Preface

The TI-PMLK BUCK-WE Edition is a hands-on learning kit for engineering students and electrical engineers, developed to study and experiment the impact of power inductors on DC-DC switching regulators. The kit is comprised of the TI-PMLK BUCK-WE board and this Experiment Book.

The TI-PMLK BUCK-WE board incorporates two independent buck switching regulators, based on TI's LM3475 and TPS54160 controllers, each one with three different inductors. Both regulators are configurable and allow individual selection of each inductor, to investigate the performances of inductors with different core materials, inductance and size, under different operating conditions, and to analyze their impact on the static and dynamic performances of switching regulators.

The kit allows analyzing the inductance of different inductors, investigating inductors saturation and thermal behavior, estimating DC and AC power losses, measuring ripple current and ripple voltage, observing continuous and discontinuous operation modes and transient response, and ultimately understanding the impact of inductors on all the performances of DC-DC switching regulators. The board features variable switching frequency, to observe its impact on inductors and on switching regulators operating with different inductors.

Each regulator incorporates an EMI input filter, to analyze the impact of inductors on conducted noise attenuation, and to compare the performances of filters with inductors selected according to different design strategies. Over-voltage, over-current, and polarity reversal protections, preserve from any user's connection or operation mistake. Current sense transformers and current shunt monitors on board allow easy inductor current measurements by means of standard voltage probes.

The TI-PMLK BUCK-WE Experiment Book includes 6 structured laboratories, covering the following topics:

- Experiment 1: Analysis of the inductance of a power inductor and its dependence on physical characteristics and DC-DC switching regulator operating conditions.
- Experiment 2: Impact of inductor power losses on the efficiency of DC-DC switching regulator, in steady-state operating conditions.
- Experiment 3: Output filter function of inductors in DC-DC switching regulator.
- Experiment 4: Input filter function of inductors in DC-DC switching regulator.

Experiment 5: Impact of inductors on continuous and discontinuous mode operation of DC-DC switching regulator.

Experiment 6: Impact of the inductor on the closed loop load-transient response of peak-current mode controlled DC-DC switching regulator.

Each experiment provides a theory background relevant to the topic to be investigated, instructions to configure and setup the instrumentation and the board, guidelines to collect and analyze the measurement results, questions on the measurement results, and a discussion of the main facts emerging from the tests. Examples of the expected waveforms are provided for each test, as a reference for measurements and support for the discussion. Expansion activities are finally suggested.

The goal of the kit is to help students and engineers understanding the fundamental role of power inductors in DC-DC switching regulators, and the reciprocal influence between power magnetics and the system they are part of. Learning the concepts underlying the behavior of devices and systems is the root of power supplies design optimization.

About the creator



Nicola Femia is Professor at the University of Salerno, Italy, where he teaches Power Electronics and Energetic Intelligence, in the Electronic Engineering and Computer Engineering Master Degree Programs. He leads the Power Electronics and Renewable Sources Laboratory. Over the past 25 years, he has promoted and directed worldwide university and industry research activities and education programs on power electronics and power design. He has been Visiting Professor at the Electrical Engineering Department of the Stanford University, Stanford, CA, where he taught Power Electronics Control and Energy Aware Design. He is also the co-creator of the Texas Instruments TI-PMLK series.

e-mail: femia@unisa.it

web: www.unisa.it/docenti/nicolafemia/index

Table of Contents

Preface 3

TI-PMLK BUCK-WE description

- Outline 6
- Circuit schematic 7
- Layers 8
- LM3475 regulator section 9
- TPS54160 regulator section 24
- Instrumentation needed for the experiments . 38
- Warnings and recommendations 39
- Additional terms, warnings, restrictions and disclaimers 40

Experiment 1

Analysis of the inductance of a power inductor and its dependence on physical characteristics and DC-DC switching regulators operating conditions 45

Experiment 2

Impact of inductor power losses on the efficiency of DC-DC switching regulators, in steady-state operating conditions 67

Experiment 3

Output filter function of inductors in DC-DC switching regulators 104

Experiment 4

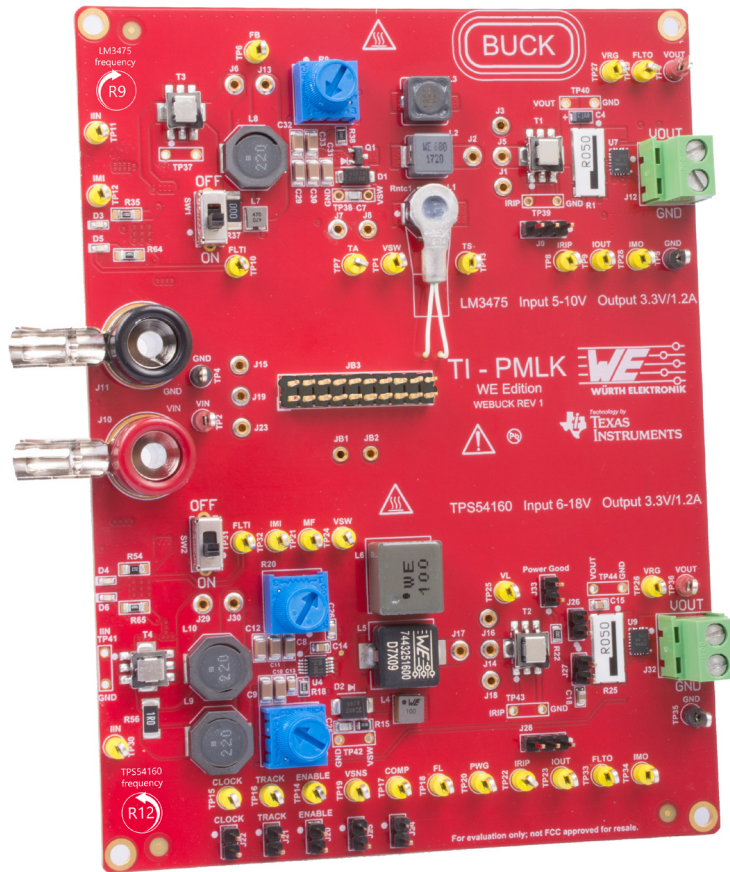
Input filter function of inductors in DC-DC switching regulators 124

Experiment 5

Impact of inductors on continuous and discontinuous mode operation of DC-DC switching regulators 145

Experiment 6

Impact of the inductor on the closed loop load-transient response of peak-current mode controlled buck regulators 162



TI-PMLK BUCK

Würth Elektronik Edition

The TI-PMLK BUCK Würth Elektronik Edition is a power board allowing experimental testing of power inductors, using two step-down switching regulators, based on hysteretic and peak current mode control.

Outline

The TI-PMLK BUCK-WE is a power board designed to perform experimental investigations on power inductors in DC-DC switching regulators.

The board allows to analyze:

- the inherent properties of power inductors, including saturation, losses and thermal effects, and their correlation with physical characteristics;
- the impact of switching regulators operating conditions on the inductors characteristics;
- the impact of inductors characteristics on the operation and performances of switching regulators.

The TI-PMLK BUCK-WE board is comprised of two parts.

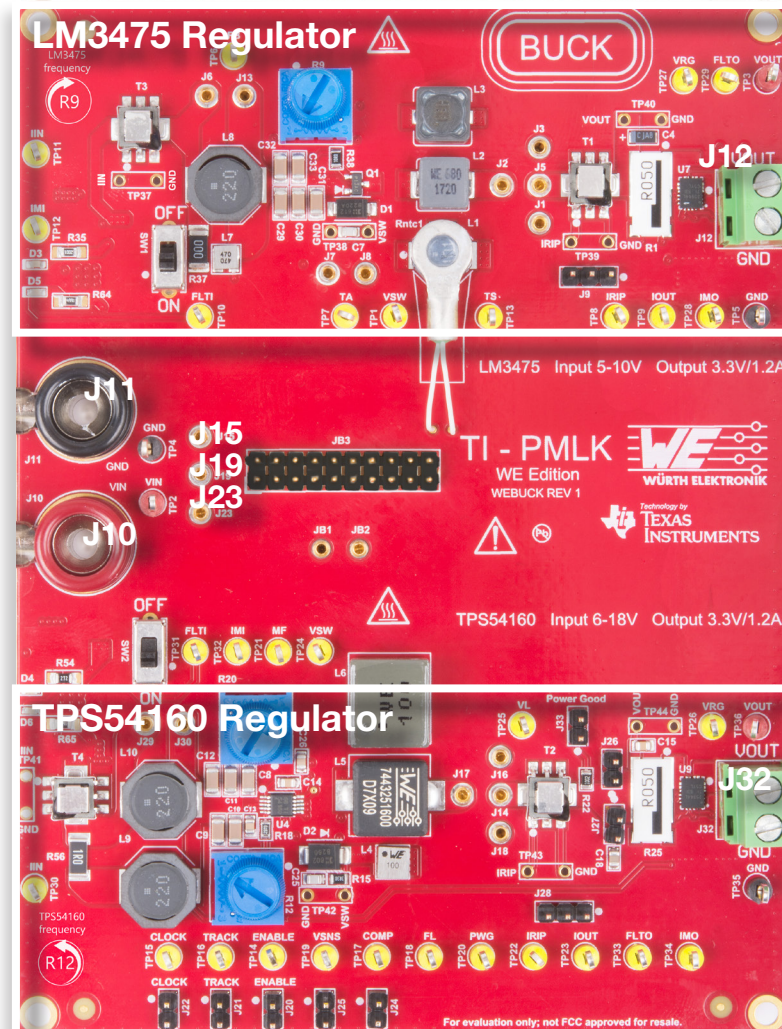
The top part implements a step-down regulator using a TI's LM3475 hysteretic controller, operating 5 V to 10 V input voltage and providing 3.3 V output voltage at maximum 1.2 A load current.

The bottom part implements a step-down regulator using a TI's TPS54160 peak-current controller, operating 6 V to 18 V input voltage, 3.3 V output voltage at maximum 1.2 A load current.

The board is powered through the banana connectors J10-J11.

The source voltage can be selectively applied to the LM3475 regulator, by shorting J15-J19, or to the TPS54160 regulator, by shorting J19-J23.

The load can be connected to the output of the LM3475 regulator through terminal block J12, and to the output of the TPS54160 regulator through terminal block J32.





Circuit Schematic

Figure 1 shows the circuit schematic of TI-PMLK BUCK-WE Board.

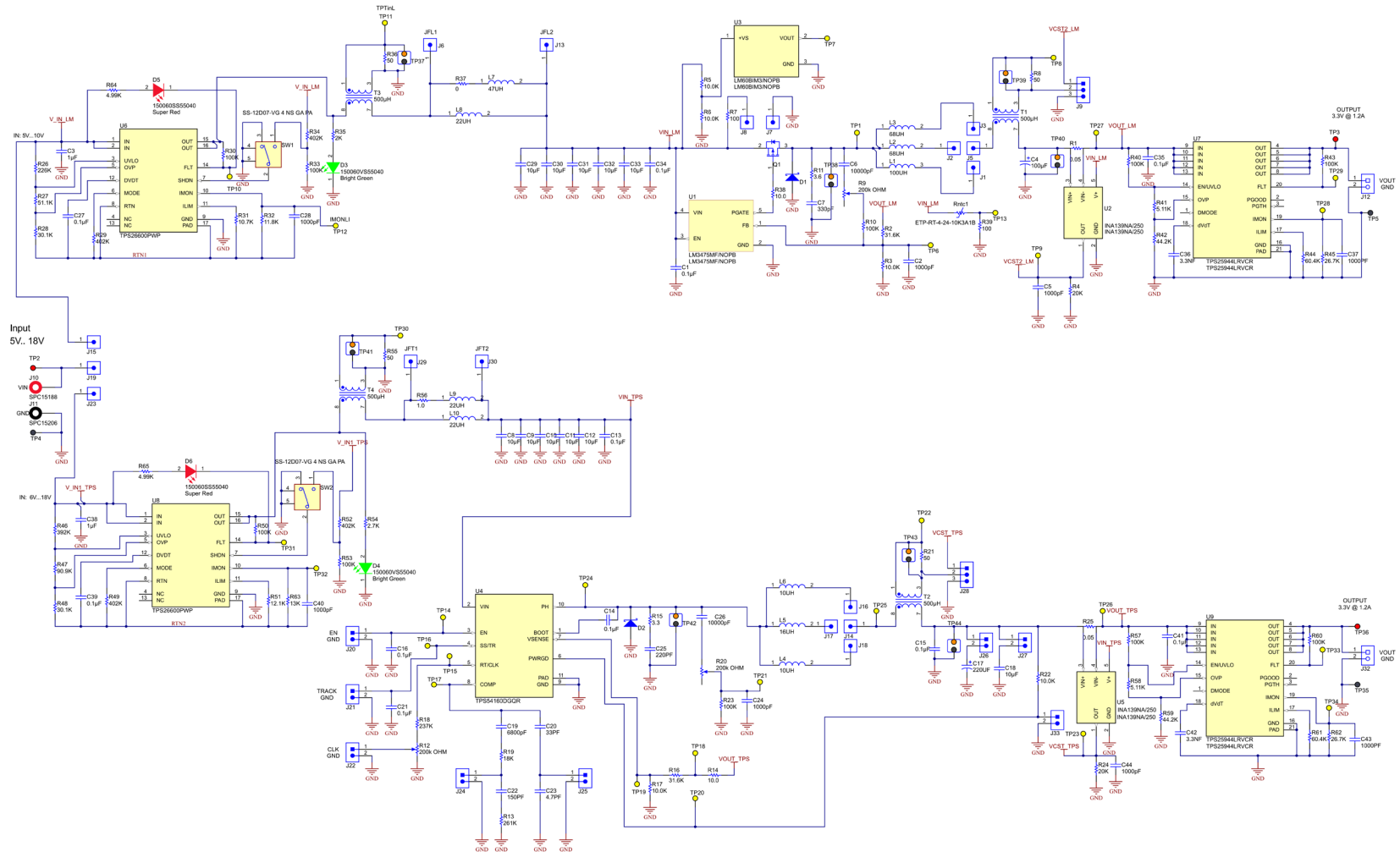
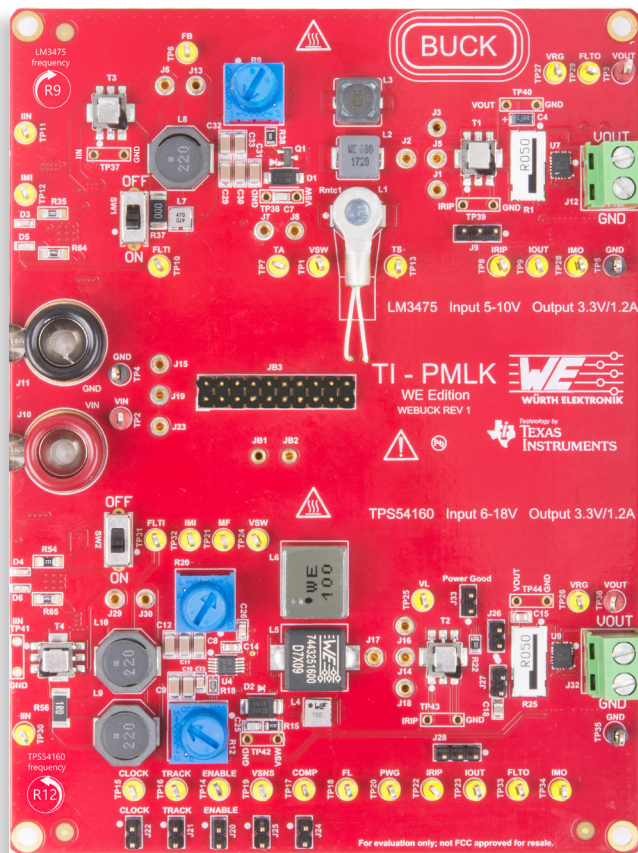


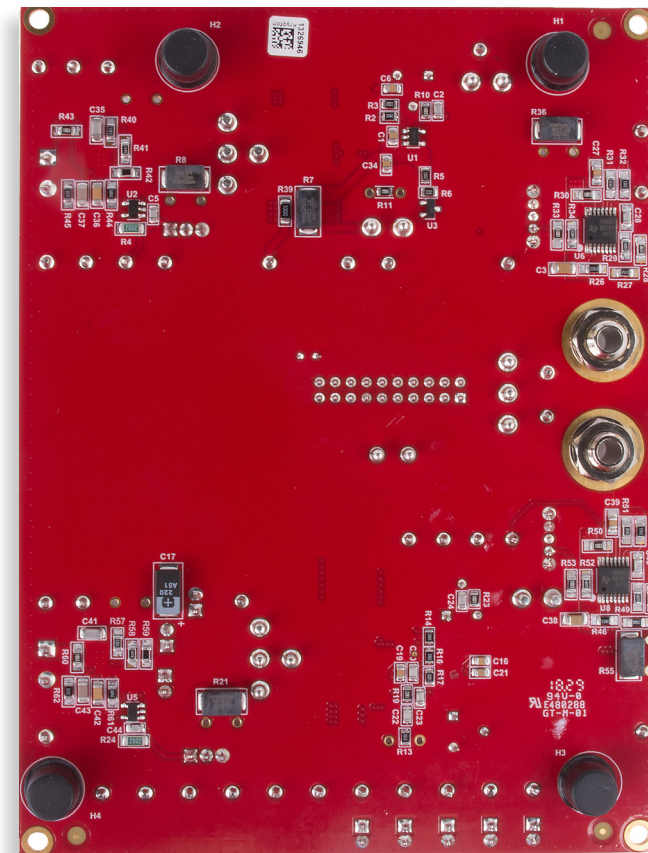
Figure 1. Circuit schematic of TI-PMLK BUCK-WE Board

Layers

The TI-PMLK BUCK-WE Board has a four layer structure, specifically designed for ease of use. The main components of interest in the tests and measurements discussed in this Experiment Book are placed on the top layer, whereas the other components are placed on the bottom layer, as shown in Figure 2. The layout has been designed to minimize the electromagnetic noise emissions, by placing the electrical connections in the intermediate layers, shielded by ground planes on top and bottom layers.



(a) Top Layer



(b) Bottom Layer

Figure 2. TI-PMLK BUCK-WE Board Layers



LM3475 Section: Top Layer

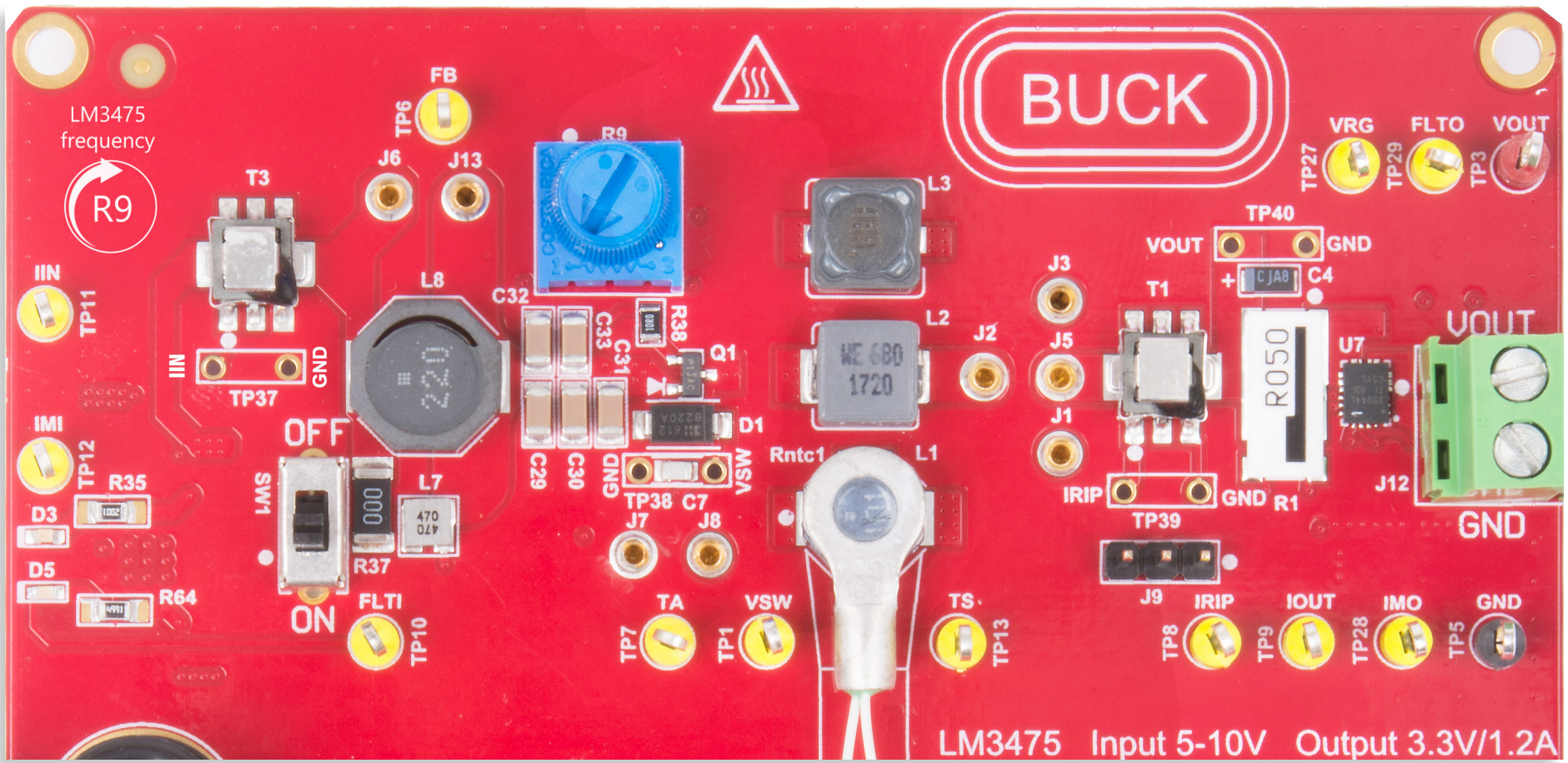


Figure 3. Top Layer of TI-PMLK BUCK-WE Board LM3475 Regulator



LM3475 Section: Bottom Layer

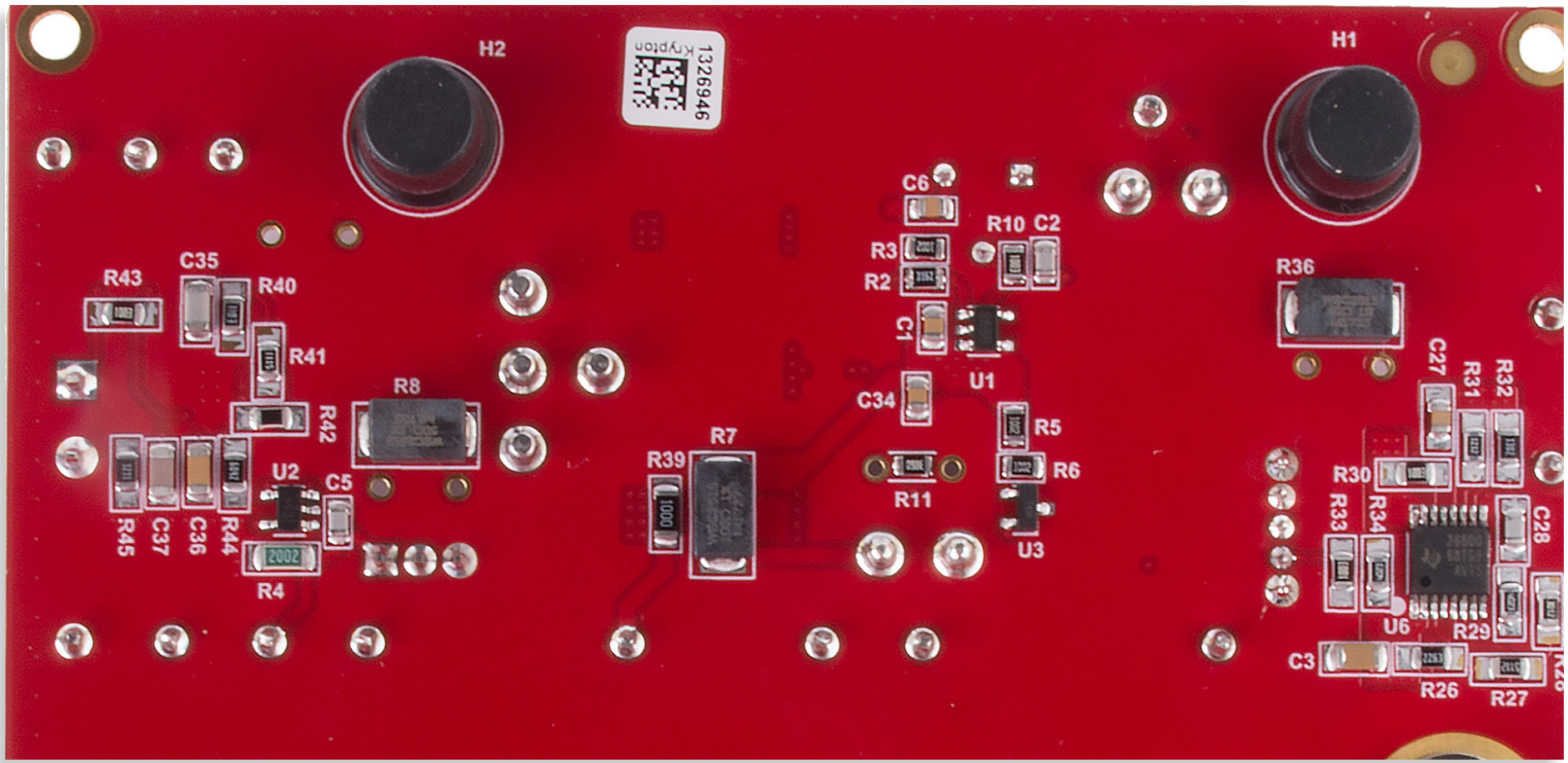


Figure 4. Bottom Layer of TI-PMLK BUCK-WE Board LM3475 Regulator



LM3475 Regulator: Input Section

The input section of LM3475 regulator incorporates a protection circuit, based on TI's TPS26600 eFuse, featuring 12 V over-voltage protection (OVP), 1.1 A over-current protection (OCP) and reverse polarity protection (RPP). The switch SW1 allows turning the TPS26600 eFuse output ON and OFF, to power on and shutdown the LM3475 regulator, respectively. In case of fault causing the protection activation, the switch SW1 allows resetting the eFuse, after the fault condition is removed, to restart the LM3475 operation. The green and red LEDs D3 and D5 indicate the ON/OFF status of the eFuse. The input current sensing circuit, comprised of transformer T3 and resistor R36 (bottom layer), allows observing the AC input ripple current at test points TP37, whereas the DC component of input current can be observed at test point TP12.

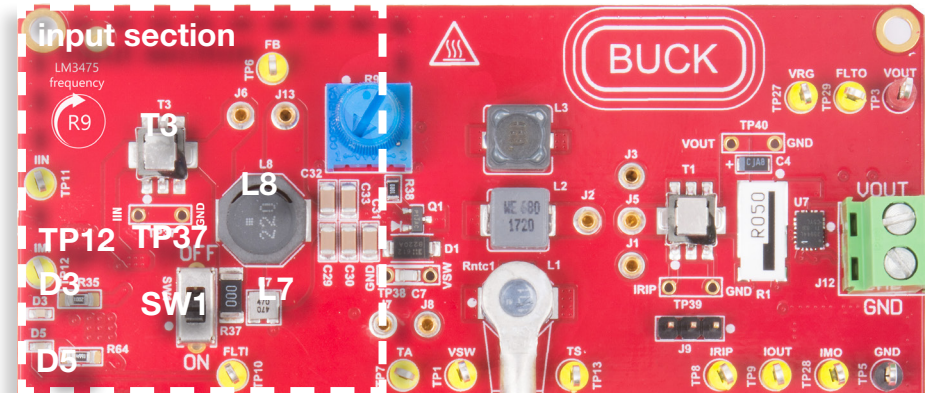


Figure 5. TI-PMLK BUCK-WE Board - LM3475 Regulator

- The input filter uses the two Würth Elektronik inductors:
- L7: WE-MAPI-3015 - 74438335470, 47 μ H, 2090 m Ω
 - L8: WE-TPC-1038 - 744066220, 22 μ H, 75 m Ω

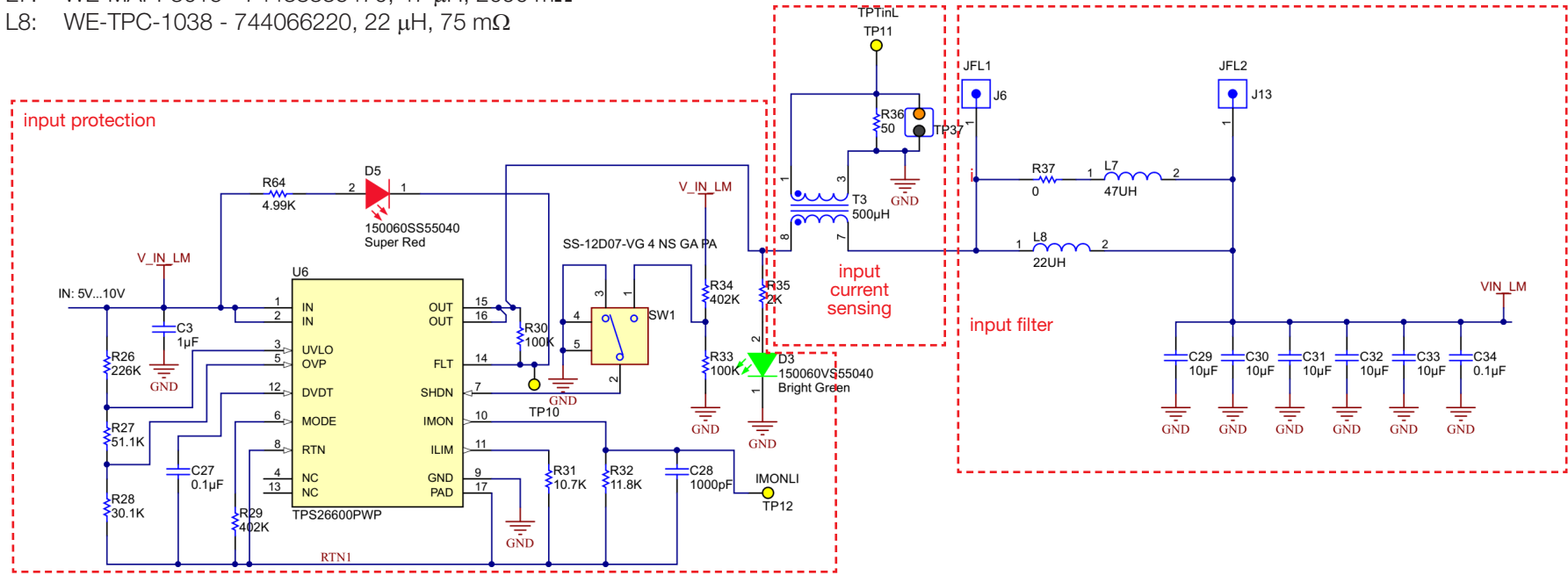
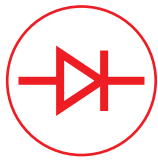


Figure 6. Circuit schematic of TI-PMLK BUCK-WE Board - LM3475 Regulator



LM3475 Regulator: Buck Section

The LM3475 regulator can use the three Würth Elektronik inductors :

- L1: WE-TPC-8043 - 744071101, 100 μ H, 270 m Ω ;
- L2: WE-LHMI-7050 - 74437349680, 68 μ H, 386 m Ω ;
- L3: WE-PD-7345 - 7447779168, 68 μ H, 239 m Ω ;

The inductors L1, L2 and L3 can be selectively connected by shorting J1-J5, J2-J5 or J3-J5, respectively, by means of one of the high current jumpers provided with the board. The LM3475 regulator incorporates a TI's LM60 sensor U3 to measure the ambient temperature at test point TP7, and a resistive sensor Rntc1 to measure the surface temperature of the inductor L1 at test point TP13.

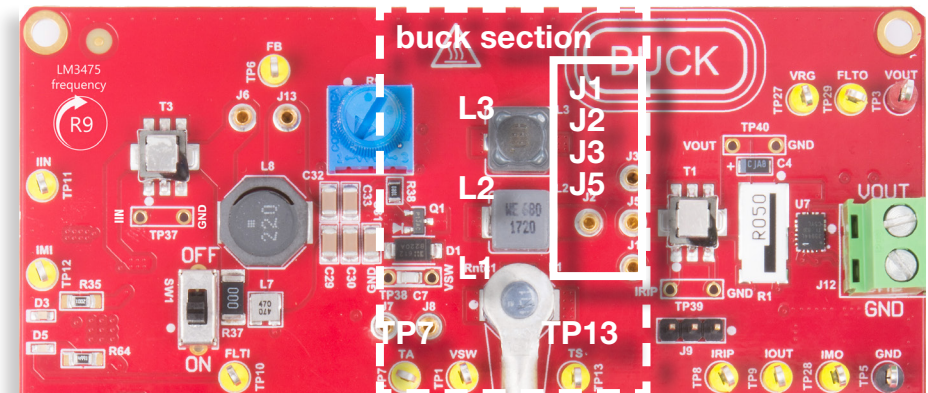


Figure 7. TI-PMLK BUCK-WE Board - LM3475 Regulator

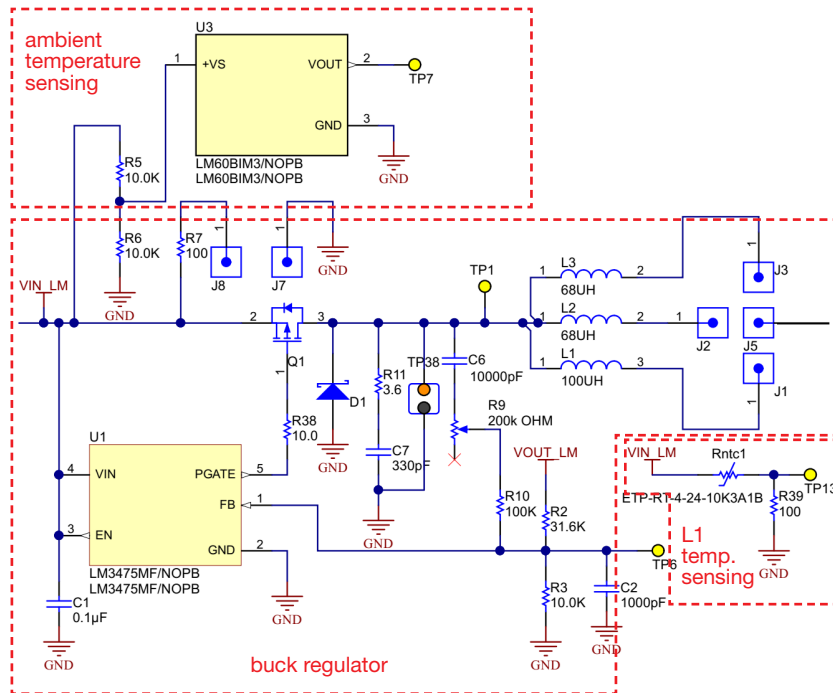


Figure 8. Circuit schematic of TI-PMLK BUCK-WE Board - LM3475 Regulator



LM3475 Regulator: Output Inductors

The output inductors L1, L2 and L3 available in the LM3475 buck regulator belong to Würth Elektronik inductors series WE-TPC, WE-LHMI, WE-PD, respectively. Their characteristics can be easily analyzed by means of the Würth Elektronik [REDEXPERT](#) on-line software. Figure 9 shows the [REDEXPERT](#) plots of inductance vs DC current for the three inductors, while Table 1 summarizes the main data.

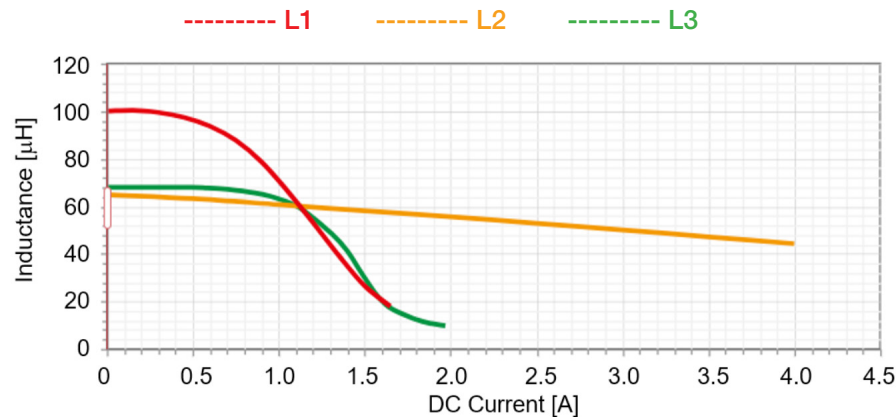


Figure 9. Inductance vs DC current at 20°C

Table 1. Inductors parameters

	L [µH]	R _{typ} [mΩ]	series	size	core material	length [mm]	width [mm]	height [mm]	vol [mm ³]
L1	100	270	WE-TPC	8043	NiZn	8.0	8.0	4.6	294.4
L2	68	386	WE-LHMI	7050	Iron P.	7.3	6.6	5.0	240.9
L3	68	239	WE-PD	7345	NiZn	7.3	7.3	4.5	239.8

The magnetic core material is a NiZn ferrite for L1 and L3 and Iron Powder for L2. The core material influences the inductance vs DC current plot, as shown in Figure 9. The two inductors L1 and L3 exhibit a sharp roll-off from the nominal inductance, at low DC current, to a much lower inductance, at high DC current, caused by the saturation of ferrite material of magnetic cores. The inductor L3, instead, is characterized by a smooth decay of the inductance as the DC

current increases, determined by the effect of the distributed micro air gaps of the powdered iron particles composing the core.

The inductance of the three inductors is 60 µH at 1.1 A DC current. Below 1.1 A DC current, the ferrite inductors L1 and L3 exhibit a higher inductance than the powder iron inductor L2, whereas the contrary happens above 1.1 A DC current.

The inductance of the inductor L1 starts rolling-off its 100 µH nominal value above 200 mA DC current, while the inductor L3 starts rolling-off its 68 µH nominal value above 500 mA DC current. The inductances of L1 and L3 are much different from each other below 1.1 A DC current, whereas they are almost equal above 1.1 A DC current.

The inductance is also influenced by the temperature. Figure 10 shows the inductance vs DC current [REDEXPERT](#) plots for inductor L3 at 30°C and 80°C.

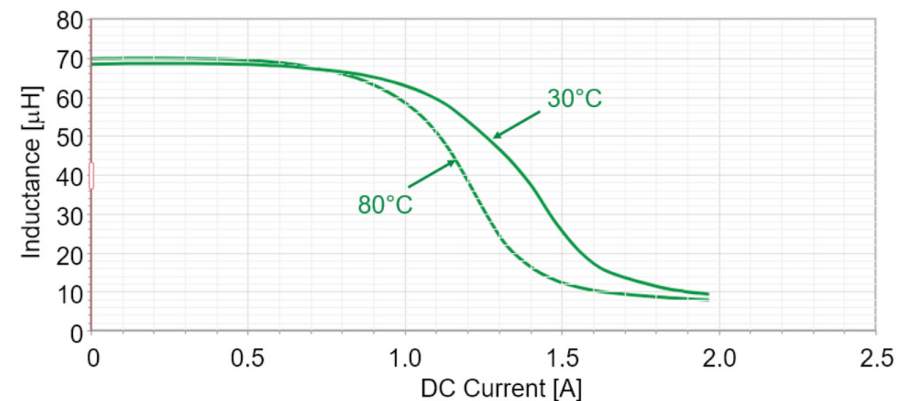


Figure 10. Inductance vs DC current at 30°C and 80°C

A left-side drift of the roll-off region can be observed at higher temperature, while the inductance at low DC current increases. This is the typical behavior of ferrite core inductors.

The temperature of the inductor L1 can be increased thanks to a heating resistor, placed in the bottom layer of the board, which allows to observe live the effects of temperature on the inductance, and the consequent impact on the LM3475 regulator operation.



LM3475 Regulator: Input Inductors

The input inductors L7 and L8 available in the LM3475 buck regulator belong to the Würth Elektronik inductors series WE-MAPI and WE-TPC, respectively. Their characteristics can be easily analyzed by means of the Würth Elektronik **REDEXPERT** on-line software. Figure 11 shows the **REDEXPERT** plots of inductance vs DC current for the two inductors, while Table 2 summarizes the main data.

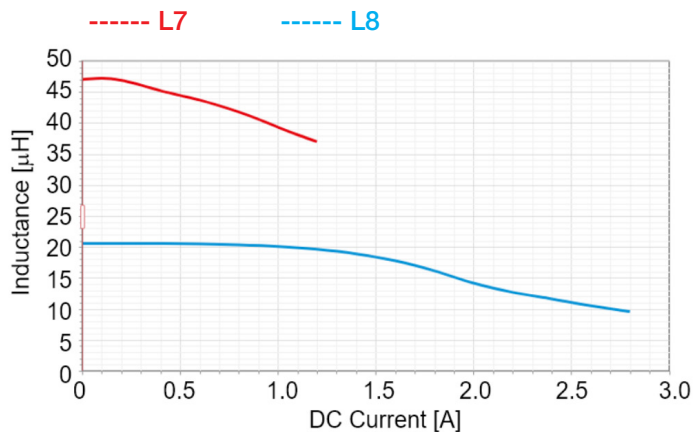


Figure 11. Inductance vs DC current at 20°C

Table 2. Inductors parameters

	L [μH]	R _{typ} [mΩ]	series	size	core material	length [mm]	width [mm]	height [mm]	vol [mm ³]
L7	47	2090	WE-MAPI	3015	Met. Alloy	3	3	1.5	13.5
L8	22	55.8	WE-TPCI	1038	NiZn	10	10	4.1	410

The magnetic core material is a metal alloy for L7 and NiZn ferrite for L8. The core material influences the inductance vs DC current plot, as shown in Figure 11. The inductor L7 is characterized by a smooth decay of the inductance as the DC current increases, above 150 mA DC current, whereas the inductor L8 exhibits a nonlinear roll-off above 1 A DC current, as a consequence of the sharper saturation of its ferrite magnetic core. The inductor L7 has a much smaller volume than inductor L8. As a consequence, at a given DC current, its

temperature rise with respect to ambient temperature is higher compared to inductor L8, as shown in Figure 12, reporting the temperature rise vs DC current **REDEXPERT** plots for the two inductors.

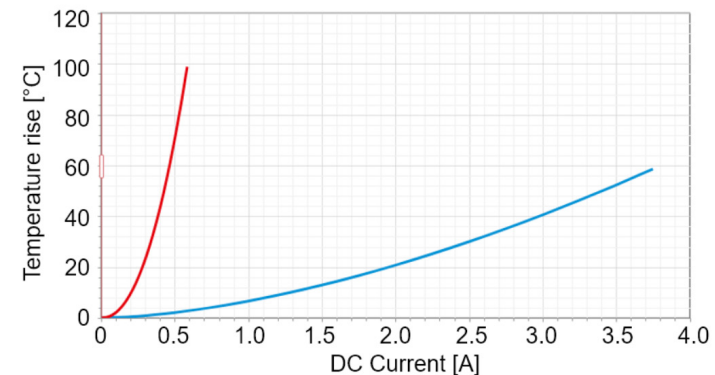


Figure 12. Temperature rise vs DC current at 20°C ambient temperature

The inductors L7 and L8 together with capacitors C29, C30, C31, C32 and C33 form the input filter of the LM3475 regulator.

The inductor L7 is characterized by a 2.09 Ω winding resistance, much higher than the 55.8 mΩ winding resistance of the inductor L8. The high winding resistance of the inductor L7 is exploited to damp the input filter. The inductors L7 and L8 operate under different conditions, due to the damping effect of the winding resistance of the inductor L7, as explained in Experiment 4. In particular, the inductor L8 sustains almost the total DC input current of the LM3475 regulator, whereas the inductor L7 shares with the inductor L8 a fraction of the very small AC input current ripple of the LM3475 regulator. Consequently, they are subjected to different power losses and temperature rise.



LM3475 Regulator: Output Section

The output (inductor) current sensing circuit is comprised of two parts.

AC current sensing. The transformer T1 and resistor R8 (bottom layer) allow observing the AC output ripple current at test point TP9. The transconductance AC gain is 1A/V.

DC current sensing. The TI's INA139 current shunt monitor U2 (bottom layer) senses the output current through the resistor R1 and generates a proportional current, that is injected into resistor R4 (bottom layer) and filtered by capacitor C5 (bottom layer). The DC component of the LM3475 regulator output current can be observed by measuring the voltage at test point TP9. The transconductance DC gain is 1 A/V.

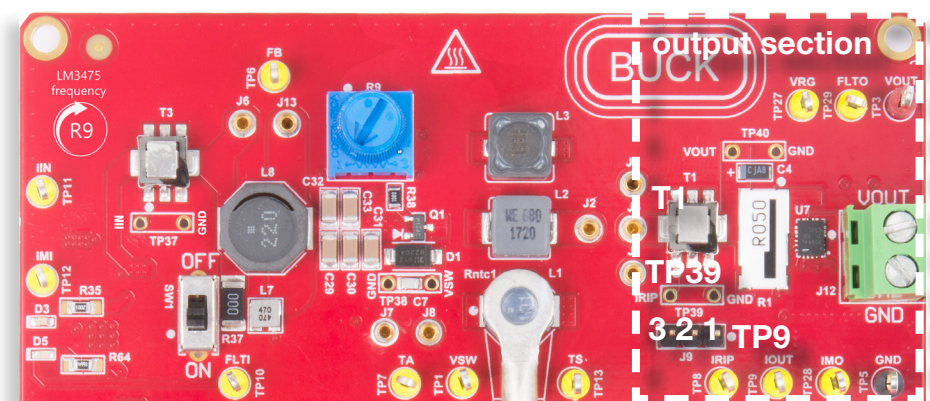


Figure 13. TI-PMLK BUCK-WE Board - LM3475 Regulator

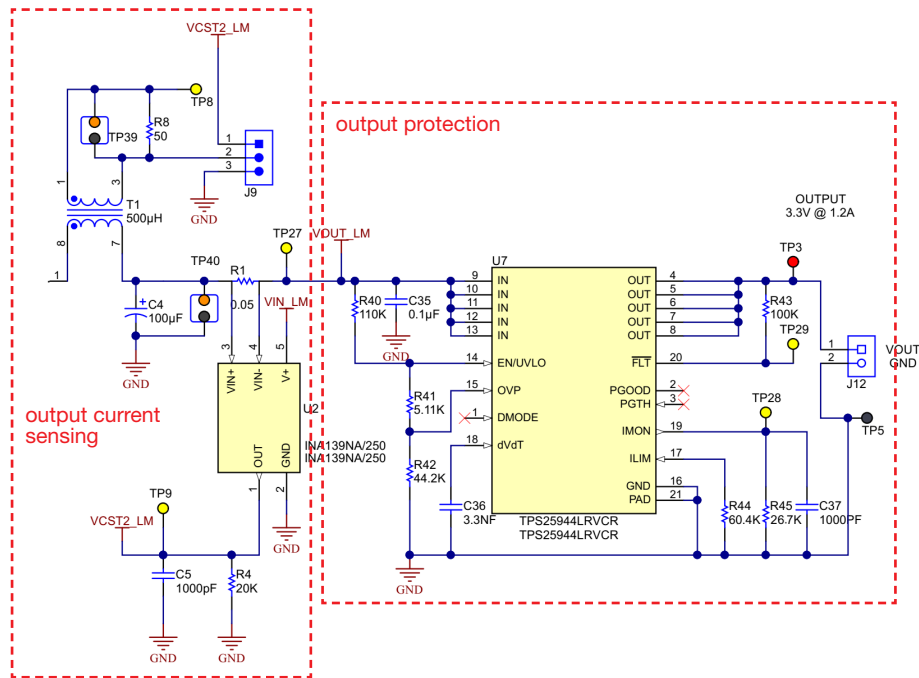


Figure 14. Circuit schematic of TI-PMLK BUCK-WE Board - LM3475 Regulator

The AC and DC components of the output current can be measured separately, by shorting pins 2 and 3 of pin header J9, or they can be summed and measured by means of a single voltage probe, by shorting pins 1 and 2 of pin header J9.

The LM3475 Section incorporates an output protection circuit, based on TI's TPS25942 eFuse, featuring 1.5 A over-current protection (OCP) and reverse polarity protection (RPP).



LM3475 Regulator: Configuration and Setup

Buck Inductors

The inductors L1, L2 and L3 can be selectively connected by shorting J1-J5, J2-J5 or J3-J5, respectively, by means of a high current jumper.

Temperature

The inductor L1 can be heated by shorting J7-J8, which connects the 100 Ω heating resistor R7, placed in the bottom layer of the board underneath the inductor, to the input voltage. The resulting temperature depends on operating conditions.

Switching Frequency

The switching frequency can be adjusted by means of the *one-turn* trimmer R9. Turning the knob clockwise from the left-side stop position to the right-side stop position increases the switching frequency from 275 to 700 kHz, at 10 V input voltage and 1.2 A load current, and from 100 to 300 kHz, at 5 V input voltage and 1.2 A load current.

Input Filter

The input filter can be bypassed by shorting J6-J13.

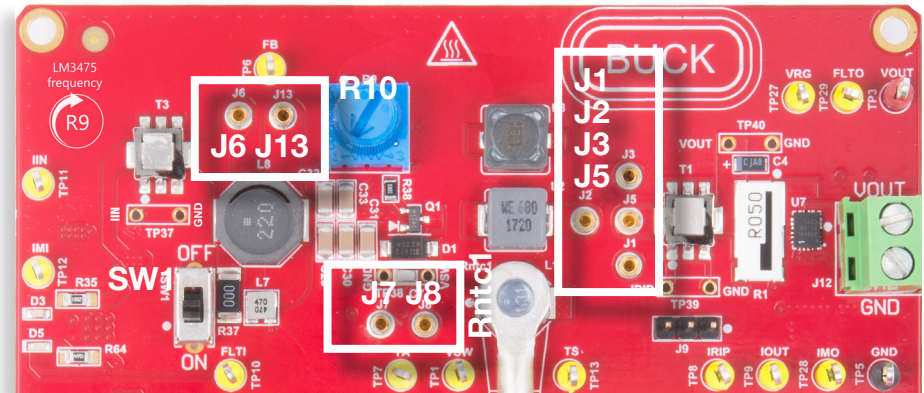


Figure 15. TI-PMLK BUCK-WE Board - LM3475 Regulator

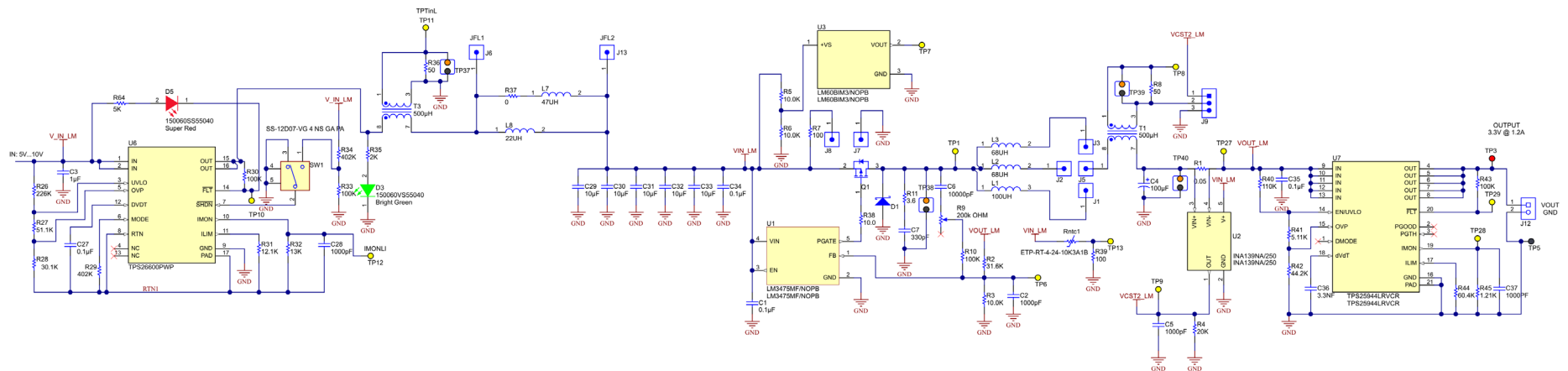


Figure 16. Circuit schematic of TI-PMLK BUCK-WE Board - LM3475 Regulator



LM3475 Regulator: Connectors, Jumpers and Test Points

Connectors

J_{12} : output load screw drive connector

Jumpers

J_9 : 1-2 **shorted**, connects the negative output pin of the current sense transformer T_1 to the positive output pin of current shunt monitor U2;
2-3 **shorted**, connects the negative output pin of the current sense transformer T_1 to the ground.

High Current Jumpers

$J_1 - J_5$ **shorted**: connects inductor L_1 (100 μ H, 270 $m\Omega$)
 $J_2 - J_5$ **shorted**: connects inductor L_2 (68 μ H, 386 $m\Omega$)
 $J_3 - J_6$ **shorted**: connects inductor L_3 (68 μ H, 239 $m\Omega$)
 $J_7 - J_8$ **shorted**: connects heating resistor R_7 (100 Ω) to input voltage
 $J_6 - J_{13}$ **shorted**: by-passes the inductors L_7 and L_8 of input filter

Test Points

TP_1 : switching node voltage
 TP_2 : positive pole of input voltage
 TP_3 : positive pole of output voltage
 TP_4 : ground pole of input voltage
 TP_5 : ground pole of output voltage
 TP_6 : feedback voltage
 TP_7 : ambient temperature
 TP_8 : inductor ripple current
 TP_9 : inductor average current
 TP_{10} : input protection fault monitor
 TP_{11} : input current ripple
 TP_{12} : average input current
 TP_{13} : inductor L_1 surface temperature
 TP_{27} : regulated output voltage
 TP_{28} : average output current
 TP_{29} : output protection fault monitor
 TP_{37} : input current ripple (low noise measurement)
 TP_{38} : switching node voltage (low noise measurement)
 TP_{39} : inductor ripple current (low noise measurement)
 TP_{40} : output capacitor voltage (low noise measurement)



LM3475 Regulator: Current Measurements

OUTPUT CURRENT MEASUREMENT

• Total DC+AC Output Inductor Current Measurement (J_9 short 1-2)

- Connect a voltage probe to TP_8 (positive pole) and TP_5 (GND) to measure the total DC + AC inductor current



• Separate DC and AC Output Inductor Current Measurement (J_9 short 2-3)

- **AC (ripple)** **Option A.** Use a voltage probe with ground spring, by inserting the probe positive pole tip into the hole of TP_{39} labeled "IRIP" and the tip of ground spring into the hole of TP_{39} labeled "GND", as shown in Figure 18.



Figure 18. Test point TP39

[Note. This type of measurement is used to prevent the noise effects caused by the parasitic inductance of voltage probe ground wire, and yields low noise measurements].

Option B. Use a voltage probe with ground wire, by connecting the positive pin of the voltage probe to TP_8 and the ground wire clamp to TP_5 .

[Note. This type of measurement is used to observe the noise effects caused by the parasitic inductance of voltage probe ground wire, and yields high noise measurements].

- **DC (average)** Connect a voltage probe, or a multimeter, to TP_9 (positive pole) and TP_5 (ground) to measure the inductor DC average current

INPUT CURRENT MEASUREMENT

• DC Input Current Measurement

- connect a voltage probe, or a multimeter, to TP_{12} (positive pole) and TP_4 (ground) to measure the input DC average current

• AC Input Current Measurement

- **Option A.** Use a voltage probe with ground spring, by inserting the probe positive pole tip into the hole of TP_{37} labeled "IIN", and the tip of ground spring into the hole of TP_{37} labeled "GND", as shown in Figure 19.

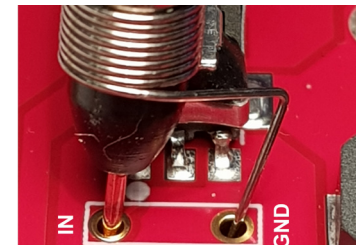


Figure 19. Test point TP37

[Note. This type of measurement is used to prevent the noise effects caused by the parasitic inductance of voltage probe ground wire, and yields low noise measurements].

- **Option B.** Use a voltage probe with ground wire, by connecting the positive pin of the voltage probe to TP_{11} and the ground wire clamp to TP_4 .

[Note. This type of measurement is used to observe the noise effects caused by the parasitic inductance of voltage probe ground wire, and yields high noise measurements].



LM3475 Regulator: Voltage Measurements

SWITCHING NODE VOLTAGE MEASUREMENT

The switching node voltage can be observed in two ways:

Option A.

Use a voltage probe with ground spring, by inserting the probe positive pole tip into the hole of TP_{38} labeled "VSW", and the tip of ground spring into the hole of TP_{38} labeled "GND", as shown in Figure 20.



Figure 20. Test point TP_{38}

[Note. This type of measurement is used to prevent the noise effects caused by the parasitic inductance of voltage probe ground wire, and yields low noise measurements].

Option B.

Use a voltage probe with ground wire, by connecting the positive pin of the voltage probe to TP_1 and the ground wire clamp to TP_5 (or TP_4).

[Note. This type of measurement is used to observe the noise effects caused by the parasitic inductance of voltage probe ground wire, and yields high noise measurements].

OUTPUT VOLTAGE MEASUREMENT

Three different test points are available to observe and measure the output voltage of the LM3475 regulator:

Measure 1.

The test point TP_{40} is used to observe the voltage of the 100 μ F output capacitor of the LM3475 regulator: use a voltage probe with ground spring, by inserting the probe positive pole tip into the hole of TP_{40} labeled "VOUT", and the tip of ground spring into the hole of TP_{40} labeled "GND", as shown in Figure 21.

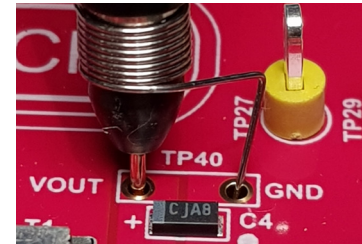


Figure 21. Test point TP_{40}

Measure 2.

The test point TP_{27} is used to observe the voltage regulated by the LM3475 controller, including the voltage drop across the 50 m Ω resistance of current sensing resistor R1: use a voltage probe with ground wire, by connecting the positive pin of the voltage probe to TP_{27} and the ground wire clamp to TP_5 .

Measure 3.

The test point TP_3 is used to observe the voltage at the output of the LM3475 controller, including the voltage drop across the 42 m Ω R_{ds}, on resistance of eFuse U7 internal MOSFET: use a voltage probe with ground wire, by connecting the positive pin of the voltage probe to TP_3 and the ground wire clamp to TP_5 .



LM3475 Regulator: temperature measurements (1)

AMBIENT TEMPERATURE MEASUREMENT

The ambient temperature can be determined with a digital multimeter, or an oscilloscope, by measuring the DC voltage at the output test point TP_7 of the TI's LM60 sensor U3 (<http://www.ti.com/lit/ds/symlink/lm60.pdf> ) , shown in Figure 22.

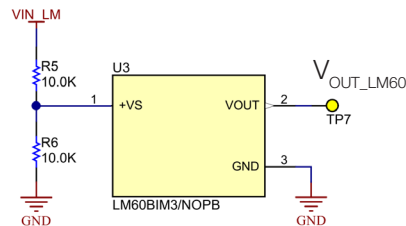


Figure 22. Ambient temperature sensor

The LM60 device is a precision integrated-circuit temperature sensor that can sense a $-40\text{ }^{\circ}\text{C}$ to $+125\text{ }^{\circ}\text{C}$ temperature range. The output voltage of the device is composed of a DC offset of 424 mV plus a variable component linearly proportional to the temperature, with a $6.25\text{ mV}/^{\circ}\text{C}$ gain, as shown in Equation (1):

$$(1) \quad V_{\text{OUT_LM60}} = 424\text{ mV} + 6.25\text{ mV}/^{\circ}\text{C} \times T_a$$

The ambient Celsius temperature can be obtained from the voltage $V_{\text{OUT_LM60}}$ measured at the test point TP_7 , as shown in Equation (2):

$$(2) \quad T_a = (V_{\text{OUT_LM60}} - 424) / 6.25$$

where $V_{\text{OUT_LM60}}$ is in mV. The offset allows reading negative temperatures without the need for a negative supply. The nominal output voltage of the device ranges from 174 mV to 1205 mV for a $-40\text{ }^{\circ}\text{C}$ to $+125\text{ }^{\circ}\text{C}$ temperature range. The device is calibrated to provide accuracies of $\pm 2\text{ }^{\circ}\text{C}$ at room temperature and $\pm 3\text{ }^{\circ}\text{C}$ over the full $-25\text{ }^{\circ}\text{C}$ to $+125\text{ }^{\circ}\text{C}$ temperature range.

INDUCTOR L1 SURFACE TEMPERATURE MEASUREMENT

The surface temperature of inductor L1 can be determined with a digital multimeter, or an oscilloscope, by measuring the DC voltage at the test point TP_{13} of the Variohm's ETP-RT-4-24-10K3A1B resistive sensor Rntc1 (https://www.variohm.com/images/datasheets/Variohm_ETP-RT_temperature_sensor_1208_F.pdf ) , shown in Figure 23.

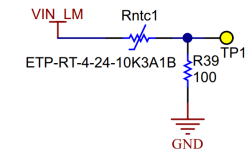
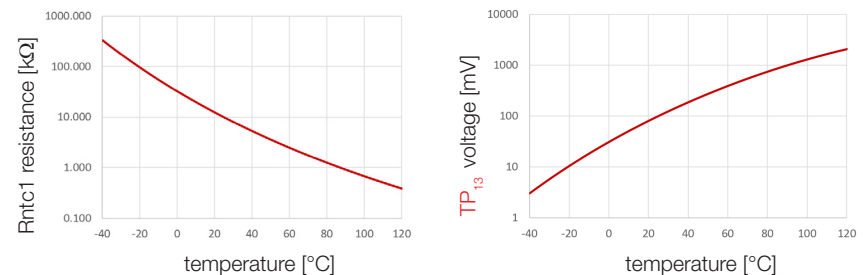


Figure 23. Surface temperature sensor

The ETP-RT-4-24-10K3A1B device is a negative temperature coefficient (NTC) resistor that can sense a $-40\text{ }^{\circ}\text{C}$ to $+125\text{ }^{\circ}\text{C}$ temperature range. The resistance of the sensor decreases as the temperature increases, as shown in Figure 24(a), whereas the voltage at the test point TP_{13} increases as shown in Figure 24(b). The sensor is characterized by a $\pm 0.2\%$ resistance tolerance from 0 to $70\text{ }^{\circ}\text{C}$. The TP_{13} voltage is proportional to the LM3475 input voltage.



(a) Rntc1 resistance vs temperature (b) voltage at TP_{13} vs temperature
Figure 24. Rntc1 resistance and TP_{13} voltage vs temperature at 10V input voltage

The Tables I, II and III on next page allow to calculate the surface temperature of the inductor L1, given the input voltage of the LM3475 regulator and the voltage measured at test point TP_{13} .



LM3475 Regulator: temperature measurements (2)

Table.I. Rntc1 conversion table at 5V input voltage

V_{TP13} [V]	T_s [°C]						
0.015	0	0.059	29	0.180	58	0.452	87
0.016	1	0.061	30	0.187	59	0.465	88
0.017	2	0.064	31	0.193	60	0.479	89
0.018	3	0.067	32	0.200	61	0.492	90
0.019	4	0.069	33	0.207	62	0.506	91
0.020	5	0.072	34	0.214	63	0.520	92
0.021	6	0.075	35	0.222	64	0.534	93
0.022	7	0.079	36	0.229	65	0.549	94
0.023	8	0.082	37	0.237	66	0.564	95
0.024	9	0.085	38	0.245	67	0.579	96
0.025	10	0.089	39	0.253	68	0.594	97
0.026	11	0.092	40	0.261	69	0.610	98
0.027	12	0.096	41	0.270	70	0.626	99
0.029	13	0.100	42	0.279	71	0.642	100
0.030	14	0.104	43	0.288	72	0.659	101
0.032	15	0.108	44	0.297	73	0.676	102
0.033	16	0.112	45	0.307	74	0.693	103
0.035	17	0.116	46	0.316	75	0.710	104
0.036	18	0.121	47	0.326	76	0.728	105
0.038	19	0.125	48	0.337	77	0.746	106
0.040	20	0.130	49	0.347	78	0.764	107
0.042	21	0.135	50	0.358	79	0.782	108
0.043	22	0.140	51	0.369	80	0.801	109
0.045	23	0.145	52	0.380	81	0.820	110
0.047	24	0.151	53	0.391	82	0.839	111
0.050	25	0.156	54	0.403	83	0.859	112
0.052	26	0.162	55	0.415	84	0.878	113
0.054	27	0.168	56	0.427	85	0.898	114
0.056	28	0.174	57	0.440	86	0.919	115

Table.II. Rntc1 conversion table at 7.5V input voltage

V_{TP13} [V]	T_s [°C]						
0.023	0	0.088	29	0.270	58	0.679	87
0.024	1	0.092	30	0.280	59	0.698	88
0.025	2	0.096	31	0.290	60	0.718	89
0.027	3	0.100	32	0.300	61	0.738	90
0.028	4	0.104	33	0.311	62	0.759	91
0.029	5	0.109	34	0.321	63	0.780	92
0.031	6	0.113	35	0.332	64	0.802	93
0.032	7	0.118	36	0.344	65	0.823	94
0.034	8	0.123	37	0.355	66	0.846	95
0.036	9	0.128	38	0.367	67	0.868	96
0.037	10	0.133	39	0.380	68	0.892	97
0.039	11	0.138	40	0.392	69	0.915	98
0.041	12	0.144	41	0.405	70	0.939	99
0.043	13	0.150	42	0.418	71	0.964	100
0.045	14	0.155	43	0.432	72	0.988	101
0.047	15	0.162	44	0.446	73	1.014	102
0.050	16	0.168	45	0.460	74	1.039	103
0.052	17	0.174	46	0.475	75	1.065	104
0.054	18	0.181	47	0.490	76	1.092	105
0.057	19	0.188	48	0.505	77	1.118	106
0.060	20	0.195	49	0.521	78	1.146	107
0.062	21	0.203	50	0.537	79	1.173	108
0.065	22	0.210	51	0.553	80	1.201	109
0.068	23	0.218	52	0.570	81	1.230	110
0.071	24	0.226	53	0.587	82	1.259	111
0.074	25	0.235	54	0.605	83	1.288	112
0.078	26	0.243	55	0.622	84	1.318	113
0.081	27	0.252	56	0.641	85	1.348	114
0.084	28	0.261	57	0.659	86	1.378	115

Table.III. Rntc1 conversion table at 10V input voltage

V_{TP13} [V]	T_s [°C]						
0.015	0	0.059	29	0.180	58	0.452	87
0.016	1	0.061	30	0.187	59	0.465	88
0.017	2	0.064	31	0.193	60	0.479	89
0.018	3	0.067	32	0.200	61	0.492	90
0.019	4	0.069	33	0.207	62	0.506	91
0.020	5	0.072	34	0.214	63	0.520	92
0.021	6	0.075	35	0.222	64	0.534	93
0.022	7	0.079	36	0.229	65	0.549	94
0.023	8	0.082	37	0.237	66	0.564	95
0.024	9	0.085	38	0.245	67	0.579	96
0.025	10	0.089	39	0.253	68	0.594	97
0.026	11	0.092	40	0.261	69	0.610	98
0.027	12	0.096	41	0.270	70	0.626	99
0.029	13	0.100	42	0.279	71	0.642	100
0.030	14	0.104	43	0.288	72	0.659	101
0.032	15	0.108	44	0.297	73	0.676	102
0.033	16	0.112	45	0.307	74	0.693	103
0.035	17	0.116	46	0.316	75	0.710	104
0.036	18	0.121	47	0.326	76	0.728	105
0.038	19	0.125	48	0.337	77	0.746	106
0.040	20	0.130	49	0.347	78	0.764	107
0.042	21	0.135	50	0.358	79	0.782	108
0.043	22	0.140	51	0.369	80	0.801	109
0.045	23	0.145	52	0.380	81	0.820	110
0.047	24	0.151	53	0.391	82	0.839	111
0.050	25	0.156	54	0.403	83	0.859	112
0.052	26	0.162	55	0.415	84	0.878	113
0.054	27	0.168	56	0.427	85	0.898	114
0.056	28	0.174	57	0.440	86	0.919	115



LM3475 Section: Bill of Materials (1)

Designator	Description	Manufacturer	Part Number
C1, C27, C34	CAP CER, 0.1 uF, 50 V, X7R, 0805	Würth Elektronik	885012207098
C2, C5, C28	CAP CER, 1000 pF, 50 V, C0G/NP0, 0805	AVX Corporation	08055A102FAT2A
C3	CAP CER, 1 uF, 50 V, X7R, 1206	Taiyo Yuden	HMK316B7105KL-T
C4	CAP TANT POLY, 100 uF, 6 V, 1206	Kemet	T5271107M006ATE100
C6	CAP CER, 10000 pF, 50 V, X7R, 0805	Würth Elektronik	885012207092
C7	CAP CER, 330 pF, 50 V, C0G/NP0, 0805	Würth Elektronik	885012007060
C29, C30, C31, C32, C33	CAP CER, 10 uF, 50 V, X5R, 1206	TDK Corporation	C3216X5R1H106K
C35	CAP CER, 0.1 uF, 16 V, X7R, 1206	Murata	GRM31C5C1E104JA01L
C36	CAP CER, 3.3 nF, 16 V, X7R, 1206	Würth Elektronik	885012208049
C37	CAP CER, 1000 pF, 50 V, X7R, 1206	Samsung	CL31C102JCCN9NC
D1	DIODE SCHOTTKY, 20 V, 2 A, SMA	Diodes Inc.	B220A-13-F
D3	WL-SMCD, SMD, MONO-COLOR, BRIGHT GREEN, 0603, LED	Lumex Opto Components Inc	SML-LX0603SUGW-TR
D5	WL-SMCD, SMD, MONO-COLOR, SUPER RED, 0603, LED	Lumex Opto Components Inc	SML-LX0603IW-TR
L1	FIXED IND, 100 uH, 1 A, 320 mΩ, SMD	Würth Elektronik	744071101
L2	FIXED IND, 68 uH, 1.25 A, 445 mΩ, SMD	Würth Elektronik	74437349680
L3	FIXED IND, 68 uH, 870 mA, 380 mΩ, SMD	Würth Elektronik	7447779168
L7	FIXED IND, 47 uH, 390 mA, 2.3 Ω, SMD	Würth Elektronik	74438335470
L8	FIXED IND, 22 uH, 2.5 A, 75 mΩ, SMD	Würth Elektronik	744066220
Q1	MOSFET, P-CH, 30 V, 5.9 A, SOT-23	Vishay Siliconix	SI2343CDS-T1-GE3
R1	RES, 0.05 OHM, 5W, 4320, WIDE	Ohmite	FC4L110R050FER
R2	RES, SMD, 31.6 kΩ, 1%, 1/8W, 0805	Vishay Dale	CRCW080531K6FKEA
R3, R5, R6	RES, SMD, 10 kΩ, 1%, 1/8W, 0805	Vishay Dale	CRCW080510K0FKEA
R4	RES, SMD, 20 kΩ, 0.1%, 1/4W, 1206	Vishay Dale	TNPW120620K0BEEA
R7	RES, SMD, 100 Ω, 1%, 1W, 2515	Vishay Dale	WSC2515100R0FEA
R8, R36	RES, SMD, 50 Ω, 1%, 1W, 2515	Vishay Dale	WSC251550R00FEA
R9	TRIMMER, 200 kΩ, 0.5 W, PC TH	Bourns	3386F-1-204TLF



LM3475 Section: Bill of Materials (2)

Designator	Description	Manufacturer	Part Number
R10, R30, R33, R43	RES, SMD, 100 k Ω , 1%, 1/8W, 0805	Yageo	RC0805FR-07100KL
R11	RES, SMD, 3.6 Ω , 5%, 1/8W, 0805	Stackpole Electronics Inc.	RMCF0805FT3R60
R26	RES, SMD, 226 k Ω , 1%, 1/8W, 0805	Vishay Dale	CRCW0805226KFKEA
R27	RES, SMD, 51.1 k Ω , 1%, 1/8W, 0805	Venkel	CR0805-10W-5112FT
R28, R48	RES, SMD, 30.1 k Ω , 1%, 1/8W, 0805	Panasonic Electronic Comp.	ERJ-6ENF3012V
R29, R34	RES, SMD, 402 k Ω , 1%, 1/8W, 0805	Panasonic Industrial Devices	ERJ-6ENF4023V
R35	RES, SMD, 2 k Ω , 1%, 1/8W, 0805	Panasonic Electronic Comp.	ERJ-6ENF2001V
R37	RES, 0 Ω , JUMPER, 1W, 2010	Vishay Dale	CRCW20100000Z0EFHP
R38	RES, SMD, 10 Ω , 5%, 1/8W, 0805	Vishay Dale	CRCW080510R0FKEA-
R39	RES, SMD, 100 Ω , 1%, 1/4W, 1206	Vishay Dale	CRCW1206100RFKEA
R40	RES, SMD, 110 k Ω , 1%, 1/8W, 0805	Yageo	RC0805FR-07110KL
R41	RES, SMD, 5.11 k Ω , 1%, 1/8W, 0805	Panasonic Electronic Comp.	ERJ-6ENF5111V
R42	RES, SMD, 44.2 k Ω , 1%, 1/8W, 0805	Panasonic Electronic Comp.	ERA-6AEB4422V
R44	RES, SMD, 60.4 k Ω , 1%, 1/8W, 0805	Vishay Dale	CRCW080560K4FKEA
R45	RES, SMD, 1.21 k Ω , 1%, 1/8W, 0805	Vishay Dale	CRCW08051K21FKEA
R46	RES, SMD, 392 k Ω , 1%, 1/8W, 0805	Vishay Dale	CRCW0805392KFKEA
R47	RES, SMD, 90.9 k Ω , 1%, 1/8W, 0805	Vishay Dale	CRCW080590K9FKEA
Rntc1	TEMPERATURE SENSOR SMT RING TERMINAL PROBE	Variohm EuroSensor	ETP-RT-4-24-10K3A1B
T1, T3	Current Sense Transformer	Würth Elektronik	749251050
U1	IC REG CTRLR BUCK SOT23-5	Texas Instruments	LM3475MF/NOPB
U2	IC CURRENT MONITOR 0.5% SOT23-5	Texas Instruments	INA139NA/250
U3	SENSOR TEMP ANLG VOLT SOT-23-3	Texas Instruments	LM60BIM3/NOPB
U6	IC HOT PLUG CTRLR 16HTSSOP	Texas Instruments	TPS26600PWP
U7	IC PWR MGMT EFUSE 2.7-18 V 20WQFN	Texas Instruments	TPS25944LRVCR



TPS54160 Section: Top Layer

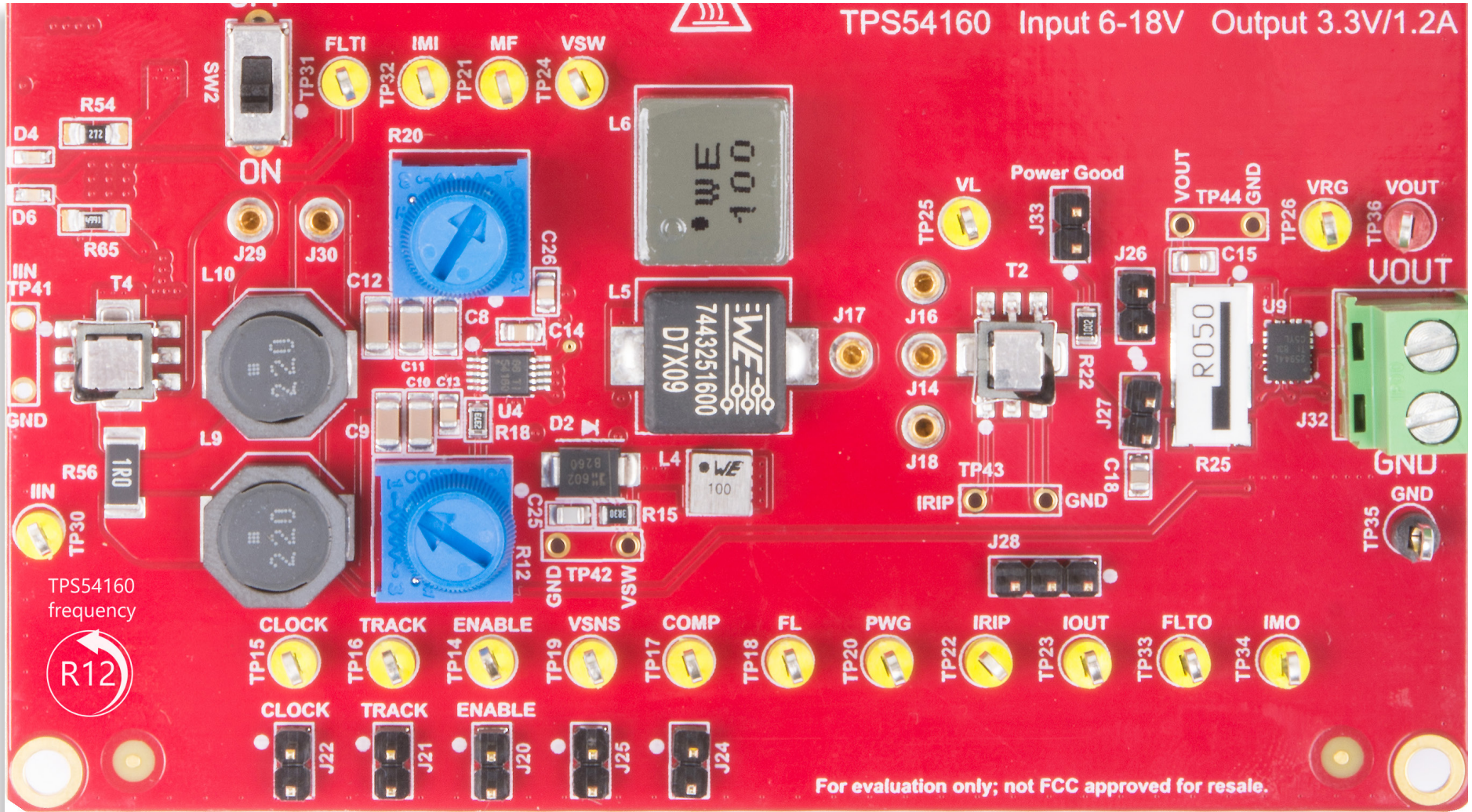


Figure 25. Top Layer of TI-PMLK BUCK-WE Board - TPS54160 Regulator



TPS54160 Section: Bottom Layer

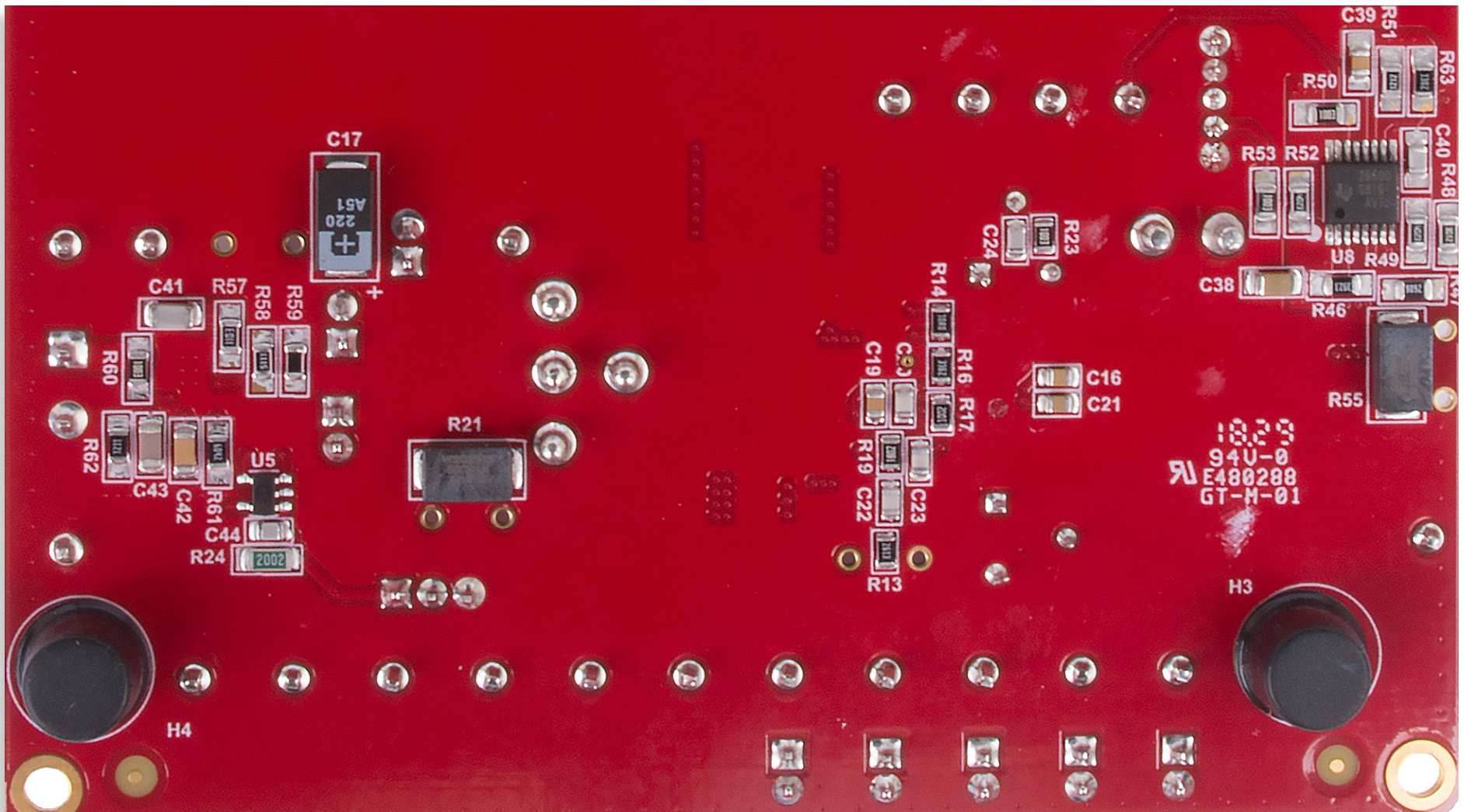


Figure 26. Bottom Layer of TI-PMLK BUCK-WE Board - TPS54160 Regulator



TPS54160 Regulator: Input Section (1)

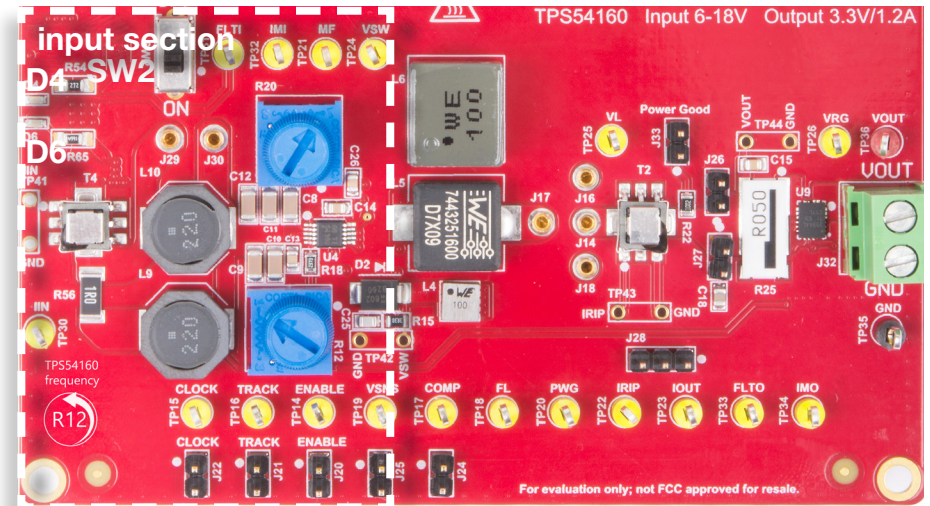
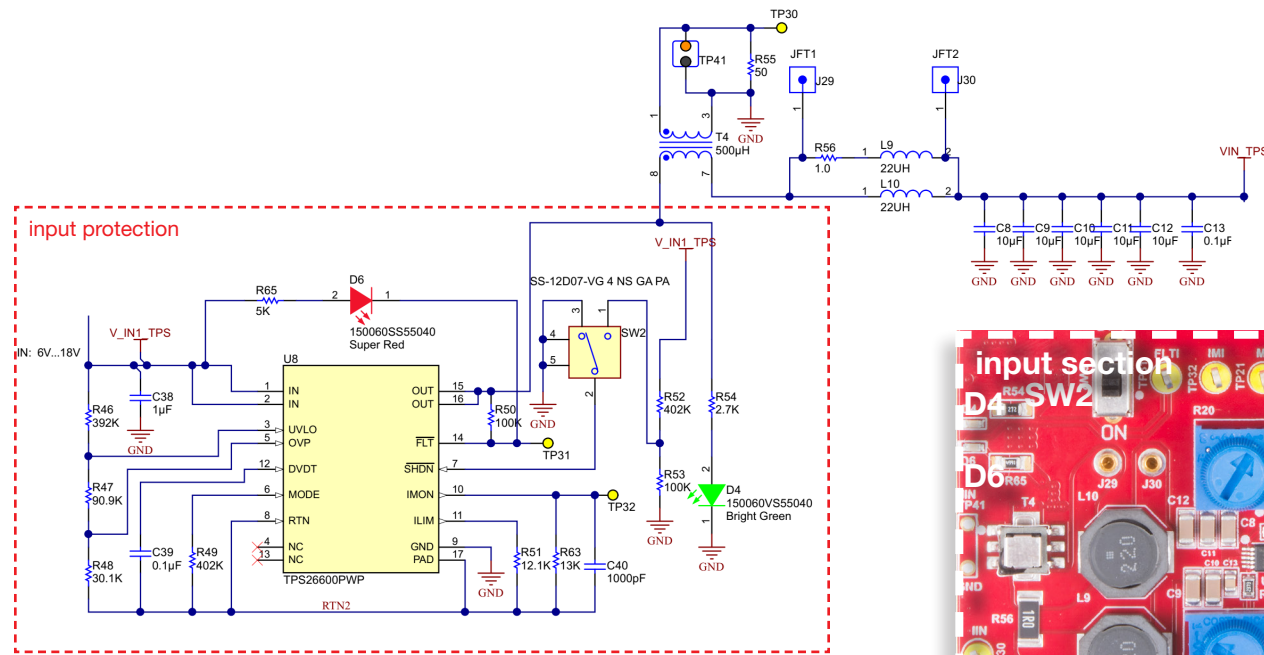


Figure 28. Circuit schematic of TI-PMLK BUCK-WE Board - TPS54160 Regulator

Figure 27. TI-PMLK BUCK-WE Board - TPS54160 Regulator

The input section of TPS54160 regulator incorporates a protection circuit, based on TI's TPS26600 eFuse, featuring 20 V over-voltage protection (OVP), 1.0 A over-current protection (OCP) and reverse polarity protection (RPP).

The switch SW2 allows turning the TPS26600 eFuse output ON and OFF, to power on and shutdown the TPS54160 regulator, respectively. In case of fault causing the protection activation, the switch SW2 allows resetting the eFuse,

after the fault condition is removed, to restart the TPS54160 operation. The green and red LEDs D4 and D6 indicate the ON/OFF status of the eFuse.



TPS54160 Regulator: Input Section (2)

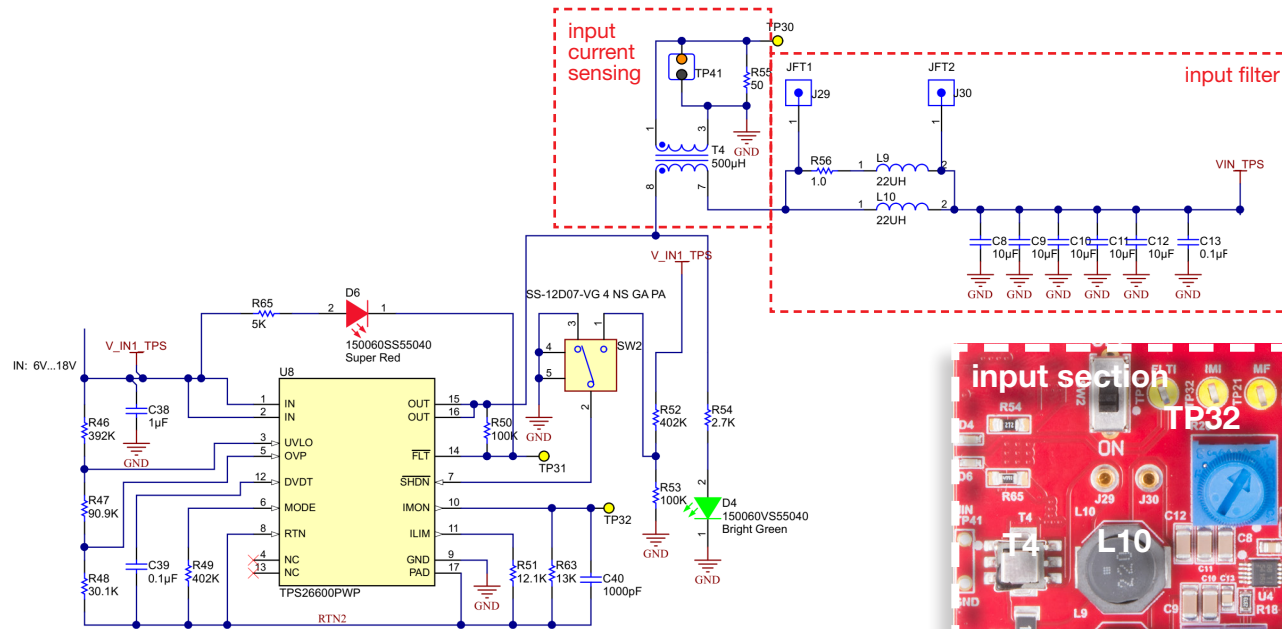


Figure 29. Circuit schematic of TI-PMLK BUCK-WE Board - TPS54160 Regulator

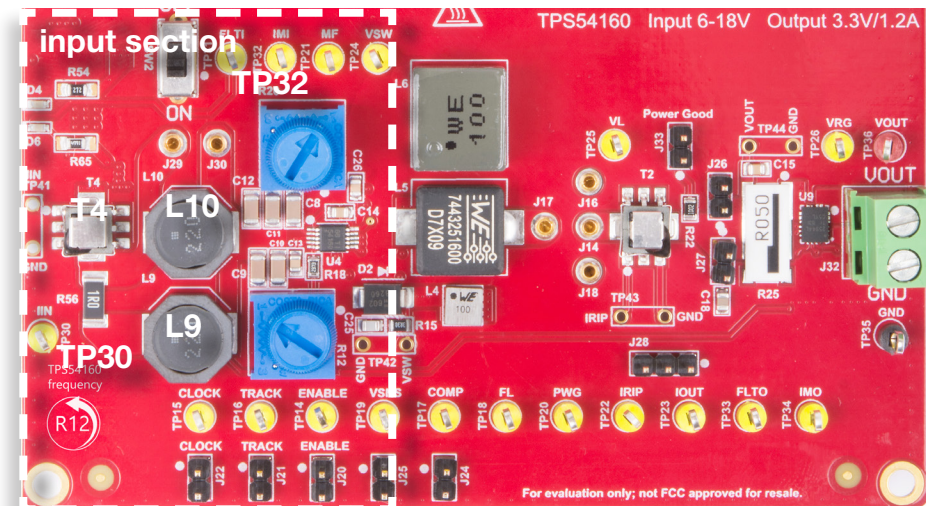


Figure 30. TI-PMLK BUCK-WE Board - TPS54160 Regulator

The input current sensing circuit, comprised of transformer T4 and resistor R55 (bottom layer), allows to observe the AC input ripple current at test points TP30, whereas the DC component of input current can be observed at test point TP32.

The input filter uses the two Würth Elektronik inductors:

- L9, L10: WE-TPC - 1038 - 744066220, 22 μ H, 75 m Ω .



TPS54160 Regulator: Buck Section

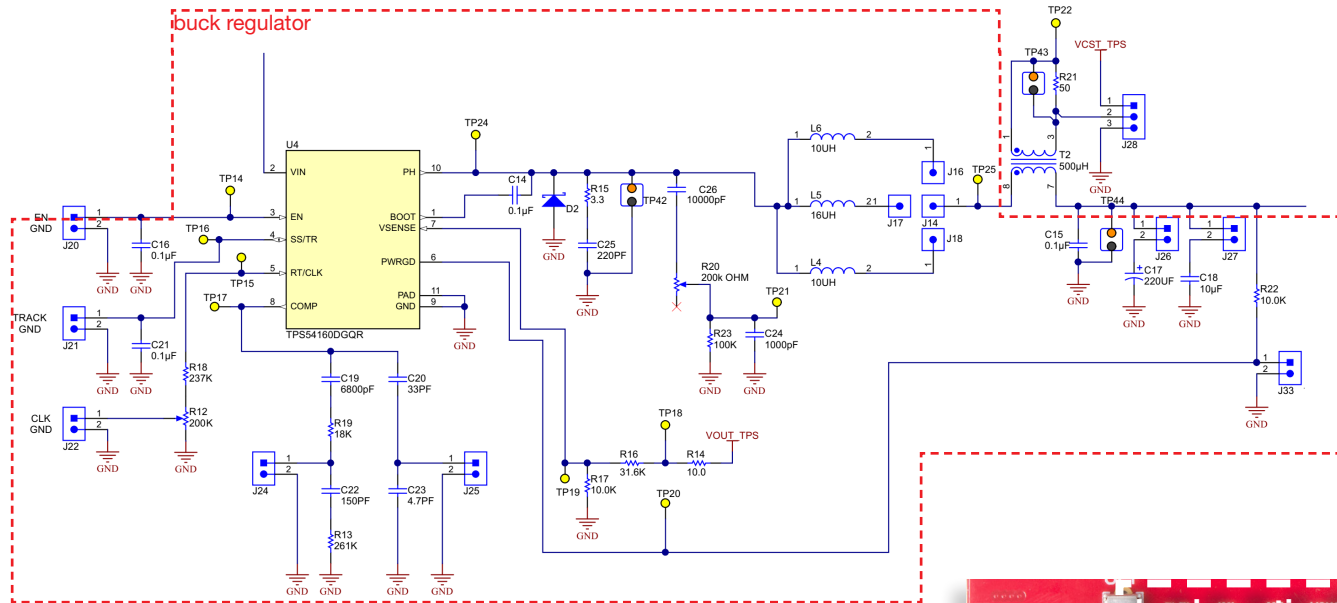


Figure 31. Circuit schematic of TI-PMLK BUCK-WE Board - TPS54160 Regulator

The TPS54160 regulator can use the three Würth Elektronik inductors :

- L4: WE-TPC-8043 - 744071101, 100 μH , 270 m Ω ;
- L5: WE-LHMI-7050 - 74437349680, 68 μH , 386 m Ω ;
- L6: WE-PD-7345 - 7447779168, 68 μH , 239 m Ω ;

The inductors L4, L5 and L6 can be selectively connected, by shorting J14-J18, J14-J17 or J14-J16, respectively.

If J22 is open, the switching frequency is fixed at 255 kHz. If J22 is shorted, the switching frequency can be adjusted by means of the *one-turn* trimmer R12. Turning the knob counterclockwise from the right-side stop position to the left-side stop position increases the switching frequency from 255 to 465 kHz.

The trimmer R20 sets the gain of the circuit comprised of C26-R20-R23-C24 used to integrate the inductor voltage and observe the inductor magnetic flux.

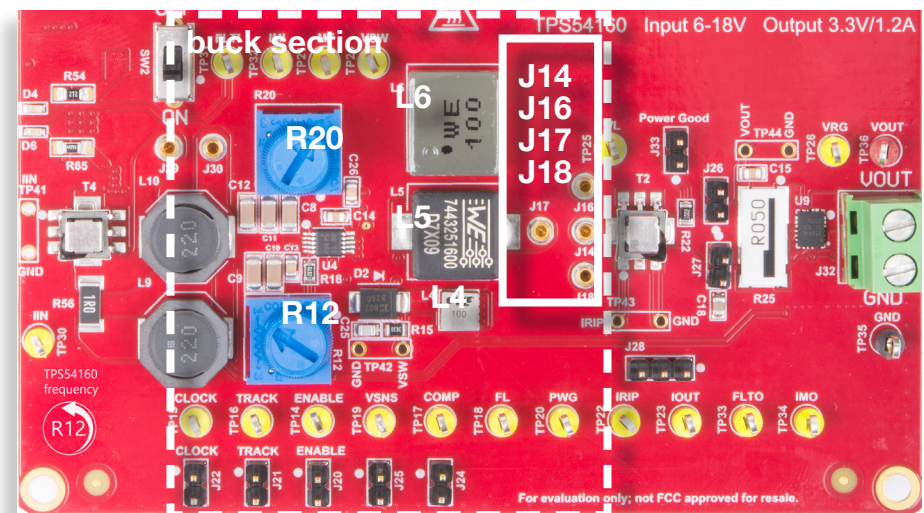


Figure 32. TI-PMLK BUCK-WE Board - TPS54160 Regulator



TPS54160 Regulator: Output Inductors

The output inductors L4, L5 and L6 available in the TPS54160 buck regulator belong to the Würth Elektronik inductors series WE-MAPI, WE-HCI, WE-XHMI, respectively. Their characteristics can be easily analyzed by means of the Würth Elektronik [REDEXPERT](#) on-line software. Figure 33 shows the [REDEXPERT](#) plots of inductance vs DC current for the three inductors, while Table 3 summarizes the main data.

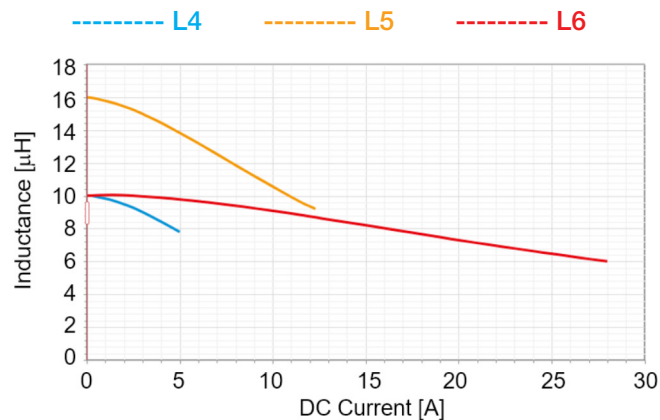


Figure 33. inductance vs DC current at 20°C

Table 3. Inductors parameters

	L [μH]	R_L [mΩ]	series	size	core material	length [mm]	width [mm]	height [mm]	vol [mm ³]
L4	10	101	WE-MAPI	4030	Met. Alloy	4.1	4.1	3.1	52.1
L5	16	34.5	WE-HCI	1050	Superflux	10.5	10.2	5.0	535.5
L6	10	11.4	WE-XHMI	1090	Hyperflux	11.6	10.5	9.1	1108

The magnetic core material is a Metal Alloy for L4, Superflux for L5 and Hyperflux for L6. The core material and size influence the inductance vs DC current characteristic and the winding resistance, as shown in Figure 33 and Table 3. The three inductors exhibit a smooth roll-off from the nominal inductance, at low DC current to lower inductance at high DC current, determined by the soft saturation of the magnetic material of cores.

Table 3 shows a big difference among the winding resistance of the three inductors. This is a direct consequence of the different size of the components. A larger size allows more room for windings, which can have larger cross-section and lower resistance.

A lower winding resistance results in lower ohmic losses.

A larger size provides better heat transfer from the inductor to the air.

The resulting effect is that, given the inductance, a bigger inductor is characterized by a lower temperature rise with respect to the ambient temperature, compared to a smaller inductor. This is highlighted in Figure 34, showing the temperature rise vs DC current [REDEXPERT](#) plots for the three inductors L4, L5 and L6.

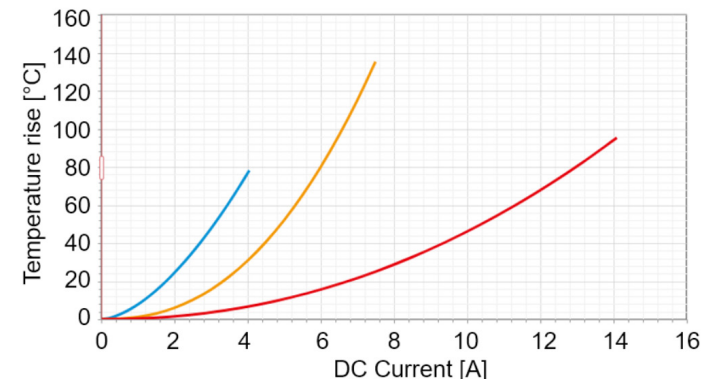


Figure 34. Temperature rise vs DC current at 20°C ambient temperature

The plots of Figure 34 are determined under DC operating conditions, with a constant DC current.

When the inductors operate under switching conditions, the current has also an AC component, which causes additional power losses in the magnetic core. These losses depend on the core material and size, on the magnitude of the magnetic flux swing and on the switching frequency.

The [REDEXPERT](#) on line software allows predicting the total DC and AC power losses of the inductors, given the operating conditions.



TPS54160 Regulator: Input Inductors

The input inductors L9 and L10 available in the TPS54160 buck regulator belong to the Würth Elektronik inductors series WE-TPC. Their characteristics can be easily analyzed by means of the Würth Elektronik [REDEXPERT](#) on-line software. Figure 35 shows the [REDEXPERT](#) plots of inductance vs DC current for the two inductors, while Table 4 summarizes the main data.

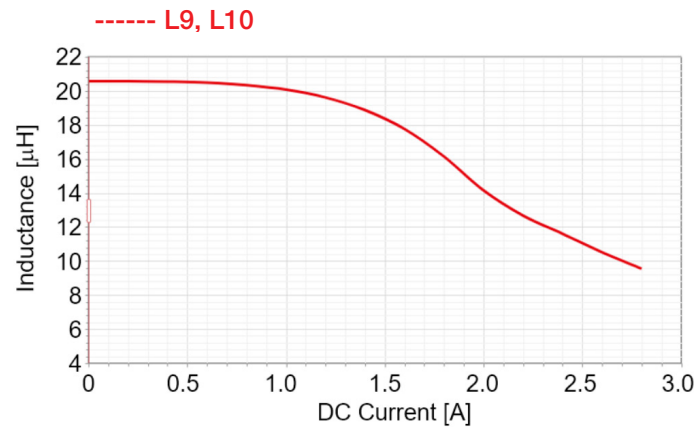


Figure 35. inductance vs DC current at 20°C

Table 4. Inductors parameters

L [μH]	R _L [mΩ]	series	size	core material	length [mm]	width [mm]	height [mm]	vol [mm ³]
22	55.8	WE-TPCI	1038	NiZn	10	10	4.1	410

The inductors L9 and L10 exhibit a nonlinear roll-off above 1 A DC current, as a consequence of the sharp saturation of their ferrite magnetic core.

Figure 36 shows the temperature rise vs DC current [REDEXPERT](#) plots for the two inductors L9 and L10.

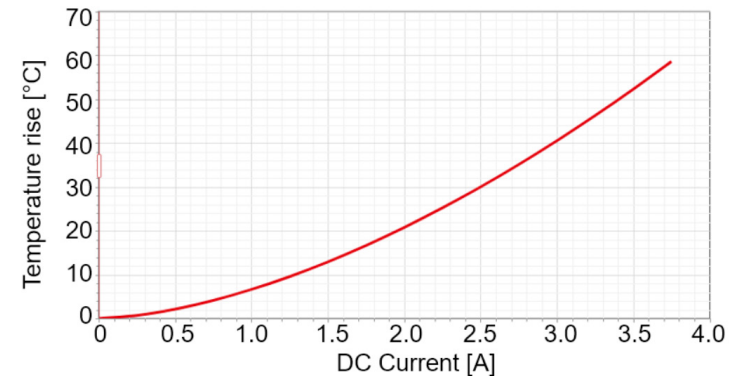


Figure 36. Temperature rise vs DC current at 20°C ambient temperature

The inductors L9 and L10 together with capacitors C8, C9, C10, C11 and C12 form the input filter of the TPS54160 regulator.

The input inductors L9 and L10 operate under different conditions, due to the effect of the damping resistor R56, as explained in Experiment 4. In particular, the inductor L10 sustains almost the total DC input current of the TPS54160 regulator, whereas the inductor L9 shares with the inductor L10 a fraction of the very small AC input current ripple of the TPS54160 regulator. Consequently, they are subjected to different power losses and temperature rise.



TPS54160 Regulator: Output Section

The output (inductor) current sensing circuit is comprised of two parts.

AC current sensing. The transformer T2 and resistor R21 (bottom layer) is used to observe the AC output ripple current at test point TP43. The transconductance AC gain is 1 A/V.

DC current sensing. The TI's INA139 current shunt monitor U5 (bottom layer) senses the output current through the resistor R25 and generates a proportional current, that is injected into resistor R24 (bottom layer) and filtered by capacitor C44 (bottom layer). The DC component of the TPS54160 regulator output current can be observed by measuring the voltage at test point TP23. The transconductance DC gain is 1 A/V.

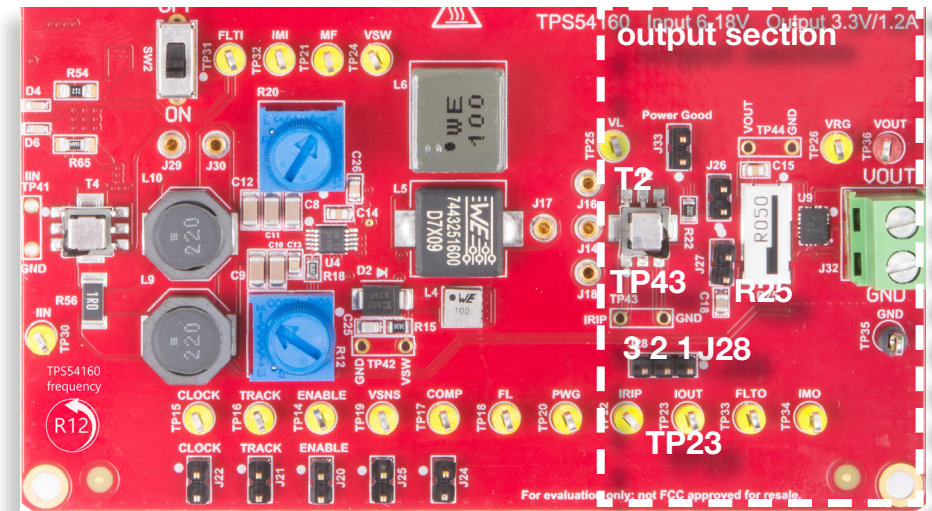


Figure 37. TI-PMLK BUCK - WE Board - TPS54160 Regulator

The AC and DC components of the output current can be measured separately, by shorting pins 2 and 3 of pin header J28, or they can be summed and measured by means of a single voltage probe, by shorting pins 1 and 2 of pin header J28.

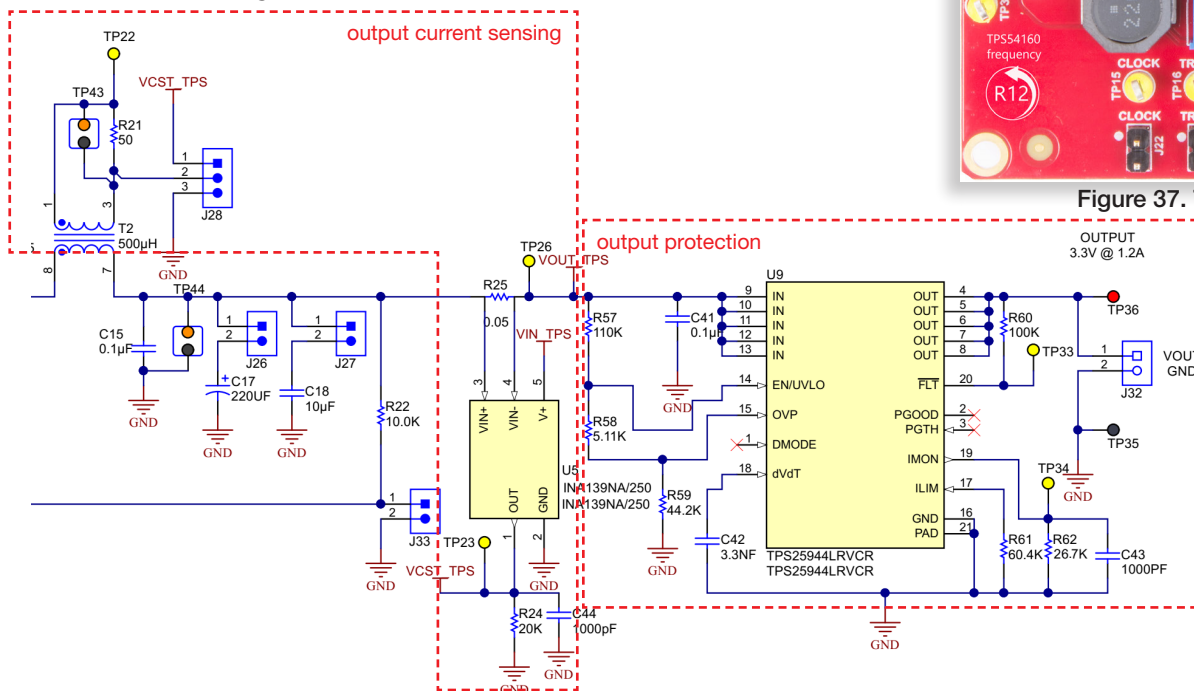


Figure 38. Circuit schematic of TI-PMLK BUCK-WE Board - TPS54160 Regulator



TPS54160 Regulator: Configuration and Setup

Buck Inductors

The inductors L4, L5 and L6 can be selectively connected by shorting J18-J14, J17-J14 or J16-J14, respectively, by means a high current jumper.

Switching Frequency

The switching frequency can be adjusted by means of the *one-turn* trimmer R12. Turning the knob counterclockwise from the right-side stop position to the left-side stop position increases the switching frequency from 255 to 465 kHz.

Input Filter

The input filter can be bypassed by shorting J29-J30.

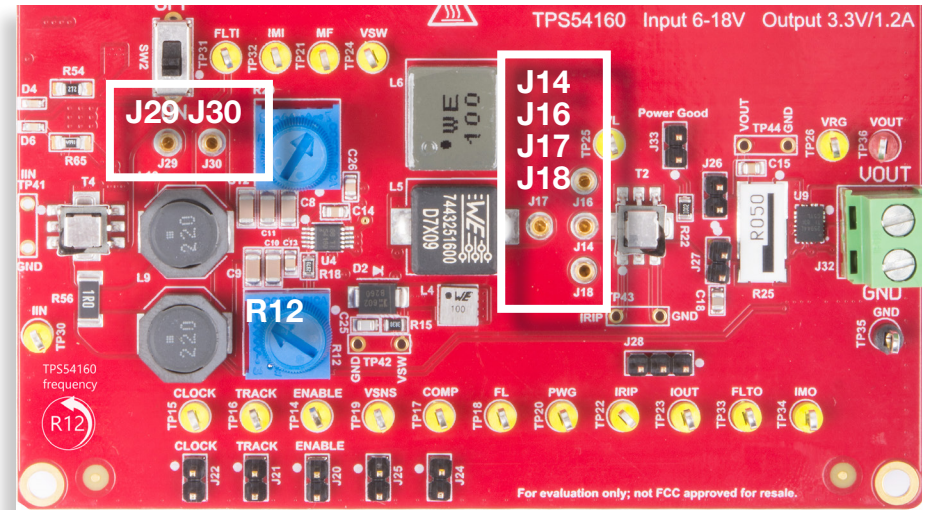
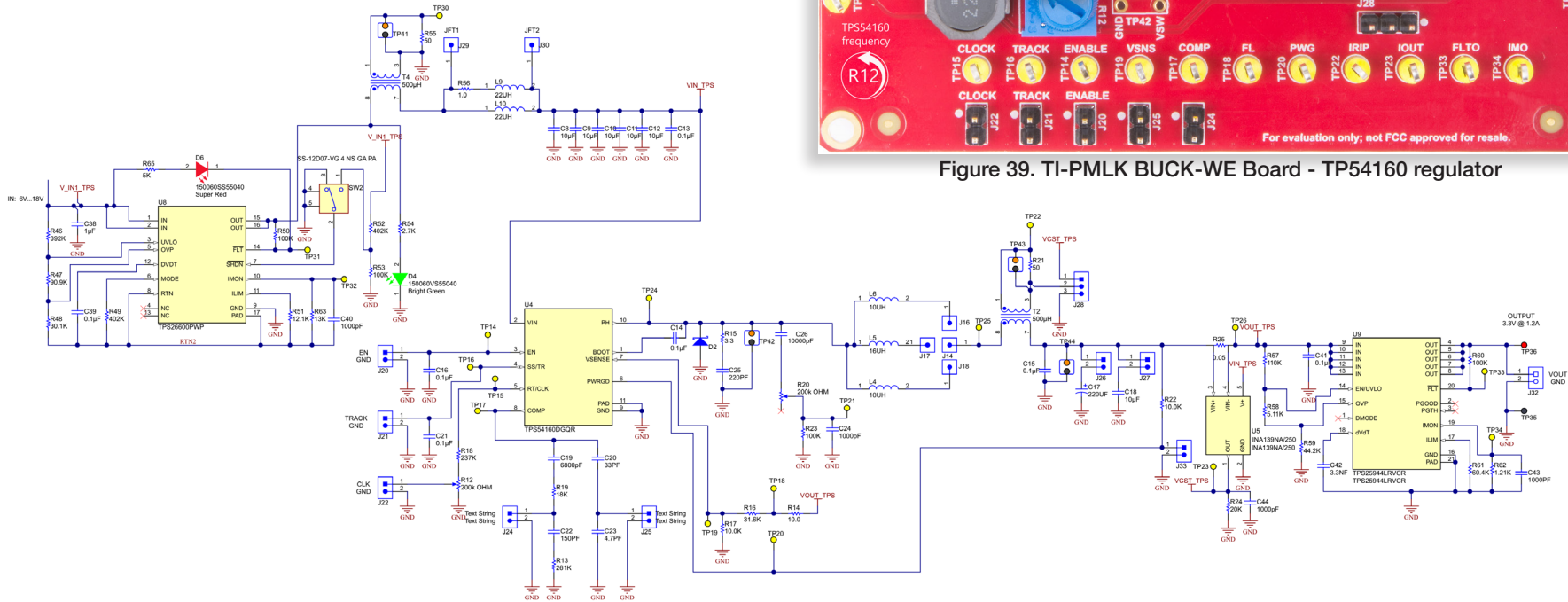


Figure 39. TI-PMLK BUCK-WE Board - TP54160 regulator





TPS54160 Section: Connectors, Jumpers and Test Pins

Connectors

- J₁₀: positive input voltage banana connector
- J₁₁: negative input voltage banana connector
- J₃₂: output load screw drive connector

Jumpers

- J₂₀: connects to external enable signal
- J₂₁: connects to external soft-start signal
- J₂₂: connects center pin of trimmer R12 to ground to allow switching frequency adjustment
- J₂₃: connects power good pin to ground
- J₂₄: bypasses the C₂₂ and R₁₃ parts to modify the error amplifier gain
- J₂₅: bypasses the C₂₃ part to modify the error amplifier gain
- J₂₈: **1-2 shorted**, connects the negative output pin of current sense transformer T₂ output to the positive output pin of current shunt monitor U5;
2-3 shorted, connects the negative output pin of current sense transformer T₂ output to ground.
- J₂₇: connects output capacitor C₁₈ (10 μF)
- J₂₆: connects output capacitor C₁₇ (220 μF)

High current jumpers

- J₁₄ - J₁₈ **shorted**: connects inductor L₄ (10 μH, 101 mΩ)
- J₁₄ - J₁₇ **shorted**: connects inductor L₅ (16 μH, 34.5 mΩ)
- J₁₄ - J₁₆ **shorted**: connects inductor L₆ (10 μH, 11.4 mΩ)
- J₂₉ - J₃₀ **shorted**: bypasses input filter inductors L₉ and L₁₀ (22 μH, 75 mΩ)

Test Points

- TP₂ : positive pole of input voltage
- TP₄ : ground pole of input voltage
- TP₁₄ : enable signal
- TP₁₅ : clock signal
- TP₁₆ : soft-start signal
- TP₁₇ : control voltage
- TP₁₈ : connection pin for loop gain measurements.
- TP₁₉ : feedback voltage
- TP₂₀ : power good signal
- TP₂₁ : inductor magnetic flux emulation signal
- TP₂₂ : inductor ripple current sensing
- TP₂₃ : inductor average current sensing
- TP₂₄ : switching node voltage
- TP₂₅ : used together with TP₄₄ to measure the voltage across the inductor.
- TP₃₀ : input ripple current sensing
- TP₃₁ : input protection fault monitor
- TP₃₂ : input average current sensing
- TP₃₃ : output protection fault monitor
- TP₃₄ : output average current sensing
- TP₃₅ : ground pole of output voltage
- TP₃₆ : positive pole of output voltage
- TP₄₁ : input ripple current sensing (low noise measurement)
- TP₄₂ : switching node voltage sensing (low noise measurement)
- TP₄₃ : inductor ripple current sensing (low noise measurement)
- TP₄₄ : output capacitor voltage sensing (low noise measurement)



TPS54160 Regulator: Current Measurements

OUTPUT CURRENT MEASUREMENT

• Total DC+AC Output Inductor Current Measurement (J_{28} short 1-2)

- Connect a voltage probe to TP_{22} (positive pole) and TP_{35} (GND) to measure the total DC + AC inductor current



• Separate DC and AC Output Inductor Current Measurement (J_{28} short 2-3)

- **AC (ripple)** **Option A.** Use a voltage probe with ground spring, by inserting the probe positive pole tip into the hole of TP_{43} labeled "IRIP" and the tip of ground spring into the hole of TP_{43} labeled "GND", as shown in Figure 41.

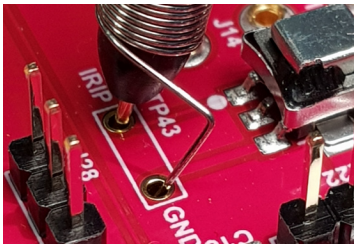


Figure 41. Test point TP43

[Note. This type of measurement is used to prevent the noise effects caused by the parasitic inductance of voltage probe ground wire, and yields low noise measurements];

Option B. Use a voltage probe with ground wire, by connecting the positive pin of the voltage probe to TP_{22} and the ground wire clamp to TP_{35} .

[Note. This type of measurement is used to observe the noise effects caused by the parasitic inductance of voltage probe ground wire, and yields high noise measurements].

- **DC (average)** Connect a voltage probe, or a multimeter, to TP_9 (positive pole) and TP_5 (ground) to measure the inductor DC average current

INPUT CURRENT MEASUREMENT

• DC Input Current Measurement

- Connect a voltage probe, or a multimeter, to TP_{32} (positive pole) and TP_4 (ground) to measure the input DC average current

• AC Input Current Measurement

- **Option A.** Use a voltage probe with ground spring, by inserting the probe positive pole tip into the hole of TP_{41} labeled "IIN", and the tip of ground spring into the hole of TP_{41} labeled "GND", as shown in Figure 42.

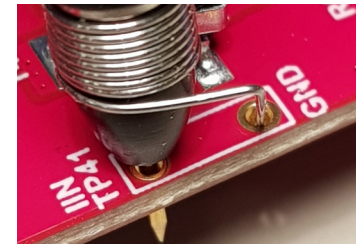


Figure 42. Test point TP41

[Note. This type of measurement is used to prevent the noise effects caused by the parasitic inductance of voltage probe ground wire, and yields low noise measurements];

- **Option B.** Use a voltage probe with ground wire, by connecting the positive pin of the voltage probe to TP_{30} and the ground wire clamp to TP_4 .

[Note. This type of measurement is used to observe the noise effects caused by the parasitic inductance of voltage probe ground wire, and yields high noise measurements].



TP54160 Regulator: Voltage Measurements

SWITCHING NODE VOLTAGE MEASUREMENT

The switching node voltage can be observed in two ways:

Option A.

Use a voltage probe with ground spring, by inserting the probe positive pole tip into the hole of TP_{42} labeled "VSW", and the tip of ground spring into the hole of TP_{42} labeled "GND", as shown in Figure 43.

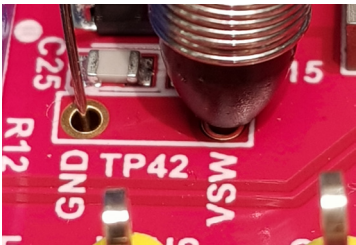


Figure 43. Test point TP42

[**Note.** This type of measurement is used to prevent the noise effects caused by the parasitic inductance of voltage probe ground wire, and yields low noise measurements];

Option B.

Use a voltage probe with ground wire, by connecting the positive pin of the voltage probe to TP_{24} and the ground wire clamp to TP_4 .

[**Note.** This type of measurement is used to observe the noise effects caused by the parasitic inductance of voltage probe ground wire, and yields high noise measurements].

OUTPUT VOLTAGE MEASUREMENT

Three different test points are available to observe and measure the output voltage of the TPS54160 regulator:

Measure 1.

The test point TP_{44} is used to observe the voltage of the output capacitors C17 and C18 of the TPS54160 regulator: use a voltage probe with ground spring, by inserting the probe positive pole tip into the hole of TP_{44} labeled "VOUT", and the tip of ground spring into the hole of TP_{44} labeled "GND", as shown in Figure 44.



Figure 44. Test point TP44

Measure 2.

The test point TP_{26} is used to observe the voltage regulated by the TPS54160 controller, including the voltage drop across the 50 mΩ resistance of current sensing resistor R25: use a voltage probe with ground wire, by connecting the positive pin of the voltage probe to TP_{26} and the ground wire clamp to TP_{35} .

Measure 3.

The test point TP_{36} is used to observe the voltage at the output of the TPS54160 controller, including the voltage drop across the 42 mΩ R_{dson} resistance of eFuse U9 internal MOSFET: use a voltage probe with ground wire, by connecting the positive pin of the voltage probe to TP_{36} and the ground wire clamp to TP_{35} .



TPS54160 Section: Bill of Materials (1)

Designator	Description	Manufacturer	PartNumber
C8, C9, C10, C11, C12	CAP CER, 10 uF, 50 V, X5R, 1206	TDK Corporation	C3216X5R1H106K
C13, C14, C15, C16, C21	CAP CER, 0.1 uF, 50 V, X7R, 0805	Würth Elektronik	885012207098
C17	CAP TANT POLY, 220 uF, 10 V ,2917	Panasonic Electronic Comp.	10TPE220ML
C18	CAP CER, 10 uF, 16 V, X5R, 0805	Samsung	CL21B106K0QNNNE
C19	CAP CER, 6800 pF, 50 V, X7R, 0805	Würth Elektronik	885012207091
C20	CAP CER, 33 pF, 50 V, COG/NP0, 0805	Yageo	CC0805JRNPO9BN330
C22	CAP CER, 150 pF, 50 V, COG/NP0, 0805	Würth Elektronik	885012007058
C23	CAP CER, 4.7 pF, 50 V, COG/NP0, 0805	Würth Elektronik	885012007049
C24	CAP CER, 1000 pF, 50 V, COG/NP0, 0805	AVX Corporation	08055A102FAT2A
C25	CAP CER, 220 pF, 50 V, COG/NP0, 0805	Würth Elektronik	885012007059
C26	CAP CER, 10000 pF, 50 V, X7R, 0805	Würth Elektronik	885012207092
C27	CAP CER, 0.1 uF, 50 V, X7R, 0805	Würth Elektronik	885012207098
C38	CAP CER, 1 uF, 50 V, X7R, 1206	Taiyo Yuden	HMK316B7105KL-T
C39	CAP CER, 0.1 uF, 50 V, X7R, 0805	Würth Elektronik	885012207098
C40	CAP CER, 1000 pF, 50 V, COG/NP0, 0805	AVX Corporation	08055A102FAT2A
C41	CAP CER, 0.1 uF, 16 V, X7R, 1206	Murata Electronics North America	GRM31C5C1E104JA01L
C42	CAP CER, 3.3 nF, 16 V, X7R, 1206	Würth Elektronik	885012208049
C43	CAP CER, 1000 pF, 50 V, X7R, 1206	Samsung	CL31C102JCCNNNC
C44	CAP CER, 1000 pF, 50 V, COG/NP0, 0805	AVX Corporation	08055A102FAT2A
D2	DIODE SCHOTTKY, 60 V, 2 A, SMB	Diodes Incorporated	B260-13-F
D4	WL-SMCD ,SMD, MONO-COLOR BRIGHT GREEN, 0603, LED	Lumex Opto Components Inc	SML-LX0603SUGW-TR
D6	WL-SMCD, SMD, MONO-COLOR SUPER RED, 0603, LED	Lumex Opto Components Inc	SML-LX0603IW-TR
L4	FIXED IND, 10 uH, 2.7 A, 110 mΩ, SMD	Würth Elektronik	74438357100
L5	FIXED IND, 16 uH, 5 A, 34.5 mΩ, SMD	Würth Elektronik	7443251600
L6	FIXED IND, 10 uH, 11.4 mΩ, SMD	Würth Elektronik	74439369100
L9, L10	FIXED IND, 22 uH, 2.5 A, 75 mΩ, SMD	Würth Elektronik	744066220
R12	TRIMMER, 200 kΩ, 0.5 W, PC TH	Bourns	3386F-1-204TLF
R13	RES SMD, 261 kΩ, 1%, 1/8W, 0805	Vishay Dale	CRCW0805261KFKEA
R14	RES SMD, 10 Ω, 1%, 1/8W, 0805	Vishay Dale	CRCW080510R0FKEA
R15	RES SMD, 3.3 Ω, 5%, 1/8W, 0805	Vishay Dale	CRCW08053R30FKEA
R16	RES SMD, 31.6 kΩ, 1%, 1/8W, 0805	Vishay Dale	CRCW080531K6FKEA
R17	RES SMD, 10 kΩ, 1%, 1/8W, 0805	Vishay Dale	CRCW080510K0FKEA-
R18	RES SMD, 237 kΩ, 1%, 1/8W, 0805	Panasonic Electronic Comp.	ERJ-6ENF2373V



TPS54160 Section: Bill of Materials (2)

Designator	Description	Manufacturer	PartNumber
R19	RES SMD, 18 k Ω , 1%, 1/8W, 0805	Yageo	RC0805FR-0718KL
R20	TRIMMER, 200 k Ω 0.5W, PC TH	Bourns	3386F-1-204TLF
R21	RES SMD, 50 Ω , 1%, 1W, 2515	Vishay Dale	WSC251550R00FEA
R22	RES SMD, 10 k Ω , 1%, 1/8W, 0805	Vishay Dale	CRCW080510K0FKEA-
R23	RES SMD, 100 k Ω , 1% ,1/8W, 0805	Yageo	RC0805FR-07100KL
R24	RES SMD, 20 k Ω , 0.1%, 1/4W, 1206	Vishay Dale	TNPW120620K0BEEA
R25	RES, 0.05 Ω , 5 W, 4320, WIDE	Ohmite	FC4L110R050FER
R46	RES SMD, 392 k Ω , 1%, 1/8W, 0805	Vishay Dale	CRCW0805392KFKEA
R47	RES SMD, 90.9 k Ω , 1%, 1/8W, 0805	Vishay Dale	CRCW080590K9FKEA
R48	RES SMD, 30.1 k Ω , 1%, 1/8W, 0805	Panasonic Electronic Comp.	ERJ-6ENF3012V
R49, R52	RES SMD, 402 k Ω , 1%, 1/8W, 0805	Panasonic Industrial Devices	ERJ-6ENF4023V
R50, R53, R60	RES SMD, 100 k Ω , 1%, 1/8W, 0805	Yageo	RC0805FR-07100KL
R54	RES SMD, 2.7 k Ω , 1%, 1/8W, 0805	Panasonic Electronic Comp.	ERJ-6ENF2701V
R55	RES SMD, 50 Ω , 1%, 1W, 2515	Vishay Dale	WSC251550R00FEA
R56	RES, 1 OHM 5%, 1W, 2010	Vishay Dale	CRM2010-JW-1R0ELF
R57	RES SMD, 110 k Ω , 1% ,1/8W, 0805	Yageo	RC0805FR-07110KL
R58	RES SMD, 5.11 k Ω , 1%, 1/8W, 0805	Panasonic Electronic Comp.	ERJ-6ENF5111V
R59	RES SMD, 44.2 k Ω , 1% ,1/8W, 0805	Panasonic Electronic Comp.	ERA-6AEB4422V
R61	RES SMD, 60.4 k Ω , 1%, 1/8W, 0805	Vishay Dale	CRCW080560K4FKEA
R62	RES SMD, 1.21 k Ω , 1%, 1/8W, 0805	Vishay Dale	CRCW08051K21FKEA
R63	RES SMD, 13 k Ω , 1%, 1/8W, 0805	Vishay Dale	CRCW080513K0FKEA
R64, R65	RES SMD, 5 k Ω , 1%, 1/8W, 0805	Panasonic - ECG	ERJ-6ENF4991V
T2,T4	CURR SENSE XFMR, 1:50, 10 A, SMD	Würth Elektronik	749251050
U4	IC REG BUCK ADJ, 1.5 A ,10MSOP	Texas Instruments	TPS54160DGQR
U5	IC CURRENT MONITOR, 0.5%, SOT23-5	Texas Instruments	INA139NA/250
U8	IC HOT PLUG CTRLR ,16HTSSOP	Texas Instruments	TPS26600PWP
U9	IC PWR MGMT EFUSE, 2.7-18 V ,20WQFN	Texas Instruments	TPS25944LRVCR



Instrumentation needed for experiments

The instrumentation needed for the execution of the experiments illustrated in this book is comprised of:

- DC power supply 0-35 V / 4 A
- DC electronic load 20 V / 10 A with dynamic current mode capability
- 250 MHz 4-channels Digital Oscilloscope
- 4-1/2 digit digital multimeters

The instrumentation used to obtain the experimental results presented in this book is comprised of:

- TTI EX354RT Power Supply 0-70 V / 4 A
- Sorensen Electronic Load SLM-4 mainframe + SLM series electronic load modules 60 V / 60 A
- Agilent Technologies MSO6034A Mixed Signals Oscilloscope, 300 MHz, 2 Gs/s, 4-channels
- FLUKE 8845A 6-1/2 digit precision multimeter



Notes, Warnings and Recommendations

NOTES

TPS54160 BUCK SECTION

- The TPS54160 feedback compensation setting with both J_{24} and J_{25} shorted is tailored for stable operation with $C_{out} = C_{18} = 10 \mu\text{F}$ (**J27 shorted**), whereas the feedback compensation setting with both J_{24} and J_{25} open is tailored for stable operation with $C_{out} = C_{17} = 220 \mu\text{F}$ (**J26 shorted**). When $C_{out} = C_{17}$ is used with J_{24} and J_{25} shorted the regulator is still stable, whereas when $C_{out} = C_{18}$ is used with J_{24} and J_{25} open the regulator is unstable, and the output voltage shows large oscillations around 3.34 V. Other combinations of capacitors C_{17} and C_{18} and jumpers J_{24} and J_{25} can lead whether to stable or to unstable operation depending on the input voltage and load current.

WARNINGS AND RECOMMENDATIONS

GENERAL

- If the board is loaded by means of an electronic load in constant current mode, the operation sequence to follow is:
 - at the turn on: turn on the input power supply, then turn on the electronic load (start with 0 A and slowly increase up to the desired DC current value)
 - at the turn off: turn off the electronic load, then turn off the input power supply
- Whatever change in the setup of jumpers has to be done, the board has to be shut down
- DO NOT operate the TPS54160 regulator in unstable conditions for more than few tens seconds
- If the regulator under test shows a behavior that looks much different with respect to what indicated in the experiment instructions, then shut down the regulator and check the board and instruments setup.
- The board has to be operated at the recommended ambient temperature 25 °C (maximum 27.5 °C)
- In case the regulator under test is shutdown by the input/output protection (red light ON), reduce the load current to 0.0 A, turn OFF the POWER SUPPLY and ELECTRONIC LOAD "OUT ON" buttons, set the switch SW1 (LM3475) , or SW2 (TPS54160), to OFF and then back to ON, and restart the test.

LM3475 BUCK SECTION

- DO NOT operate the regulator with J_1 - J_5 AND J_2 - J_5 AND J_3 - J_5 OPEN

TPS54160 BUCK SECTION

- DO NOT operate the regulator with J_{26} AND J_{27} OPEN
- DO NOT operate the regulator with J_{14} - J_{16} AND J_{14} - J_{17} AND J_{14} - J_{18} OPEN



Additional Terms, warnings, restrictions and disclaimers (1)

Additional Terms, warnings, restrictions and disclaimers of the “TI-PMLK Buck - Würth Elektronik Edition” Learning Kit (later defined as LEARNING KIT)

Würth Elektronik (later defined as WE) provides the enclosed LEARNING KIT under the following conditions: The user has to bear all responsibility and liability for the proper and safe handling with regard to this LEARNING KIT. The user shall indemnify WE from all claims arising from the handling or utilization of the LEARNING KIT. In case this LEARNING KIT does not comply with the specifications indicated in the Quick Start Guide and Experiment Book available for free download at www.we-online.com/pmlk, the LEARNING KIT may be returned to the following address within 30 days from the date of delivery for a full reimbursement of the purchase price.

Würth Elektronik eiSos GmbH & Co. KG

Max-Eyth-Straße 1
74638 Waldenburg
Germany

THE FOREGOING LIMITED WARRANTY IS THE EXCLUSIVE WARRANTY MADE BY WE TO THE USER AND IS IN LIEU OF ALL OTHER WARRANTIES, EXPRESSED, IMPLIED, OR STATUTORY, INCLUDING ANY WARRANTY OF MERCHANTABILITY OR FITNESS FOR ANY PARTICULAR PURPOSE. EXCEPT TO THE EXTENT OF THE INDEMNITY SET FORTH ABOVE, NEITHER PARTY SHALL BE LIABLE TO THE OTHER FOR ANY INDIRECT, SPECIAL, INCIDENTAL OR CONSEQUENTIAL DAMAGES.

Please read the Quick Start Guide carefully prior to handling the LEARNING KIT. This Guide contains essential safety information regarding temperatures and voltages.

No license is granted under any patent right or other intellectual property rights of WE covering or relating to any machine, process and procedure, or combination in which such the LEARNING KIT or services might be or are used. Our arrangement with the user is not exclusive as WE is currently working with a large number of customers for LEARNING KITS. WE bears no liability for applications assistance, customer product design, software performance, or infringement of patents or services described in the Quick Start Guide.

Code of federal regulations

As noted in the LEARNING KIT Quick Start Guide, this LEARNING KIT and/or accompanying hardware may or may not be subject to and compliant with the Code of Federal Regulations, Title 47, Part 15.

For LEARNING KITS annotated to comply with the Code of Federal Regulations, Title 47, Part 15. Operation is subject to the following two conditions: (1) This LEARNING KIT may not cause harmful interference, and (2) this LEARNING KIT must accept any interference received, including interference that may cause undesired operation. Changes or modifications not expressly approved by the party responsible for compliance could void the user's authority to operate the equipment. This LEARNING KIT as a Class A digital apparatus complies with Canadian ICES-003. Changes or modifications not expressly approved by the party responsible for compliance could void the users' authority to operate the equipment



Additional Terms, warnings, restrictions and disclaimers (2)

- For LEARNING KITS annotated as not subject to or compliant with the Code of Federal Regulations, Title 47, Part 15. This evaluation board is intended to be operated in a research and development environment for learning and educational purposes only. This evaluation board is not designed to fulfill requirements for CE compliance. It generates, uses, and can radiate radio frequency energy and has not been tested for compliance with the limits of computing devices pursuant to the Code of Federal Regulations, Title 47, Part 15, which are designed to provide reasonable protection against radio frequency interference. Operation of the equipment may cause interference with radio communications, in which case the user at its own expense will be required to take whatever measures may be required to correct this interference.
- **For Feasibility Evaluation Only.**
- The LEARNING KIT is intended exclusively for learning and educational purposes. Everyone using the LEARNING KIT must be aware of the dangers and application risks in connection with handling electrical mechanical components, systems and subsystems. It should not be used as an end product or as a part of an end product.
- **Your Sole Responsibility and Risk. You acknowledge, represent and agree that:**
 - a) You have unique awareness of the Federal, State and local regulatory requirements (including but not limited to Food and Drug Administration regulations, if applicable) which affect your products and which refer to your use (and/or the use of your employees, affiliates, contractors or designees) of the LEARNING KIT for evaluation, testing and other purposes.
 - b) You are unlimited and exclusively responsible for the safety of your LEARNING KIT and for the compliance with all relevant laws and other applicable regulatory requirements. Further, you have to assure the safety of any activities to be conducted by you and/or your employees, affiliates, contractors or designees, using the LEARNING KIT. You are also responsible to ensure that any interfaces (electronic and/or mechanical) between the LEARNING KIT and any human body are designed with suitable isolation and means to safely limit the accessible leakage currents to minimize the risk of electrical shock hazard.
 - c) Since the LEARNING KIT may not meet all applicable regulatory and safety compliance standards (such as UL, CSA, VDE, CE, RoHS and WEEE) which may normally be associated with similar completed products. You assume full responsibility to determine and/or assure compliance with any such standards and related certifications as may be applicable. You have to use reasonable safeguards to ensure that your use of the LEARNING KIT will not result in any property damage, injury or death, even if the LEARNING KIT should fail to perform as specified or expected.



Additional Terms, warnings, restrictions and disclaimers (3)

- **Certain Instructions.**
- It is important to handle this LEARNING KIT within WE's recommended specifications and environmental considerations as described in the Quick Start Guide. Surpassing the specified LEARNING KIT classifications (including but not limited to input and output voltage, current, power, and environmental ranges) may cause property damage, personal injury or death. If there are questions concerning these classifications please contact a WE external sales representative before connecting interface electronics including input power and intended loads. Any loads applied beyond the specified output range may result in unintended and/or inexact operation and/or possible lasting damage to the LEARNING KIT and/or interface electronics. Please consult the LEARNING KIT Quick Start Guide prior to connecting any load to the LEARNING KIT output. If there is uncertainty regarding the load specification, please contact a WE external sales representative. During normal operation, some circuit components may have case temperatures greater than 70°C as long as the input and output are maintained at a normal ambient operating temperature. These components include but are not limited to linear regulators, switching transistors, pass transistors, inductors and current sense resistors, which can be identified by using the LEARNING KIT schematic published in the LEARNING KIT Experiment Book.
- **Please be aware that the devices of the LEARNING KIT may be very warm in case of placing the measurement test setup close to the LEARNING KIT during normal procedure.**
- **Agreement to Defend, Indemnify and Hold Harmless.**
- You agree to defend, indemnify and hold WE, its licensors and their representatives harmless from and against any and all claims, damages, losses, expenses, costs and liabilities (collectively, „Claims“) arising out of or in connection with any use of the LEARNING KIT that is not in accordance with the terms of the agreement. This obligation shall apply whether Claims arise under law of tort or contract or any other legal theory, and even if the LEARNING KIT fails to perform as specified or expected.
- **Safety-Critical or Life-Critical Applications.**
- If you intend to evaluate the components for possible use in safety critical applications (such as life support) where a failure of the WE product would reasonably be expected to cause severe personal injury or death, such as devices which are classified as FDA Class III or similar classification, you have to specifically notify WE of such intent and enter into a separate Assurance and Indemnity Agreement.



Where to buy the board

You can get information on how to buy the board at www.we-online.com/pmlk  to take full advantages of the Learning Kit.

Experiment 1

The goal of this experiment is to investigate how the inductance of a power inductor changes depending on its physical characteristics and on the operating conditions, in a DC-DC switching regulator application.

The LM3475 regulator of the TI-PMLK BUCK-WE Board is used to perform the experimental tests.



Theory Background (1)

Figure 1.1 shows a simplified schematic of the LM3475 and TPS54160 buck regulators power stage, including current sensing, input filter and eFuses.

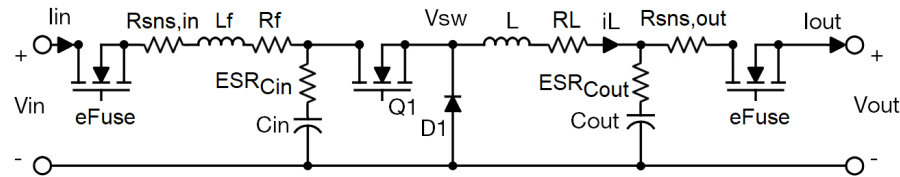


Figure 1.1. Buck converter simplified schematic

Figure 1.2 shows the theoretical voltage and current waveforms of the buck converter, obtained with **REDEXPERT** simulation under the following operating conditions:

- $V_{in} = 10 \text{ V}$
- $f_{sw} = 500 \text{ kHz}$
- $V_{out} = 3.3 \text{ V}$
- $I_{out} = 1 \text{ A}$
- $L = 10 \text{ }\mu\text{H}$

The constant input voltage V_{in} is converted into the square-wave voltage V_{sw} by the MOSFET Q_1 and the diode D_1 , which form a half-bridge, switching at frequency f_{sw} . The inductor is consequently subjected to the positive voltage (1):

$$(1) \quad V_{L+} = V_{in} - (R_{in} + R_{dson} + R_L) i_L - V_{out} \approx V_{in} - (R_{in} + R_{dson} + R_L) I_{out} - V_{out}$$

during the interval of time of duration $t_{on} = DT_{sw}$, and to the negative voltage (2):

$$(2) \quad V_{L-} = -V_{D1} - R_L i_L - V_{out} \approx -V_{D1} - R_L I_{out} - V_{out}$$

during the interval of time of duration $t_{off} = (1 - D) T_{sw}$.

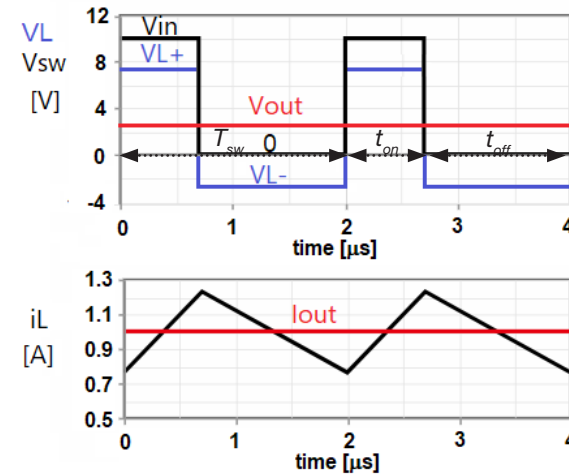


Figure 1.2. Voltage and current waveforms of buck converter

The parameters R_{in} , R_{dson} , V_{D1} , D and T_{sw} are defined as follows:

- (3) R_{in} = resistance of input eFuse and current sensing
- (4) R_{dson} = on-state resistance of the MOSFET Q_1
- (5) R_L = winding resistance of the inductor L
- (6) V_{D1} = forward voltage drop of the diode D_1
- (7) $D = t_{on} / T_{sw}$ = duty cycle of the MOSFET Q_1
- (8) $T_{sw} = 1 / f_{sw}$ = switching period



Theory Background (2)

In theory, the inductor current rises linearly during the interval of time of duration DT_{sw} , and falls linearly during the interval of time of duration $(1-D)T_{sw}$. The rise and fall slopes are determined by the value of the inductance L , and are given by (9) and (10):

$$(9) \quad \text{Rise Slope (RS)} = V_{L+} / L > 0$$

$$(10) \quad \text{Fall Slope (FS)} = V_{L-} / L < 0$$

Therefore, in steady-state operation the inductor current is expected to have a peak-peak ripple at switching frequency that can be calculated in two ways, as shown in equations (11.a) and (11.b):

$$(11.a) \quad \Delta i_{Lpp} = (V_{L+} / L) D T_{sw}$$

$$(11.b) \quad \Delta i_{Lpp} = - (V_{L-} / L) (1 - D) T_{sw}$$

Replacing (1) and (2) into (11.a) and (11.b), respectively, yields:

$$(12.a) \quad \Delta i_{Lpp} = [V_{in} - (R_{in} + R_{dson} + R_L) I_{out} - V_{out}] D / (f_{sw} L)$$

$$(12.b) \quad \Delta i_{Lpp} = [V_{D1} + R_L I_{out} + V_{out}] (1 - D) / (f_{sw} L)$$

From the equality of the peak-peak ripple current expressions Δi_{Lpp} given by (12.a) and (12.b), the value of the duty cycle D can be determined, resulting in equation (13):

$$(13) \quad D \approx (V_{out} + V_{D1} + R_L I_{out}) / [V_{in} + V_{D1} - (R_{in} + R_{dson}) I_{out}]$$



Return to previous page by:

Windows: +

Mac: +

Putting the value of the duty cycle D given by (12) into (11) provides the value of the peak-peak ripple current Δi_{Lpp} .

The inductance L is influenced by the operating conditions. Indeed, the inductance of inductors is not a constant parameter. Its value is mainly influenced by the DC current and by the ambient temperature.

Figure 1.3 shows the **REDEXPERT** plots of the inductance vs the DC current at 25 °C of the three inductors L1, L2 and L3 available in the LM3475 buck regulator of the TI-PMLK BUCK-WE Board. Table 1.1 shows the nominal value L_{nom} and the value L_{out} at 1 A DC current of the inductance of the three inductors. The DC component of the current flowing through the output inductor in a buck converter is the load current I_{out} . The decay of the inductance when the DC current increases is caused by the saturation of the magnetic core, which is influenced by the core material (see **LM3475 Regulator: Output Inductors**).

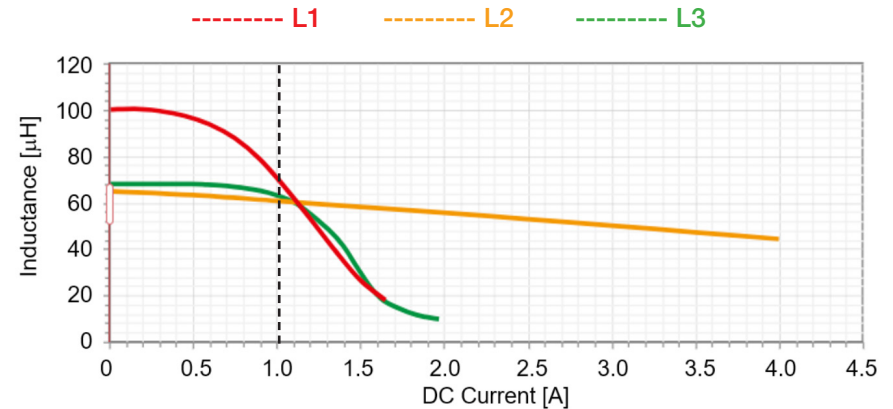


Figure 1.3. Inductance vs DC current



Theory Background (3)

Assuming that $V_{in} = 10\text{ V}$, $f_{sw} = 500\text{ kHz}$, $V_{out} = 3.3\text{ V}$, $I_{out} = 1\text{ A}$, $R_{dson} = 50\text{ m}\Omega$ and $V_{D1} = 0.4\text{ V}$, from (12.a) we get the values of duty cycle and peak-peak current ripple summarized in Table 1.1.

Table 1.1. Inductors parameters and resulting duty cycle and peak-peak current ripple in the buck converter

	L_{nom} [μH]	R_L [$\text{m}\Omega$]	$L_{out}@1\text{A}$ [μH]	$D@L_{nom}$	$\Delta i_{Lpp}@L_{nom}$ [mA]	$D@L_{out}$	$\Delta i_{Lpp}@L_{out}$ [mA]
L1	100	270	70	0.380	69	0.380	48
L2	68	386	60	0.391	82	0.391	72
L3	68	239	63	0.377	77	0.377	71

The nominal amplitude of peak-peak inductor ripple current for the three inductors L1, L2 and L3 can be quickly obtained by means of the **REDEXPERT** software. Figure 1.4, 1.5 and 1.6 show the results of inductor L1, L2 and L3 analysis.



Return to previous page by:

Windows: Alt + ← Mac: cmd + ←

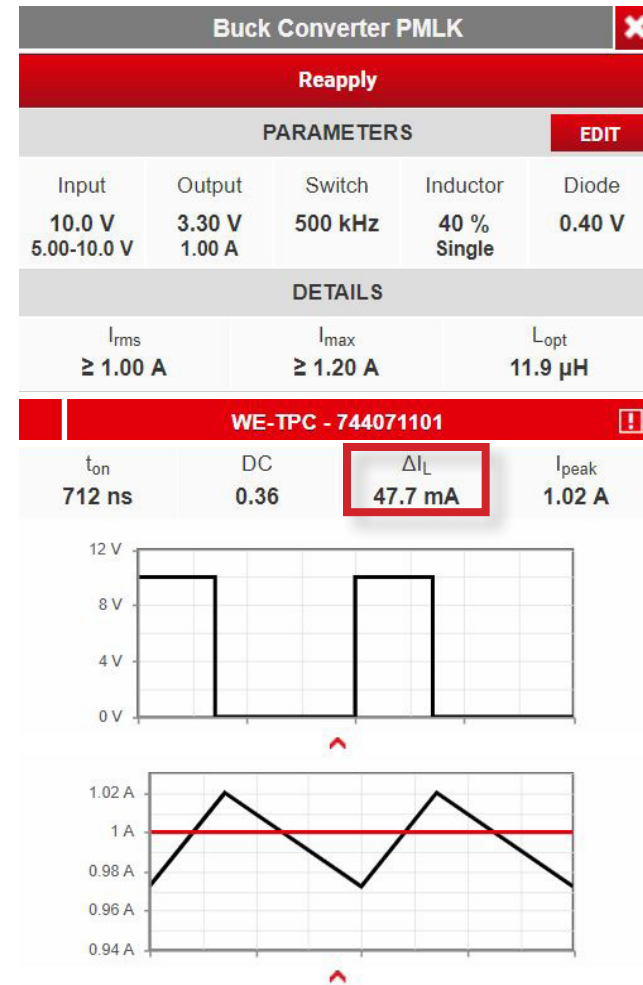


Figure 1.4. **REDEXPERT** analysis of inductor L1



Theory Background (4)

Return to previous page by:
 Windows: + Mac: +

Buck Converter PMLK				
Reapply				
PARAMETERS				EDIT
Input	Output	Switch	Inductor	Diode
10.0 V 5.00-10.0 V	3.30 V 1.00 A	500 kHz	40 % Single	0.40 V
DETAILS				
I_{rms}	I_{max}	L_{opt}		
≥ 1.00 A	≥ 1.20 A	11.9 μ H		
WE-LHMI - 74437349680				
t_{on}	DC	ΔI_L	I_{peak}	
712 ns	0.36	70.2 mA	1.04 A	

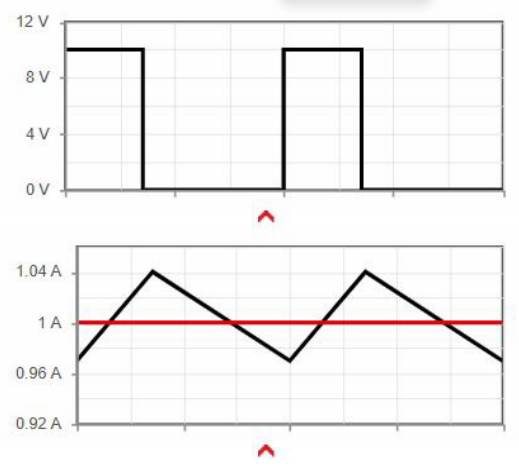


Figure 1.5. REDEXPERT analysis of inductor L2

Buck Converter PMLK				
Reapply				
PARAMETERS				EDIT
Input	Output	Switch	Inductor	Diode
10.0 V 5.00-10.0 V	3.30 V 1.00 A	500 kHz	40 % Single	0.40 V
DETAILS				
I_{rms}	I_{max}	L_{opt}		
≥ 1.00 A	≥ 1.20 A	11.9 μ H		
WE-PD - 7447779168				
t_{on}	DC	ΔI_L	I_{peak}	
712 ns	0.36	70.2 mA	1.04 A	

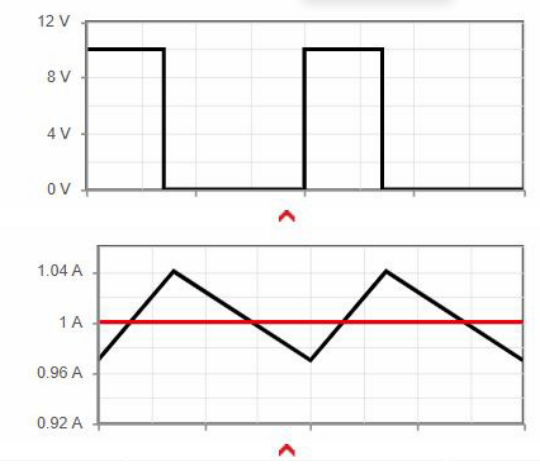


Figure 1.6. REDEXPERT analysis of inductor L3



Theory Background (5)



Return to previous page by:

Windows:



Mac:



Starting from equations (12.a) and (12.b), we have:

$$(14.a) \quad L = [V_{in} - (R_{in} + R_{dson} + R_L) I_{out} - V_{out}] D / (f_{sw} \Delta i_{Lpp})$$

$$(14.b) \quad L = [V_{D1} + R_L I_{out} + V_{out}] (1 - D) / (f_{sw} \Delta i_{Lpp})$$

Equations (14.a) and (14.b) allow to evaluate the inductance L using the measured values of the input voltage V_{in} , the output voltage V_{out} , the output current I_{out} , the duty cycle D , the switching frequency f_{sw} , and the amplitude of peak-peak inductor ripple current Δi_{Lpp} .

Given the operating parameters V_{in} , V_{out} , D and f_{sw} , if the physical parameters R_{in} , R_{dson} , R_L , and V_{D1} are known exactly, the results provided by (14.a) and (14.b) are coincident.

The parameters R_{in} , R_{dson} , R_L , and V_{D1} are characterized by different levels of accuracy, depending on the nature of devices and on the specific application.

The source resistance R_{in} is often not specified. If the source is a laboratory power supply, its value is very small and can be neglected. However, the resistances of connections, protections, current sensors and filters connected between the source and the input of the buck converter contribute to form the resistance R_{in} , which in general is not just the source resistance in the strict sense, but rather the equivalent resistance between the source and the input of the buck converter.

The MOSFET on-state resistance R_{dson} is subjected to a large uncertainty, as it is influenced by the gate driver voltage and by the temperature. Data and graphs of R_{dson} are provided in the MOSFETs datasheets, under different operating conditions.

The inductor resistance R_L , also called DC resistance and labeled as R_{DC} , is provided in the datasheets. Its value is quite reliable.

The diode forward voltage drop V_{D1} is subjected to a large uncertainty, as it is influenced by the forward current and by the temperature. It can be easily obtained by measuring the low value of the switching node voltage during the buck converter operation.

In conclusion, R_{in} and R_{dson} are the parameters affected by the highest uncertainty.

Defining $R_x = R_{in} + R_{ds}$ allows to rewrite equation (12.a) and (12.b) as follows:

$$(15.a) \quad \Delta i_{Lpp} = [V_{in} - (R_x + R_L) I_{out} - V_{out}] D / (f_{sw} L)$$

$$(15.b) \quad \Delta i_{Lpp} = [V_{D1} + R_L I_{out} + V_{out}] (1 - D) / (f_{sw} L)$$

Solving equations (15.a) and (15.b) with respect to R_x and L_{out} yields:

$$(16.a) \quad R_x = [D V_{in} + (1 - D) V_{D1} + R_L I_{out} + V_{out}] / (D I_{out})$$

$$(16.b) \quad L = [V_{D1} + R_L I_{out} + V_{out}] (1 - D) / (f_{sw} \Delta i_{Lpp})$$

Equation (16.b) is equal to equation (14.b). Therefore, the inductance can be determined by means of equation (14.b), using the measured values of V_{D1} , I_{out} , V_{out} , D , f_{sw} and Δi_{Lpp} and the datasheet value of R_L .

If reliable values of R_{in} and R_{dson} are available, then the inductance can be determined by means of equation (14.a), using the measured values of V_{in} , I_{out} , V_{out} , D , f_{sw} , and Δi_{Lpp} and the datasheet values of R_L , R_{dson} , and R_{in} .

In the next section, the equations discussed above will be used to evaluate the inductance of the three inductors L1, L2 and L3 of the LM3475 regulator, based on experimental measurements.



Case Study

The goal of this experiment is to evaluate the inductance of the inductors L1, L2 and L3, by using the results of experimental measurements performed on the LM3475 regulator, under different operating conditions.

In particular, equation (14.a) provided in the **Theory and Background** section will be used to evaluate the inductance L , using the measured values of the input voltage V_{in} , the output voltage V_{out} , the output current I_{out} , the on-time t_{on} , the switching period T_{sw} , and the amplitude of peak-peak inductor ripple current Δi_{Lpp} .

The value of R_{in} is determined as the sum of the internal resistance of the eFuse U6, the secondary coil output resistance R36 of current sense transformer T3 reflected to the primary coil, and the resistance of input filter inductors L7 and L8.

The values of R_{dson} and V_{D1} are available in the datasheets of the MOSFET Q1 (Vishay Siliconix SI2343CDS-T1-GE3 30 V / 5.9 A P-channel MOSFET) and diode D1 (Diodes Incorporated B220A-13-F 20 V / 2 A Schottky diode). The datasheet value of R_L of the three inductors L1, L2 and L3 are used.

The following test points of the LM3475 regulator will be used:

- **TP₂**, to measure the input voltage, V_{in}
- **TP₇**, to measure the ambient temperature, T_a
- **TP₉**, to measure the DC inductor current, I_{out}
- **TP₁₃**, to measure the surface temperature of inductor L1, T_s
- **TP₂₇**, to measure the output voltage, V_{out}
- **TP₃₈**, to measure the switching period, T_{sw} , and the duty cycle, D
- **TP₃₉**, to measure the peak-peak amplitude of inductor current ripple, Δi_{Lpp}

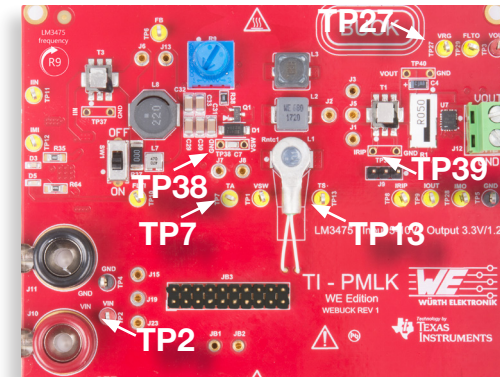


Figure 1.5. LM3475 regulator test points used to analyze inductors L1, L2 and L3



Experiment set-up: configuration

The instruments needed for this experiment are: a DC POWER SUPPLY, a MULTIMETER, an OSCILLOSCOPE and a DC ELECTRONIC LOAD. Figure 1.6 shows the instruments connections. Follow the instructions provided in next page to set-up the **connections**.

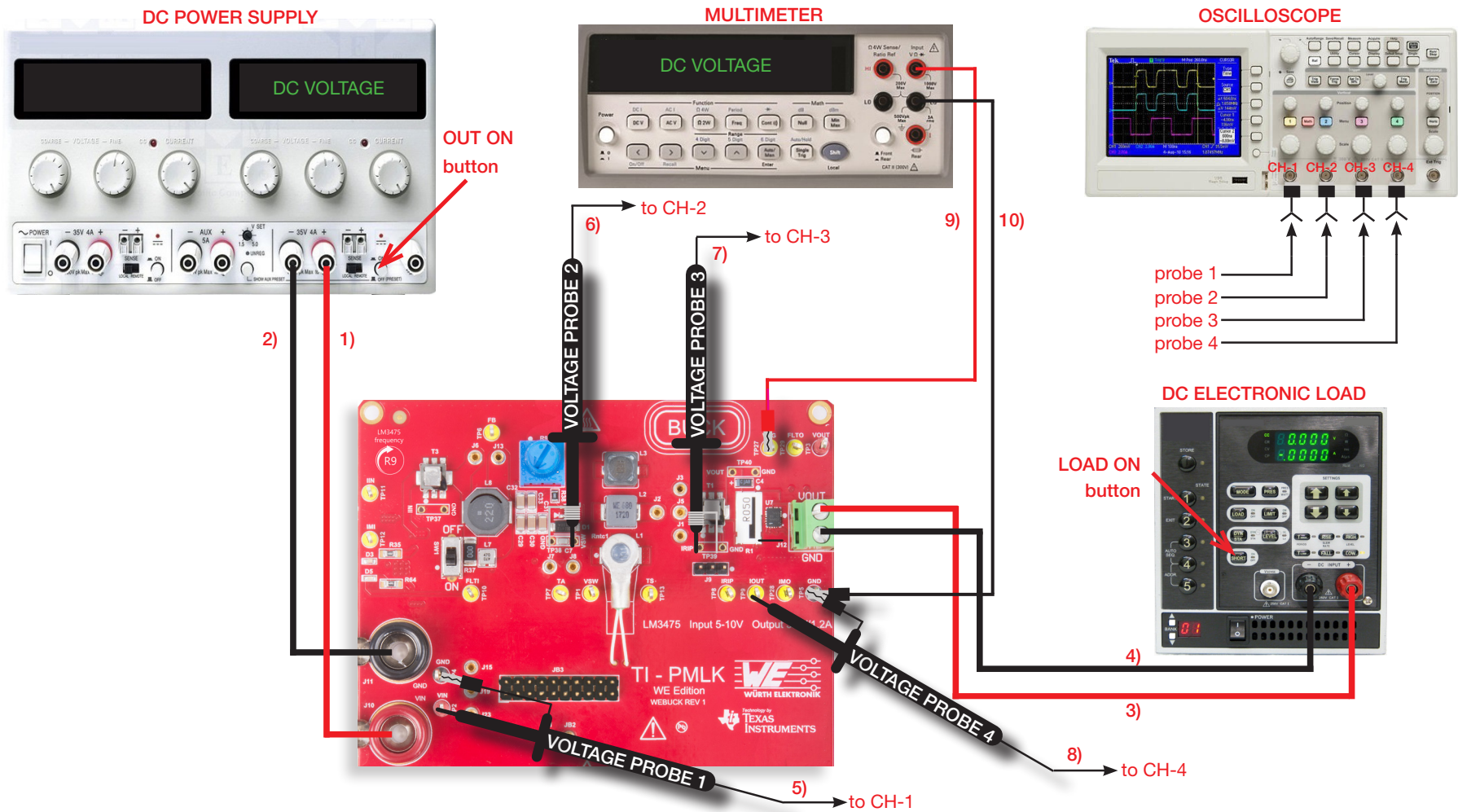


Figure 1.6. Experiment set-up



Experiment set-up: instructions

With all the instruments off, make the following **connections** (see Figure 1.7):

1. Connect the POSITIVE (RED) OUTPUT of the DC POWER SUPPLY to the POSITIVE INPUT (VIN) banana connector J_{10} of the TI-PMLK BUCK-WE board.
2. Connect the NEGATIVE (BLACK) OUTPUT of the DC POWER SUPPLY to the GROUND (GND) banana connector J_{11} of the TI-PMLK BUCK-WE board.
3. Connect the POSITIVE OUTPUT (VOUT) of the J_{12} screw terminal of LM3475 regulator to the POSITIVE (RED) INPUT of the ELECTRONIC LOAD
4. Connect the NEGATIVE (BLACK) INPUT of the ELECTRONIC LOAD to the GROUND (GND) of the J_{12} screw terminal of LM3475 regulator
5. Connect a standard voltage probe to channel 1 of the OSCILLOSCOPE, hang its tip to the test point TP_2 and its ground clamp to test point TP_4
6. Connect a voltage probe with ground spring to channel 2 of the OSCILLOSCOPE, insert its positive tip into the hole of test point TP_{38} labeled "VSW" and its ground spring tip into the hole of test point TP_{38} labeled "GND". [WARNING: DO NOT INVERT THE POSITIVE AND GROUND CONNECTIONS OF THE VOLTAGE PROBE]
7. Connect a voltage probe with ground spring to channel 3 of the OSCILLOSCOPE, insert its positive tip into the hole of test point TP_{39} labeled "IRIP" and its ground spring tip into the hole of test point TP_{39} labeled "GND". [WARNING: DO NOT INVERT THE POSITIVE AND GROUND CONNECTIONS OF THE VOLTAGE PROBE]
8. Connect a standard voltage probe to channel 4 of the OSCILLOSCOPE, hang its tip to the test point TP_9 and its ground clamp to test point TP_5
9. Connect the POSITIVE (RED) INPUT of the MULTIMETER to the test point TP_{27}
10. Connect the NEGATIVE (BLACK) INPUT of the MULTIMETER to test point TP_5



Test#1: instructions (1)

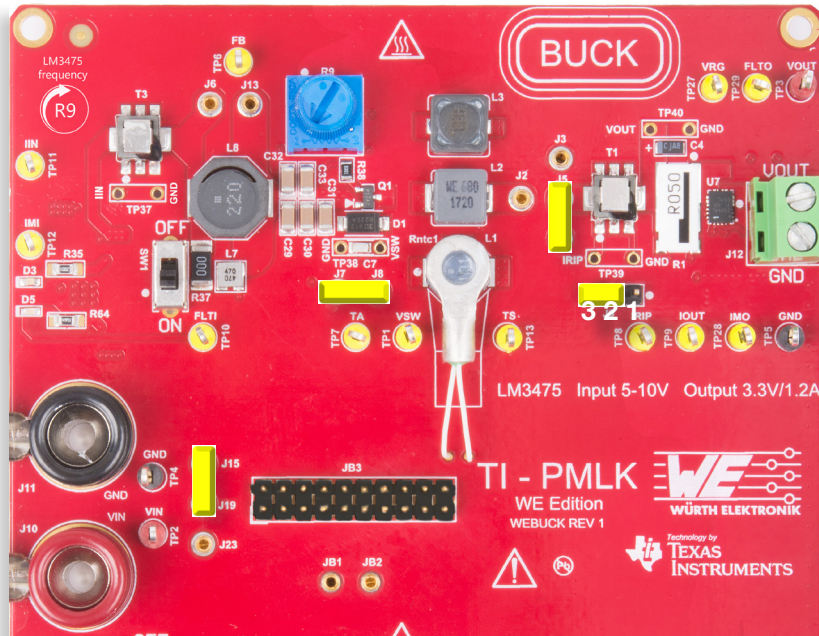


Figure 1.7. LM3475 jumpers set-up for Test#1

Initial set-up (see Figure 1.7, jumpers not mentioned are open):

- short J_{15} - J_{19} , LM3475 regulator connected to power input
- short J_1 - J_5 , inductor L_1 connected
- short J_9 on 2-3, separate AC and DC inductor currents
- turn R_9 right until it stops

Test Procedure:

1. Switch ON the SCOPE, set all channels in DC $1\text{ M}\Omega$ coupling mode with 20 MHz BW limit, the time base to 500 ns/div, the trigger on CH-2 rising edge, the vertical scale to 5 V/div on CH-1 and CH-2, to 20 mV/div on CH-3 and to 500 mV/div on CH-4, and CH-3 on 8 sweeps average acquisition mode.
2. Switch ON the MULTIMETER and set DC Voltage measurement.
3. Switch ON the POWER SUPPLY, set the "OUT ON" button OFF, output voltage to 10 V, and CURRENT LIMIT to 1.5 A.
4. Switch ON the ELECTRONIC LOAD, set the "OUT ON" button OFF, CONSTANT CURRENT MODE, and input current to 0.0 A.
5. Switch the POWER SUPPLY "OUT ON" button ON and the ELECTRONIC LOAD "LOAD ON" button ON. Under these conditions, you should see about 3.36 V DC output voltage V_{out} on the MULTIMETER, 10.0 V input voltage V_{in} on the SCOPE CH-1.
6. Rise slowly the ELECTRONIC LOAD current until you read 1.0 V on the SCOPE CH-4. Adjust the DC POWER SUPPLY finr regulation knob, if needed, until you get $V_{in} = 10.0\text{ V}$.
7. Watch the switching frequency f_{sw} on the SCOPE CH-2 (switching node voltage V_{sw}) while turning the knob of trimmer R9 until you get $f_{sw} = 500\text{ kHz}$. Under these conditions, you should see a triangle voltage on the SCOPE CH-3 with about 80mV peak-peak amplitude. As the current sensor's gain is 1 A/V, the voltage reading provides directly the current (set 4 or 8 sweeps average acquisition mode on SCOPE CH-3, to get a less noisy waveform).

[WARNING. If the measurements do not look as described above, switch OFF the "OUT ON" button of the ELECTRONIC LOAD and POWER SUPPLY, check the connections, the jumpers setup, the instruments setup and repeat the procedure]



Test#1: instructions (2)

8. Measure the average input voltage V_{in} on the SCOPE CH-1.
9. Measure the duty cycle D of the switching node voltage V_{sw} on the SCOPE CH-2.

[Note: normally, oscilloscopes have frequency and duty cycle measurement features for square waves like the switching node voltage V_{sw} ; in case these features are not available in your oscilloscope, use horizontal cursors placed on the rising and falling edges of switching node voltage V_{sw} to measure the period T_{sw} and the on-time t_{on} shown in Figure 1.8 to get $D = t_{on}/T_{sw}$; the switching period T_{sw} and the on-time t_{on} can be measured on the inductor ripple current waveform too, by means of horizontal cursors on the peak and valley corners of the triangle waveform]

10. Measure the amplitude of the peak-peak inductor ripple current Δi_{Lpp} on the SCOPE CH-3
11. Measure the average output current I_{out} on the SCOPE CH-4
12. Record the measured values in Table 1.2.
13. Reduce the current of the ELECTRONIC LOAD to 0.0 A, switch its “LOAD ON” button OFF, and switch the “OUT ON” button of the POWER SUPPLY OFF.
14. Short J_2 - J_5 to connect inductor L2 and repeat steps 5 to 13.
15. Short J_3 - J_5 to connect inductor L3 and repeat steps 5 to 13.
16. Switch OFF the ELECTRONIC LOAD, the POWER SUPPLY, the MULTIMETER, and the SCOPE.

Figures 1.8 and 1.9 show the expected switching node voltage and the inductor ripple current with inductor L1, at 0.2 A and 1.2 A load current. Figure 1.9 highlights the forward voltage drop V_{D1} of the diode D1 during the off time t_{OFF} .

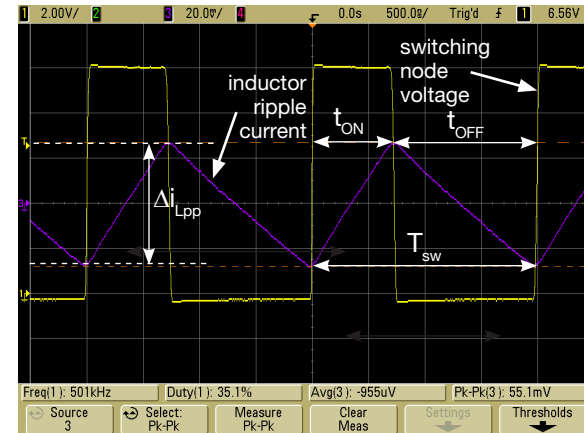


Figure 1.8. Measured waveforms in Test#1 with inductor L1 at 0.2 A load current

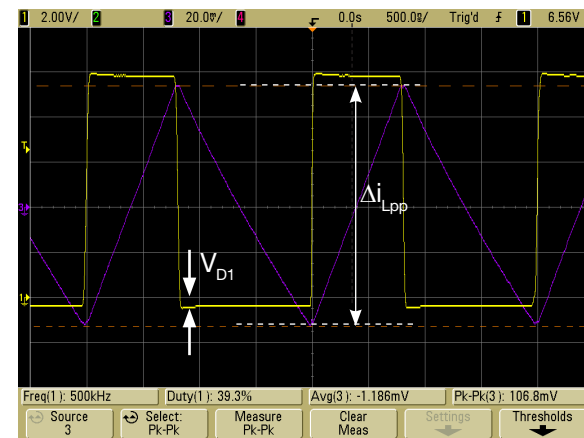


Figure 1.9. Measured waveforms in Test#1 with inductor L1 at 1.2 A load current



Test#1: measure and calculate

Use the measured values of the input voltage V_{in} , the output voltage V_{out} , the output current I_{out} , the duty cycle D , and the amplitude of peak-peak inductor ripple current Δi_{Lpp} collected in Table 1 to determine the inductance of inductors L1, L2 and L3 in the given operating conditions, using equation (14.a) discussed in the *Theory and Background* section. Analyze the results and answer the questions.

COMPONENTS DATA AND OPERATING PARAMETERS

Input eFuse U6

$$R_{fuse} = 150 \text{ m}\Omega$$

Input current sensing

$$R_{sns} = 20 \text{ m}\Omega$$

Input Filter Inductors

$$R_{L7}/R_{L8} = R_{filter} = 55 \text{ m}\Omega$$

MOSFET Q1

$$R_{dson} = 50 \text{ m}\Omega$$

Diode D1

$$V_{D1} = 400 \text{ mV@1.0 A}$$

Table 1.2. Evaluation of the inductance of inductors L1, L2 and L3 based on experimental measurements

inductor	V_{in} [V]	V_{out} [V]	I_{out} [A]	D	Δi_{Lpp} [mA]	$L@1A$ [μH]	L_{nom} [μH]	R_L [m Ω]	$L@1A/L_{nom}$ [%]
L1									
L2									
L3									

Answer:

- Which inductor is determining the peak-peak ripple current with biggest amplitude? L1 L2 L3
- Which inductor is characterized by the biggest nominal inductance? L1 L2 L3
- Which inductor is characterized by the smallest inductance at 1 A? L1 L2 L3
- Which inductor is characterized by the smallest ratio $L@1A/L_{nom}$? L1 L2 L3
- Does the inductor with biggest nominal value provide the smallest peak-peak ripple current? yes no

Please comment your answers: _____



Test#2: instructions (1)

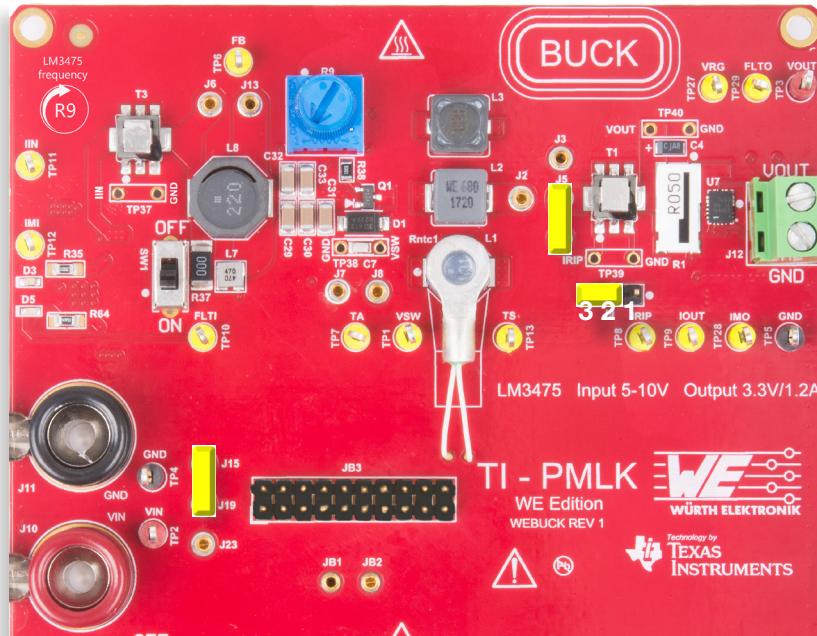


Figure 1.10. LM3475 jumpers set-up for Test#2

Initial set-up (see Figure 1.10, jumpers not mentioned are open):

- short J_{15} - J_{19} ; LM3475 regulator connected to power input
- short J_1 - J_5 ; inductor L1 connected
- short J_9 on 2-3, separate AC and DC inductor currents
- turn R_9 right until it stops

Test Procedure:

1. Switch ON the SCOPE, set all channels in DC 1 M Ω coupling mode with 20 MHz BW limit, the time base to 500 ns/div, the trigger on CH-2 rising edge, the vertical scale to 5 V/div on CH-1 and CH-2, to 20 mV/div on CH-3 and to 500 mV/div on CH-4.
2. Switch ON the MULTIMETER and set DC Voltage measurement.
3. Switch ON the POWER SUPPLY, set the "OUT ON" button OFF, set the voltage to 10 V, and set the CURRENT LIMIT to 1.5 A.
4. Switch ON the ELECTRONIC LOAD, set the "OUT ON" button OFF, set CONSTANT CURRENT MODE
5. Set the ELECTRONIC LOAD current to 0.0 A.
6. Switch the POWER SUPPLY "OUT ON" button ON and the ELECTRONIC LOAD "LOAD ON" button ON. You should see about 3.36 V DC output voltage V_{out} on the MULTIMETER, 10.0 V input voltage V_{in} on the SCOPE CH-1.
7. Rise slowly the ELECTRONIC LOAD DC current until you read 0.2 V on the SCOPE CH-4. Adjust the POWER SUPPLY fine regulation knob, if needed, until you get $V_{in} = 10.0$ V.
8. Watch the switching frequency f_{sw} on the SCOPE CH-2 (switching node voltage V_{sw}) while turn the knob of trimmer R9 until you get $f_{sw} = 500$ kHz. Under these conditions, you should see a triangle voltage on SCOPE CH-3 with about 55 mV peak-peak amplitude. As the current sensors gain is 1 A/V, the voltage reading provides directly the current (set 4 or 8 sweeps average acquisition mode on SCOPE CH-3, to get a less noisy waveform). **[WARNING. If the measurements do not look as described above, switch OFF the "OUT ON" button of the ELECTRONIC LOAD and POWER SUPPLY, check the connections, the jumpers setup, the instruments setup and repeat the procedure]**



Test#2: instructions (2)

9. Measure the the duty cycle D of the switching node voltage V_{sw} on the SCOPE CH-2, the amplitude of the peak-peak inductor ripple current Δi_{Lpp} on the SCOPE CH-3, the average output current I_{out} on the SCOPE CH-4, and record the measured values in Table 1.3.
10. Connect the MULTIMETER to test point TP_7 , read the voltage in millivolt, convert the voltage into Celsius degrees by using **Equation (2)** on Page 21, and record the resulting value of ambient temperature T_a in Table 1.3.
11. Connect the MULTIMETER to test point TP_{13} , read the voltage in volt with three decimal digits, convert the voltage into Celsius degrees by means of **Table III** on Page 22, and record resulting value of inductor surface temperature T_s in Table 1.3.
12. Connect the MULTIMETER to the test point TP_{27}
13. Repeat steps 6 to 11, by increasing the load current of 400 mA steps up to 1.4 A.
14. Short J_7 - J_8 to connect the heating resistor of inductor L1, repeat steps 6 to 13, record the measured value in Table 1.4 and open J_7 - J_8 .
15. Switch OFF the “LOAD ON” button of the ELECTRONIC LOAD and the “OUT ON” button of the POWER SUPPLY.
16. Short J_2 - J_5 to connect inductor L2, repeat steps 5 to 15 (skip steps 10, 11, 12 and 14), and record the measured values in Table 1.5.
17. Short J_3 - J_5 to connect inductor L3, repeat steps 5 to 15 (skip steps 10, 11, 12 and 14), and record the measured values in Table 1.6.
18. Switch OFF the ELECTRONIC LOAD, the POWER SUPPLY, the MULTIMETER, and the SCOPE.

Figures 1.11 and 1.12 show examples of the expected waveforms. The violet trace of Figure 1.12, highlights the effect of a higher operating temperature on the inductance of the inductor L1, causing a larger peak-peak ripple current amplitude compared to Figure 1.11.

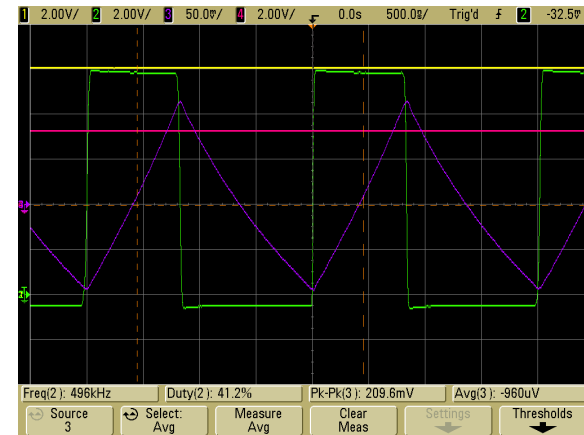


Figure 1.11. Measured waveforms in Test#2 at 1.4A with inductor L1 not heated:
■ input voltage, ■ switching node voltage, ■ output voltage, ■ ripple current

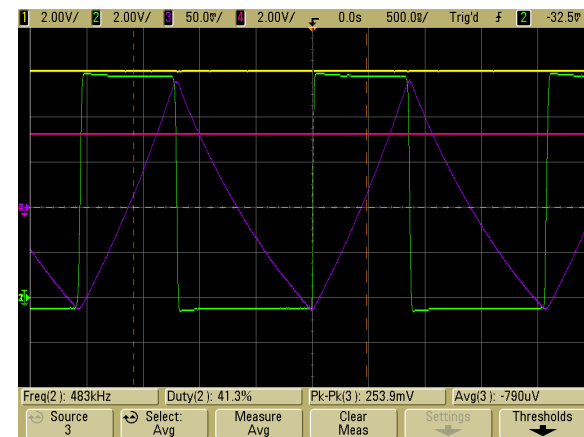


Figure 1.12. Measured waveforms in Test#2 at 1.4A with inductor L1 heated:
■ input voltage, ■ switching node voltage, ■ output voltage, ■ ripple current



Test#2: measure and calculate (1)

Use the measured values of the input voltage V_{in} , the output voltage V_{out} , the duty cycle D , and the amplitude of peak-peak inductor ripple current Δi_{Lpp} collected in Tables 1.3, 1.4, 1.5 and 1.6 to determine the inductance of the inductors L1, L2 and L3 in the given operating conditions, using equation (14.a) discussed in the *Theory and Background* section. Analyze the results and answer the questions.

COMPONENTS DATA AND OPERATING PARAMETERS

Input voltage

$$V_{in} = 10.0 \text{ V}$$

Switching Freq.

$$f_{sw} = 500 \text{ kHz}$$

Switching Period

$$T_{sw} = 2 \text{ } \mu\text{s}$$

Nominal Ind.

$$L1_{nom} = 100 \text{ } \mu\text{H}$$

$$L2_{nom} = 68 \text{ } \mu\text{H}$$

$$L3_{nom} = 68 \text{ } \mu\text{H}$$

Inductor Resist.

$$R_{L1} = 270 \text{ m}\Omega \text{ (Typ.)}$$

$$R_{L2} = 386 \text{ m}\Omega \text{ (Typ.)}$$

$$R_{L3} = 239 \text{ m}\Omega \text{ (Typ.)}$$

Other Resist.

$$R_{fuse} = 150 \text{ m}\Omega$$

$$R_{sns} = 20 \text{ m}\Omega$$

$$R_{filter} = 55 \text{ m}\Omega$$

MOSFET Resist.

$$R_{dson} = 50 \text{ m}\Omega$$

Diode D1

$$V_{D1} = 0.4 \text{ V@1.0 A}$$

Table 1.3. Evaluation of the inductance of inductor L1 based on experimental measurements with J7-J8 open

I_{out} [mA]	200	600	1000	1400
V_{out} [V]				
D				
Δi_{Lpp} [mA]				
$L1$ [μH]				
$L1/L1_{nom}$ [%]				
T_a [$^{\circ}\text{C}$]				
T_s [$^{\circ}\text{C}$]				

Table 1.4. Evaluation of the inductance of inductor L1 based on experimental measurements with J7-J8 shorted

I_{out} [mA]	200	600	1000	1400
V_{out} [V]				
D				
Δi_{Lpp} [mA]				
$L1$ [μH]				
$L1/L1_{nom}$ [%]				
T_a [$^{\circ}\text{C}$]				
T_s [$^{\circ}\text{C}$]				



Test#2: measure and calculate (2)

COMPONENTS DATA AND OPERATING PARAMETERS

Input voltage

$$V_{in} = 10.0 \text{ V}$$

Switching Freq.

$$f_{sw} = 500 \text{ kHz}$$

Switching Period

$$T_{sw} = 2 \text{ } \mu\text{s}$$

Nominal Ind.

$$L1_{nom} = 100 \text{ } \mu\text{H}$$

$$L2_{nom} = 68 \text{ } \mu\text{H}$$

$$L3_{nom} = 68 \text{ } \mu\text{H}$$

Inductor Resist.

$$R_{L1} = 270 \text{ m}\Omega \text{ (Typ.)}$$

$$R_{L2} = 386 \text{ m}\Omega \text{ (Typ.)}$$

$$R_{L3} = 239 \text{ m}\Omega \text{ (Typ.)}$$

Other Resist.

$$R_{fuse} = 150 \text{ m}\Omega$$

$$R_{sns} = 20 \text{ m}\Omega$$

$$R_{filter} = 55 \text{ m}\Omega$$

MOSFET Resist.

$$R_{ds(on)} = 50 \text{ m}\Omega$$

Diode D1

$$V_{D1} = 0.4 \text{ V@1.0 A}$$

Table 1.5. Evaluation of the inductance of inductor L2 based on experimental measurements

I_{out} [mA]	200	600	1000	1400
V_{out} [V]				
D				
Δi_{Lpp} [mA]				
$L2$ [μH]				
$L2/L2_{nom}$ [%]				

Table 1.6. Evaluation of the inductance of inductor L3 based on experimental measurements

I_{out} [mA]	200	600	1000	1400
V_{out} [V]				
D				
Δi_{Lpp} [mA]				
$L3$ [μH]				
$L3/L3_{nom}$ [%]				



Observe and Answer

1 What is the trend of the inductance as the load current increases? it increases it decreases other: _____

Please comment your answer: _____

2 Are the variations of the inductance uniform as the load current increases? yes no

Please comment your answer: _____

3 What is the trend of the peak-peak ripple as the load current increases? it increases it decreases other: _____

Please comment your answer: _____

4 Are the peak-peak ripple variations uniform as the load current increases? yes no

Please comment your answer: _____

5 Which inductor does exhibit the largest inductance decrease as the current increases ? L1 L2 L3

Please comment your answer: _____

6 Which inductor does exhibit the largest peak-peak ripple increase as the current increases ? L1 L2 L3

Please comment your answer: _____

7 Which inductor does determine the smallest peak-peak ripple at 0.2A load current ? L1 L2 L3

Please comment your answer: _____

8 Which inductor does determine the smallest peak-peak ripple at 1.4A load current ? L1 L2 L3

Please comment your answer: _____

9 What is the effect of a higher temperature on the inductance and peak-peak ripple current of the inductor L1? _____



Discussion (1)

Equations (12.a) and (12.b) provided in the **Theory Background** section highlights that the amplitude Δi_{Lpp} of the peak-peak inductor ripple current is influenced by several factors. Given the regulated output voltage V_{out} , the major influence factors are the inductance of the inductor L , the input voltage V_{in} , and switching frequency f_{sw} . In particular, the ripple increases when a) the inductance decreases, b) the input voltage increases and c) the switching frequency decreases. The input voltage and the output voltage also determine the value of the duty cycle D , as shown in equation (13).

The output current I_{out} is an influence factor. In theory, the inductor current ripple should be insensitive to the load current. The impact of the load current on the duty cycle and on the amplitude of the peak-peak inductor current ripple depends on the voltage drops it causes in the parasitic resistances of the power components, current sensing and protections placed along the power train from the source to the load. In the very high efficiency regulators, these resistances are very small, so that the output current is not expected to influence considerably the amplitude of the duty cycle and of the amplitude of the peak-peak inductor current ripple. However, when the load current increases, the duty cycle slightly increases to compensate the higher ohmic losses. Consequently, a change of the inductor ripple current can be observed according to equations (12.a) and (12.b). The forward voltage drop V_{D1} of the diode D1 also influences the losses, the duty cycle, and then the inductor current ripple. Schottky diodes are used to reduce these effects.

The **Theory Background** discussion and the results of measurements highlight that inductors are subjected to different rates of de-rating of the inductance as the DC current increases, depending on the magnetic core characteristics. Comparing the behavior of the ferrite core inductors L1 and L3 to the powdered iron core inductor L2 highlights that the ferrite inductors involve a higher rate of increase of the peak-peak inductor ripple current as the load current increases, compared to powdered iron inductors. Inductors with ferrite and powdered iron cores are primarily used in switch-mode power supplies. A large variety of parts is available today, allowing different trade-off among inductance, size, power losses and temperature rise (**Experiment 2** investigates inductors losses and temperature issues).

Given the input voltage V_{in} , the output voltage V_{out} , the maximum load current $I_{out,max}$, the switching frequency f_{sw} and the peak-peak inductor ripple current Δi_{Lpp} specifications of a switching power supply, the inductors is normally selected so that its worst case peak current $I_{out,max} + \Delta i_{Lpp} / 2$ does not exceed the value of current involving 10% (or 20%) of inductance de-rating with respect to the nominal inductance value. This rule is based on the intention to avoid excessive losses and temperature rise deriving from big peak-peak inductor ripple current because of inductance de-rating caused by saturation. In this regard, powdered iron core inductors allow a easier control of peak-peak inductor ripple current, as they exhibit a much smoother rate of decay of the inductance as DC current increases, compared to ferrite core inductors.

This experiment shows that, given the input voltage V_{in} , the output voltage V_{out} , the load current I_{out} , and the switching frequency f_{sw} , a ferrite core inductor of higher nominal inductance (e.g. L1) can operate with a de-rate of inductance of about 50% with respect to its nominal value, while providing values of inductance and peak-peak current ripple equivalent to those ones of an inductor with lower nominal value (e.g. L3) operating with about 10% de-rate of inductance with respect to its nominal value. Recent studies have proved that this concept can be exploited to reduce size and weight of switching power supplies, by selecting smaller inductors with higher nominal inductance to work in moderate saturation, while complying with ripple, losses and temperature rise specifications.

Finally, the experiment shows that an increase of temperature results in a decrease of the DC current threshold determining the saturation of ferrite inductor L1.



Discussion (2)

Figure 1.13 shows the inductance of inductors L1, L2 and L3, calculated by means of the peak-peak ripple current measurements.

Figure 1.14 shows the ambient temperature and the surface temperature of inductor L1, measured by means of the temperature sensors on board.

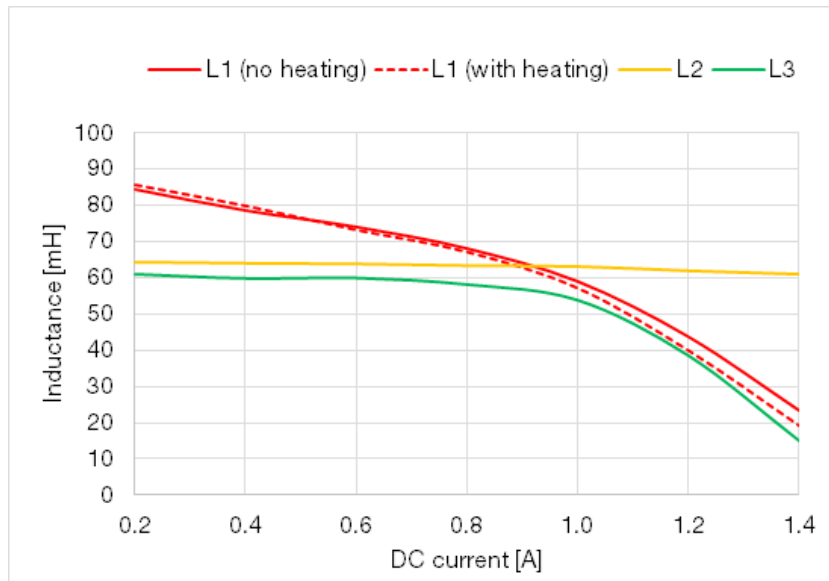


Figure 1.13. Inductance vs DC current
(calculated by means of the peak-peak ripple current measurements)

The plots of Figure 1.13 look similar to the [REDEXPERT](#)  curves shown in Figure 9. The small differences are caused by the operating temperature of the inductors. In particular, the solid and dashed red curves in Figure 1.13 highlight the impact of an increase of the temperature on the inductance of the inductor L1. It is interesting to observe that the inductance decreases at high current and slightly increases at low current. This is a characteristic of ferrite inductor, also highlighted in the [REDEXPERT](#)  plots of Figure 9, relevant to inductor L3.

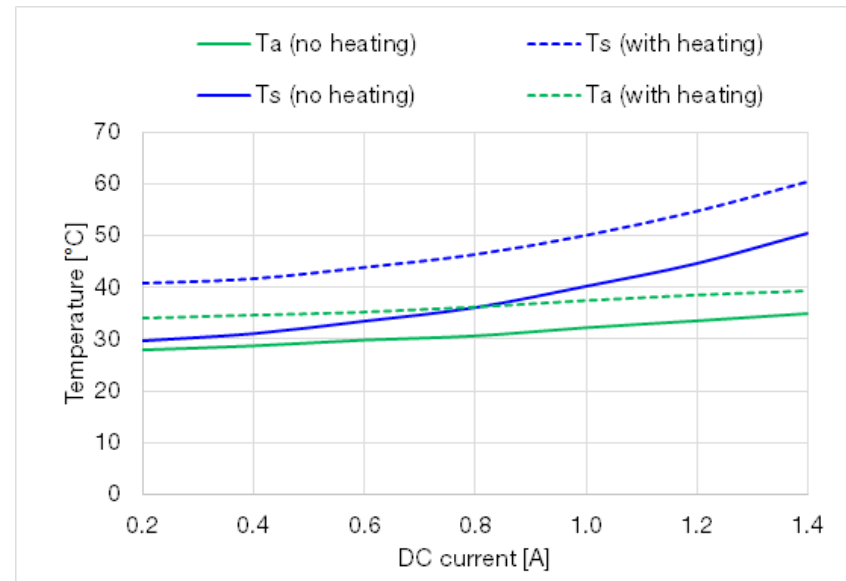


Figure 1.14. Ambient temperature and surface temperature of the inductor L1
(measured by means of temperature sensors on board)

The plots of Figure 1.14 highlight that the heating resistor determines an increase of the ambient temperature and of the inductor surface temperature. However, the temperature rise of the inductor at higher ambient temperature is larger than at lower ambient temperature, especially at high current. This is the result of a loop of effects:

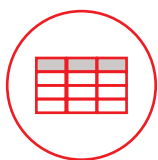
- the higher temperature causes a decrease of the inductance;
- the lower inductance causes a larger peak-peak inductor ripple current;
- the larger ripple current causes an increase of AC inductor losses;
- the higher AC losses cause an increase of the inductor temperature.

Experiment 2  insights inductor losses.



Expansion Activities

- Repeat the experiment under different input voltage V_{in} and switching frequency f_{sw} conditions, to verify the impact of these operating parameters on the peak-peak inductor current ripple. The input voltage can range from 5 V to 10 V. The switching frequency can be varied by means of the trimmer R9.
- Repeat the experiment with $J_6 - J_{13}$ shorted, to evaluate the effect of the input filter resistance on the duty cycle and on peak-peak inductor current ripple.
- Use the [REDEXPERT](#)  simulation features to analyze the performance of inductors L1, L2 and L3 in boost and buck-boost DC-DC converters. Ensure that the converters operating conditions are set appropriately to fulfill the restrictions indicated in the [REDEXPERT](#)  for each topology.



Tables of measurements (1)

The tables shown in this section are filled with values obtained by performing measurements on the TI-PMLK BUCK-WE board according to the previous test instructions. **[WARNING. The values reported in the tables are purely indicative. The results of your measurements on the TI-PMLK BUCK-WE board can be different due to tolerances and thermal effects of power components, and can be influenced by the accuracy and calibration of the instruments].**

Table 1.2. Evaluation of the inductance of inductors L1, L2 and L3 based on experimental measurements

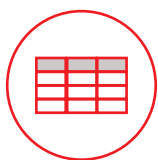
inductor	V_{in} [V]	V_{out} [V]	I_{out} [A]	D	Δi_{Lpp} [mA]	$L@1A$ [μ H]	L_{nom} [μ H]	R_L [m Ω]	$L@1A/L_{nom}$ [%]
L1	10.0	3.367	1.0	0.398	85	56.9	100.0	270	56.9
L2	10.0	3.367	1.0	0.410	80	61.2	68.0	386	90.0
L3	10.0	3.367	1.0	0.403	95	51.9	68.0	239	76.3

Table 1.3. Evaluation of the inductance of inductor L1 based on experimental measurements with J7-J8 open

I_{out} [mA]	200	600	1000	1400
V_{out} [V]	3.372	3.369	3.368	3.367
D	0.365	0.378	0.394	0.410
Δi_{Lpp} [mA]	56.5	64.5	81.5	206.5
$L1$ [μ H]	84.2	73.9	58.9	23.3
$L1/L1_{nom}$ [%]	84.2	73.9	58.9	23.3
T_a [$^{\circ}$ C]	27.9	29.8	32.2	34.9
T_s [$^{\circ}$ C]	29.6	33.4	40.1	50.3

Table 1.4. Evaluation of the inductance of inductor L1 based on experimental measurements with J7-J8 shorted

I_{out} [mA]	200	600	1000	1400
V_{out} [V]	3.372	3.369	3.369	3.369
D	0.365	0.375	0.395	0.415
Δi_{Lpp} [mA]	55.5	64.5	84.0	252.5
$L1$ [μ H]	85.7	73.3	57.2	19.3
$L1/L1_{nom}$ [%]	85.7	73.3	57.2	19.3
T_a [$^{\circ}$ C]	34.0	34.6	37.5	39.4
T_s [$^{\circ}$ C]	40.8	43.9	50.1	60.5



Tables of measurements (2)

The tables shown in this section are filled with values obtained by performing measurements on the TI-PMLK BUCK-WE board according to the previous test instructions. **[WARNING. The values reported in the tables are purely indicative. The results of your measurements on the TI-PMLK BUCK-WE board can be different due to tolerances and thermal effects of power components, and can be influenced by the accuracy and calibration of the instruments].**

Table 1.5. Evaluation of the inductance of inductor L2 based on experimental measurements

I_{out} [mA]	200	600	1000	1400
V_{out} [V]	3.371	3.368	3.367	3.367
D	0.366	0.389	0.412	0.438
Δi_{Lpp} [mA]	74.2	76.2	78.1	81.8
$L2$ [μ H]	64.1	63.7	63.0	61.1
$L2/L2_{nom}$ [%]	94.3	93.6	92.7	89.9

Table 1.6. Evaluation of the inductance of inductor L3 based on experimental measurements

I_{out} [mA]	200	600	1000	1400
V_{out} [V]	3.372	3.370	3.368	3.367
D	0.365	0.382	0.402	0.422
Δi_{Lpp} [mA]	78.2	80.5	91.2	334.5
$L3$ [μ H]	60.9	59.8	53.7	14.8
$L3/L3_{nom}$ [%]	89.5	88.0	78.9	21.8

Experiment 2

The goal of this experiment is to investigate the impact of inductor power losses on the efficiency of a DC-DC switching regulator, in steady-state operating conditions.

The LM3475 and TPS54160 regulators of the TI-PMLK BUCK-WE board are used to perform the experimental tests.



Theory Background (1)

Figure 2.1 shows a simplified schematic of the LM3475 and TPS54160 buck regulators power stage, including current sensing, input filter and eFuses.

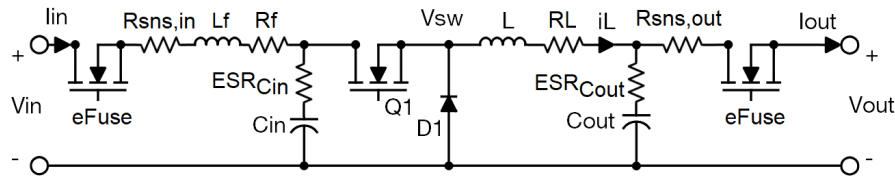


Figure 2.1. Buck converter simplified schematic

Figure 2.2 shows the theoretical voltage and current waveforms of the buck converter, in steady-state operation. The MOSFET Q1 conducts during the on time t_{ON} , whereas the diode D1 conducts during the off time t_{OFF} .

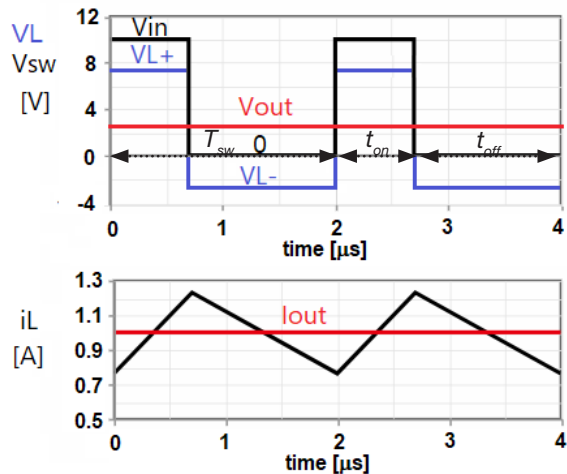


Figure 2.2. Voltage and current waveforms of buck converter



Return to previous page by:

Windows: + Mac: +

The output average power $P_{out} = V_{out} I_{out}$ is always lower than the average input power $P_{in} = V_{in} I_{in}$, as the power components of all DC-DC converters are affected by power losses. The total power losses P_{loss} of power components determine the efficiency η of the converter:

$$(1) \quad \eta = P_{out} / P_{in} = P_{out} / (P_{out} + P_{loss})$$

The main losses of the buck converter are summarized below.

1. MOSFET conduction losses

During the ON time, the MOSFET behaves like a resistor, whose resistance R_{dson} is determined by its gate driver voltage V_{dr} , by the voltage and current operating conditions imposed by the converter, and by the ambient temperature T_a . The MOSFET conduction losses can be evaluated by means of equation (2)

$$(2) \quad P_{MOScon} = R_{dson} D (I_{out}^2 + \Delta i_{Lpp}^2 / 12) = P_{MOScon,DC} + P_{MOScon,AC}$$

where D is the duty cycle, I_{out} is the load current and Δi_{Lpp} is the peak-peak amplitude of the inductor ripple current, $P_{MOScon,DC} = R_{dson} D I_{out}^2$, and $P_{MOScon,AC} = R_{dson} D \Delta i_{Lpp}^2 / 12$.

2. MOSFET switching losses

During the ON-OFF and OFF-ON transitions, the MOSFET is affected by losses determined by the overlapping of voltage and current. These switching losses can be evaluated by means of equations (3) and (4):

$$(3) \quad P_{MOSswon} = \frac{1}{2} (V_{in} + V_{D1}) (I_{out} - \Delta i_{Lpp} / 2) f_{sw} t_{swon}$$

$$(4) \quad P_{MOSswoff} = \frac{1}{2} (V_{in} + V_{D1}) (I_{out} + \Delta i_{Lpp} / 2) f_{sw} t_{swoff}$$

where V_{D1} is the forward voltage drop of diode D1, f_{sw} is the switching frequency, t_{swon} is the OFF-ON transition time and t_{swoff} is the ON-OFF transition time.



Theory Background (2)

3. MOSFET gate losses

The average power required to turn on and off the MOSFET at each switching period is given by equation (5):

$$(5) \quad P_{MOSgate} = Q_g V_{dr} f_{sw}$$

where Q_g is the MOSFET gate charge required at the MOSFET gate-to-source voltage V_{dr} imposed by the gate driver.

4. DIODE conduction losses

The average power loss of the diode D1 is given by equation (6):

$$(6) \quad P_{D1} = (1 - D) V_{D1} I_{out}$$

5. Current sensing and eFuse conduction losses

The average power losses of the input and output current sensing devices and eFuse protections are given by equations (7) and (8):

$$(7) \quad P_{insf} = (R_{sns,in} + R_{fuse,in}) (D I_{out})^2$$

$$(8) \quad P_{outsf} = (R_{sns,out} + R_{fuse,out}) I_{out}^2$$

where $R_{sns,in}$ and $R_{fuse,in}$ are the input current sensing resistance and on-state resistance of the eFuse MOSFET, and $R_{sns,out}$ and $R_{fuse,out}$ are the output current sensing resistance and on-state resistance of the eFuse MOSFET.

6. Capacitors losses

The average power losses of the input and output capacitors are given by the simplified equations (9) and (10):

$$(9) \quad P_{Cin} = ESR_{Cin} D (1 - D) I_{out}^2$$

$$(10) \quad P_{Cout} = ESR_{Cout} \Delta i_{Lpp}^2 / 12$$

where ESR_{Cin} and ESR_{Cout} are the equivalent series resistances of the input and output capacitors, respectively.

7. Inductor losses

Inductors are affected by DC losses and AC losses.

The DC losses depend on the winding DC resistance R_{LDC} and on the DC component of the inductor current flowing through it, as shown in equation (11):

$$(11) \quad P_{w,DC} = R_{LDC} I_{out}^2$$

The winding DC resistance R_{LDC} is provided in the power inductors datasheets and can be easily measured by means of a multimeter.

The AC losses include the high frequency losses in the windings and the hysteresis and eddy current losses in the magnetic core. The AC winding losses can be described by means of simplified equation (12):

$$(12) \quad P_{w,AC} = R_{LAC} \Delta i_{Lpp}^2 / 12$$

The value of the winding AC equivalent resistance R_{LAC} is influenced by several factors, including the switching frequency, the duty cycle, the winding wire cross-section and the number of winding layers. These elements play an important role when the skin depth of AC current flowing through the winding is smaller than the wire radius. As the switching frequency increases, the skin depth decreases and the AC equivalent resistance R_{LAC} increases. Some analytical formulae allow predicting an approximated value of the AC equivalent resistance R_{LAC} , which can be applied to inductors characterized by simple geometric symmetry and operating in sinusoidal AC current conditions.

Using Litz wires to make the inductor winding helps mitigating the impact of the skin effect. However, this solution is quite expensive and it is not adopted for commercial power inductors used in low power DC-DC switching regulators.



Return to previous page by:

Windows: +

Mac: +



Theory Background (3)

The AC core losses can be described by means of different equations, depending on the magnetic core material, geometry and size. The main operating parameters influencing the inductor AC core losses in a DC-DC converter are:

- the switching frequency f_{sw} ;
- the magnetic flux peak-peak swing amplitude $\Delta\Phi_{pp} = (V_{in} - V_{out}) D T_{sw}$;
- the DC component of the inductor current $I_L = I_{out}$.

If the DC component of the inductor current I_L is in the region of weak saturation, then $\Delta\Phi_{pp} = L_{nom} \Delta i_{Lpp}$, where L_{nom} is the nominal inductance of the inductor.

Modeling core losses of commercial power inductors for switching power converters is not easy, because of:

- the complexity of mathematical models and computations required to account for the non linearity of magnetic materials and the sharp-cornered geometry of commercial magnetic cores;
- the non-sinusoidal operating conditions imposed by switching power converters;
- the wide ranges of current, voltage, switching frequency, and ambient temperature occurring in switching power supply applications.

A core loss model can be obtained, in principle, by performing the inductor electromagnetic analysis, using dedicated computer programs, over the operating conditions ranges of interest in the application field. The results of computations, however, require an experimental validation to assess the model reliability.

For low-power commercial power inductors, core loss formulae are mostly determined through curve fitting of loss data acquired by means of experimental measurements.

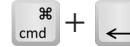


Return to previous page by:

Windows:



Mac:



A well known simplified formula allowing the evaluation of ferrite core losses is the Steinmetz equation:

$$(13) \quad P_{coreAC} = K_{fe} f_{sw}^{\alpha} \Delta B_{pp}^{\beta}$$

where ΔB_{pp} is the peak-peak amplitude of the magnetic flux density in the core. The parameters K_{fe} , α and β depend on the core material, geometry and size, on the frequency f_{sw} , on the DC bias current I_{out} and on the ambient temperature T_a . Several enhanced versions of the Steinmetz equation have been proposed over the last decades, allowing to improve the reliability of the loss prediction. If the inductor operates in the weak saturation region, equation (13) can be rewritten as follows:

$$(14) \quad P_{coreAC} = K_{fe} f_{sw}^{\alpha} (\gamma \Delta i_{Lpp})^{\beta} = K_1 f_{sw}^{\alpha-\beta} [\gamma (V_{in} - V_{out} - (R_{MOS} + R_{LDC}) I_{out}) D / L_{nom}]^{\beta}$$

where γ is a factor depending on the core characteristics. For ferrite cores, the value of parameter α is typically between 1.1 and 1.9, whereas the parameter β is between 1.6 and 3. Based on equation (13), it is expected that the core losses decrease as the switching frequency increases.

The **REDEXPERT**  software implements enhanced AC loss models of power inductors used in the TI-PMLKBUCK-WE board. These models have been developed by using large data sets of inductors power losses measurements, over voltage, current and switching frequency values covering the operating ranges of LM3475 and TPS54160 regulators implemented in the TI-PMLKBUCK-WE board.

All the parameters of winding and core loss formulae depend on the operating temperature. In general, the temperatures of winding and core are different. They depend on the operating conditions and on the structure of the inductor. In shielded inductors, winding and core temperatures may likely get closer, compared to unshielded inductors.



Theory Background (4)

For small size shielded inductors, it is reasonable to assume that the winding and the core operate at the same temperature, which can be predicted by means of equation (15):

$$(15) \quad T_{ind} = T_a + P_{ind} R_{\theta}$$

where T_a is the ambient temperature, $P_{ind} = P_{w,DC} + P_{w,AC} + P_{c,AC}$ is the total inductor power loss, and R_{θ} is the inductor equivalent thermal resistance. The thermal resistance R_{θ} can be approximately evaluated starting from the temperature rise plots of the inductor in DC current operation. Figure 2.3 shows the **REDEXPERT** plots of temperature rise for inductors L1, L2 and L3.

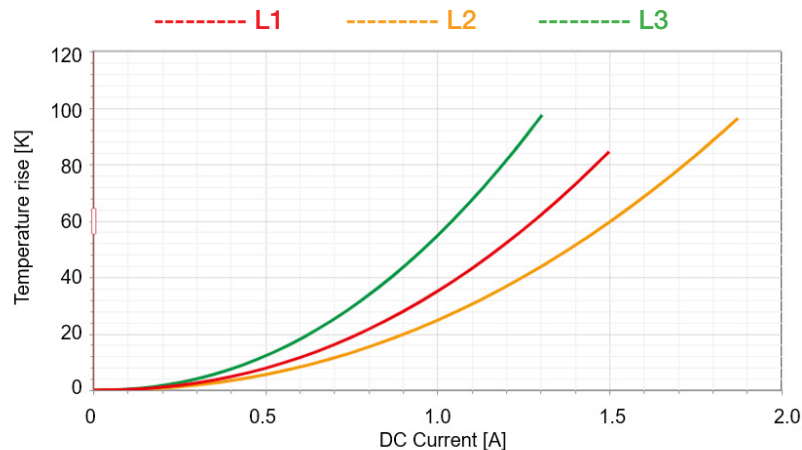


Figure 2.3. core loss density of a MnZn ferrite

Taking the temperature rise at 1 A DC current, ΔT_{1A} , the thermal resistance is given by equation (16):

$$(16) \quad R_{\theta} = \Delta T_{1A} / R_{LDC}$$

where R_{LDC} is the DC winding resistance.



Return to previous page by:

Windows: Alt + ←

Mac: ⌘ + ←

A realistic prediction of the temperature is needed to assess the reliability of the inductor operation. Indeed, the core losses density has a non-monotonic behavior with respect to the temperature, as shown in Figure 2.4.

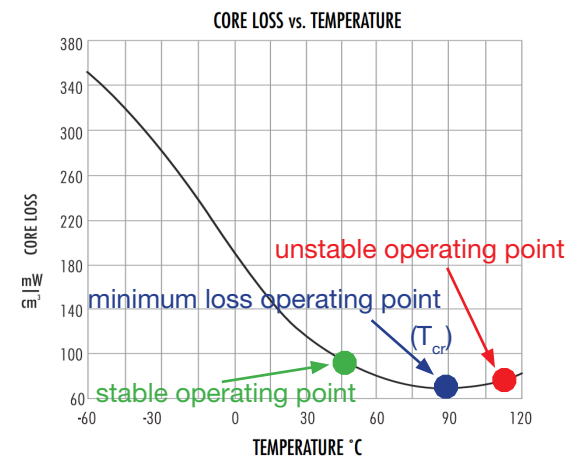


Figure 2.4. Core loss density versus temperature of Magnetics Type R MnZn ferrite, operating with 0.1 T AC magnetic flux density at 100 kHz

If the power losses determine a core temperature lower than the minimum loss critical temperature T_{cr} , then the inductor is thermally stable, as an increase of losses involves a reduction of the temperature and vice versa. If the core temperature increases beyond T_{cr} , then the inductor becomes thermally unstable, as an increase of the temperature involves an increase of losses. In these conditions, a thermal drift may occur, resulting in unpredictable effects. In particular, if the material exceeds the Curie temperature, its magnetic permeability drops and the inductor behaves almost like a short. The shape of the loss vs temperature curve and the location of the minimum loss point depend on the operating frequency and on the amplitude of the AC magnetic flux density ΔB_{pp} .



Case Study

The goal of this experiment is to compare the power losses of different inductors, under given operating conditions. The converter efficiency given by equation (1) will be analyzed based on the measurement of the input voltage V_{in} , the input current I_{in} , the output voltage V_{out} , and the output current I_{out} . The duty cycle D and the amplitude of peak-peak inductor ripple current Δi_{Lpp} will be also measured to analyze the inductors operating conditions. Both regulators LM3475 and TPS54160 will be used to perform the experiment, configured to operate in the same voltage, current and frequency conditions. The values of parameters introduced in loss equations from (2) to (10) will be determined starting from components datasheets.

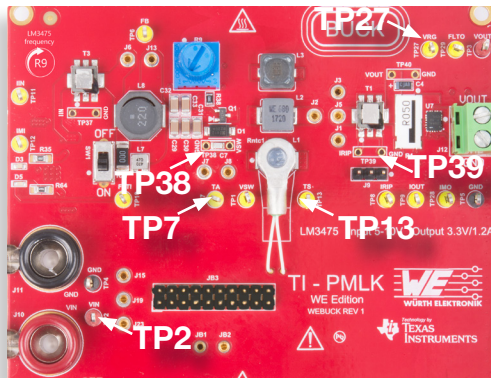


Figure 2.5. Test points used to analyze buck converter efficiency in the LM3475 regulator

The ambient temperature and the surface temperature of the inductor L1 will also be measured, to analyze the impact of temperature on the inductor performance.

The following test points of the LM3475 regulator will be used:

- **TP₃₉**, to measure the peak-peak amplitude of inductor current ripple Δi_{Lpp}
- **TP₃₈**, to measure the switching period T_{sw} and the duty cycle D
- **TP₂**, to measure the input voltage V_{in}
- **TP₂₇**, to measure the output voltage V_{out}
- **TP₇**, to measure the ambient temperature T_a
- **TP₁₃**, to measure the surface temperature of inductor L1 T_s

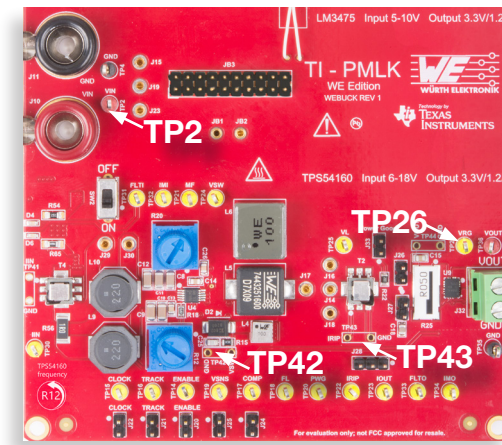


Figure 2.6. Test points used to analyze buck converter efficiency in the TPS54160 regulator

The following test points of the LM3475 regulator will be used:

- **TP₄₃**, to measure the peak-peak amplitude of inductor current ripple Δi_{Lpp}
- **TP₄₂**, to measure the switching period T_{sw} and the duty cycle D
- **TP₂**, to measure the input voltage V_{in}
- **TP₂₆**, to measure the output voltage V_{out}



Experiment set-up for LM3475 regulator: configuration

The instruments needed for this experiment are: a DC POWER SUPPLY, four MULTIMETERS, an OSCILLOSCOPE and a DC ELECTRONIC LOAD. Figure 2.7 shows the instruments connections for measurements on LM3475 regulator. Follow the instructions provided in next page to set-up the **connections**.

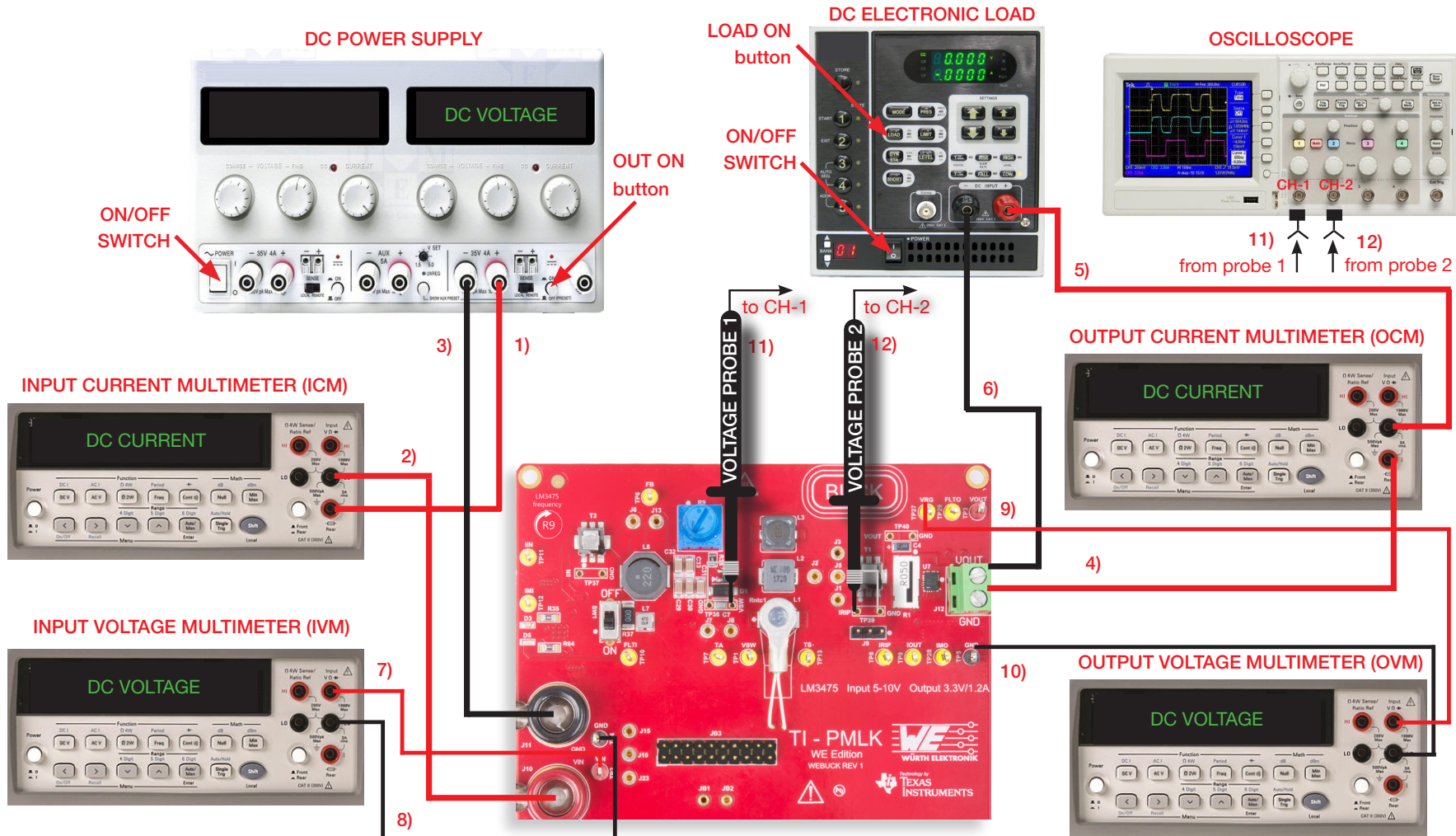


Figure 2.7. Experiment set-up for measurements on LM3475 regulator



Experiment set-up for LM3475 regulator: instructions

With all the instruments turned off, make the following **connections**:

1. Connect the POSITIVE (RED) OUTPUT of the DC POWER SUPPLY to the POSITIVE (RED) CURRENT INPUT of the INPUT CURRENT MULTIMETER (ICM) **[WARNING: THE POSITIVE INPUT OF THE MULTIMETER FOR CURRENT MEASUREMENT IS DIFFERENT FROM THE POSITIVE INPUT FOR VOLTAGE MEASUREMENT]**
2. Connect the NEGATIVE (BLACK) CURRENT INPUT of the INPUT CURRENT MULTIMETER (ICM) to the POSITIVE INPUT (VIN) banana connector J_{10} of the TI-PMLK BUCK-WE board
3. Connect the NEGATIVE (BLACK) OUTPUT of the DC POWER SUPPLY to the GROUND (GND) banana connector J_{11} of the TI-PMLK BUCK-WE board
4. Connect the POSITIVE OUTPUT (VOUT) of the screw terminal J_{12} of the LM3475 regulator to the POSITIVE (RED) CURRENT INPUT of the OUTPUT CURRENT MULTIMETER (OCM) **[WARNING: THE POSITIVE INPUT OF THE MULTIMETER FOR CURRENT MEASUREMENT IS DIFFERENT FROM THE POSITIVE INPUT FOR VOLTAGE MEASUREMENT]**
5. Connect the NEGATIVE (BLACK) CURRENT INPUT of the OUTPUT CURRENT MULTIMETER (OCM) to the POSITIVE (RED) INPUT of the ELECTRONIC LOAD.
6. Connect the NEGATIVE (BLACK) INPUT of the ELECTRONIC LOAD to the GROUND (GND) of the screw terminal J_{12} of the LM3475 regulator
7. Connect the POSITIVE (RED) VOLTAGE INPUT of the INPUT VOLTAGE MULTIMETER (IVM) to the test point TP_2 of the TI-PMLK BUCK-WE board
8. Connect the NEGATIVE (BLACK) VOLTAGE INPUT of the INPUT VOLTAGE MULTIMETER (IVM) to the test point TP_4 of the TI-PMLK BUCK-WE board
9. Connect the POSITIVE (RED) VOLTAGE INPUT of the OUTPUT VOLTAGE MULTIMETER (OVM) to the test point TP_{27} of the LM3475 regulator
10. Connect the NEGATIVE (BLACK) VOLTAGE INPUT of the OUTPUT VOLTAGE MULTIMETER (OVM) to the test point TP_5 of the LM3475 regulator
11. Connect a voltage probe with ground spring to channel 1 of the OSCILLOSCOPE, insert its positive tip into the hole of test point TP_{38} labeled "VSW" and its ground spring tip into the hole of test point TP_{38} labeled "GND". **[WARNING: DO NOT INVERT THE POSITIVE AND GROUND CONNECTIONS OF THE VOLTAGE PROBE]**
12. Connect a voltage probe with ground spring to channel 2 of the OSCILLOSCOPE, insert its positive tip into the hole of test point TP_{39} labeled "IRIP" and its ground spring tip into the hole of test point TP_{39} labeled "GND". **[WARNING: DO NOT INVERT THE POSITIVE AND GROUND CONNECTIONS OF THE VOLTAGE PROBE]**



Test#1: instructions (1)

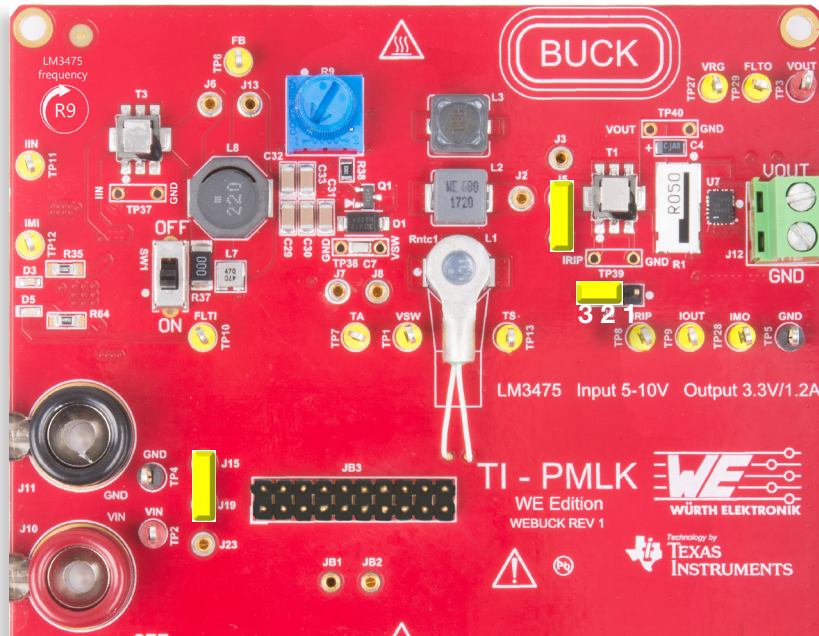


Figure 2.8. LM3475 jumpers set-up for Test#1

Initial set-up (see Figure 2.8, jumpers not mentioned are open):

- short J_{15} - J_{19} , LM3475 regulator connected to power input
- short J_1 - J_5 , inductor L1 connected
- short 2-3 of J_9 , separate AC and DC inductor currents
- turn R_9 right until it stops

Test Procedure:

1. Switch ON the SCOPE, set CH-1 and CH-2 in DC 1 M Ω coupling mode with 20 MHz BW limit, the time base to 1 μ s/div, the trigger on CH-2 rising edge, the vertical scale to 5 V/div on CH-1 and 20 mV/div on CH-2.
2. Switch ON the MULTIMETERS, select DC voltage measurement on IVM and OVM, and DC current measurement on ICM and OCM (see Figure 2.7).
3. Switch ON the POWER SUPPLY, set the "OUT ON" button OFF, output voltage to 10 V, and CURRENT LIMIT to 1.5 A.
4. Switch ON the ELECTRONIC LOAD, set the "OUT ON" button OFF, CONSTANT CURRENT MODE, and input current to 0.0 A.
5. Switch the POWER SUPPLY "OUT ON" button ON and the ELECTRONIC LOAD "LOAD ON" button ON. Under these conditions, you should see about 3.36 V on OVM display.
6. Rise slowly the ELECTRONIC LOAD current until you read 400 mA on the OCM. Adjust the DC POWER SUPPLY fine regulation knob, if needed, until you read $V_{in} = 10.0$ V on the IVM.
7. Watch the switching frequency f_{sw} of the waveform on SCOPE CH-1 (switching node voltage V_{sw}), while turning the knob of trimmer R9, until you get $f_{sw} = 300$ kHz. Under these conditions, you should see the inductor AC ripple current triangle waveform on SCOPE CH-3, with about 100 mA peak-peak amplitude (as the current sensor gain is 1 A/V, the voltage reading provides directly the current). Set 4 or 8 sweeps average acquisition mode on the SCOPE CH-2, to get a less noisy waveform, if needed.

[WARNING. If the measurements do not look as described above, switch OFF the "OUT ON" button of the ELECTRONIC LOAD and POWER SUPPLY, check the connections, the jumpers setup, the instruments setup, and repeat the procedure]



Test#1: instructions (2)

8. Read the measurements of input voltage on the IVM, input current on the ICM, output voltage on the OVM, output current on the OCM, and record the results in Table 2.1.
9. Measure the duty cycle of the switching node voltage V_{sw} on the SCOPE CH-1, and record the results in Table 2.1.
10. Measure the amplitude of the peak-peak inductor ripple current Δi_{Lpp} on the SCOPE CH-2, and record the results in Table 2.1.
11. Connect the OVM to test point TP_7 , read the voltage in millivolt, convert the voltage into Celsius degrees by using **Equation (2)**  on Page 21, and record the resulting value of ambient temperature T_a in Table 2.1.
12. Connect the OVM to test point TP_{13} , read the voltage in volt with three decimal digits, convert the voltage into Celsius degrees by means of **Table III**  on Page 22, and record resulting value of inductor surface temperature T_s in Table 2.1.

[NOTE. You may need to wait for a while to get stable values of voltage at test points TP_7 and TP_{13} , because of the slow settling of the temperature. Ensure the air surrounding the board is steady, as even a weak air flow may cause the temperature to float].
13. Connect the OVM positive connection to test point TP_{27} .
14. Repeat the steps 7 to 13, by increasing the load current of 400 mA steps, up to 1.2 A.
15. Watch the switching frequency f_{sw} of the waveform on the SCOPE CH-2, while turning the knob of trimmer R9, until you get $f_{sw} = 450$ kHz, set the load current to 400 mA, and adjust the DC POWER SUPPLY fine regulation knob, if needed, until you read $V_{in} = 10.0V$ on the IVM.
16. Repeat the steps 8 to 14.
17. Reduce the current of the ELECTRONIC LOAD to 0.0 A, switch its “LOAD ON” button OFF, and switch the POWER SUPPLY “OUT ON” button OFF.
18. Short J_2 - J_5 to connect inductor L2, repeat the steps 5 to 17 (skip the steps 11, 12, and 13), and record the measurement results in Table 2.2.
19. Short J_3 - J_5 to connect inductor L3, repeat steps 5 to 17 (skip the steps 11, 12, and 13), and record the measurement results in Table 2.3.
20. Switch OFF the ELECTRONIC LOAD, the MULTIMETERs, the POWER SUPPLY, and the SCOPE.
21. Summarize the measurement results in Table 2.4.



Test#1: measure and calculate (1)

Use the measured values of the input voltage V_{in} , input current I_{in} , output voltage V_{out} , output current I_{out} , switching frequency f_{sw} , duty cycle D , and amplitude of peak-peak inductor ripple current Δi_{Lpp} collected in Table 2.1 to determine the buck converter percent efficiency η [%] = $(V_{out} I_{out}) / (V_{in} I_{in}) \times 100$. Use **REDEXPERT**  to evaluate the inductors losses.

COMPONENTS DATA AND OPERATING PARAMETERS

Input Resistances

$$\begin{aligned} R_{fuse} &= 150 \text{ m}\Omega \\ R_{sns} &= 20 \text{ m}\Omega \\ R_{filter} &= 55 \text{ m}\Omega \end{aligned}$$

MOSFET

$$\begin{aligned} R_{dson} &= 50 \text{ m}\Omega & t_{sw,on} &= 5 \text{ ns} \\ Q_g &= 13.5 \text{ nC} & t_{sw,off} &= 20 \text{ ns} \end{aligned}$$

Diode D1

$$\begin{aligned} V_{D1} &= 300 \text{ mV@0.2 A} \\ V_{D1} &= 340 \text{ mV@0.6 A} \\ V_{D1} &= 400 \text{ mV@1.2 A} \end{aligned}$$

Inductor Resist.

$$\begin{aligned} R_{L1} &= 270 \text{ m}\Omega \text{ (Typ.)} \\ R_{L3} &= 386 \text{ m}\Omega \text{ (Typ.)} \\ R_{L3} &= 239 \text{ m}\Omega \text{ (Typ.)} \end{aligned}$$

Output Resist.

$$\begin{aligned} R_{sns} &= 70 \text{ m}\Omega \\ R_{fuse} &= 42 \text{ m}\Omega \end{aligned}$$

Input Capacitor

$$ESR_{Cin} = 1 \text{ m}\Omega$$

Output Capacitor

$$ESR_{Cout} = 100 \text{ m}\Omega$$

Table 2.1. Evaluation of losses and efficiency of LM3475 regulator with inductor L1 at 10V input voltage

f_{sw} [kHz]	300			450		
I_{out} [mA]	400	800	1200	400	800	1200
V_{out} [V]						
I_{in} [mA]						
D [%]						
Δi_{Lpp} [mA]						
P_{loss} [mW] = $V_{in} I_{in} - V_{out} I_{out}$						
η [%] = $(V_{out} I_{out}) / (V_{in} I_{in}) \times 100$						
T_a [°C]						
T_s [°C]						
P_{insf} [mW] eq. (7)						
P_{MOS} [mW] eqs. (2), (3), (4) and (5)						
P_{D1} [mW] eq. (6)						
P_{outsf} [mW] eq. (8)						
$P_{wDC} + P_{wAC}$ [mW] eqs (11)(12)						
P_{core} [mW] REDEXPERT						



Test#1: measure and calculate (2)

Use the measured values of the input voltage V_{in} , input current I_{in} , output voltage V_{out} , output current I_{out} , switching frequency f_{sw} , duty cycle D , and amplitude of peak-peak inductor ripple current Δi_{Lpp} collected in Table 2.2 to determine the buck converter percent efficiency η [%] = $(V_{out} I_{out}) / (V_{in} I_{in}) \times 100$. Use **REDEXPERT**  to evaluate the inductors losses.

COMPONENTS DATA AND OPERATING PARAMETERS

Input Resistances

$$\begin{aligned} R_{fuse} &= 150 \text{ m}\Omega \\ R_{sns} &= 20 \text{ m}\Omega \\ R_{filter} &= 55 \text{ m}\Omega \end{aligned}$$

MOSFET

$$\begin{aligned} R_{dson} &= 50 \text{ m}\Omega & t_{sw,on} &= 5 \text{ ns} \\ Q_g &= 13.5 \text{ nC} & t_{sw,off} &= 20 \text{ ns} \end{aligned}$$

Diode D1

$$\begin{aligned} V_{D1} &= 300 \text{ mV@0.2 A} \\ V_{D1} &= 340 \text{ mV@0.6 A} \\ V_{D1} &= 400 \text{ mV@1.2 A} \end{aligned}$$

Inductor Resist.

$$\begin{aligned} R_{L1} &= 270 \text{ m}\Omega \text{ (Typ.)} \\ R_{L3} &= 386 \text{ m}\Omega \text{ (Typ.)} \\ R_{L3} &= 239 \text{ m}\Omega \text{ (Typ.)} \end{aligned}$$

Output Resist.

$$\begin{aligned} R_{sns} &= 70 \text{ m}\Omega \\ R_{fuse} &= 42 \text{ m}\Omega \end{aligned}$$

Input Capacitor

$$ESR_{Cin} = 1 \text{ m}\Omega$$

Output Capacitor

$$ESR_{Cout} = 100 \text{ m}\Omega$$

Table 2.2. Evaluation of losses and efficiency of LM3475 regulator with inductor L2 at 10V input voltage

f_{sw} [kHz]	300			450		
I_{out} [mA]	400	800	1200	400	800	1200
V_{out} [V]						
I_{in} [mA]						
D [%]						
Δi_{Lpp} [mA]						
P_{loss} [mW] = $V_{in} I_{in} - V_{out} I_{out}$						
η [%] = $(V_{out} I_{out}) / (V_{in} I_{in}) \times 100$						
P_{insf} [mW] eq. (7)						
P_{MOS} [mW] eqs. (2), (3), (4) and (5)						
P_{D1} [mW] eq. (6)						
P_{outsf} [mW] eq. (8)						
$P_{wDC} + P_{wAC}$ [mW] eqs (11)(12)						
P_{core} [mW] REDEXPERT						



Test#1: measure and calculate (3)

Use the measured values of the input voltage V_{in} , input current I_{in} , output voltage V_{out} , output current I_{out} , switching frequency f_{sw} , duty cycle D , and amplitude of peak-peak inductor ripple current Δi_{Lpp} collected in Table 2.3 to determine the buck converter percent efficiency η [%] = $(V_{out} I_{out}) / (V_{in} I_{in}) \times 100$. Use **REDEXPERT**  to evaluate the inductors losses.

COMPONENTS DATA AND OPERATING PARAMETERS

Input Resistances

$$\begin{aligned} R_{fuse} &= 150 \text{ m}\Omega \\ R_{sns} &= 20 \text{ m}\Omega \\ R_{filter} &= 55 \text{ m}\Omega \end{aligned}$$

MOSFET

$$\begin{aligned} R_{dson} &= 50 \text{ m}\Omega & t_{sw,on} &= 5 \text{ ns} \\ Q_g &= 13.5 \text{ nC} & t_{sw,off} &= 20 \text{ ns} \end{aligned}$$

Diode D1

$$\begin{aligned} V_{D1} &= 300 \text{ mV@0.2 A} \\ V_{D1} &= 340 \text{ mV@0.6 A} \\ V_{D1} &= 400 \text{ mV@1.2 A} \end{aligned}$$

Inductor Resist.

$$\begin{aligned} R_{L1} &= 270 \text{ m}\Omega \text{ (Typ.)} \\ R_{L3} &= 386 \text{ m}\Omega \text{ (Typ.)} \\ R_{L3} &= 239 \text{ m}\Omega \text{ (Typ.)} \end{aligned}$$

Output Resist.

$$\begin{aligned} R_{sns} &= 70 \text{ m}\Omega \\ R_{fuse} &= 42 \text{ m}\Omega \end{aligned}$$

Input Capacitor

$$ESR_{Cin} = 1 \text{ m}\Omega$$

Output Capacitor

$$ESR_{Cout} = 100 \text{ m}\Omega$$

Table 2.3. Evaluation of losses and efficiency of LM3475 regulator with inductor L3 at 10V input voltage

f_{sw} [kHz]	300			450		
I_{out} [mA]	400	800	1200	400	800	1200
V_{out} [V]						
I_{in} [mA]						
D [%]						
Δi_{Lpp} [mA]						
$P_{loss} \text{ [mW]} = V_{in} I_{in} - V_{out} I_{out}$						
η [%] = $(V_{out} I_{out}) / (V_{in} I_{in}) \times 100$						
P_{insf} [mW] eq. (7)						
P_{MOS} [mW] eqs. (2), (3), (4) and (5)						
P_{D1} [mW] eq. (6)						
P_{outsf} [mW] eq. (8)						
$P_{wDC} + P_{wAC}$ [mW] eqs (11)(12)						
P_{core} [mW] REDEXPERT						



Test#1: measure and calculate (4)

Summarize the measurements and the inductors losses in Table 2.4.

Table 2.4. Comparative evaluation of LM3475 regulator losses and efficiency with inductors L1, L2 and L3

ind.	f_{sw} [kHz]	300			450		
	I_{out} [mA]	400	800	1200	400	800	1200
L1	Δi_{Lpp} [mA]						
	$P_{wDC} + P_{wAC}$ [mW] eqs. (11)(12)						
	P_{ind} [mW] REDEXPERT						
	P_{loss} [mW]						
	η [%]						
L2	Δi_{Lpp} [mA]						
	$P_{wDC} + P_{wAC}$ [mW] eqs. (11)(12)						
	P_{ind} [mW] REDEXPERT						
	P_{loss} [mW]						
	η [%]						
L3	Δi_{Lpp} [mA]						
	$P_{wDC} + P_{wAC}$ [mW] eqs. (11)(12)						
	P_{ind} [mW] REDEXPERT						
	P_{loss} [mW]						
	η [%]						



Test#1: measure and calculate (5)

Answer:

1 How does the efficiency vary as the load current increases? it increases it decreases other: _____

Please comment your answer: _____

2 How does the efficiency vary as the switching frequency increases? it increases it decreases other: _____

Please comment your answer: _____

3 What inductor does determine the highest efficiency? L1 L2 L3 other: _____

Please comment your answer: _____



Experiment set-up for TPS54160 regulator: configuration

The instruments needed for this experiment are: a DC POWER SUPPLY, four MULTIMETERS, an OSCILLOSCOPE and a DC ELECTRONIC LOAD. Figure 2.9 shows the instruments connections for measurements on TPS54160 regulator. Follow the instructions provided in next page to set-up the **connections**.

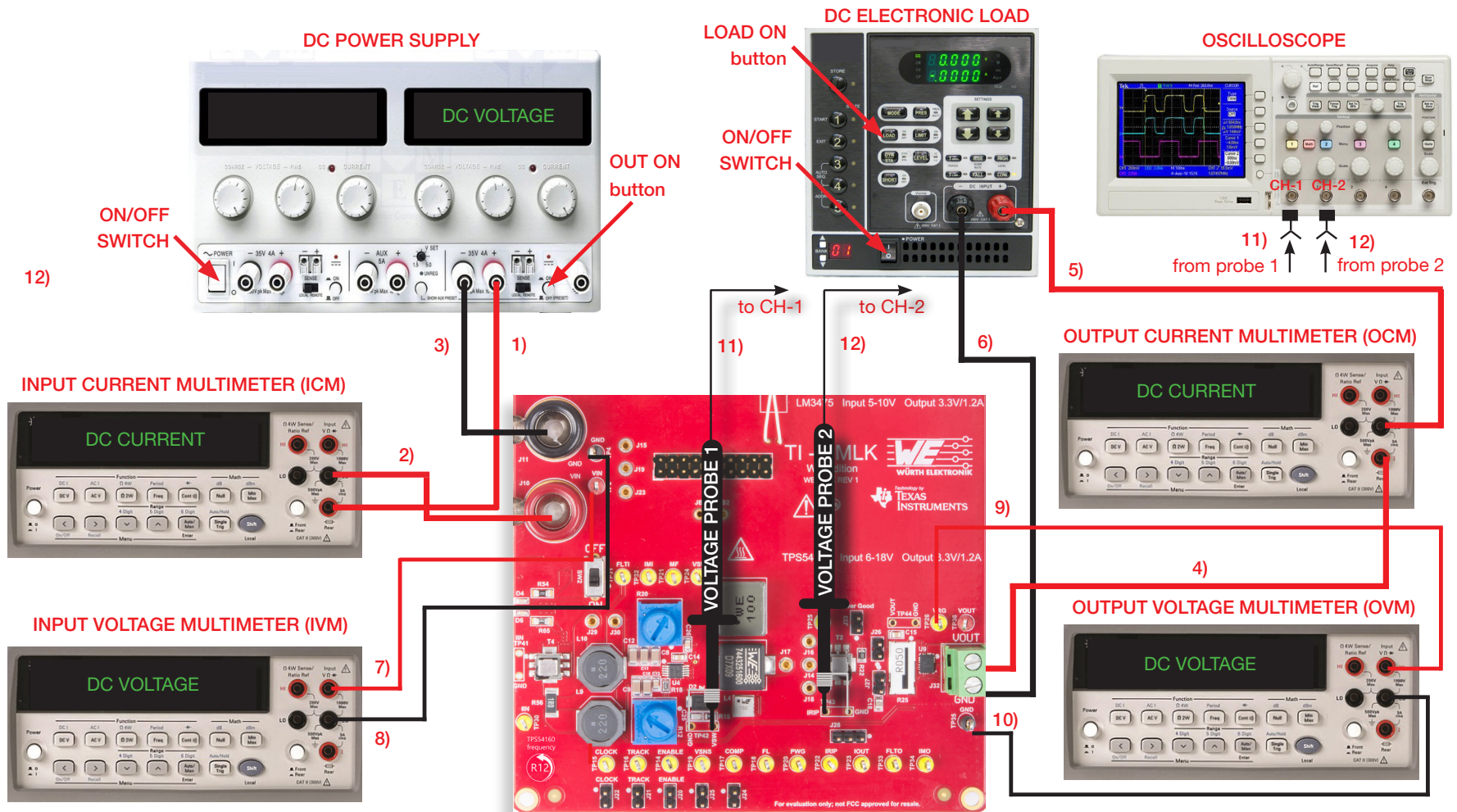


Figure 2.9. Experiment set-up for measurements on TPS54160 regulator



Experiment set-up for TPS54160 regulator: instructions

With all the instruments turned off, make the following **connections**:

1. Connect the POSITIVE (RED) OUTPUT of the DC POWER SUPPLY to the POSITIVE (RED) CURRENT INPUT of the INPUT CURRENT MULTIMETER (ICM) **[WARNING: THE POSITIVE INPUT OF THE MULTIMETER FOR CURRENT MEASUREMENT IS DIFFERENT FROM THE POSITIVE INPUT FOR VOLTAGE MEASUREMENT]**
2. Connect the NEGATIVE (BLACK) CURRENT INPUT of the INPUT CURRENT MULTIMETER (ICM) to the POSITIVE INPUT (VIN) banana connector J_{10} of the TI-PMLK BUCK-WE board
3. Connect the NEGATIVE (BLACK) OUTPUT of the DC POWER SUPPLY to the GROUND (GND) banana connector J_{11} of the TI-PMLK BUCK-WE board
4. Connect the POSITIVE OUTPUT (VOUT) of the screw terminal J_{32} of the TPS54160 regulator to the POSITIVE (RED) CURRENT INPUT of the OUTPUT CURRENT MULTIMETER (OCM) **[WARNING: THE POSITIVE INPUT OF THE MULTIMETER FOR CURRENT MEASUREMENT IS DIFFERENT FROM THE POSITIVE INPUT FOR VOLTAGE MEASUREMENT]**
5. Connect the NEGATIVE (BLACK) CURRENT INPUT of the OUTPUT CURRENT MULTIMETER (OCM) to the POSITIVE (RED) INPUT of the ELECTRONIC LOAD.
6. Connect the NEGATIVE (BLACK) INPUT of the ELECTRONIC LOAD to the GROUND (GND) of the screw terminal J_{32} of the TPS54160 regulator
7. Connect the POSITIVE (RED) VOLTAGE INPUT of the INPUT VOLTAGE MULTIMETER (IVM) to the test point TP_2 of the TI-PMLK BUCK-WE board
8. Connect the NEGATIVE (BLACK) VOLTAGE INPUT of the INPUT VOLTAGE MULTIMETER (IVM) to the test point TP_4 of the TI-PMLK BUCK-WE board
9. Connect the POSITIVE (RED) VOLTAGE INPUT of the OUTPUT VOLTAGE MULTIMETER (OVM) to the test point TP_{26} of the TPS54160 regulator
10. Connect the NEGATIVE (BLACK) VOLTAGE INPUT of the OUTPUT VOLTAGE MULTIMETER (OVM) to the test point TP_{35} of the TPS54160 regulator
11. Connect a voltage probe with ground spring to channel 1 of the OSCILLOSCOPE, insert its positive tip into the hole of test point TP_{42} labeled "VSW" and its ground spring tip into the hole of test point TP_{42} labeled "GND". **[WARNING: DO NOT INVERT THE POSITIVE AND GROUND CONNECTIONS OF THE VOLTAGE PROBE]**
12. Connect a voltage probe with ground spring to channel 2 of the OSCILLOSCOPE, insert its positive tip into the hole of test point TP_{43} labeled "IRIP" and its ground spring tip into the hole of test point TP_{43} labeled "GND". **[WARNING: DO NOT INVERT THE POSITIVE AND GROUND CONNECTIONS OF THE VOLTAGE PROBE]**



Test#2: instructions (1)

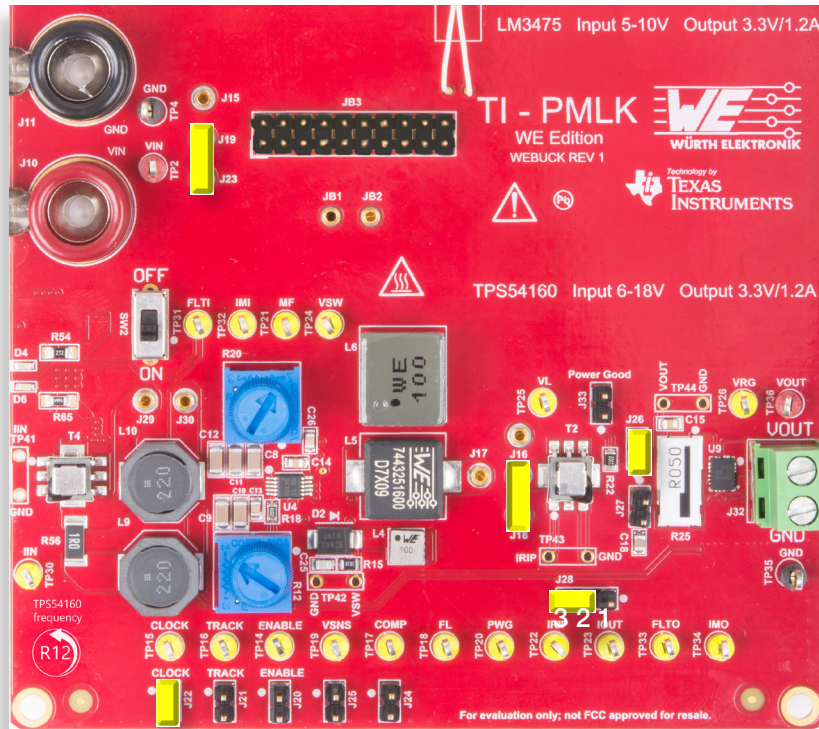


Figure 2.10. TPS54160 jumpers set-up for Test#2

Initial set-up (see Figure 2.10, jumpers not mentioned are open):

- short J_{19} - J_{23} , TPS54160 regulator connected to power input
- short J_{14} - J_{18} , inductor L_4 connected
- short pins 2-3 of J_{28} , separate AC and DC inductor currents
- short J_{22} , switching frequency adjust enabled
- short J_{26} , output capacitor C_{18} connected
- turn R_{12} left until it stops

Test Procedure:

1. Switch ON the SCOPE, set CH-1 and CH-2 in DC 1 M Ω coupling mode with 20 MHz BW limit, the time base to 1 μ s/div, the trigger on CH-2 rising edge, the vertical scale to 5 V/div on CH-1 and 20 mV/div on CH-2.
2. Switch ON the MULTIMETERS, select DC voltage measurement on IVM and OVM, and DC current measurement on ICM and OCM (see Figure 2.9).
3. Switch ON the POWER SUPPLY, set the "OUT ON" button OFF, output voltage to 10 V, and CURRENT LIMIT to 1.5 A.
4. Switch ON the ELECTRONIC LOAD, set the "OUT ON" button OFF, CONSTANT CURRENT MODE, and input current to 0.0 A.
5. Switch the POWER SUPPLY "OUT ON" button ON and the ELECTRONIC LOAD "LOAD ON" button ON. Under these conditions, you should see about 3.36 V on the OVM.
6. Rise slowly the ELECTRONIC LOAD current until you read 400 mA on the OCM. Adjust the DC POWER SUPPLY fine regulation knob, if needed, until you read $V_{in} = 10.0$ V on the IVM.
7. Watch the switching frequency f_{sw} of the waveform on the SCOPE CH-1 (switching node voltage V_{sw}), while turning the knob of trimmer R_{12} , until you get $f_{sw} = 300$ kHz. Under these conditions, you should see the inductor AC ripple current triangle waveform on the SCOPE CH-3, with about 770 mA peak-peak amplitude (as the current sensor gain is 1 A/V, the voltage reading provides directly the current). Set 4 or 8 sweeps average acquisition mode on the SCOPE CH-2 to get a less noisy waveform, if needed.

[WARNING. If the measurements do not look as described above, switch OFF the "OUT ON" button of the ELECTRONIC LOAD and POWER SUPPLY, check the connections, the jumpers setup, the instruments setup and repeat the procedure]



Test#2: instructions (2)

8. Read the measurements of input voltage on the IVM, input current on the ICM, output voltage on the OVM, output current on the OCM, and record the results in Table 2.5.
9. Measure the switching frequency f_{sw} and the duty cycle D of the switching node voltage V_{sw} on the SCOPE CH-1, and record the results in Table 2.5.
10. Measure the amplitude of the peak-peak inductor ripple current Δi_{Lpp} on the SCOPE CH-2, and record the results in Table 2.5.
11. Repeat the steps 7 to 10, by increasing the load current of 400 mA steps, up to 1.2 A.
12. Watch the switching frequency f_{sw} of the waveform on SCOPE CH-2, while turning the knob of trimmer R12, until you get $f_{sw} = 450$ kHz, and adjust the DC POWER SUPPLY fine regulation knob, if needed, until you read $V_{in} = 10.0$ V on the IVM.
13. Repeat the steps 8 to 11.
14. Reduce the current of the ELECTRONIC LOAD to 0.0 A, switch its “LOAD ON” button OFF, and switch the POWER SUPPLY “OUT ON” button OFF.
15. Short J_{14} - J_{17} to connect the inductor L5, repeat the steps 5 to 14, and record the measurement results in Table 2.6.
16. Short J_{14} - J_{16} to connect the inductor L6 and repeat the steps 5 to 14, and record the measurement results in Table 2.7.
17. Switch OFF the ELECTRONIC LOAD, the POWER SUPPLY, the MULTIMETER and the SCOPE.
18. Summarize the measurement results in Table 2.8.

Figures 2.11 and 2.12 show the waveform of the switching node voltage (yellow) and inductor current ripple (violet) at MOSFET commutations. The switching times of the TPS54160 internal MOSFET can be measured as shown in the Figures. The switching times decrease at higher load current.

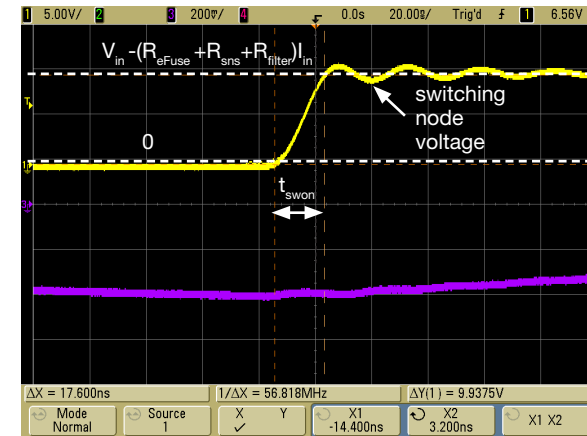


Figure 2.11. Measurement of the MOSFET turn on time t_{swon} , at 10 V input voltage, 0.4 A load current, 300 kHz frequency, with inductor L4

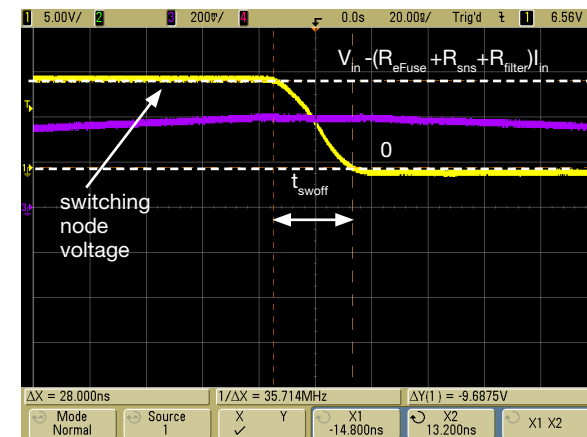


Figure 2.12. Measurement of the MOSFET turn off time t_{swoff} , at 10 V input voltage, 0.4 A load current, 300 kHz frequency, with inductor L4



Test#2: measure and calculate (1)

Use the measured values of the input voltage V_{in} , input current I_{in} , output voltage V_{out} , output current I_{out} , switching frequency f_{sw} , duty cycle D , and amplitude of peak-peak inductor ripple current Δi_{Lpp} collected in Table 2.5 to determine the buck converter percent efficiency η [%] = $(V_{out} I_{out}) / (V_{in} I_{in}) \times 100$. Use **REDEXPERT** to evaluate the inductors losses.

COMPONENTS DATA AND OPERATING PARAMETERS

Input Resistances

$$R_{fuse} = 150 \text{ m}\Omega$$

$$R_{sns} = 20 \text{ m}\Omega$$

$$R_{filter} = 75 \text{ m}\Omega$$

TPS54160 MOSFET

$$R_{dson} = 200 \text{ m}\Omega$$

$$Q_g = 3 \text{ nC}$$

$$t_{sw,on} = 17.6 \text{ ns@0.4 A}$$

$$16.0 \text{ ns@1.2 A}$$

$$t_{sw,off} = 28.0 \text{ ns@0.4 A}$$

$$19.2 \text{ ns@1.2 A}$$

Diode D1

$$V_{D1} = 420 \text{ mV@0.2 A}$$

$$V_{D1} = 480 \text{ mV@0.6 A}$$

$$V_{D1} = 520 \text{ mV@1.2 A}$$

Inductor Resist.

$$R_{L4} = 110 \text{ m}\Omega$$

$$R_{L5} = 34.5 \text{ m}\Omega$$

$$R_{L6} = 11.4 \text{ m}\Omega$$

Output Resist.

$$R_{sns} = 70 \text{ m}\Omega$$

$$R_{fuse} = 42 \text{ m}\Omega$$

Input Capacitor

$$ESR_{Cin} = 1 \text{ m}\Omega$$

Output Capacitor

$$ESR_{Cout} = 25 \text{ m}\Omega$$

Table 2.5. Evaluation of losses and efficiency of TPS54160 regulator with inductor L4 at 10V input voltage

f_{sw} [kHz]	300			450		
I_{out} [mA]	400	800	1200	400	800	1200
V_{out} [V]						
I_{in} [mA]						
D [%]						
Δi_{Lpp} [mA]						
P_{loss} [mW] = $V_{in} I_{in} - V_{out} I_{out}$						
η [%] = $(V_{out} I_{out}) / (V_{in} I_{in}) \times 100$						
P_{insf} [mW] eq. (7)						
P_{MOS} [mW] eqs. (2), (3), (4) and (5)						
P_{D1} [mW] eq. (6)						
P_{outsf} [mW] eq. (8)						
$P_{wDC} + P_{wAC}$ [mW] eqs (11)(12)						
P_{core} [mW] REDEXPERT						



Test#2: measure and calculate (2)

Use the measured values of the input voltage V_{in} , input current I_{in} , output voltage V_{out} , output current I_{out} , switching frequency f_{sw} , duty cycle D , and amplitude of peak-peak inductor ripple current Δi_{Lpp} collected in Table 2.6 to determine the buck converter percent efficiency η [%] = $(V_{out} I_{out}) / (V_{in} I_{in}) \times 100$. Use [REDEXPERT](#) to evaluate the inductors losses.

COMPONENTS DATA AND OPERATING PARAMETERS

Input Resistances

$$R_{fuse} = 150 \text{ m}\Omega$$

$$R_{sns} = 20 \text{ m}\Omega$$

$$R_{filter} = 75 \text{ m}\Omega$$

TPS54160 MOSFET

$$R_{dson} = 200 \text{ m}\Omega$$

$$Q_g = 3 \text{ nC}$$

$$t_{sw,on} = 17.6 \text{ ns@0.4 A}$$

$$16.0 \text{ ns@1.2 A}$$

$$t_{sw,off} = 28.0 \text{ ns@0.4 A}$$

$$19.2 \text{ ns@1.2 A}$$

Diode D1

$$V_{D1} = 420 \text{ mV@0.2 A}$$

$$V_{D1} = 480 \text{ mV@0.6 A}$$

$$V_{D1} = 520 \text{ mV@1.2 A}$$

Inductor Resist.

$$R_{L4} = 110 \text{ m}\Omega$$

$$R_{L5} = 34.5 \text{ m}\Omega$$

$$R_{L6} = 11.4 \text{ m}\Omega$$

Output Resist.

$$R_{sns} = 70 \text{ m}\Omega$$

$$R_{fuse} = 42 \text{ m}\Omega$$

Input Capacitor

$$ESR_{Cin} = 1 \text{ m}\Omega$$

Output Capacitor

$$ESR_{Cout} = 25 \text{ m}\Omega$$

Table 2.6. Evaluation of losses and efficiency of TPS54160 regulator with inductor L5 at 10V input voltage

f_{sw} [kHz]	300			450		
I_{out} [mA]	400	800	1200	400	800	1200
V_{out} [V]						
I_{in} [mA]						
D [%]						
Δi_{Lpp} [mA]						
P_{loss} [mW] = $V_{in} I_{in} - V_{out} I_{out}$						
η [%] = $(V_{out} I_{out}) / (V_{in} I_{in}) \times 100$						
P_{insf} [mW] eq. (7)						
P_{MOS} [mW] eqs. (2), (3), (4) and (5)						
P_{D1} [mW] eq. (6)						
P_{outsf} [mW] eq. (8)						
$P_{wDC} + P_{wAC}$ [mW] eqs (11)(12)						
P_{core} [mW] REDEXPERT						



Test#2: measure and calculate (3)

Use the measured values of the input voltage V_{in} , input current I_{in} , output voltage V_{out} , output current I_{out} , switching frequency f_{sw} , duty cycle D , and amplitude of peak-peak inductor ripple current Δi_{Lpp} collected in Table 2.7 to determine the buck converter percent efficiency η [%] = $(V_{out} I_{out}) / (V_{in} I_{in}) \times 100$. Use [REDEXPERT](#) to evaluate the inductors losses.

COMPONENTS DATA AND OPERATING PARAMETERS

Input Resistances

$$R_{fuse} = 150 \text{ m}\Omega$$

$$R_{sns} = 20 \text{ m}\Omega$$

$$R_{filter} = 75 \text{ m}\Omega$$

TPS54160 MOSFET

$$R_{dson} = 200 \text{ m}\Omega$$

$$Q_g = 3 \text{ nC}$$

$$t_{sw,on} = 17.6 \text{ ns@0.4 A}$$

$$16.0 \text{ ns@1.2 A}$$

$$t_{sw,off} = 28.0 \text{ ns@0.4 A}$$

$$19.2 \text{ ns@1.2 A}$$

Diode D1

$$V_{D1} = 420 \text{ mV@0.2 A}$$

$$V_{D1} = 480 \text{ mV@0.6 A}$$

$$V_{D1} = 520 \text{ mV@1.2 A}$$

Inductor Resist.

$$R_{L4} = 110 \text{ m}\Omega$$

$$R_{L5} = 34.5 \text{ m}\Omega$$

$$R_{L6} = 11.4 \text{ m}\Omega$$

Output Resist.

$$R_{sns} = 70 \text{ m}\Omega$$

$$R_{fuse} = 42 \text{ m}\Omega$$

Input Capacitor

$$ESR_{Cin} = 1 \text{ m}\Omega$$

Output Capacitor

$$ESR_{Cout} = 25 \text{ m}\Omega$$

Table 2.7. Evaluation of losses and efficiency of TPS54160 regulator with inductor L6 at 10V input voltage

f_{sw} [kHz]	300			450		
I_{out} [mA]	400	800	1200	400	800	1200
V_{out} [V]						
I_{in} [mA]						
D [%]						
Δi_{Lpp} [mA]						
P_{loss} [mW] = $V_{in} I_{in} - V_{out} I_{out}$						
η [%] = $(V_{out} I_{out}) / (V_{in} I_{in}) \times 100$						
P_{insf} [mW] eq. (7)						
P_{MOS} [mW] eqs. (2), (3), (4) and (5)						
P_{D1} [mW] eq. (6)						
P_{outsf} [mW] eq. (8)						
$P_{wDC} + P_{wAC}$ [mW] eqs (11)(12)						
P_{core} [mW] REDEXPERT						



Test#2: measure and calculate (4)

Summarize the measurements and the inductors losses in Table 2.8.

Table 2.8. Comparative evaluation of TPS54160 regulator losses and efficiency with inductors L4, L5 and L6

ind.	f_{sw} [kHz]	300			450		
	I_{out} [mA]	400	800	1200	400	800	1200
L4	Δi_{Lpp} [mA]						
	$P_{wDC} + P_{wAC}$ [mW] eqs. (11)(12)						
	P_{ind} [mW] REDEXPERT						
	P_{loss} [mW]						
	η [%]						
L5	Δi_{Lpp} [mA]						
	$P_{wDC} + P_{wAC}$ [mW] eqs. (11)(12)						
	P_{ind} [mW] REDEXPERT						
	P_{loss} [mW]						
	η [%]						
L6	Δi_{Lpp} [mA]						
	$P_{wDC} + P_{wAC}$ [mW] eqs. (11)(12)						
	P_{ind} [mW] REDEXPERT						
	P_{loss} [mW]						
	η [%]						



Observe and Answer

Answer:

1 How does the efficiency vary as the load current increases? it increases it decreases other: _____

Please comment your answer: _____

2 How does the efficiency vary as the switching frequency increases? it increases it decreases other: _____

Please comment your answer: _____

3 What inductor determines the highest efficiency? L4 L5 L6 other: _____

Please comment your answer: _____



Discussion (1)

Equation (11) highlights that the DC ohmic losses in the inductor winding increase with the load current. Similarly, the DC ohmic losses of all power components increase with load current, including the MOSFET, the current sensing resistors and the eFuses. Therefore, it is realistic that the efficiency of the converter decreases while the load current increases. The measurements show that this happens indeed, but only above a certain value of the load current, where the converter efficiency exhibits a maximum. The decrease of efficiency at low current is mainly caused by the impact of MOSFET AC conduction losses (equation (2)) and switching losses (equations (3), (4), (5)), of inductor AC losses (equations (12), (13), (14)). Other minor losses contributing to decrease the efficiency at low load current are the capacitors losses (equations (9), (10)) and the losses determined by the quiescent currents of ICs (these currents are from tens to hundreds of micro Ampères).

The inductor core losses are not as easy to determine as the winding ohmic losses. Given the voltage, current, duty cycle and switching frequency conditions imposed by the DC-DC converter, the amount of core losses is determined by the core material and by the balance among the core size and the inductance. In case of ferrite inductors, a given core can be used to construct inductors of different inductance, with windings of different number of turns using strands of different cross section. In particular, the inductance of a gapped ferrite core inductor, is

$$(17) \quad L = N^2 \mu_0 \mu_r A_c / (l_m + \mu_r l_g)$$

where N is the number of turns, μ_0 is the free space permeability, μ_r is the relative permeability of the core material, A_c is the core cross-section, l_m is the magnetic path length of the core, and l_g is the air gap length. With a given core, a larger inductance can be obtained by using a larger number of turns. A larger number of turns involves a smaller wire gauge cross section $A_w = W_A K_u / N$, where W_A is the winding allocation area of the core, and $K_u < 1$ is the utilization factor of the allocation area W_A (there are empty interspaces between winding strand turns). The resulting DC resistance of the inductor winding is:

$$(18) \quad R_{LDC} = l_{MLT} N \rho / A_w$$

where l_{MLT} is the mean length of each winding turn, and ρ is the copper resistivity.

For an inductor operating in the weak saturation region, the peak-peak amplitude of the AC magnetic flux density is approximately given by:

$$(19) \quad \Delta B_{pp} = (V_{in} - V_{out}) D / (f_{sw} A_c N)$$

Combining equations (17), (18) and (19) with equations (11), (12) and (13) highlights that an inductor with a bigger inductance is likely affected by higher winding losses and lower core losses [Note. If the skin effect is negligible, then $R_{LAC} = R_{LDC}$ in equation (12)].

Increasing the switching frequency reduces the inductor core losses and the AC ohmic losses of all power components, thanks to the reduction of the peak-peak amplitude Δi_{Lpp} of the inductor ripple current.



Discussion (2)

Figures 2.13 to 2.16 show the plots of inductors winding losses (P_w), core losses (P_c), and ripple current, at 300 kHz and 450 kHz, and resulting efficiency of LM3475 regulator.

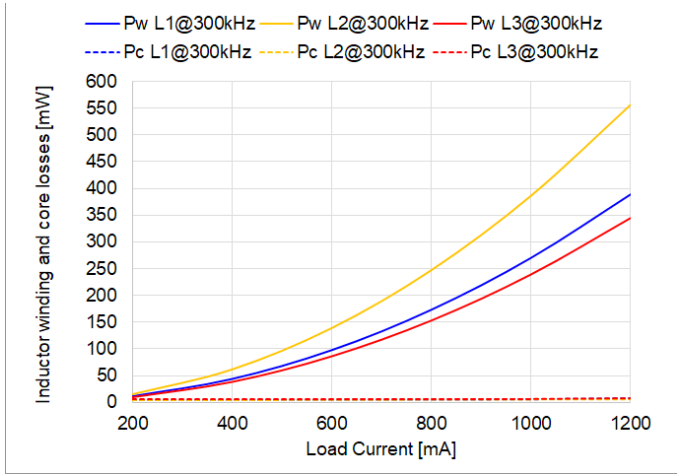


Figure 2.13. Inductor losses at 300kHz (calculated)

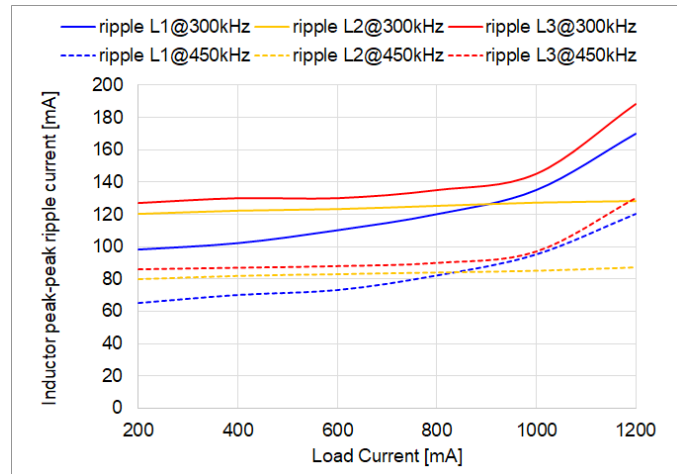


Figure 2.15. Inductor ripple current (measured)

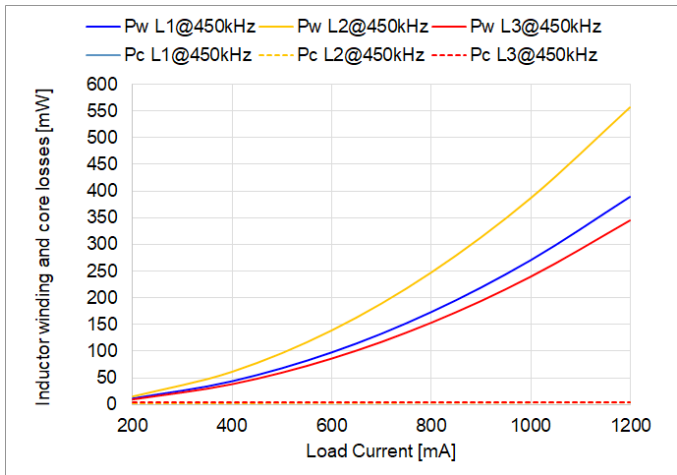


Figure 2.14. Inductor losses at 450kHz (calculated)

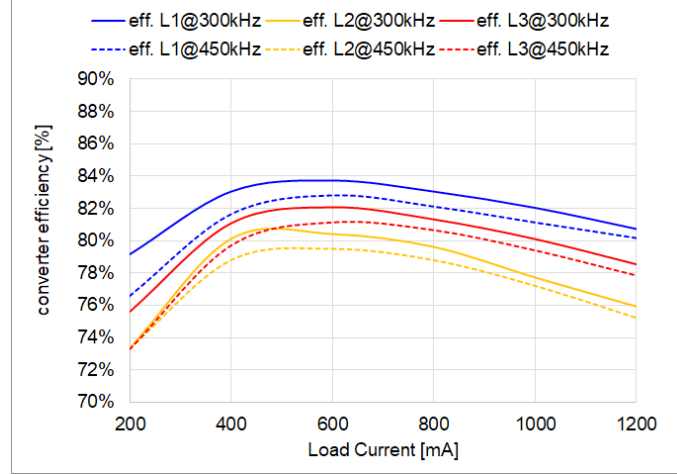


Figure 2.16. LM3475 regulator efficiency (measured)



Discussion (3)

Figures 2.17 to 2.20 show the plots of inductors winding losses (P_w), core losses (P_c), and ripple current, at 300 kHz and 450 kHz, and resulting efficiency of TPS54160 regulator.

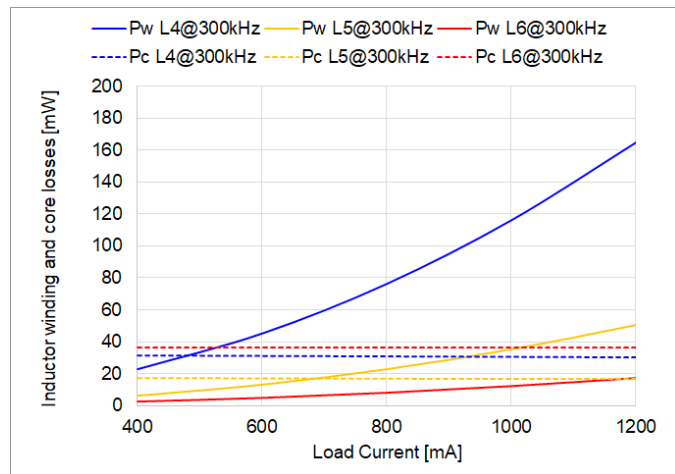


Figure 2.17. Inductor losses at 300kHz (calculated)

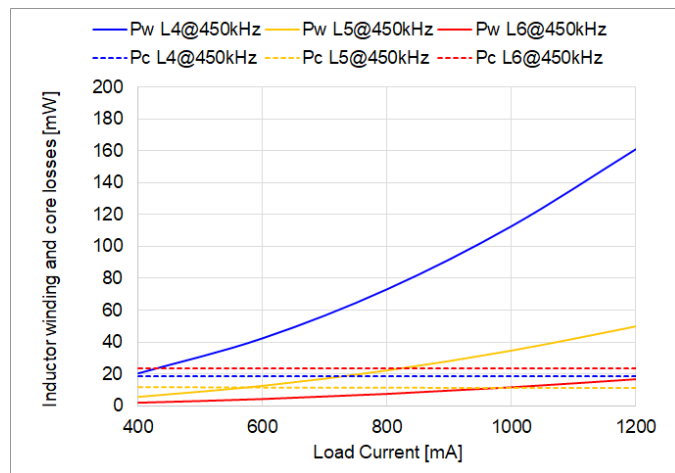


Figure 2.18. Inductor losses at 450kHz (calculated)

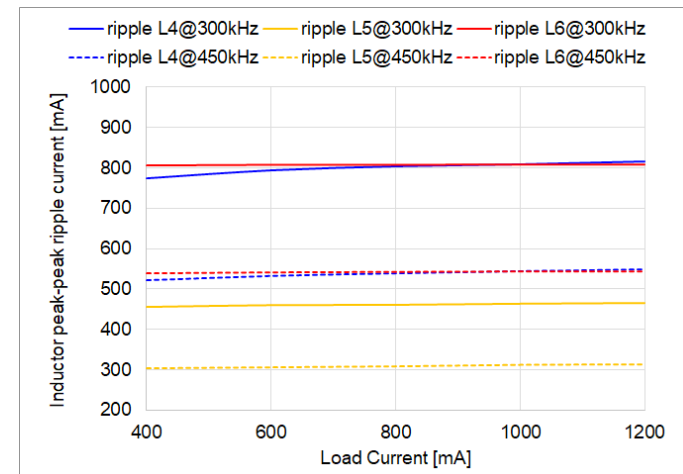


Figure 2.19. Inductor ripple current (measured)

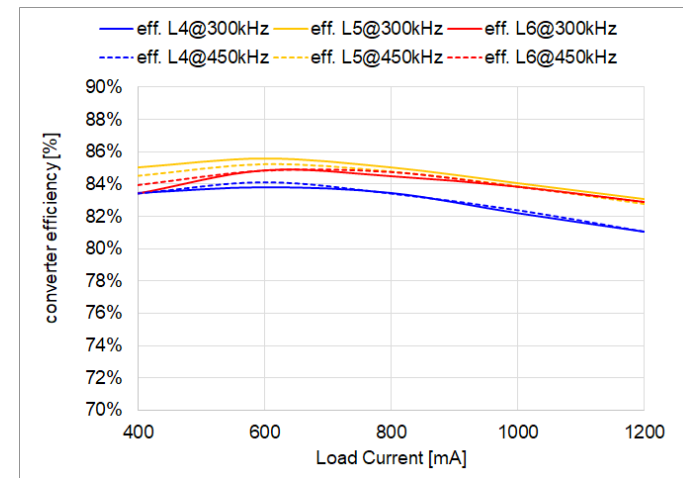


Figure 2.20. TPS54160 regulator efficiency (measured)



Discussion (4)

The results of measurements and calculations shown in the plots of Figures 2.13 to 2.20 highlight that the efficiency of the LM3475 regulator is lower than the efficiency of the TPS54160 regulator, under identical operating conditions. This is the effect of the type of inductors of the two regulators.

The inductors L1, L2 and L3 of the LM3475 regulator have much bigger inductance compared to the inductors L4, L5 and L6 of the TPS54160 regulator. According to equations (17), (18) and (19), the DC winding resistances of inductors L1, L2 and L3 are much larger compared to the inductors L4, L5 and L6. This is why we have very small core losses in inductors L1, L2 and L3 compared to winding losses, as shown in Figures 2.13 and 2.14 [NOTE: the values of surface temperature of inductor L1 in Test#1 at 300 kHz and 450 kHz are similar]. Conversely, the inductors L4, L5 and L6 have much smaller winding losses and higher core losses, as shown in Figures 2.17 and 2.18.

The inductors L5 and L6 have a larger size than inductors L1, L2 and L3, whereas the inductor L4 is much smaller. The smaller size of inductor L4 is the origin of its higher winding resistance and relevant losses, compared to inductors L5 and L6, as the smaller space available for windings involves the use of strands with smaller cross section.

Overall, the inductors L4, L5 and L6 have lower losses than inductors L1, L2 and L3, as they ensure a better balance between winding and core losses. This results in the higher efficiency of the TPS54160 regulator compared to the LM3475 regulator. In this regard, it is worth remarking that the inductors L4, L5 and L6 determine a much higher peak-peak inductor ripple current amplitude compared to inductors L1, L2 and L3, and that the internal MOSFET of TPS54160 chip has a larger on-state resistance $R_{ds(on)}$ compared to the MOSFET of the LM3475 regulator. Nevertheless, the resulting efficiency of TPS54160 regulator is higher.

The results of the experiment and the previous discussion prove that a larger peak-peak inductor ripple current amplitude does not necessarily cause a decrease of the efficiency of DC-DC converters. Indeed, although in principle a ripple current of larger amplitude may involve higher AC conduction losses and higher core losses, a careful selection of the inductor can lead to the identification of parts providing optimal performance with a large ripple. A large ripple may also have a positive impact on MOSFETs, which can benefit of a reduction of switching losses, thanks to the matching of the ripple current amplitude with the MOSFET parameters determining the switching losses. The conduction and switching losses of MOSFETs can be minimized, indeed, if the MOSFET and the inductor are well matched, by selecting the components that ensure at same time an efficiency complying with specifications. Surprisingly, the inductor ensuring such optimal condition may have minimum volume.

The inductor L4 of TPS54160, is an example of efficiency vs volume trade-off. The increase of efficiency provided by inductors L5 and L6 is paid with 10 times to 20 times larger inductor volume. Other inductors, may provide lower volume and higher losses, and vice versa, depending on the MOSFET characteristics. A good design consists in searching the components providing the best balance between MOSFETs and inductors for the given specifications.



Expansion Activities

- Repeat the experiment with different input voltage V_{in} . The input voltage can range from min 5 V to max 10 V in LM3475 regulator, and from min 6 V to max 18 V in TPS54160 regulator.

[Note. 1) The TPS54160 can operate in discontinuous conduction mode at high input voltage and low load current. The resulting loss equations of power components are different. 2) The TPS54160 regulator features a skip-cycle mode, determining an automatic reduction of switching frequency at low load current. This may result in discontinuous conduction mode operation. 3) See [Experiment 5](#) to investigate the impact of inductors on discontinuous conduction mode].

- Use the [REDEXPERT](#) simulation features to analyze the performance of inductors L1, L2, L3, L4, L5 and L6 in boost and buck-boost DC-DC converters. Ensure that the converters operating conditions are set appropriately to fulfill the restrictions indicated in the [REDEXPERT](#) for each topology.

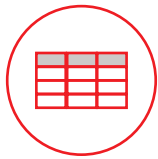


Tables of measurements (1)

The tables shown in this section are filled with values obtained by performing measurements on the TI-PMLK BUCK-WE board according to the previous test instructions. **[WARNING. The values reported in the tables are purely indicative. The results of your measurements on the TI-PMLK BUCK-WE board can be different due to tolerances and thermal effects of power components, and can be influenced by the accuracy and calibration of the instruments].**

Table 2.1. Evaluation of losses and efficiency of LM3475 regulator with inductor L1 at 10V input voltage

f_{sw} [kHz]	300			450		
I_{out} [mA]	400	800	1200	400	800	1200
V_{out} [V]	3.364	3.364	3.364	3.368	3.367	3.367
I_{in} [mA]	162	324	500	165	328	504
D [%]	37.3	39.0	40.5	37.5	39.0	41.0
ΔI_{Lpp} [mA]	102	120	170	70	82	120
P_{loss} [mW] = $V_{in} I_{in} - V_{out} I_{out}$	274.4	548.8	963.2	302.8	586.4	999.6
η [%] = $(V_{out} I_{out}) / (V_{in} I_{in}) \times 100$	0.831	0.831	0.807	0.816	0.821	0.802
T_a [°C]	26.2	27.5	28.8	28.2	29.1	29.8
T_s [°C]	28.7	32.1	38.4	31.8	36.0	39.8
P_{insf} [mW] eq. (7)	6.1	24.5	58.3	6.4	25.1	59.3
P_{MOS} [mW] eqs. (2), (3), (4) and (5)	63.2	91.5	127.5	92.9	130.6	176.4
P_{D1} [mW] eq. (6)	80.3	175.7	285.6	80.0	175.7	283.2
P_{outsf} [mW] eq. (8)	11.2	44.8	100.8	11.2	44.8	100.8
$P_{wDC} + P_{wAC}$ [mW] eqs. (11)(12)	43.4	173.1	389.5	43.3	173.0	389.1
P_{core} [mW] REDEXPERT	5.1	5.7	7.9	3.5	3.9	5.1

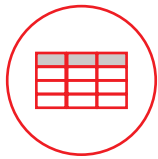


Tables of measurements (2)

The tables shown in this section are filled with values obtained by performing measurements on the TI-PMLK BUCK-WE board according to the previous test instructions. **[WARNING. The values reported in the tables are purely indicative. The results of your measurements on the TI-PMLK BUCK-WE board can be different due to tolerances and thermal effects of power components, and can be influenced by the accuracy and calibration of the instruments].**

Table 2.2. Evaluation of losses and efficiency of LM3475 regulator with inductor L2 at 10V input voltage

f_{sw} [kHz]	300			450		
I_{out} [mA]	400	800	1200	400	800	1200
V_{out} [V]	3.364	3.363	3.363	3.368	3.367	3.367
I_{in} [mA]	168	338	532	171	342	537
D	36.3	38.5	41.0	36.8	39.2	41.5
Δi_{Lpp} [mA]	122	125	128	82	84	87
P_{loss} [mW] = $V_{in} I_{in} - V_{out} I_{out}$	334	690	1284	363	726	1330
η [%] = $(V_{out} I_{out}) / (V_{in} I_{in}) \times 100$	0.801	0.796	0.759	0.788	0.788	0.752
P_{insf} [mW] eq. (7)	6.6	26.7	66.0	6.8	27.3	67.3
P_{MOS} [mW] eqs. (2), (3), (4) and (5)	63.2	91.4	127.5	93.0	130.7	176.4
P_{D1} [mW] eq. (6)	81.5	177.1	283.2	80.9	175.1	280.8
P_{outsf} [mW] eq. (8)	11.2	44.8	100.8	11.2	44.8	100.8
$P_{wDC} + P_{wAC}$ [mW] eqs. (11)(12)	62.2	247.5	556.4	62.0	247.3	556.1
P_{ind} [mW] REDEXPERT	4.6	5.1	5.7	2.9	3.3	3.7

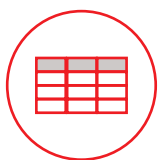


Tables of measurements (3)

The tables shown in this section are filled with values obtained by performing measurements on the TI-PMLK BUCK-WE board according to the previous test instructions. **[WARNING. The values reported in the tables are purely indicative. The results of your measurements on the TI-PMLK BUCK-WE board can be different due to tolerances and thermal effects of power components, and can be influenced by the accuracy and calibration of the instruments].**

Table 2.3. Evaluation of losses and efficiency of LM3475 regulator with inductor L3 at 10V input voltage

f_{sw} [kHz]	300			450		
I_{out} [mA]	400	800	1200	400	800	1200
V_{out} [V]	3.364	3.364	3.364	3.368	3.368	3.367
I_{in} [mA]	166	331	514	169	334	519
D	36.0	38.0	39.5	36.4	38.2	40.5
Δi_{Lpp} [mA]	130	135	188	87	90	130
P_{loss} [mW] = $V_{in} I_{in} - V_{out} I_{out}$	314	619	1103	343	646	1150
η [%] = $(V_{out} I_{out}) / (V_{in} I_{in}) \times 100$	0.811	0.813	0.785	0.797	0.807	0.778
P_{insf} [mW] eq. (7)	6.4	25.6	61.6	6.7	26.0	62.9
P_{MOS} [mW] eqs. (2), (3), (4) and (5)	63.3	91.3	126.9	93.0	130.4	176.1
P_{Dt} [mW] eq. (6)	81.9	178.6	290.4	81.4	178.0	285.6
P_{outsf} [mW] eq. (8)	11.2	44.8	100.8	11.2	44.8	100.8
$P_{wDC} + P_{wAC}$ [mW] eqs. (11)(12)	38.6	153.3	344.9	38.4	153.1	344.5
P_{ind} [mW] REDEXPERT	5.3	5.5	7.2	3.2	3.3	4.3

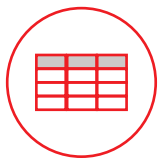


Tables of measurements (4)

The tables shown in this section are filled with values obtained by performing measurements on the TI-PMLK BUCK-WE board according to the previous test instructions. **[WARNING. The values reported in the tables are purely indicative. The results of your measurements on the TI-PMLK BUCK-WE board can be different due to tolerances and thermal effects of power components, and can be influenced by the accuracy and calibration of the instruments].**

Table 2.4. Comparative evaluation of LM3475 regulator losses and efficiency with inductors L1, L2 and L3

ind.	f_{sw} [kHz]	300			450		
	I_{out} [mA]	400	800	1200	400	800	1200
L1	Δi_{Lpp} [mA]	102	120	170	70	82	120
	$P_{wDC} + P_{wAC}$ [mW] eqs. (11)(12)	43.4	173.1	389.5	43.3	173.0	389.1
	P_{ind} [mW] REDEXPERT	5.1	5.7	7.9	3.5	3.9	5.1
	P_{loss} [mW]	274.4	548.8	963.2	302.8	586.4	999.6
	η [%]	83.1	83.1	80.7	81.6	82.1	80.2
L2	Δi_{Lpp} [mA]	122	125	128	82	84	87
	$P_{wDC} + P_{wAC}$ [mW] eqs. (11)(12)	62.2	247.5	556.4	62.0	247.3	556.1
	P_{ind} [mW] REDEXPERT	4.6	5.1	5.7	2.9	3.3	3.7
	P_{loss} [mW]	334.0	690.0	1284.0	363.0	726.0	1330.0
	η [%]	80.1	79.6	75.9	78.8	78.8	75.2
L3	Δi_{Lpp} [mA]	130	135	188	87	90	130
	$P_{wDC} + P_{wAC}$ [mW] eqs. (11)(12)	38.6	153.3	344.9	38.4	153.1	344.5
	P_{ind} [mW] REDEXPERT	5.3	5.5	7.2	3.2	3.3	4.3
	P_{loss} [mW]	314.4	618.8	1103.2	342.8	645.6	1149.6
	η [%]	81.1	81.3	78.5	79.7	80.7	77.8

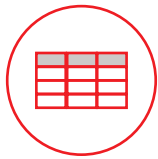


Tables of measurements (5)

The tables shown in this section are filled with values obtained by performing measurements on the TI-PMLK BUCK-WE board according to the previous test instructions. **[WARNING. The values reported in the tables are purely indicative. The results of your measurements on the TI-PMLK BUCK-WE board can be different due to tolerances and thermal effects of power components, and can be influenced by the accuracy and calibration of the instruments].**

Table 2.5. Evaluation of losses and efficiency of TPS54160 regulator with inductor L4 at 10V input voltage

f_{sw} [kHz]	300			450		
I_{out} [mA]	400	800	1200	400	800	1200
V_{out} [V]	3.337	3.337	3.337	3.337	3.337	3.337
I_{in} [mA]	160	320	494	160	320	494
D	36.0	37.7	39.2	35.6	37.4	38.9
Δi_{Lpp} [mA]	773	803	815	523	539	548
P_{loss} [mW] = $V_{in} I_{in} - V_{out} I_{out}$	265.2	530.4	935.6	265.2	530.4	935.6
η [%] = $(V_{out} I_{out}) / (V_{in} I_{in}) \times 100$	83.4	83.4	81.1	83.4	83.4	81.1
P_{insf} [mW] eq. (7)	6.0	23.9	56.9	6.0	23.9	56.9
P_{MOS} [mW] eqs. (2), (3), (4) and (5)	55.3	119.2	210.9	51.6	114.9	206.0
P_{Dt} [mW] eq. (6)	112.6	239.2	379.4	113.3	240.4	381.3
P_{outsf} [mW] eq. (8)	11.2	44.8	100.8	11.2	44.8	100.8
$P_{wDC} + P_{wAC}$ [mW] eqs. (11)(12)	23.1	76.3	164.5	20.1	73.1	161.2
P_{ind} [mW] REDEXPERT	31.6	31.0	30.3	18.8	18.6	18.4

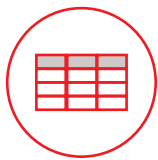


Tables of measurements (6)

The tables shown in this section are filled with values obtained by performing measurements on the TI-PMLK BUCK-WE board according to the previous test instructions. **[WARNING. The values reported in the tables are purely indicative. The results of your measurements on the TI-PMLK BUCK-WE board can be different due to tolerances and thermal effects of power components, and can be influenced by the accuracy and calibration of the instruments].**

Table 2.6. Evaluation of losses and efficiency of TPS54160 regulator with inductor L5 at 10V input voltage

f_{sw} [kHz]	300			450		
I_{out} [mA]	400	800	1200	400	800	1200
V_{out} [V]	3.337	3.337	3.337	3.337	3.337	3.337
I_{in} [mA]	157	314	482	158	315	484
D	35.9	37.2	38.4	35.6	36.9	38.3
Δi_{Lpp} [mA]	455	461	466	305	309	313
P_{loss} [mW] = $V_{in} I_{in} - V_{out} I_{out}$	334.0	690.0	1284.0	363.0	726.0	1330.0
η [%] = $(V_{out} I_{out}) / (V_{in} I_{in}) \times 100$	85.0	85.0	83.1	84.5	84.7	82.7
P_{insf} [mW] eq. (7)	5.8	23.0	54.2	5.8	23.2	54.7
P_{MOS} [mW] eqs. (2), (3), (4) and (5)	50.9	113.7	203.5	49.2	111.6	201.4
P_{Dt} [mW] eq. (6)	112.8	241.2	384.4	113.3	242.3	385.0
P_{outsf} [mW] eq. (8)	11.2	44.8	100.8	11.2	44.8	100.8
$P_{wDC} + P_{wAC}$ [mW] eqs. (11)(12)	6.1	22.7	50.3	5.8	22.4	50.0
P_{ind} [mW] REDEXPERT	17.3	17.1	17.0	11.9	11.5	11.3

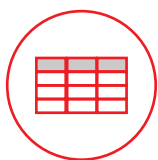


Tables of measurements (7)

The tables shown in this section are filled with values obtained by performing measurements on the TI-PMLK BUCK-WE board according to the previous test instructions. **[WARNING. The values reported in the tables are purely indicative. The results of your measurements on the TI-PMLK BUCK-WE board can be different due to tolerances and thermal effects of power components, and can be influenced by the accuracy and calibration of the instruments].**

Table 2.7. Evaluation of losses and efficiency of TPS54160 regulator with inductor L6 at 10V input voltage

f_{sw} [kHz]	300			450		
I_{out} [mA]	400	800	1200	400	800	1200
V_{out} [V]	3.337	3.337	3.337	3.337	3.337	3.337
I_{in} [mA]	160	316	483	159	315	483
D	35.8	37.0	38.2	35.6	36.6	37.8
Δi_{Lpp} [mA]	805	807	808	540	543	544
P_{loss} [mW] = $V_{in} I_{in} - V_{out} I_{out}$	265.2	490.4	825.6	255.2	480.4	825.6
η [%] = $(V_{out} I_{out}) / (V_{in} I_{in}) \times 100$	83.4	84.5	82.9	83.9	84.7	82.9
P_{insf} [mW] eq. (7)	6.0	23.3	54.4	5.9	23.2	54.4
P_{MOS} [mW] eqs. (2), (3), (4) and (5)	55.7	118.3	207.8	51.8	113.9	202.7
P_{Dt} [mW] eq. (6)	113.0	241.9	385.6	113.3	243.5	388.1
P_{outsf} [mW] eq. (8)	11.2	44.8	100.8	11.2	44.8	100.8
$P_{wDC} + P_{wAC}$ [mW] eqs. (11)(12)	2.4	7.9	17.0	2.1	7.6	16.7
P_{ind} [mW] REDEXPERT	36.3	36.3	36.3	23.6	23.6	23.6



Tables of measurements (8)

The tables shown in this section are filled with values obtained by performing measurements on the TI-PMLK BUCK-WE board according to the previous test instructions. **[WARNING. The values reported in the tables are purely indicative. The results of your measurements on the TI-PMLK BUCK-WE board can be different due to tolerances and thermal effects of power components, and can be influenced by the accuracy and calibration of the instruments].**

Table 2.8. Comparative evaluation of TPS54160 regulator losses and efficiency with inductors L4, L5 and L6

ind.	f_{sw} [kHz]	300			450		
	I_{out} [mA]	400	800	1200	400	800	1200
L4	Δi_{Lpp} [mA]	773	803	815	523	539	548
	$P_{wDC} + P_{wAC}$ [mW] eqs. (11)(12)	23.1	76.3	164.5	20.1	73.1	161.2
	P_{ind} [mW] REDEXPERT	31.6	31.0	30.3	18.8	18.6	18.4
	P_{loss} [mW]	265.2	530.4	935.6	265.2	530.4	935.6
	η [%]	83.4	83.4	81.1	83.4	83.4	81.1
L5	Δi_{Lpp} [mA]	455	461	466	305	309	313
	$P_{wDC} + P_{wAC}$ [mW] eqs. (11)(12)	6.1	22.7	50.3	5.8	22.4	50.0
	P_{ind} [mW] REDEXPERT	17.3	17.1	17.0	11.9	11.5	11.3
	P_{loss} [mW]	334.0	690.0	1284.0	363.0	726.0	1330.0
	η [%]	85.0	85.0	83.1	84.5	84.7	82.7
L6	Δi_{Lpp} [mA]	805	807	808	540	543	544
	$P_{wDC} + P_{wAC}$ [mW] eqs. (11)(12)	2.4	7.9	17.0	2.1	7.6	16.7
	P_{ind} [mW] REDEXPERT	36.3	36.3	36.3	23.6	23.6	23.6
	P_{loss} [mW]	265.2	490.4	825.6	255.2	480.4	825.6
	η [%]	83.4	84.5	82.9	83.9	84.7	82.9

Experiment 3

The goal of this experiment is to analyze the output filtering functions of inductors in DC-DC switching converters. The impact of the inductance on the output ripple voltage is investigated.

The TPS54160 buck regulator is used for this experiment.



Theory Background (1)

Figure 3.1 shows a simplified schematic of the TPS54160 buck regulator power stage, including current sensing, input filter and eFuses.

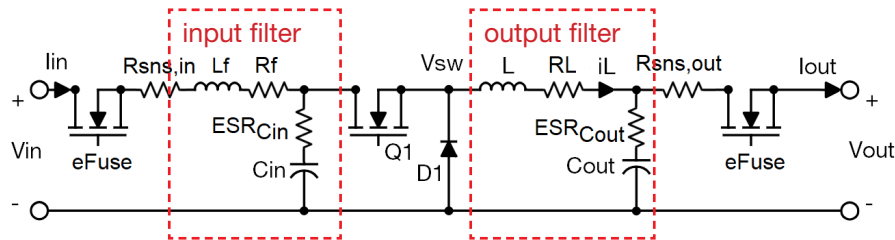


Figure 3.1. Buck converter simplified schematic

In the **output filter**, the function of the output capacitor is to bypass the inductor ripple current, to ensure the compliance of the output ripple voltage peak-peak amplitude Δv_{outpp} with the restrictions imposed by the design specifications. Typically, the maximum allowed amplitude $\Delta v_{outpp,max}$ of the peak-peak output ripple voltage is about 1% of the average output voltage.

Figures 3.2 and 3.3 show two examples of the expected theoretical voltage and current waveforms of the TPS54160 buck regulator, in steady-state operation at 10 V input voltage, 3.3 V output voltage, 400 mA load current, 500 kHz switching frequency, 10 μ H inductor, with two different types of capacitors.

Figure 3.2 refers to the 220 μ F, 25 m Ω tantalum capacitor C17, whereas Figure 3.3 refers to the 10 μ F, 5 m Ω ceramic capacitor C18. The plots show that the same inductor ripple current determines different types of output ripple voltage.

In the tantalum capacitor, the equivalent series resistance ESR_{Cout} is dominant with respect the impedance of the capacitance at the switching frequency, given by $1 / (2 \pi C_{out} f_{sw})$. Thus, the ripple voltage is determined by the ESR. In the ceramic capacitor, instead, it is $1 / (2 \pi C_{out} f_{sw}) \gg ESR_{Cout}$. Thus, the ripple voltage waveform is the integral of the ripple current and shows a 90° phase lag.



Return to previous page by:

Windows: Alt + ←

Mac: cmd + ←

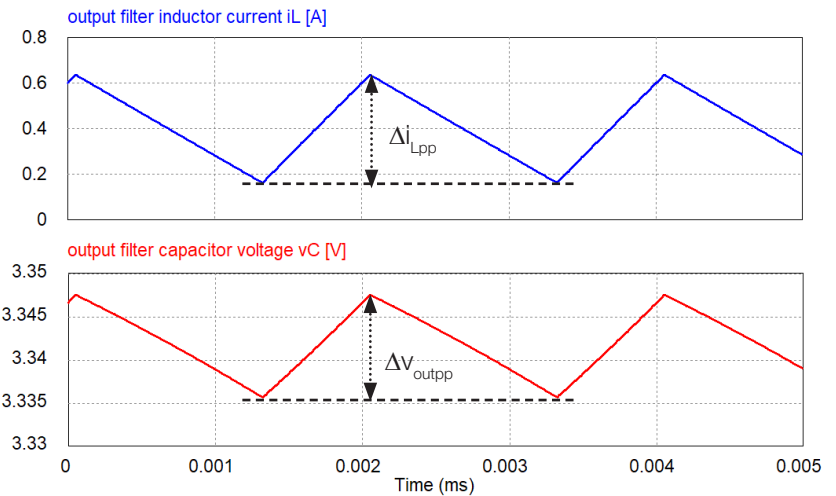


Figure 3.2. Output filter current and voltage waveforms with tantalum capacitor

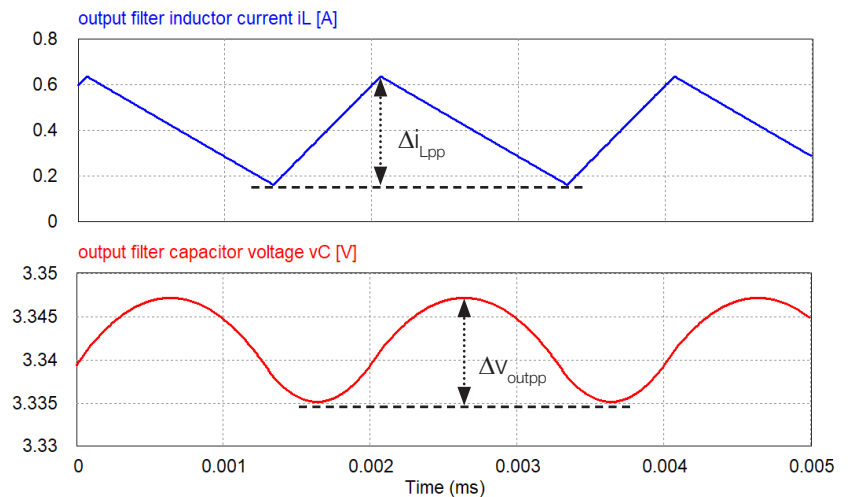


Figure 3.3. Output filter current and voltage waveforms with ceramic capacitor



Theory Background (2)

The output ripple voltage peak-peak amplitude is consequently determined by the type and parameters of the output capacitor. In high ESR capacitors (e.g. electrolytic), the peak-peak ripple voltage is mainly determined by the $ESR_{C_{out}}$:

$$(1) \quad \Delta V_{outpp} = ESR_{C_{out}} \Delta i_{Lpp}$$

In low ESR capacitors (e.g. ceramic), the peak-peak ripple voltage is mainly determined by the capacitance C_{out} :

$$(2) \quad \Delta V_{outpp} = \Delta i_{Lpp} / (8 f_{sw} C_{out})$$

Equations (1) and (2) highlight that a larger peak-peak inductor ripple current Δi_{Lpp} causes a larger peak-peak output ripple voltage ΔV_{outpp} , in any case. Given the maximum peak-peak inductor ripple current $\Delta i_{Lpp,max}$, equations (3) and (4) provide the maximum equivalent series resistance ESR (for high ESR capacitors) and the minimum capacitance (for low ESR capacitors) ensuring the compliance with maximum peak-peak output ripple voltage $\Delta V_{outpp,max}$:

$$(3) \quad ESR_{C_{out}} < \Delta V_{outpp,max} / \Delta i_{Lpp,max}$$

$$(4) \quad C_{out} > \Delta i_{Lpp,max} / (8 f_{sw} \Delta V_{outpp,max})$$

Normally, the ESR of capacitors is inversely proportional to the capacitance. Consequently, a larger peak-peak inductor ripple current $\Delta i_{Lpp,max}$ requires a capacitor of larger capacitance.

The inductance required to achieve the desired peak-peak inductor ripple current $\Delta i_{Lpp,max}$ is given by equation (5):

$$(5) \quad L > [V_{in} - V_{out} - (R_{eFuse} + R_{sns} + R_f + R_{MOS} + R_L) I_{out}] D / (f_{sw} \Delta i_{Lpp,max})$$

Given a power loss budget for the inductor, the size of the component increases with the inductance L [see [Experiment 2](#) to insight inductors power loss issues].



Return to previous page by:

Windows: Alt + ←

Mac: ⌘ + ←

Equations (3), (4) and (5) highlight that, for a given maximum peak-peak output ripple voltage $\Delta V_{outpp,max}$, a larger peak-peak inductor ripple current $\Delta i_{Lpp,max}$ results in a smaller inductor and a larger capacitor, and viceversa. Moreover, for a given output capacitor, an increase of the peak-peak inductor ripple current results in a larger peak-peak output ripple voltage. Finally, for given inductor and output capacitor, an increase of the switching frequency f_{sw} results in a decrease of the peak-peak inductor ripple current and peak-peak output ripple voltage.

The parasitic inductances of the output capacitor and layout affect the shape and peak-peak amplitude of the output ripple voltage, as shown in Figure 3.4.

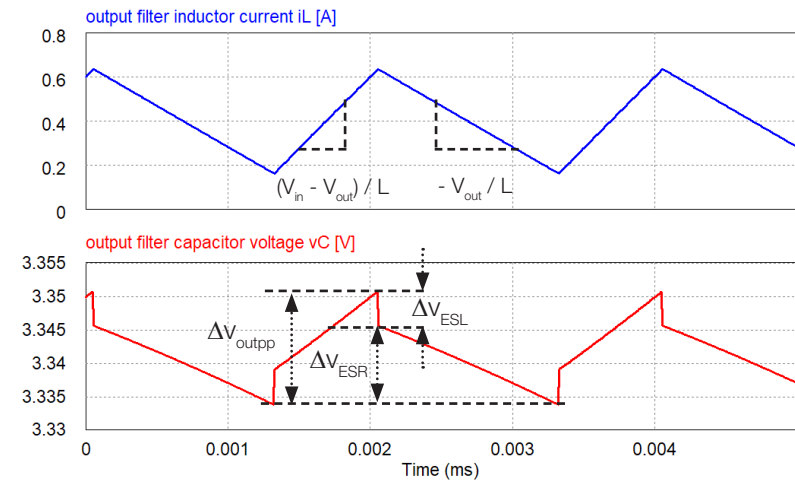


Figure 3.4. Impact of parasitic inductance on electrolytic capacitor voltage

Figure 3.4 refers to an electrolytic capacitor. The amplitude ΔV_{ESL} of the voltage step caused by the ESL on the output ripple voltage waveform is given by:

$$(6) \quad \Delta V_{ESL} = ESL [(V_{in} - V_{out}) / L - (-V_{out}) / L] = ESL V_{in} / L$$

where ESL is the equivalent series parasitic inductance.



Theory Background (3)

Equation (6) highlights that a smaller inductance L magnifies the effect of parasitic inductance ESL . Indeed, the voltage step ΔV_{ESL} is proportional to the change of the inductor current slope between the rise and fall, highlighted in Equation (6).

Figure 3.5 shows the effect of the ESL on the voltage waveform of a ceramic capacitor.

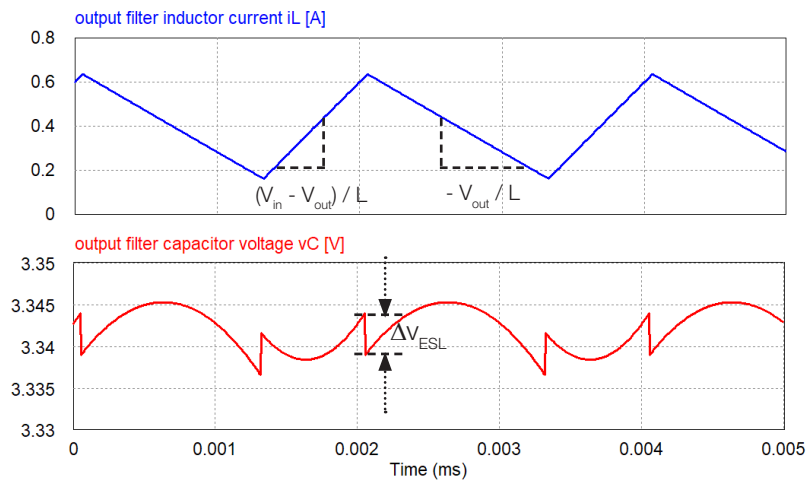


Figure 3.5. Impact of parasitic inductance on ceramic capacitor voltage

It is worth mentioning that the impact of the parasitic inductance ESL on the electrolytic capacitor is worse than the impact on the ceramic capacitor, in terms of increase of output ripple voltage peak-peak amplitude. In fact, while in the electrolytic capacitor the voltage step ΔV_{ESL} is in phase with the triangle ripple voltage determined by the ESR, in the ceramic capacitor it is characterized by a 90 degrees phase lead with respect to the quasi-sinusoidal ripple voltage determined by the capacitance C_{out} . Moreover, the inherent parasitic inductance ESL is smaller in ceramic capacitors than in electrolytic capacitors. Overall, ceramic capacitors provide better performance than electrolytic capacitors.



Return to previous page by:

Windows: Alt + ←

Mac: ⌘ + ←

However, they are more expensive, have lower capacitances, and their small ESR may have a negative impact on dynamic response, thus requiring extra phase lead to achieve the stability of the closed loop regulator (see [Experiment 5](#) ↗).

Capacitances can resonate with parasitic inductances and cause a ringing on the output voltage. Figure 3.6 shows the resulting waveforms observed in real switching converters.

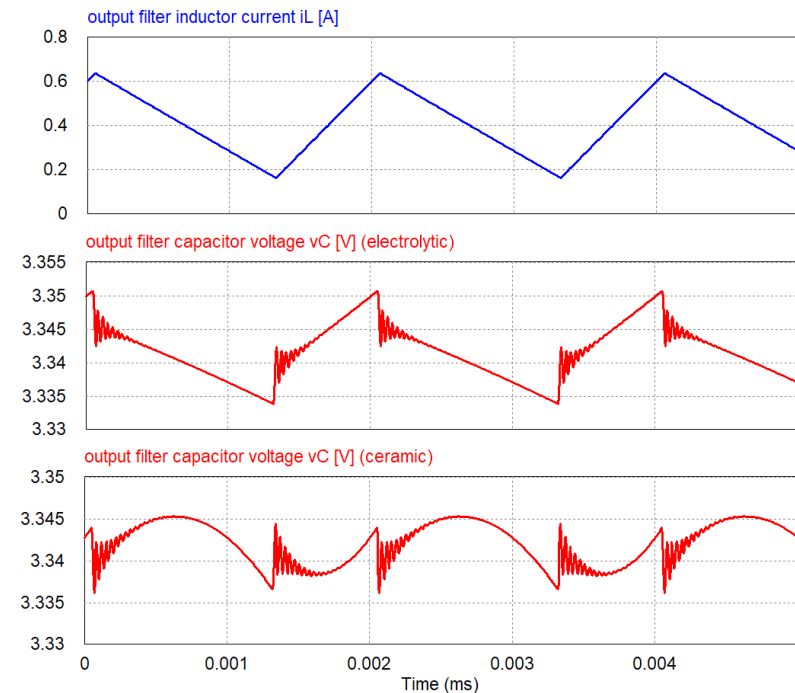


Figure 3.6. Impact of parasitic inductances and capacitances on output voltage

[**Note.** The oscilloscope voltage probes can introduce parasitic inductances, generating large amplitude ringing (Please refer to the [Introduction](#) ↗)]



Case Study

The goal of this experiment is to analyze the output filter capacitor voltage, with different inductors and capacitors, under different operating conditions.

The regulator TPS54160 will be used to perform the experiment, with varying input voltage V_{in} and switching frequency f_{sw} .

The peak-peak amplitude of the inductor ripple current Δi_{Lpp} and output capacitor ripple voltage Δv_{outpp} will be measured. Equations (1) and (2) will be used to evaluate the ESR of the tantalum capacitor C17 and the capacitance C_{out} of the ceramic capacitor C18 available in the TPS54160.

The following test points of the TPS54160 regulator will be used:

- **TP₄₃**, to measure the peak-peak amplitude of inductor current ripple Δi_{Lpp}
- **TP₄₂**, to measure the duty cycle D
- **TP₂**, to measure the input voltage V_{in}
- **TP₂₆**, to measure the DC output voltage V_{out}
- **TP₄₄**, to measure the output voltage ripple ΔV_{outpp}

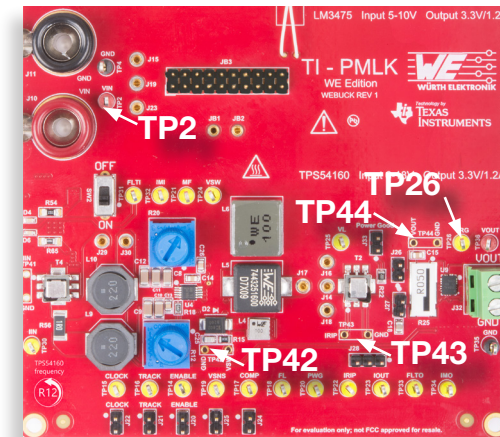


Figure 3.7. Test points used to analyze buck converter output voltage ripple in the TPS54160 regulator



Experiment set-up: configuration

The instruments needed for this experiment are: a DC POWER SUPPLY, an OSCILLOSCOPE and a DC ELECTRONIC LOAD. Figure 3.8 shows the instruments connections. Follow the instructions provided in next page to set-up the **connections**.

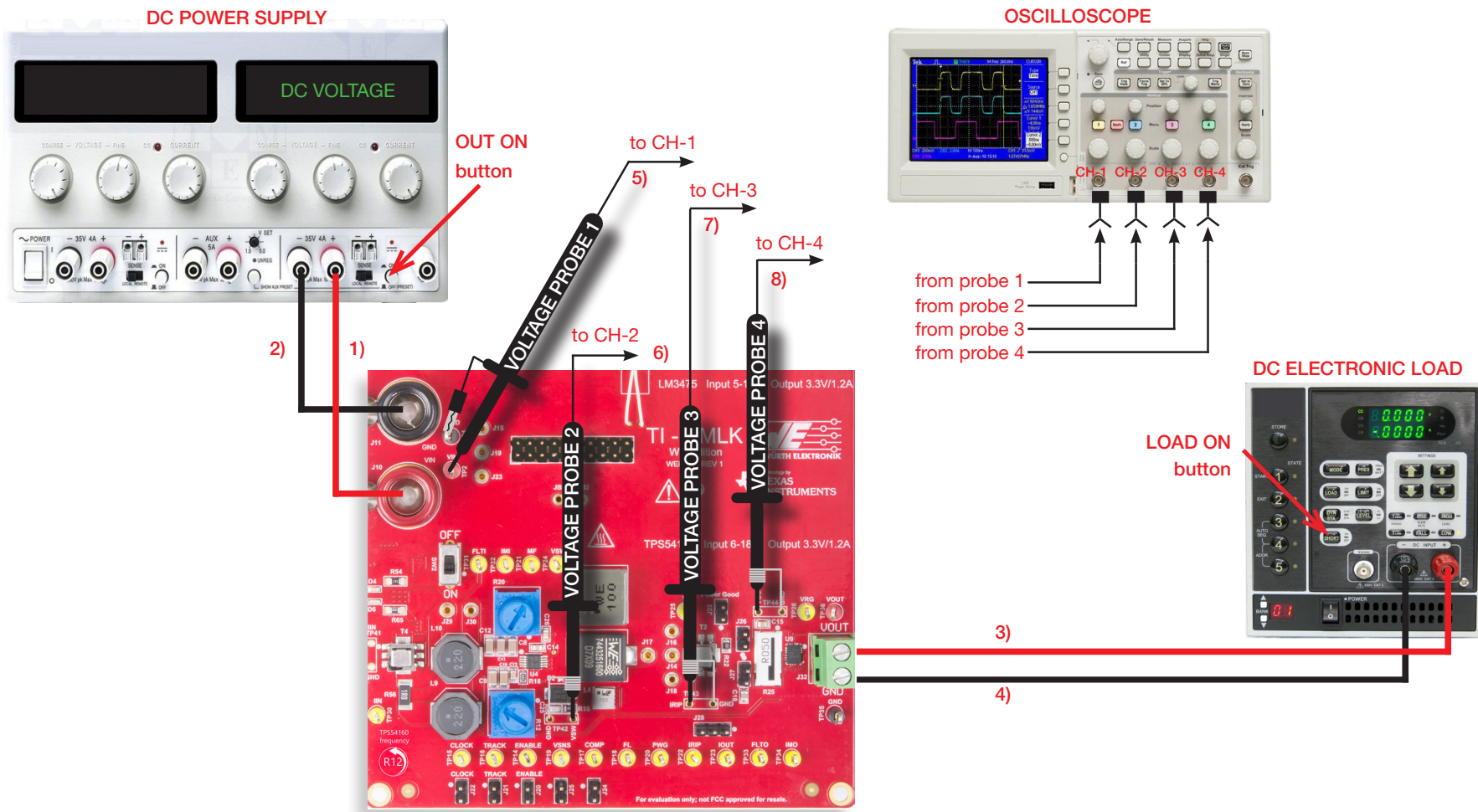


Figure 3.8. Experiment set-up



Experiment set-up: instructions

With all the instruments turned off, make the following **connections**:

1. Connect the POSITIVE (RED) OUTPUT of the DC POWER SUPPLY to the POSITIVE INPUT (VIN) banana connector J_{10} of the TI-PMLK BUCK-WE board
2. Connect the NEGATIVE (BLACK) OUTPUT of the DC POWER SUPPLY to the GROUND (GND) banana connector J_{11} of the TI-PMLK BUCK-WE board
3. Connect the POSITIVE OUTPUT (VOUT) of the screw terminal J_{32} of the TPS54160 regulator to the POSITIVE (RED) INPUT of the ELECTRONIC LOAD.
4. Connect the NEGATIVE (BLACK) INPUT of the ELECTRONIC LOAD to the GROUND (GND) of the screw terminal J_{32} of the TPS54160 regulator
5. Connect a standard voltage probe to channel 1 of the OSCILLOSCOPE, hang its tip to the test point TP_2 and its ground clamp to test point TP_4
6. Connect a voltage probe with ground spring to channel 2 of the OSCILLOSCOPE, insert its positive tip into the hole of test point TP_{42} labeled "VSW" and its ground spring tip into the hole of test point TP_{42} labeled "GND". **[WARNING: DO NOT INVERT THE POSITIVE AND GROUND CONNECTIONS OF THE VOLTAGE PROBE]**
7. Connect a voltage probe with ground spring to channel 3 of the OSCILLOSCOPE, insert its positive tip into the hole of test point TP_{43} labeled "IRIP" and its ground spring tip into the hole of test point TP_{43} labeled "GND". **[WARNING: DO NOT INVERT THE POSITIVE AND GROUND CONNECTIONS OF THE VOLTAGE PROBE]**
8. Connect a voltage probe with ground spring to channel 4 of the OSCILLOSCOPE, insert its positive tip into the hole of test point TP_{44} labeled "VOUT" and its ground spring tip into the hole of test point TP_{44} labeled "GND". **[WARNING: DO NOT INVERT THE POSITIVE AND GROUND CONNECTIONS OF THE VOLTAGE PROBE]**



Test#1: instructions (1)

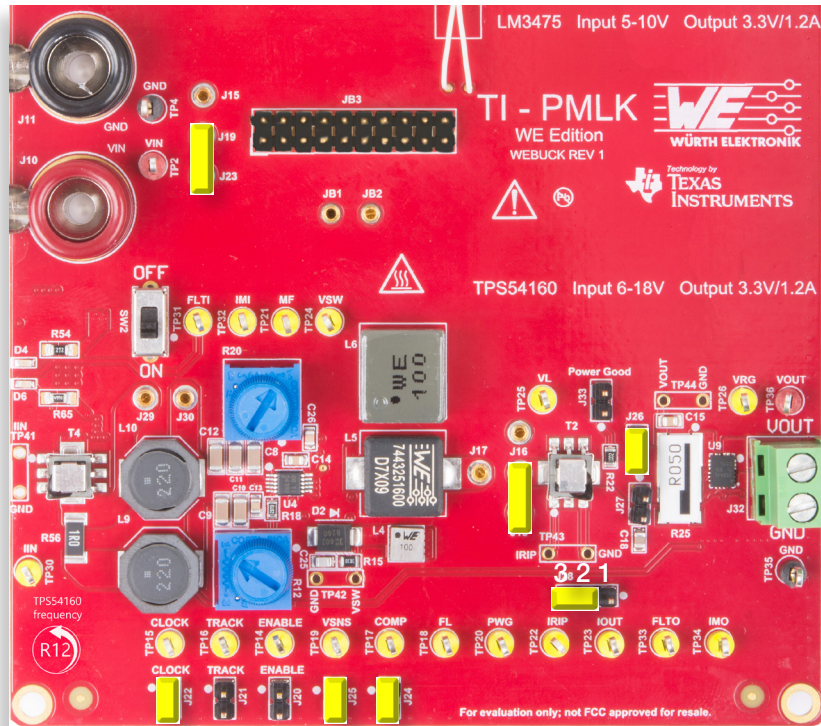


Figure 3.9. TPS54160 jumpers set-up for Test#1

Initial set-up (see Figure 3.9, jumpers not mentioned are open):

- short J_{19} - J_{23} , TPS54160 regulator connected to power input
- short J_{14} - J_{18} , inductor L_4 connected
- short pins 2-3 of J_{28} , separate AC and DC inductor currents
- short J_{22} , switching frequency adjust enabled
- short J_{26} , tantalum output capacitor C17 connected
- short J_{24} and J_{25} , compensation for high voltage
- turn R_{12} left until it stops

Test Procedure:

1. Switch ON the SCOPE, set all channels in DC 1 M Ω coupling mode with 20 MHz BW limit, the time base at 1 μ s/div, the trigger on CH-2 rising edge, the vertical scale to 10 V/div on CH-1 and CH-2, 200 mV/div on CH-3, and 1 V/div on CH-4.
 2. Switch ON the POWER SUPPLY and the ELECTRONIC LOAD
 3. Set the POWER SUPPLY output voltage to 6.0 V, the CURRENT LIMIT to 1.5 A, and switch the POWER SUPPLY "OUT ON" button ON
 4. Set the ELECTRONIC LOAD in CONSTANT CURRENT MODE, switch the "OUT ON" button ON, and rise slowly the output current to 1.2 A.
 5. Under these conditions, you should see the flat 6 V voltage V_{in} on the SCOPE CH-1, the flat 3.34 V output voltage V_{out} on the SCOPE CH-4, and the triangle inductor current ripple Δi_L on the SCOPE CH-3.
 6. Watch the switching frequency f_{sw} of the waveform on the SCOPE CH-2 (switching node voltage V_{sw}), while turning the knob of trimmer R12, until you get $f_{sw} = 300$ kHz. Under these conditions, you should see the inductor AC ripple current triangle waveform on the SCOPE CH-3, with about 460 mA peak-peak amplitude (as the current sensor gain is 1 A/V, the voltage reading provides directly the current). Set 4 or 8 sweeps average acquisition mode on the SCOPE CH-3 to get a less noisy waveform, if needed.
- [WARNING. If the measurements do not look as described above, switch OFF the "OUT ON" button of the ELECTRONIC LOAD and POWER SUPPLY, check the connections, the jumpers setup, the instruments setup and repeat the procedure]**
7. Set the SCOPE CH-4 in AC 1 M Ω coupling mode and the vertical scale to 20 mV/div.



Test#1: instructions (2)

8. Check the DC POWER SUPPLY, and adjust it by using the fine regulation knob, if needed.
9. Measure the amplitude of the peak-peak inductor ripple current Δi_{Lpp} on the SCOPE CH-3, and record the measured values in Table 3.1.
10. Measure the amplitude of the peak-peak output voltage ripple voltage Δv_{outpp} on the SCOPE CH-4, and record the measured values in Table 3.1.
11. Measure the amplitude of the *ESL* step voltage Δv_{ESL} on the SCOPE CH-4 (see Figure 3.10 and 3.11), and record the measured values in Table 3.1.
12. Repeat the steps 8 to 11, by increasing the input voltage of 3 V steps, up to 18 V.
13. Watch the switching frequency f_{sw} of the waveform on the SCOPE CH-2, while turning the knob of trimmer R12, until you get $f_{sw} = 450$ kHz, and adjust the POWER SUPPLY voltage until you read 6 V on the SCOPE CH-1.
14. Repeat the steps 8 to 12.
15. Reduce the current of the ELECTRONIC LOAD to 0.0 A, switch its “LOAD ON” button OFF, and switch the POWER SUPPLY “OUT ON” button OFF.
16. Short J_{14} - J_{17} to connect the inductor L5, repeat the steps 3 to 14, and record the measurement results in Table 3.2.
17. Reduce the current of the ELECTRONIC LOAD to 0.0 A, switch its “LOAD ON” button OFF, and switch the POWER SUPPLY “OUT ON” button OFF.
18. Switch the ELECTRONIC LOAD and the POWER SUPPLY OFF.

Figure 3.10 and 3.11 show the expected inductor ripple current and capacitor ripple voltage with inductor L4, at $f_{sw} = 300$ kHz, with capacitor C17, at $V_{in} = 6$ V and $V_{in} = 18$ V, respectively. Figure 3.11 highlights the heavier impact of the ESL on the output ripple voltage at higher input voltage (4 mV @ $V_{in} = 6$ V vs 12 mV @ $V_{in} = 18$ V).

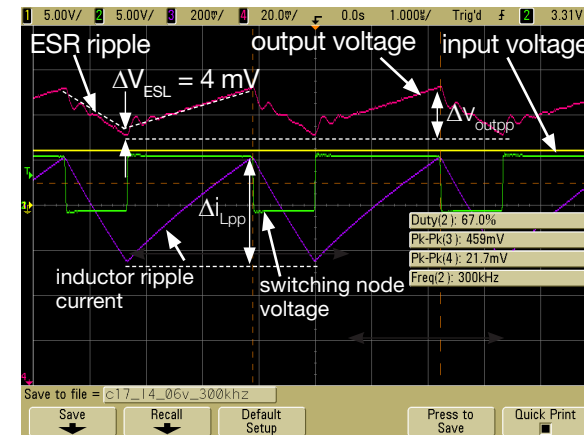


Figure 3.10. Measured waveforms in Test#1 with inductor L4 at 6V input voltage

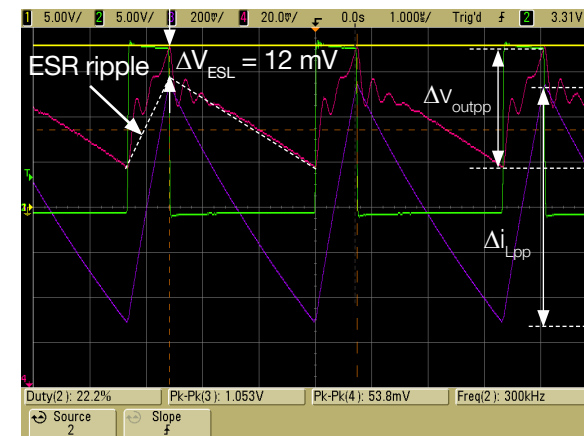


Figure 3.11. Measured waveforms in Test#1 with inductor L4 at 18V input voltage



Test#1: measure and calculate

Collect in Tables 3.1 and 3.2 the measured values of the input voltage V_{in} , the amplitude of peak-peak inductor ripple current Δi_{Lpp} , the amplitude of peak-peak output ripple voltage Δv_{outpp} , and the amplitude of the *ESL* step voltage Δv_{ESL} , and calculate the equivalent series resistance $ESR = (\Delta v_{outpp} - \Delta v_{ESL}) / \Delta i_{Lpp}$ of the tantalum capacitor.

[**Note.** The ESL can be estimated by measuring the step voltage Δv_{ESL} at $V_{in} = 18$ V, when it is better visible. Given Δv_{ESL} , from Equation (6)  we have $ESL = \Delta v_{ESL} L / V_{in}$. At $V_{in} = 18$ V we have about $\Delta v_{ESL} \approx 12$ mV, so that $ESL = 12 \text{ mV} \times 10 \text{ } \mu\text{H} / 18 \text{ V} \approx 6.7 \text{ nH}$.]

Table 3.1. TPS54160 regulator output ripple voltage, with tantalum capacitor C17 and 10 μH inductor L4, at 1.2 A load current

ind.	f_{sw} [kHz]	300					450				
	V_{in} [V]	6	9	12	15	18	6	9	12	15	18
L4	Δi_{Lpp} [mA]										
	Δv_{outpp} [mV]										
	Δv_{ESL} [mV]										
	ESR [m Ω]										

Table 3.2. TPS54160 regulator output ripple voltage, with tantalum capacitor C17 and 16 μH inductor L5, at 1.2 A load current

ind.	f_{sw} [kHz]	300					450				
	V_{in} [V]	6	9	12	15	18	6	9	12	15	18
L5	Δi_{Lpp} [mA]										
	Δv_{outpp} [mV]										
	Δv_{ESL} [mV]										
	ESR [m Ω]										



Test#2: instructions (1)

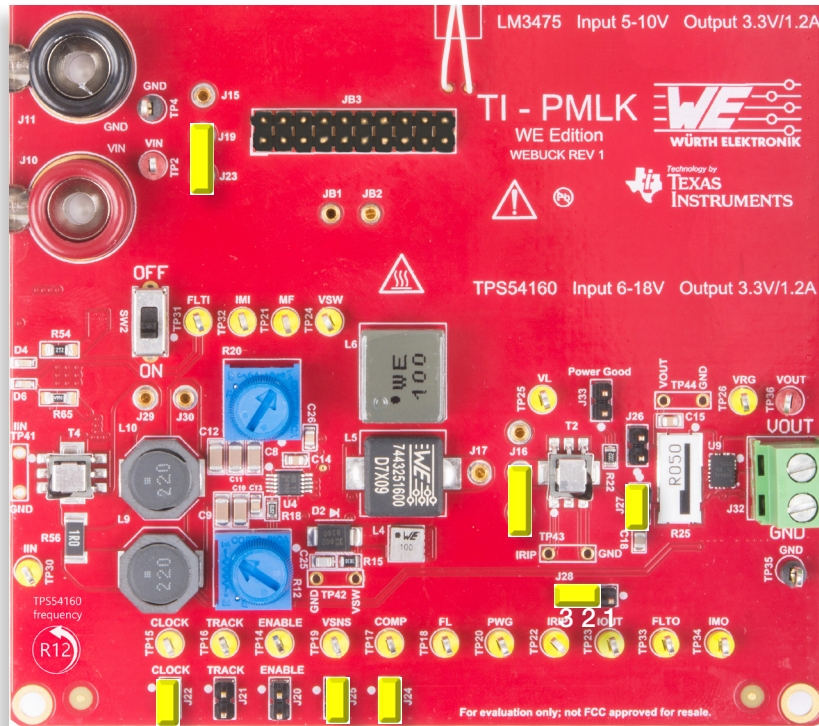


Figure 3.12. TPS54160 jumpers set-up for Test#2

Initial set-up (see Figure 3.12, jumpers not mentioned are open):

- short J_{19} - J_{23} , TPS54160 regulator connected to power input
- short J_{14} - J_{18} , inductor L4 connected
- short pins 2-3 of J_{28} , separate AC and DC inductor currents
- short J_{22} , switching frequency adjust enabled
- short J_{27} , ceramic output capacitor C18 connected
- short J_{24} and J_{25} , compensation for C18
- turn R_{12} left until it stops

Test Procedure:

1. Switch ON the SCOPE, set all channels in DC $1\text{M}\Omega$ coupling mode with 20 MHz BW limit, the time base to $1\ \mu\text{s}/\text{div}$, the trigger on CH-2 rising edge, the vertical scale to 10 V/div on CH-1 and CH-2, 200 mV/div on CH-3, and 1 V/div on CH-4.
2. Switch ON the POWER SUPPLY and the ELECTRONIC LOAD.
3. Set the POWER SUPPLY output voltage at 6V, the CURRENT LIMIT at 1.5 A, and switch the POWER SUPPLY "OUT ON" button ON.
4. Set the ELECTRONIC LOAD in CONSTANT CURRENT MODE, switch the "OUT ON" button ON, and rise slowly the output current to 1.2 A.
5. Under these conditions, you should see the flat 6 V voltage V_{in} on the SCOPE CH-1, the flat 3.34 V output voltage V_{out} on the SCOPE CH-4, and the triangle inductor current ripple ΔI_L on the SCOPE CH-3.
6. Watch the switching frequency f_{sw} of the waveform on the SCOPE CH-2 (switching node voltage V_{sw}), while turning the knob of trimmer R12, until you get $f_{sw} = 300\ \text{kHz}$. Under these conditions, you should see the inductor AC ripple current triangle waveform on the SCOPE CH-3, with about 460 mA peak-peak amplitude (as the current sensor gain is 1 A/V, the voltage reading provides directly the current). Set 4 or 8 sweeps average acquisition mode on the SCOPE CH-3 to get a less noisy waveform, if needed.
7. Set the SCOPE CH-4 in AC $1\ \text{M}\Omega$ coupling mode and the vertical scale to 20 mV/div.

[WARNING. If the measurements do not look as described above, switch OFF the "OUT ON" button of the ELECTRONIC LOAD and POWER SUPPLY, check the connections, the jumpers setup, the instruments setup and repeat the procedure]



Test#2: instructions (2)

8. Check the DC POWER SUPPLY, and adjust it by using the fine regulation knob, if needed.
9. Measure the amplitude of the peak-peak inductor ripple current Δi_{Lpp} on the SCOPE CH-3, and record the measured values in Table 3.3.
10. Measure the amplitude of the peak-peak output voltage ripple voltage Δv_{outpp} on the SCOPE CH-4, and record the measured values in Table 3.3.
11. Repeat the steps 8 to 10, by increasing the input voltage of 3 V steps, up to 18 V.
12. Watch the switching frequency f_{sw} of the waveform on the SCOPE CH-2, while turning the knob of trimmer R12, until you get $f_{sw} = 450$ kHz, and adjust the POWER SUPPLY voltage until you read 6V on the SCOPE CH-1.
13. Repeat the steps 8 to 11.
14. Reduce the current of the ELECTRONIC LOAD to 0.0 A, switch its “LOAD ON” button OFF, and switch the POWER SUPPLY “OUT ON” button OFF.
15. Short J_{14} - J_{17} to connect the inductor L5, repeat the steps 3 to 13, and record the measurement results in Table 3.4.
16. Reduce the current of the ELECTRONIC LOAD to 0.0 A, switch its “LOAD ON” button OFF, and switch the POWER SUPPLY “OUT ON” button OFF.
17. Switch the ELECTRONIC LOAD and the POWER SUPPLY OFF.

Figure 3.13 and 3.14 show the expected inductor ripple current and capacitor ripple voltage with inductor L4, at $f_{sw} = 300$ kHz, with capacitor C18, at $V_{in} = 6$ V and $V_{in} = 18$ V, respectively. Comparing Figures 3.13 and 3.14 to Figures 3.10 and 3.11 relevant to Test #1 highlights that the *ESL* of ceramic capacitor is negligible compared to tantalum capacitor, as no step is visible on the output ripple voltage.

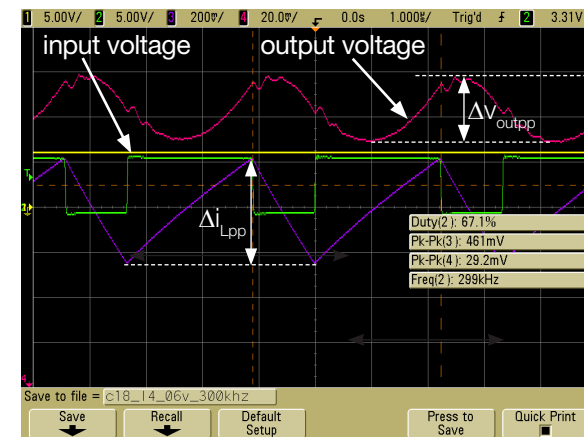


Figure 3.13. Measured waveforms in Test#2 with inductor L4 at 6 V input voltage

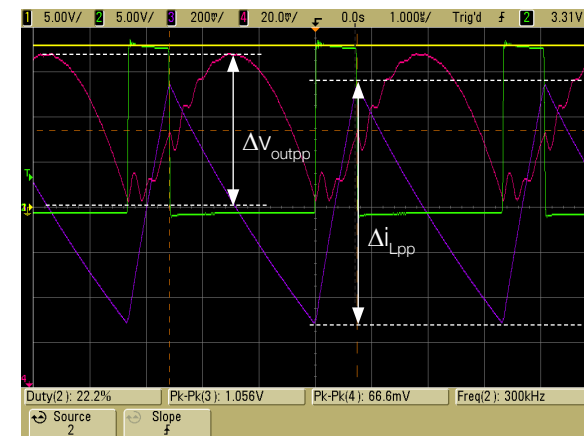


Figure 3.14. Measured waveforms in Test#2 with inductor L4 at 18 V input voltage



Test#2: measure and calculate

Collect in Tables 3.3 and 3.4 the measured values of the input voltage V_{in} , the amplitude of peak-peak inductor ripple current Δi_{Lpp} , and the amplitude of peak-peak output ripple voltage Δv_{outpp} , and evaluate the capacitance of the ceramic capacitor $C_{out} = \Delta i_{Lpp} / (8 \Delta V_{outpp} f_{sw})$.

Table 3.3 TPS54160 regulator output ripple voltage, with ceramic capacitor C18 and 10 μ H inductor L4, at 1.2 A load current

ind.	f_{sw} [kHz]	300					450				
	V_{in} [V]	6	9	12	15	18	6	9	12	15	18
L4	Δi_{Lpp} [mA]										
	Δv_{outpp} [mV]										
	C_{out} [μ F]										

Table 3.4. TPS54160 regulator output ripple voltage, with ceramic capacitor C18 and 16 μ H inductor L5, at 1.2 A load current

ind.	f_{sw} [kHz]	300					450				
	V_{in} [V]	6	9	12	15	18	6	9	12	15	18
L5	Δi_{Lpp} [mA]										
	Δv_{outpp} [mV]										
	C_{out} [μ F]										



Observe and Answer

1 How does the peak-peak amplitude of the output ripple voltage vary as the input voltage increases?

it increases

it decreases

other: _____

Please comment your answer: _____

2 How do the inductors influence the peak-peak amplitude of the output ripple voltage?

the amplitude is larger with L4

the amplitude is larger with L5

other: _____

Please comment your answer: _____

3 How does the switching frequency f_{sw} influence the peak-peak amplitude of the output ripple voltage?

the amplitude is larger with higher f_{sw}

the amplitude is larger with lower f_{sw}

other: _____

Please comment your answer: _____

4 How does the capacitor influence the peak-peak amplitude of the output ripple voltage?

the amplitude is larger with C17

the amplitude is larger with C18

other: _____

Please comment your answer: _____



Discussion (1)

The measurement results show the joint impact of inductors and capacitors parameters and of parasitics on the output ripple voltage.

In Tests #1 and #2, we observe that the 10 μH inductor L4 causes a larger peak-peak output ripple voltage compared to the 16 μH inductor L5, with both capacitors C17 and C18. This is the consequence of the larger peak-peak amplitude of the inductor ripple current determined by the smaller inductance of L4.

In Tests #1 and #2, we observe the effect of parasitics, causing the high-frequency ringing on the output voltage at switching instants. The ringing influences the peak-peak amplitude of output ripple voltage, and it influences the estimation of the *ESR* of capacitor C17 and of the capacitance of capacitor C18. For example, Figures 3.15(a)-(c) show that, as the input voltage increases from 6 V to 12 V, the ringing caused by parasitics is increasingly influential on the valley of the output ripple voltage of ceramic capacitor C18. For the input voltage between 6 V and 8 V, the peak-peak output ripple voltage is not much influenced by the ringing caused by parasitics. These are preferred conditions to better estimate the capacitance of the ceramic capacitor.

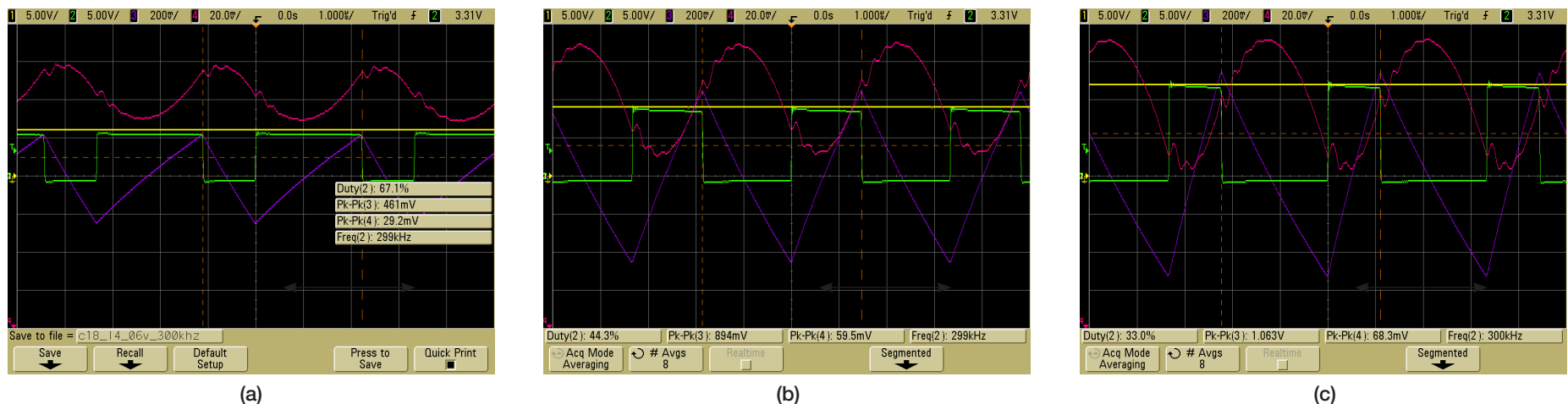


Figure 3.15. Waveforms in with 10 μF ceramic capacitor C18, inductor L4, $f_{sw} = 300 \text{ kHz}$ and (a) 6 V, (b) 9 V and (c) 12 V input voltage

In Test #1, we observe the impact of the inductor on the step voltage caused by the *ESL* of the tantalum capacitor C17 on the output ripple voltage at switching instants. In particular, we see that a larger inductance reduces the impact of the *ESL*, and that the impact of the *ESL* increases at higher input voltage. Therefore, the estimation of the *ESR* of the tantalum capacitor C17 can be better performed with larger inductance and lower input voltage.

Overall, the Tests #1 and #2 show a larger influence of the inductor on tantalum capacitor ripple voltage compared to ceramic capacitor, mainly because of the *ESL* effect. This involves that a larger inductance can be needed to keep the output ripple voltage below the given specification limit if capacitors with high *ESR*, like electrolytic capacitors, are used. Nevertheless, the high *ESR* of electrolytic capacitors helps in the control loop design when high cross-over frequency is required.



Discussion (2)

Figures 3.16 to 3.19 show the datasheet characteristics of the ceramic capacitor C18, which highlight that the real capacitance of a ceramic capacitor can be much lower than its nominal value, due to DC bias, tolerance and thermal effects.

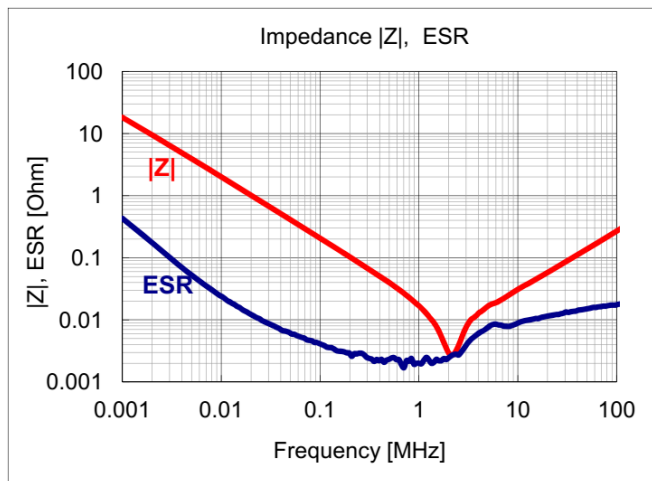


Figure 3.16. Impedance and ESR of capacitor C18 vs frequency

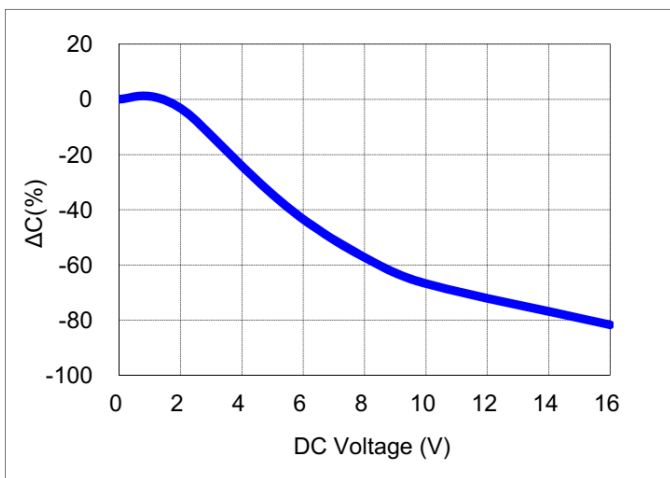


Figure 3.17. Capacitance de-rating of capacitor C18 vs DC bias voltage

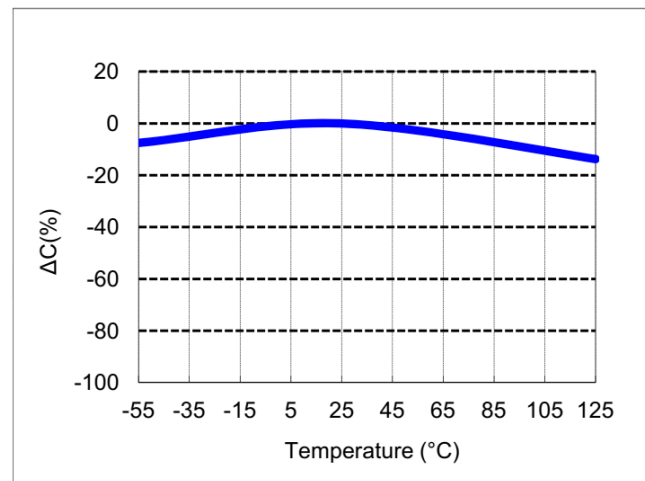


Figure 3.18. Capacitance de-rating of capacitor C18 vs temperature

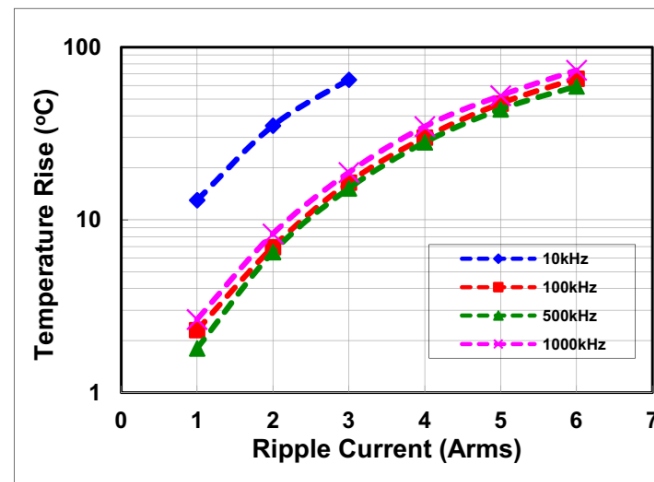


Figure 3.19. Temperature rise of capacitor C18 vs ripple current



Discussion (3)

Figure 3.16 shows that the *ESR* of the ceramic capacitor C18 is minimum in the range of frequency from 300 kHz to 2 MHz, wherein its value is approximately 1 mΩ, whereas the total impedance *Z* is about ten times larger. This confirms that the impedance $1 / (2 \pi f_{sw} C_{out})$ of the capacitance C_{out} is dominant with respect to the *ESR* in the switching frequency range [300 kHz, 450 kHz] adopted for Test #2.

Figure 3.17 shows that the capacitance of the ceramic capacitor C18 is affected by a de-rating of about -20% at the 3.3 V DC voltage, which is the voltage applied to the capacitor in the TPS54160 regulator.

Figures 3.18 and 3.19 show that a further de-rating of the capacitance of the ceramic capacitor C18 can derive from the increase of its temperature, which depends on the switching frequency and on the amplitude of the rms ripple current, given by $\Delta i_{Lpp} / \sqrt{12}$.

Finally, the the ceramic capacitor C18 is affected by a 10% tolerance.

The combined effects of the above influence factors explain why in Test #2 we obtain an evaluation of C_{out} between 6.2 μF and 7.2 μF, which is much lower than the nominal 10 μF capacitance of capacitor C18.

[Note. The accuracy of measurements influence the estimation of the capacitance of capacitor C18. In this regard, voltage probes compensation is recommended before performing the measurements with the oscilloscope, in particular for probes used to measure the inductor ripple current and the output ripple voltage].

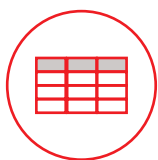


Expansion Activities

- Repeat the experiment with inductor L6 of TPS54160 regulator.
- Repeat the experiment with TPS54160 load current lower than 1.2 A.

[**Note. 1)** The TPS54160 can operate in discontinuous conduction mode at high input voltage and low load current. The ripple current and ripple voltage equations are different. **2)** The TPS54160 regulator features a skip-cycle mode, determining an automatic reduction of switching frequency at low load current. This may result in discontinuous conduction mode operation. **3)** See **Experiment 5** [↗](#) to investigate the impact of inductors on discontinuous conduction mode].

- Repeat the experiment with LM3475 regulator.



Tables of measurements (1)

The tables shown in this section are filled with values obtained by performing measurements on the TI-PMLK BUCK-WE board according to the previous test instructions. **[WARNING. The values reported in the tables are purely indicative. The results of your measurements on the TI-PMLK BUCK-WE board can be different due to tolerances and thermal effects of power components, and can be influenced by the accuracy and calibration of the instruments].**

Table 3.1. TPS54160 regulator output ripple voltage, with tantalum capacitor C17 and 10 μ H inductor L4, at 1.2 A load current

ind.	f_{sw} [kHz]	300					450				
	V_{in} [V]	6	9	12	15	18	6	9	12	15	18
L4	Δi_{Lpp} [mA]	536	887	1059	1162	1226	360	599	717	785	833
	Δv_{outpp} [mV]	26	41	49	55	61	19	30	37	42	48
	Δv_{ESL} [mV]	4	6	8	10	12	4	6	8	10	12
	ESR [m Ω]	41	39	39	39	40	41	41	41	41	43

Table 3.2. TPS54160 regulator output ripple voltage, with tantalum capacitor C17 and 16 μ H inductor L5, at 1.2 A load current

ind.	f_{sw} [kHz]	300					450				
	V_{in} [V]	6	9	12	15	18	6	9	12	15	18
L5	Δi_{Lpp} [mA]	312	509	600	656	694	211	343	405	443	470
	Δv_{outpp} [mV]	15	25	29	32	35	12	19	22	26	28
	Δv_{ESL} [mV]	2.5	3.8	5.0	6.3	7.5	2.5	3.8	5.0	6.3	7.5
	ESR [m Ω]	41	41	40	39	40	44	44	43	44	44



Tables of measurements (2)

The tables shown in this section are filled with values obtained by performing measurements on the TI-PMLK BUCK-WE board according to the previous test instructions. **[WARNING. The values reported in the tables are purely indicative. The results of your measurements on the TI-PMLK BUCK-WE board can be different due to tolerances and thermal effects of power components, and can be influenced by the accuracy and calibration of the instruments].**

Table 3.3 TPS54160 regulator output ripple voltage, with ceramic capacitor C18 and 10 μ H inductor L4, at 1.2 A load current

ind.	f_{sw} [kHz]	300					450				
	V_{in} [V]	6	9	12	15	18	6	9	12	15	18
L4	Δi_{Lpp} [mA]	538	892	1065	1165	1233	360	603	717	786	833
	Δv_{outpp} [mV]	35	56	66	73	76	15	23	28	33	35
	C_{out} [μ F]	6.4	6.6	6.8	6.7	6.8	6.6	7.2	7.1	6.7	6.6

Table 3.4. TPS54160 regulator output ripple voltage, with ceramic capacitor C18 and 16 μ H inductor L5, at 1.2 A load current

ind.	f_{sw} [kHz]	300					450				
	V_{in} [V]	6	9	12	15	18	6	9	12	15	18
L5	Δi_{Lpp} [mA]	314	512	604	662	697	211	343	406	443	470
	Δv_{outpp} [mV]	21	33	39	42	44	9	14	16	19	21
	C_{out} [μ F]	6.2	6.5	6.5	6.6	6.5	6.3	6.8	6.9	6.6	6.2

Experiment 4

The goal of this experiment is to analyze the input filtering functions of inductors in DC-DC switching converters. The impact of the inductance on input ripple current is investigated.

The LM3475 and TPS54160 buck regulators are used for this experiment.



Theory Background (1)

Figure 4.1 shows a simplified schematic of the LM3475 and TPS54160 buck regulators power stage, including current sensing, input filter and eFuses.

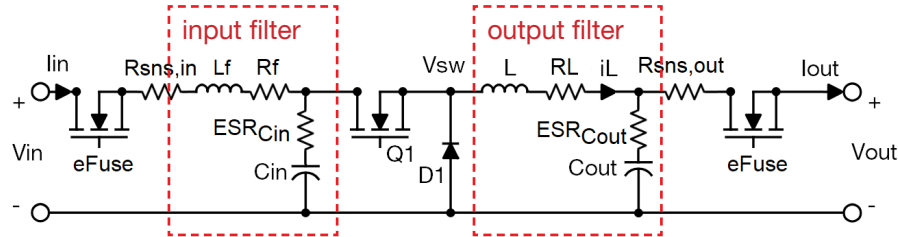


Figure 4.1. Buck converter simplified schematic

Figure 4.2 shows an example of the theoretical input current waveforms of a buck regulator, in steady-state operation at 10 V input voltage, 200 mA load current, and 500kHz switching frequency. Figure 4.2 highlights that, while the MOSFET current is affected by a large peak-peak ripple current at switching frequency, the input current is expected to have a much smaller peak-peak ripple.

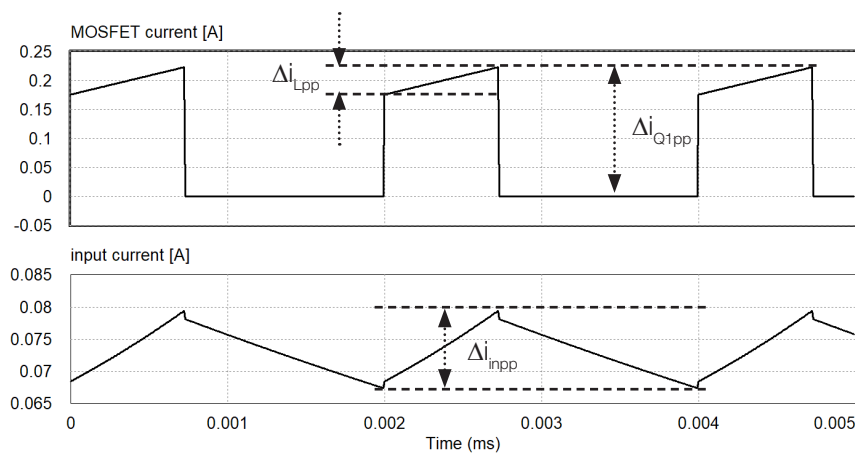


Figure 4.2. MOSFET and input current waveforms of a buck regulator



Return to previous page by:

Windows:



Mac:



In the **input filter**, the function of the input inductor is to increase the line impedance at high frequency. This action helps reducing the size of the input capacitor C_{in} needed to bypass the MOSFET square-wave ripple current, and to ensure the compliance of the peak-peak input ripple current Δi_{inpp} with the maximum conducted limit $\Delta i_{inpp,max}$, imposed by the Electromagnetic Compatibility (EMC) norms in force in the country where the switching regulator is used. This kind of input filter is called **differential mode filter**, as it filters the differential mode noise caused by the inherent switch-mode operation of DC-DC buck regulators. The capacitor and the inductor of the input filter are selected with inductance L_f and capacitance C_{in} ensuring the required attenuation $Att_{f_{sw}}$ at the switching frequency f_{sw} , which can be calculated by means of the simplified Equation (1):

$$(1) \quad Att_{f_{sw}} = \Delta i_{Q1pp} @ f_{sw} / \Delta i_{inpp,max} @ f_{sw} \quad (*)$$

The resonance frequency f_o of the input filter ensuring the required attenuation $Att_{f_{sw}}$ at the switching frequency f_{sw} is given by Equation (2):

$$(2) \quad f_o = 1 / [2 \pi \sqrt{ (L_f C_{in}) }] = f_{sw} / \sqrt{ (Att_{f_{sw}})}$$

Given the capacitance C_{in} , the inductance required to achieve the required attenuation $Att_{f_{sw}}$ at the switching frequency f_{sw} is given by Equation (3):

$$(3) \quad L_{fdes} = Att_{f_{sw}} / (4 \pi^2 C_{in} f_{sw}^2)$$

The commercial inductor to be selected for the input filter has to be characterized by a nominal inductance $L_{nom} > L_{fdes}$, by a saturation current $I_{sat} > I_{inDC,max}$, where $I_{inDC,max}$ is the maximum input DC current of the converter at maximum load current and minimum input voltage, and by a winding DC resistance R_{LDC} dissipating a power $R_{LDC} (I_{inDC,max})^2$ complying with the converter efficiency specifications.

(*) The real differential mode noise generated by the converter in the 150 kHz to 30 MHz frequency range (this range can change with the Norm) must be measured by means of a LISN and a spectrum analyzer, to perform a rigorous design of the differential mode filter



Theory Background (2)

The AC losses of the input filter inductor are very small, and can be neglected. Indeed, the input AC ripple current, resulting from the action of the inductor itself, is very small.

The input filter designed by means of the elementary procedure outlined through Equations (1), (2) and (3) may cause some instability issue in the buck regulator, if the resulting output impedance of the input filter is too high compared to the input impedance of the buck converter power stage, comprised of the switching cell Q1-D1 and of the output filter $L-C_{out}$. The input filter, indeed, needs a damping in order to limit its quality factor Q within a safety margin, thus preventing ringing and instability issues.

An effective way to damp the input filter is to add an L_d-R_d branch in parallel to the filter inductor L_f , as shown in Figure 4.3

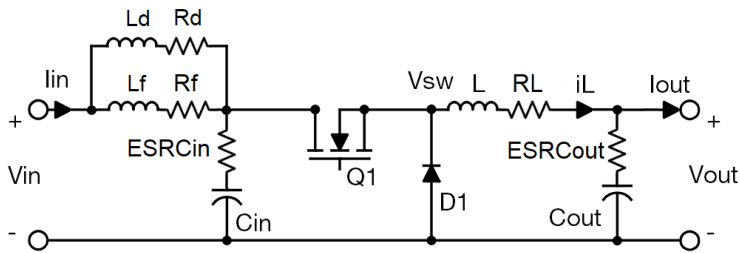


Figure 4.3. Buck converter with damped input filter

In principle, a resistor in parallel to the inductor L_f could be sufficient to damp the input filter, but it would involve a degradation of the filter efficiency and a degradation of the attenuation at switching frequency. The inductor L_d in series to R_d helps achieving a trade-off between efficiency and attenuation.

Assuming that $L_f = L_{fdes}$, where L_{fdes} is given by Equation (3), if we take a damping inductor with inductance $L_d = \alpha L_f$, where α can be greater or smaller than 1, and a damping resistor with resistance $R_d << 2 \pi f_{sw} L_d$, we have an

equivalent filter inductance:

$$(4) \quad L_{eq} = L_{fdes} / (1 + 1 / \alpha)$$

resulting in a degradation of the attenuation at the switching frequency f_{sw} of a factor $1/(1+1/\alpha)$, according to Equation (3). In order to prevent such degradation, the inductance L_f must be increased by a factor $(1+1/\alpha)$. The values of L_f and L_d ensuring that $L_{eq} = L_{fdes}$ are given by Equations (5):

$$(5.a) \quad L_f = (1 + 1 / \alpha) L_{fdes} = (1 + 1 / \alpha) Att_{fsw} / (4 \pi^2 C_{in} f_{sw}^2)$$

$$(5.b) \quad L_d = (1 + \alpha) L_{fdes} = (1 + \alpha) Att_{fsw} / (4 \pi^2 C_{in} f_{sw}^2)$$

Therefore, an increase of the damping inductance L_d results in a decrease of the filter inductance L_f . If the damping resistance R_d is much larger than the winding DC resistance R_{LfDC} of the filter inductor L_f , the DC input current of the buck converter mostly flows through the filter inductor L_f . This means that it is convenient to take a damping inductor with inductance L_d greater than the inductance L_f of the filter inductor. In fact, due to the very small DC current it must withstand, it can be selected with small saturation current, thus resulting in a very small size inductor. The resulting winding resistance of the damping inductor will likely be much greater than the winding DC resistance R_{LfDC} of the filter inductor L_f , and it can be exploited as damping resistance R_d . This way, the input filter can be damped without a significant increase of parts size and cost. Given the ratio α , the value of the damping resistance R_d determining the maximum damping of the input filter resonance peak is given by Equation (6):

$$(6) \quad R_{d,opt} = 1 / (2 \pi C_{in} f_{sw}) \times \sqrt{[Att_{fsw}(1+\alpha)(3+4\alpha)(1+2\alpha)] / [2(1+4\alpha)]}$$

The optimal damping inductor is characterized by inductance and resistance given by Equations (5.b) and (6), respectively, and by a saturation current $I_{sat} > I_{in,max} R_{LfDC} / (R_{LfDC} + R_{d,opt})$, where $I_{in,max}$ is the maximum DC input current of the buck converter.



Return to previous page by:

Windows:



Mac:





Theory Background (3)

The input filter of the LM3475 regulator is comprised of capacitors C29 to C33, providing total input capacitance $C_{in} = 50 \mu\text{F}$, and inductors L7 (47 μH , max 2.3 Ω) and L8 (22 μH , max 75 m Ω), playing the role of damping inductor L_d and main filter inductor L_f , respectively. The damping inductor L7 has very small size (13.5 mm³) compared to the filter inductor L8 (410 mm³). This results in the 2.3 Ω winding resistance of inductor L7, much larger than the 75 m Ω winding resistance of the inductor L8. The DC input current is then distributed between the two inductors with a percent amount of about 3% to inductor L7 and 97% to inductor L8. The saturation current of inductor L7 is 1.18 A, whereas the saturation current of inductor L8 is 2.3 A. The high resistance of the inductor L7 is used as damping resistance R_d . The two inductors L7 and L8 can be bypassed by shorting J_6 and J_{13} (see page 17 of Introduction). This allows analyzing the LM3475 input filter response $H = \Delta i_{in} / \Delta i_{Q1}$ determined by capacitors C29 to C33 alone, or with the inductors L7 and L8 connected:

$$(7) \quad H_{Cin} = \Delta i_{in} / \Delta i_{Q1} |_{L7, L8 \text{ bypassed}} = 1 / (1 + s R_{in} C_{in})$$

$$(8) \quad H_{LM, CinLin} = \Delta i_{in} / \Delta i_{Q1} |_{L7, L8 \text{ connected}} = 1 / (1 + s Z_{in, LM} C_{in})$$

where R_{in} is the total 170 m Ω resistance of input eFuse and current sensing and:

$$(9) \quad Z_{in, LM} = R_{in} + (R_{L7} + s L_7)(R_{L8} + s L_8) / [R_{L7} + R_{L8} + s(L_7 + L_8)]$$

The input filter of the TPS54160 regulator is comprised of capacitors C8 to C12, providing total input capacitance $C_{in} = 50 \mu\text{F}$, and 22 μH , 75m Ω inductors L9 and L10, playing the role of damping inductor L_d and main filter inductor L_f .

The inductor L9 is connected in series to the 1 Ω external damping resistor R56. The resulting input filter response is given by Equations (10):

$$(10) \quad H_{TPS, CinLin} = \Delta i_{in} / \Delta i_{Q1} |_{L9, L10 \text{ connected}} = 1 / (1 + s Z_{in, TPS} C_{in})$$

where R_{in} is the total 170 m Ω resistance of input eFuse and current sensing and:

$$(12) \quad Z_{in, TPS} = R_{in} + (R_{L9} + R_{56} + s L_9)(R_{L10} + s L_{10}) / [R_{L9} + R_{56} + R_{L10} + s(L_9 + L_{10})]$$

Figure 4.4 shows the Bode plots of the input filter responses H_{Cin} , $H_{LM, CinLin}$ and $H_{TPS, CinLin}$. The plots show that connecting the inductors L7 and L8 provides an improvement of the LM3475 input filter attenuation at high frequency, as the response rolls off -40 dB/decade instead of -20 dB/decade. At 400 kHz frequency (which is the switching frequency used in this experiment) this results in -73.5 dB attenuation with L7 and L8 connected, instead of -26.6 dB attenuation with L7 and L8 bypassed. The Bode plot of TPS54160 input filter response $H_{TPS, CinLin}$ shows that connecting the inductors L9 and L10 also provides an improvement of the filter attenuation at high frequency, as the filter response rolls off -40 dB/decade instead of -20 dB/decade. At 400 kHz frequency this results in -70.8 dB attenuation with L9 and L10 connected instead of -26.6 dB attenuation with L9 and L10 bypassed. The LM3475 input filter provides about 2.7 dB more attenuation.

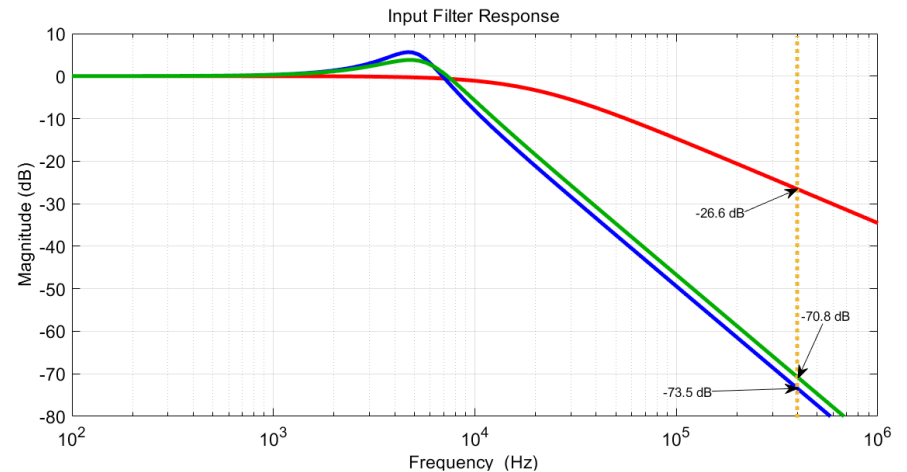


Figure 4.4. LM3475 and TPS54160 input filter responses:

red = H_{Cin} ; blue = $H_{LM, CinLin}$; green = $H_{TPS, CinLin}$



Case Study

The goal of this experiment is to compare the filtering and efficiency performance of the two different input filters of LM3475 and TPS54160 buck regulators, in the same operating conditions. The input ripple current will be analyzed, under different input voltage V_{in} and load current I_{out} , without the input filter inductors and with the input filter inductors. The regulators LM3475 and TPS54160 will be configured to operate in the same voltage, current and frequency conditions.

The following test points of the LM3475 regulator will be used:

- **TP₂**, to measure the input voltage V_{in}
- **TP₂₇**, to measure the output voltage V_{out}
- **TP₃₇**, to measure the peak-peak amplitude of input ripple current Δi_{inpp}
- **TP₃₈**, to observe the switching node voltage V_{sw}

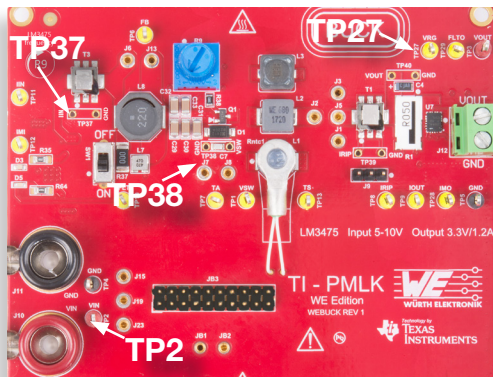


Figure 4.5. Test points used to analyze the LM3475 regulator input filter

The following test points of the TPS54160 regulator will be used:

- **TP₂**, to measure the input voltage V_{in}
- **TP₂₆**, to measure the output voltage V_{out}
- **TP₄₁**, to measure the peak-peak amplitude of input ripple current Δi_{inpp}
- **TP₄₂**, to observe the switching node voltage V_{sw}

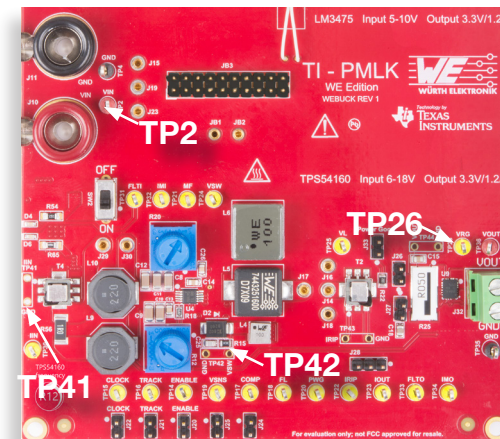


Figure 4.6. Test points used to analyze the TPS54160 regulator input filter



Experiment set-up for LM3475 regulator: configuration

The instruments needed for this experiment are: a DC POWER SUPPLY, four MULTIMETERS, an OSCILLOSCOPE and a DC ELECTRONIC LOAD. Figure 4.7 shows the instruments connections for measurements on LM3475 regulator. Follow the instructions provided in next page to set-up the **connections**.

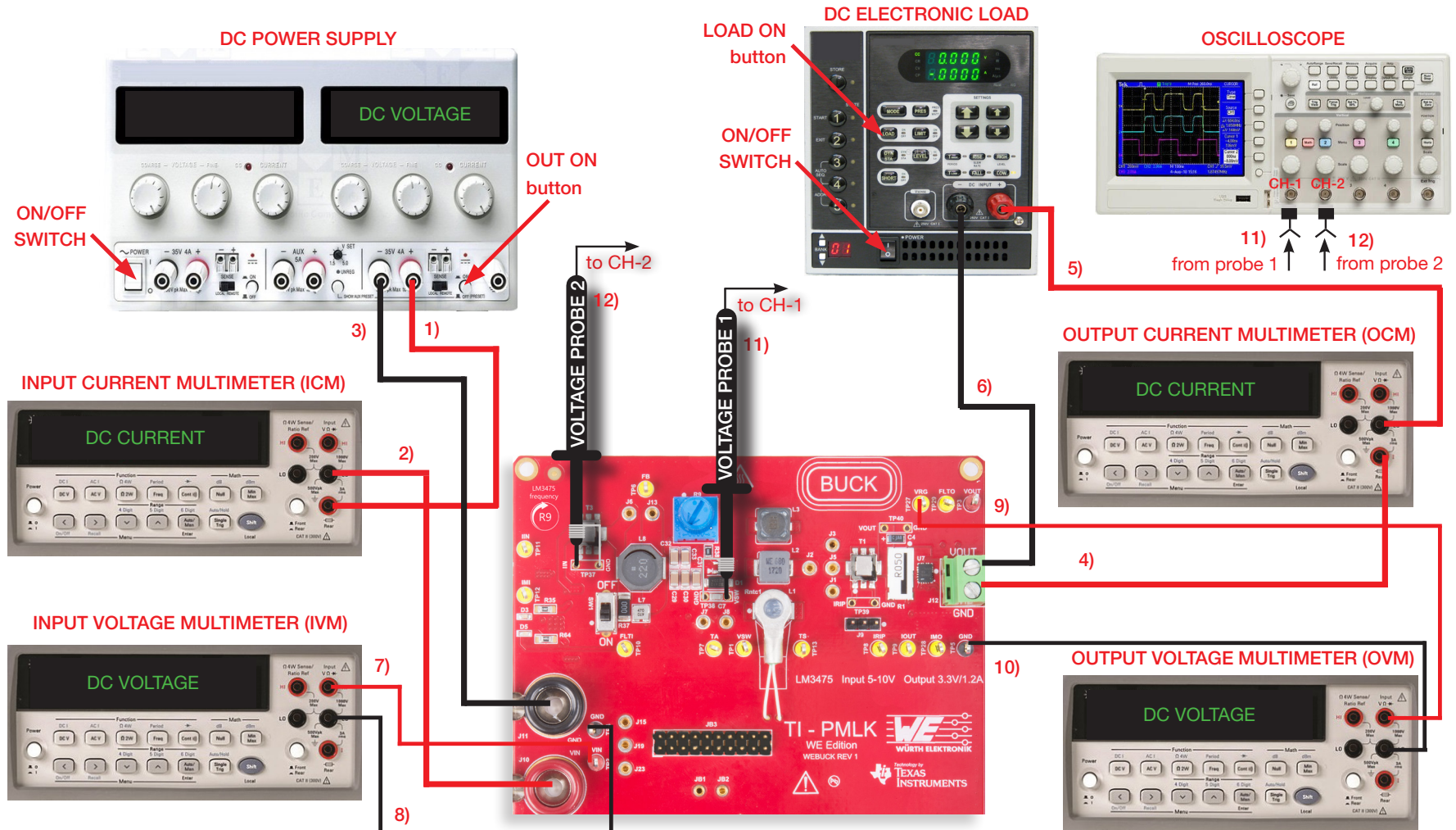


Figure 4.7. Experiment set-up for measurements on LM3475 regulator



Experiment set-up for LM3475 regulator: instructions

With all the instruments turned off, make the following **connections**:

1. Connect the POSITIVE (RED) OUTPUT of the DC POWER SUPPLY to the POSITIVE (RED) CURRENT INPUT of the INPUT CURRENT MULTIMETER (ICM) **[WARNING: THE POSITIVE INPUT OF THE MULTIMETER FOR CURRENT MEASUREMENT IS DIFFERENT FROM THE POSITIVE INPUT FOR VOLTAGE MEASUREMENT]**
2. Connect the NEGATIVE (BLACK) CURRENT INPUT of the INPUT CURRENT MULTIMETER (ICM) to the POSITIVE INPUT (VIN) banana connector J_{10} of the TI-PMLK BUCK-WE board
3. Connect the NEGATIVE (BLACK) OUTPUT of the DC POWER SUPPLY to the GROUND (GND) banana connector J_{11} of the TI-PMLK BUCK-WE board
4. Connect the POSITIVE OUTPUT (VOUT) of the screw terminal J_{12} of the LM3475 regulator to the POSITIVE (RED) CURRENT INPUT of the OUTPUT CURRENT MULTIMETER (OCM) **[WARNING: THE POSITIVE INPUT OF THE MULTIMETER FOR CURRENT MEASUREMENT IS DIFFERENT FROM THE POSITIVE INPUT FOR VOLTAGE MEASUREMENT]**
5. Connect the NEGATIVE (BLACK) CURRENT INPUT of the OUTPUT CURRENT MULTIMETER (OCM) to the POSITIVE (RED) INPUT of the ELECTRONIC LOAD.
6. Connect the NEGATIVE (BLACK) INPUT of the ELECTRONIC LOAD to the GROUND (GND) of the screw terminal J_{12} of the LM3475 regulator
7. Connect the POSITIVE (RED) VOLTAGE INPUT of the INPUT VOLTAGE MULTIMETER (IVM) to the test point TP_2 of the TI-PMLK BUCK-WE board
8. Connect the NEGATIVE (BLACK) VOLTAGE INPUT of the INPUT VOLTAGE MULTIMETER (IVM) to the test point TP_4 of the TI-PMLK BUCK-WE board
9. Connect the POSITIVE (RED) VOLTAGE INPUT of the OUTPUT VOLTAGE MULTIMETER (OVM) to the test point TP_{27} of the LM3475 regulator
10. Connect the NEGATIVE (BLACK) VOLTAGE INPUT of the OUTPUT VOLTAGE MULTIMETER (OVM) to the test point TP_5 of the LM3475 regulator
11. Connect a voltage probe with ground spring to channel 1 of the OSCILLOSCOPE, insert its positive tip into the hole of test point TP_{38} labeled "VSW" and its ground spring tip into the hole of test point TP_{38} labeled "GND". **[WARNING: DO NOT INVERT THE POSITIVE AND GROUND CONNECTIONS OF THE VOLTAGE PROBE]**
12. Connect a voltage probe with ground spring to channel 2 of the OSCILLOSCOPE, insert its positive tip into the hole of test point TP_{37} labeled "IIN" and its ground spring tip into the hole of test point TP_{37} labeled "GND". **[WARNING: DO NOT INVERT THE POSITIVE AND GROUND CONNECTIONS OF THE VOLTAGE PROBE]**



Test#1: instructions (1)

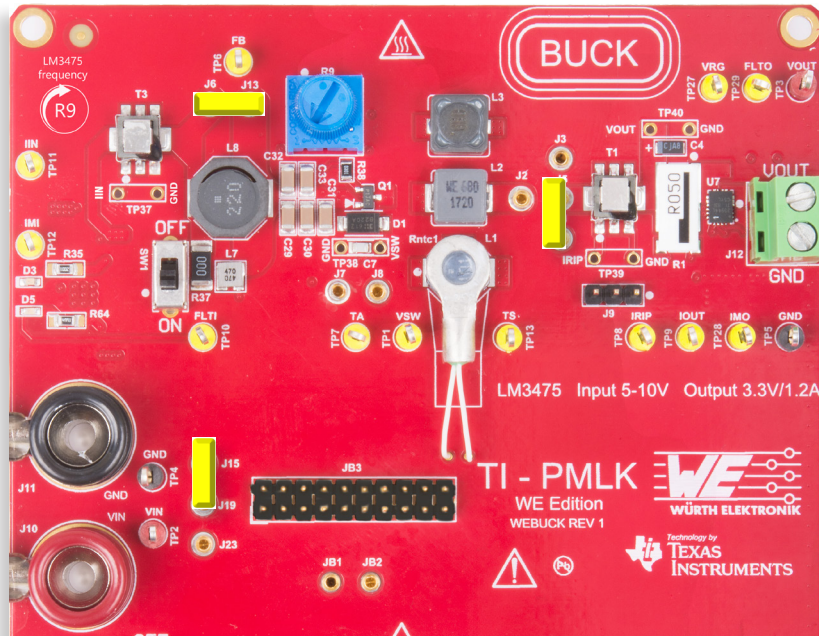


Figure 4.8. LM3475 jumpers set-up for Test#1

Initial set-up (see Figure 4.8, jumpers not mentioned are open):

- short J_{15} - J_{19} , LM3475 regulator connected to power input
- short J_1 - J_5 , inductor L1 connected
- short J_6 - J_{13} , input filter inductors L7 and L8 bypassed
- turn R_9 right until it stops

Test Procedure:

1. Switch ON the SCOPE, set CH-1 and CH-2 in DC 1 M Ω coupling mode with 20 MHz BW limit, the time base to 1 μ s/div, the trigger on CH-1 rising edge, the vertical scale to 5 V/div on CH-1 and 20 mV/div on CH-2.
2. Switch ON the MULTIMETERS, select DC voltage measurement on IVM and OVM, and DC current measurement on ICM and OCM (see Figure 4.7).
3. Switch ON the POWER SUPPLY, set the "OUT ON" button OFF, output voltage at 6.0 V, and CURRENT LIMIT at 1.5 A.
4. Switch ON the ELECTRONIC LOAD, set the "OUT ON" button OFF, CONSTANT CURRENT MODE, and input current at 0.0 A.
5. Switch the POWER SUPPLY "OUT ON" button ON and the ELECTRONIC LOAD "LOAD ON" button ON. Under these conditions, you should see about 3.36 V on OVM display.
6. Slowly increase the ELECTRONIC LOAD current until you read 0.6 A on the OCM. Adjust the DC POWER SUPPLY fine regulation knob, if needed, until you read $V_{in} = 6.0$ V on the IVM.
7. Watch the switching frequency f_{sw} of the waveform on SCOPE CH-1 (switching node voltage V_{sw}), while turning the knob of trimmer R9, until you get $f_{sw} = 400$ kHz. Under these conditions, you should see the input AC ripple current waveform on SCOPE CH-2, with about 28 mA peak-peak amplitude (as the current sensor gain is 1 A/V, the voltage reading provides directly the current). Set 4 or 8 sweeps average acquisition mode on the SCOPE CH-2, to get a less noisy waveform, if needed.

[WARNING. If the measurements do not look as described above, switch OFF the "OUT ON" button of the ELECTRONIC LOAD and POWER SUPPLY, check the connections, the jumpers setup, the instruments setup, and repeat the procedure]



Test#1: instructions (2)

8. Read the measurements of input voltage on the IVM, input current on the ICM, output voltage on the OVM, output current on the OCM, and record the results in Table 4.1.
9. Measure the the duty cycle of the switching node voltage V_{sw} on the SCOPE CH-1, and record the results in Table 4.1.
10. Measure the amplitude of the peak-peak input ripple current Δi_{inpp} on the SCOPE CH-2, and record the results in Table 4.1.
11. Set the POWER SUPPLY voltage to 10 V.
12. Watch the switching frequency f_{sw} of the waveform on the SCOPE CH-1, while turning the knob of trimmer R9, until you get $f_{sw} = 400$ kHz, and adjust the DC POWER SUPPLY fine regulation knob, if needed, until you read $V_{in} = 10.0$ V on the IVM.
13. Repeat the steps 8 to 10.
14. Set the DC POWER SUPPLY voltage to 6.0 V and the ELECTRONIC LOAD current to 1.2 A.
15. Repeat the steps 7 to 13.
16. Reduce the current of the ELECTRONIC LOAD to 0.0 A, switch its "LOAD ON" button OFF, and switch the POWER SUPPLY "OUT ON" button OFF.
17. Short J_2 - J_5 to connect inductor L_2 , repeat the steps 5 to 16, and record the measurement results in Table 4.1.
18. Open J_6 - J_{13} to connect input filter inductors L_7 and L_8 , repeat steps 5 to 17, and record the measurement results in Table 4.2. [Note. The peak-peak amplitude of the input ripple current can be lower than 1 mA. Use scope zoom feature, if available, to improve measurement accuracy]
19. Switch OFF the ELECTRONIC LOAD, the POWER SUPPLY, the MULTIMETERS and the SCOPE.

Figures 4.9 and 4.10 show the waveforms of the LM3475 switching node voltage (yellow) and input ripple current (green) with inductor L_1 , at 10 V input voltage, 1.2 A load current, with input filter inductors L_7 and L_8 bypassed and connected, respectively.



Figure 4.9. Measured waveforms with input filter inductors bypassed

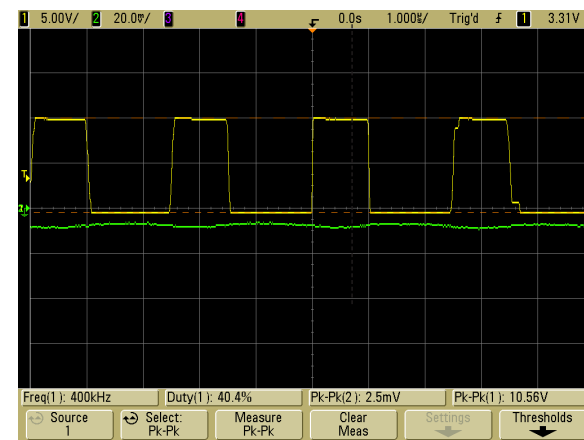


Figure 4.10. Measured waveforms with input filter inductors connected



Test#1: measure and calculate

Collect in Tables 4.1 and 4.2 the measured values of the input voltage V_{in} , output voltage V_{out} , input current I_{in} , output current I_{out} , amplitude of peak-peak input ripple current $\Delta i_{inpp,n}$ (with L7 and L8 bypassed) and $\Delta i_{inpp,f}$ (with L7 and L8 connected), evaluate the percent efficiency of the regulator η [%] = $V_{out} I_{out} / (V_{in} I_{in}) \times 100$, calculate the input ripple current attenuation in decibel determined by the connection of the input filter inductors L7 and L8, given by $20 \times \log_{10} (\Delta i_{inpp,f} / \Delta i_{inpp,n})$, and report the results in Tables 4.1 and 4.2.

Table 4.1. LM3475 regulator input ripple current and efficiency, at 400 kHz switching frequency, with inductors L1 and L2, and input filter inductors L7 and L8 bypassed

inductor	L1				L2			
I_{out} [A]	0.6		1.2		0.6		1.2	
V_{in} [V]	6	10	6	10	6	10	6	10
input current I_{in} [mA]								
output voltage V_{out} [V]								
efficiency η [%]								
peak-peak input ripple current $\Delta i_{inpp,n}$ [mA]								

Table 4.2. LM3475 regulator input ripple current and efficiency, at 400 kHz switching frequency, with inductors L1 and L₂, and input filter inductors L7 and L8 connected

inductor	L1				L2			
I_{out} [A]	0.6		1.2		0.6		1.2	
V_{in} [V]	6	10	6	10	6	10	6	10
input current I_{in} [A]								
output voltage V_{out} [V]								
efficiency η [%]								
peak-peak input ripple current $\Delta i_{inpp,f}$ [mA]								
input ripple current attenuation [dB]								



Experiment set-up for TPS54160 regulator: configuration

The instruments needed for this experiment are: a DC POWER SUPPLY, four MULTIMETERS, an OSCILLOSCOPE and a DC ELECTRONIC LOAD. Figure 4.11 shows the instruments connections for measurements on TPS54160 regulator. Follow the instructions provided in next page to set-up the **connections**.

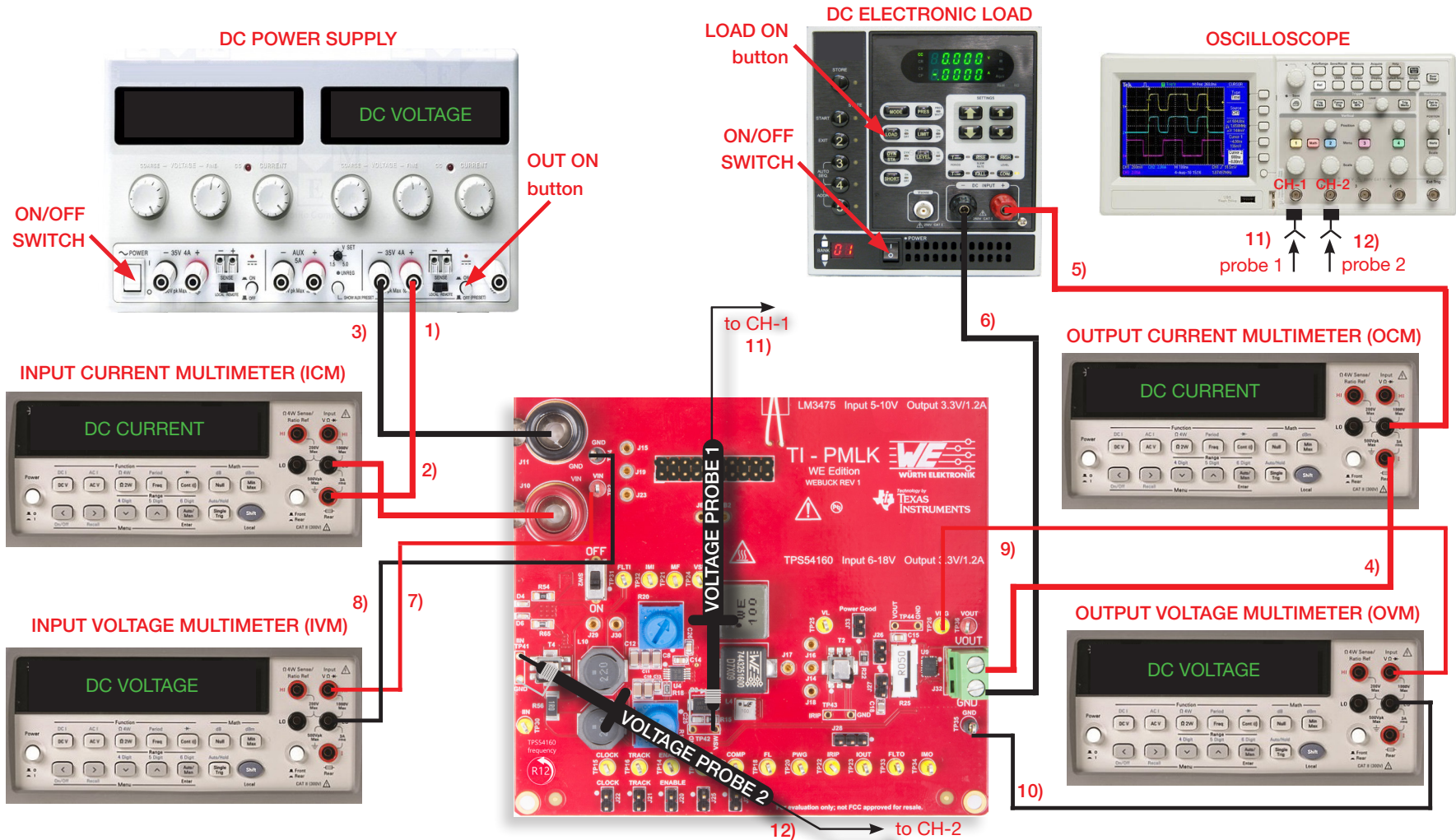


Figure 4.11. Experiment set-up for measurements on TPS54160 regulator



Experiment set-up for TPS54160 regulator: instructions

With all the instruments turned off, make the following **connections**:

1. Connect the POSITIVE (RED) OUTPUT of the DC POWER SUPPLY to the POSITIVE (RED) CURRENT INPUT of the INPUT CURRENT MULTIMETER (ICM) **[WARNING: THE POSITIVE INPUT OF THE MULTIMETER FOR CURRENT MEASUREMENT IS DIFFERENT FROM THE POSITIVE INPUT FOR VOLTAGE MEASUREMENT]**
2. Connect the NEGATIVE (BLACK) CURRENT INPUT of the INPUT CURRENT MULTIMETER (ICM) to the POSITIVE INPUT (VIN) banana connector J_{10} of the TI-PMLK BUCK-WE board
3. Connect the NEGATIVE (BLACK) OUTPUT of the DC POWER SUPPLY to the GROUND (GND) banana connector J_{11} of the TI-PMLK BUCK-WE board
4. Connect the POSITIVE OUTPUT (VOUT) of the screw terminal J_{32} of the TPS54160 regulator to the POSITIVE (RED) CURRENT INPUT of the OUTPUT CURRENT MULTIMETER (OCM) **[WARNING: THE POSITIVE INPUT OF THE MULTIMETER FOR CURRENT MEASUREMENT IS DIFFERENT FROM THE POSITIVE INPUT FOR VOLTAGE MEASUREMENT]**
5. Connect the NEGATIVE (BLACK) CURRENT INPUT of the OUTPUT CURRENT MULTIMETER (OCM) to the POSITIVE (RED) INPUT of the ELECTRONIC LOAD.
6. Connect the NEGATIVE (BLACK) INPUT of the ELECTRONIC LOAD to the GROUND (GND) of the screw terminal J_{22} of the TPS54160 regulator
7. Connect the POSITIVE (RED) VOLTAGE INPUT of the INPUT VOLTAGE MULTIMETER (IVM) to the test point TP_2 of the TI-PMLK BUCK-WE board
8. Connect the NEGATIVE (BLACK) VOLTAGE INPUT of the INPUT VOLTAGE MULTIMETER (IVM) to the test point TP_4 of the TI-PMLK BUCK-WE board
9. Connect the POSITIVE (RED) VOLTAGE INPUT of the OUTPUT VOLTAGE MULTIMETER (OVM) to the test point TP_{26} of the TPS54160 regulator
10. Connect the NEGATIVE (BLACK) VOLTAGE INPUT of the OUTPUT VOLTAGE MULTIMETER (OVM) to the test point TP_{35} of the TPS54160 regulator
11. Connect a voltage probe with ground spring to channel 1 of the OSCILLOSCOPE, insert its positive tip into the hole of test point TP_{42} labeled "VSW" and its ground spring tip into the hole of test point TP_{42} labeled "GND". **[WARNING: DO NOT INVERT THE POSITIVE AND GROUND CONNECTIONS OF THE VOLTAGE PROBE]**
12. Connect a voltage probe with ground spring to channel 2 of the OSCILLOSCOPE, insert its positive tip into the hole of test point TP_{41} labeled "IIN" and its ground spring tip into the hole of test point TP_{41} labeled "GND". **[WARNING: DO NOT INVERT THE POSITIVE AND GROUND CONNECTIONS OF THE VOLTAGE PROBE]**



Test#2: instructions (1)

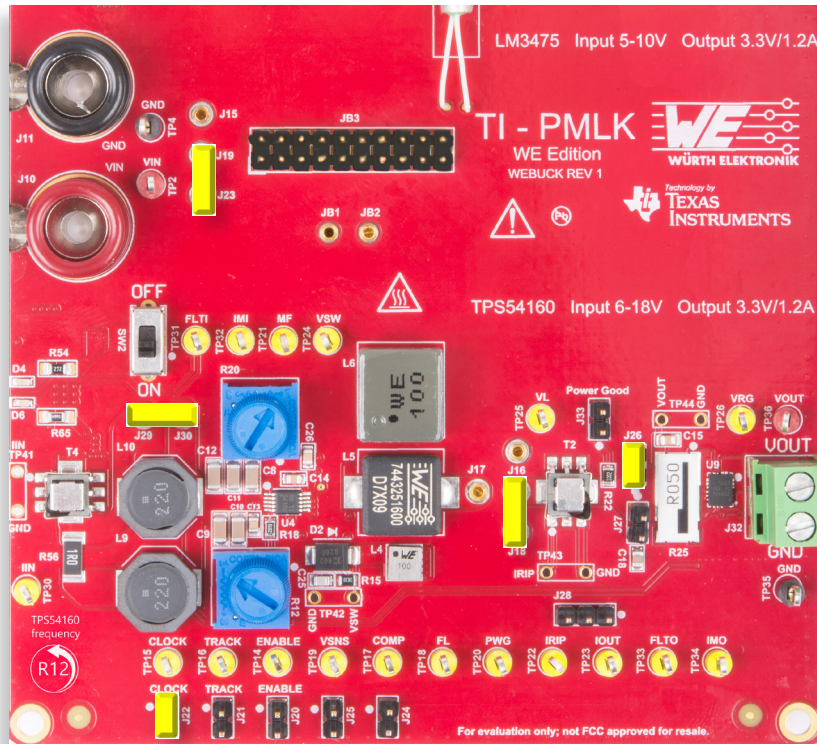


Figure 4.12. TPS54160 jumpers set-up for Test#1

Initial set-up (see Figure 4.12 jumpers not mentioned are open):

- short J_{19} - J_{23} , TPS54160 regulator connected to power input
- short J_{14} - J_{18} , inductor L4 connected
- short J_{22} , switching frequency adjust enabled
- short J_{26} , tantalum output capacitor C17 connected
- short J_{29} - J_{30} , input filter inductors L9 and L10 bypassed
- turn R_{12} left until it stops

Test Procedure:

1. Switch ON the SCOPE, set CH-1 and CH-2 in DC 1 M Ω coupling mode with 20 MHz BW limit, the time base to 1 μ s/div, the trigger on CH-1 rising edge, the vertical scale to 5 V/div on CH-1 and 20 mV/div on CH-2.
2. Switch ON the MULTIMETERS, select DC voltage measurement on IVM and OVM, and DC current measurement on ICM and OCM (see Figure 4.11).
3. Switch ON the POWER SUPPLY, set the "OUT ON" button OFF, output voltage at 6.0 V, and CURRENT LIMIT at 1.5 A.
4. Switch ON the ELECTRONIC LOAD, set the "OUT ON" button OFF, CONSTANT CURRENT MODE, and input current at 0.0 A.
5. Switch the POWER SUPPLY "OUT ON" button ON and the ELECTRONIC LOAD "LOAD ON" button ON. Under these conditions, you should see about 3.34 V on OVM display.
6. Slowly increase the ELECTRONIC LOAD current until you read 0.6 A on the OCM. Adjust the DC POWER SUPPLY fine regulation knob, if needed, until you read $V_{in} = 6.0$ V on the IVM.
7. Watch the switching frequency f_{sw} of the waveform on SCOPE CH-1 (switching node voltage V_{sw}), while turning the knob of trimmer R12, until you get $f_{sw} = 400$ kHz. Under these conditions, you should see the input AC ripple current waveform on SCOPE CH-2, with about 26 mA peak-peak amplitude (as the current sensor gain is 1 A/V, the voltage reading provides directly the current). Set 4 or 8 sweeps average acquisition mode on the SCOPE CH-2, to get a less noisy waveform, if needed.

[WARNING. If the measurements do not look as described above, switch OFF the "OUT ON" button of the ELECTRONIC LOAD and POWER SUPPLY, check the connections, the jumpers setup, the instruments setup, and repeat the procedure].



Test#2: instructions (2)

8. Read the measurements of input voltage on the IVM, input current on the ICM, output voltage on the OVM, output current on the OCM, and record the results in Table 4.3.
9. Measure the the duty cycle of the switching node voltage V_{sw} on the SCOPE CH-1, and record the results in Table 4.3.
10. Measure the amplitude of the peak-peak input ripple current Δi_{inpp} on the SCOPE CH-2, and record the results in Table 4.3.
11. Set the POWER SUPPLY voltage to 10.0 V.
12. Watch the switching frequency f_{sw} of the waveform on the SCOPE CH-1, while turning the knob of trimmer R12, until you get $f_{sw} = 400$ kHz, and adjust the DC POWER SUPPLY fine regulation knob, if needed, until you read $V_{in} = 6.0$ V on the IVM.
13. Repeat the steps 8 to 10.
14. Set the DC POWER SUPPLY voltage to 6.0 V and the ELECTRONIC LOAD current to 1.2 A.
15. Repeat the steps 7 to 13.
16. Reduce the current of the ELECTRONIC LOAD to 0.0 A, switch its “LOAD ON” button OFF, and switch the POWER SUPPLY “OUT ON” button OFF.
17. Short J_{14} - J_{17} to connect inductor L5, repeat the steps 5 to 16, and record the measurement results in Table 4.4.
18. Open J_{29} - J_{30} to connect input filter inductors L9 and L10, repeat steps 5 to 17, and record the measurement results in Table 4.4. [Note. The peak-peak amplitude of the input ripple current can be lower than 1 mA. Use scope zoom feature, if available, to improve measurement accuracy]
19. Switch OFF the ELECTRONIC LOAD, the POWER SUPPLY, the MULTIMETERS and the SCOPE.

Figures 4.13 and 4.14 show the waveforms of the TPS54160 switching node voltage (yellow) and input ripple current (green) with inductor L_4 , at 10 V input voltage, 1.2 A load current, with input filter inductors L_9 and L_{10} bypassed and connected, respectively.



Figure 4.13. Measured waveforms with input filter inductors bypassed

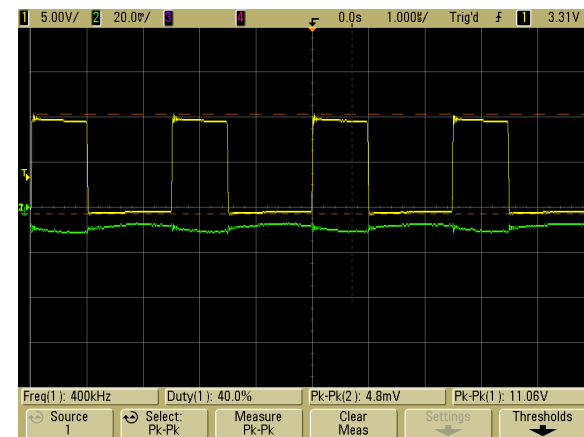


Figure 4.14. Measured waveforms with input filter inductors connected



Test#2: measure and calculate

Collect in Tables 4.3 and 4.4 the measured values of the input voltage V_{in} , output voltage V_{out} , input current I_{in} , output current I_{out} , amplitude of peak-peak input ripple current $\Delta i_{inpp,n}$ (with L_9 and L_{10} bypassed) and $\Delta i_{inpp,f}$ (with L_9 and L_{10} connected), evaluate the percent efficiency of the regulator η [%] = $V_{out} I_{out} / (V_{in} I_{in}) \times 100$, calculate the input ripple current attenuation in decibel determined by the connection of the input filter inductors L_9 and L_{10} , given by $20 \times \log_{10} (\Delta i_{inpp,f} / \Delta i_{inpp,n})$, and report the results in Tables 4.3 and 4.4.

Table 4.3. TPS54160 regulator input ripple current and efficiency, at 400 kHz switching frequency, with inductor L4 and L5, and input filter inductors L9 and L10 bypassed

inductor	L1				L2			
I_{out} [A]	0.6		1.2		0.6		1.2	
V_{in} [V]	6	10	6	10	6	10	6	10
input current I_{in} [mA]								
output voltage V_{out} [V]								
efficiency η [%]								
peak-peak input ripple current $\Delta i_{inpp,n}$ [mA]								

Table 4.4. TPS54160 regulator input ripple current and efficiency, at 400 kHz switching frequency, with inductor L4 and L5, and input filter inductors L9 and L10 connected

inductor	L1				L2			
I_{out} [A]	0.6		1.2		0.6		1.2	
V_{in} [V]	6	10	6	10	6	10	6	10
input current I_{in} [A]								
output voltage V_{out} [V]								
efficiency η [%]								
peak-peak input ripple current $\Delta i_{inpp,f}$ [mA]								
input ripple current attenuation [dB]								



Observe and Answer

1 How does the peak-peak amplitude of the input ripple current vary when the input filter inductors are connected in LM3475 and TPS54160 regulators?

it increases

it decreases

other: _____

Please comment your answer: _____

2 How do the output filter inductors L_1 and L_2 (LM3475) and L_4 and L_5 (TPS54160) influence the peak-peak amplitude of the input ripple current?

they are strongly influential

they are weakly influential

other: _____

Please comment your answer: _____

3 Is the peak-peak input ripple current attenuation better in the LM3475 input filter or in the TPS54160 input filter?

better in LM3475 regulator

better in TPS54160 regulator

other: _____

Please comment your answer: _____

4 Which operating parameter is more influential on the peak-peak input ripple current?

the input voltage V_{in}

the load current I_{out}

other: _____

Please comment your answer: _____



Discussion (1)

Figures 4.15 and 4.16 show the plots of inductance vs DC bias current of LM3475 regulator output filter inductors L1, L2 and L3 and input filter inductors L7 and L8. In Test #1 we operate at 0.6 A and 1.2 A load current, with output filter inductors L1 and L2. At 0.6 A, the inductances of inductors L1 and L2 are about 94 μH and 63 μH , respectively. Thus, given the input voltage V_{in} and the switching frequency f_{sw} operating conditions, the peak-peak amplitude of the ripple current with the output inductor L2 is expected to be $94/63 \approx 1.5$ times larger than the peak-peak amplitude of the ripple current with output inductor L1. At 1.2 A, the inductances of inductors L1 and L2 are about 53 μH and 60 μH , respectively. Therefore, given the input voltage V_{in} and the switching frequency f_{sw} , the peak-peak amplitude of the ripple current with the output inductor L2 is expected to be $53/60 \approx 0.9$ times smaller than the peak-peak amplitude of the ripple current with output inductor L1.

The results of measurements performed in Test #1 show that the LM3475 regulator DC input current ranges from 245 mA at $\{V_{in} = 10.0 \text{ V}, I_{out} = 0.6 \text{ A}\}$ up to 820 mA at $\{V_{in} = 6.0 \text{ V}, I_{out} = 1.2 \text{ A}\}$. Given the 2.3 Ω and 75 m Ω winding resistances of inductors L7 and L8, respectively, the DC input current is splitted into a 3% part flowing through inductor L7 and a 97% part flowing through inductor L8. Consequently, inductors L7 and L8 withstand a maximum DC current of 25 mA and 795 mA respectively. The plots of Figure 4.16 show that both inductors L7 and L8 operate in the weak saturation region, resulting in inductance values almost equal to their own nominal values.

The measurement results collected in Table 4.1 highlight that there is a very weak influence of the inductors L1 and L2 on the peak-peak amplitude of input ripple current, despite of the large change of inductance L1 compared to inductance L₂. Inductors L1 and L2 mostly influence the LM3475 regulator efficiency. Indeed, the peak-peak amplitude of the input ripple current is mostly determined by the square-wave component of the MOSFET current (see Figure 4.2 in the **Theory Background** section), which is influenced by the input voltage V_{in} , determining the duty cycle D , and by the load current I_{out} , determining the amplitude. The results collected in Table 4.1 highlight such influence.

The improvement of the input filter attenuation at switching frequency determined by the inductors L7 and L8 is witnessed by the much smaller values of peak-peak amplitude of input ripple current obtained with L7 and L8 connected. The largest

increase of the attenuation of input ripple current peak-peak amplitude determined by the inductors L7 and L8 is about -34 dB, not as large as the -46 dB expected from theoretical predictions provided by the analytical model shown in the **Theory Background** section. Indeed, the theoretical model considers the first harmonic of the MOSFET current, whereas the input ripple current is comprised also of harmonics which are caused by parasitics (see Figure 4.9). Moreover, the very small ripple amplitude involves a degradation of measurement accuracy.

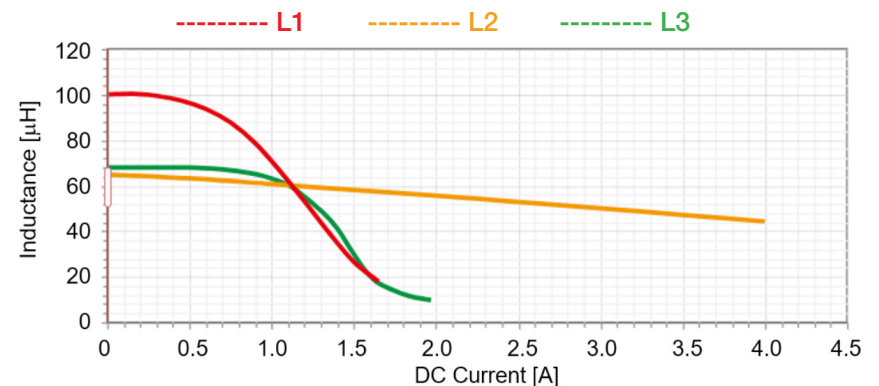


Figure 4.15. Inductance vs DC current at 20 °C

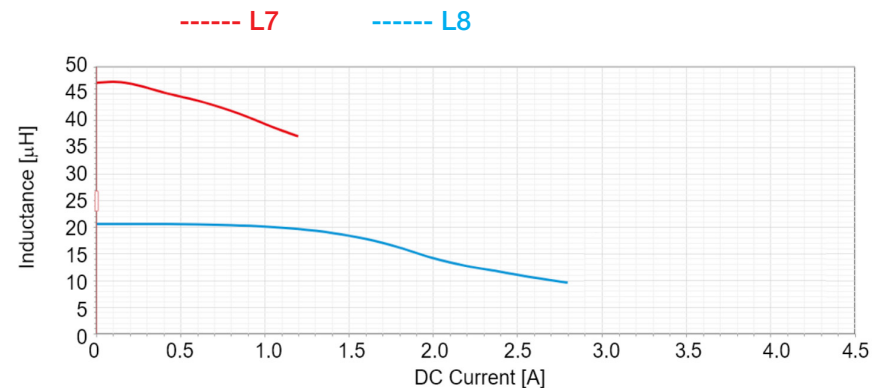


Figure 4.16. Inductance vs DC current at 20 °C



Discussion (2)

Figures 4.17 and 4.18 show the plots of inductance vs DC bias current of TPS54160 regulator output filter inductors L4, L5 and L6 and input filter inductors L9 and L10. In Test #2 we operate at 0.6 A and 1.2 A load current, with output filter inductors L4 and L5. In this current range, the inductances of inductors L4 and L5 are close to their nominal values 10 μH and 16 μH , respectively, as they operate in the weak saturation region. Thus, given the input voltage V_{in} and the switching frequency f_{sw} operating conditions, the peak-peak amplitude of the ripple current with the output inductor L4 is expected to be $16/10 = 1.6$ times larger than the peak-peak amplitude of the ripple current with output inductor L5.

The results of measurements performed in Test #2 show that the TPS54160 regulator DC input current ranges from 235 mA at $\{V_{in} = 10.0 \text{ V}, I_{out} = 0.6 \text{ A}\}$ up to 810 mA at $\{V_{in} = 6.0 \text{ V}, I_{out} = 1.2 \text{ A}\}$. Given the 1 Ω damping resistance R56 in series to the damping inductor L9, and the 75 m Ω winding resistances of both inductors L9 and L10, the DC input current is splitted into a 6.5% part flowing through inductor L9 and a 93.5% part flowing through inductor L10. Consequently, inductors L9 and L10 withstand a maximum DC current of 52.5 mA and 757.5 mA respectively. The plots of Figure 4.18 show that both inductors L9 and L10 operate in the weak saturation region, resulting in inductance values almost equal to their own nominal values.

As in the case of the LM3475 regulator, the measurement results collected in Table 4.3 highlight that there is a very weak influence of the inductors L4 and L5 on the peak-peak amplitude of input ripple current, despite of the large difference between the inductances L4 and L5. The inductors L5 moderately increases the TPS54160 regulator efficiency, due to its smaller winding resistance.

The input filter attenuation at switching frequency is improved by the inductors L9 and L10, as highlighted by the much smaller values of peak-peak amplitude of input ripple current obtained with L9 and L10 connected. Comparing the measurement results of the TPS54160 input filter with the measurement results of the LM3475 regulator in the same operating conditions, highlights a slightly better performance of the LM3475 regulator input filter, providing few decibels more of attenuation, in agreement with plots of Figure 4.4. Indeed, the inductance of the LM3475 damping inductor L7 (47 μH) is larger than the inductance of the TPS54160 damping inductor L9 (22 μH), and this determines a larger equivalent inductance of the input filter (see Equation (4) in the [Theory Background](#) section), involving better attenuation.

Overall, the comparison between the input filters of the LM3475 and TPS54160 regulators shows that effective attenuation and damping performances can be achieved with small size, large inductance, high-resistance damping inductors, like the inductor L7 used in the LM3475 regulator.

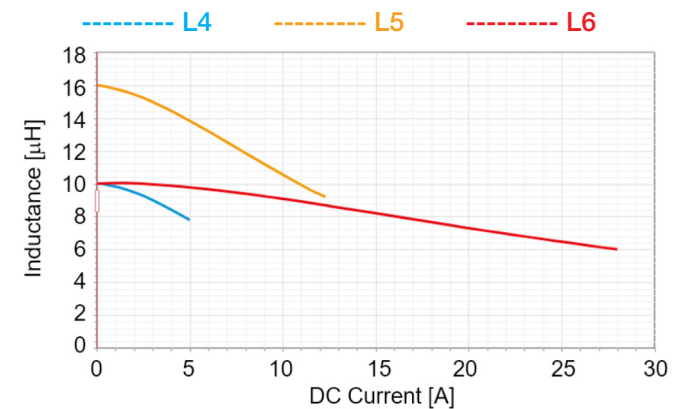


Figure 4.17. inductance vs DC current at 20 °C

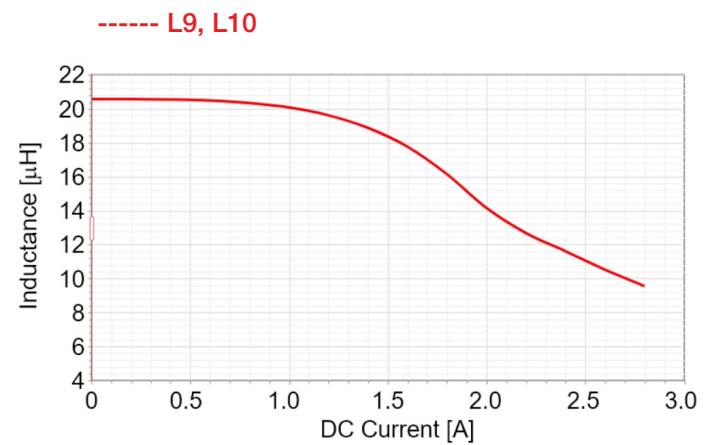


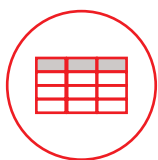
Figure 4.18. inductance vs DC current at 20 °C



Expansion Activities

- Repeat the experiment with different switching frequency, input voltage and load current.

[Note. 1) The TPS54160 can operate in discontinuous conduction mode at high input voltage, low load current and low switching frequency. 2) The TPS54160 regulator features a skip-cycle mode, determining an automatic reduction of switching frequency at low load current. 3) The LM3475 regulator may exhibit jittering at low switching frequency. 4) See [Experiment 5](#) to investigate the impact of inductors on discontinuous conduction mode].



Tables of measurements (1)

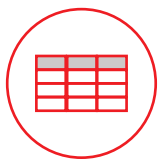
The tables shown in this section are filled with values obtained by performing measurements on the TI-PMLK BUCK-WE board according to the previous test instructions. **[WARNING. The values reported in the tables are purely indicative. The results of your measurements on the TI-PMLK BUCK-WE board can be different due to tolerances and thermal effects of power components, and can be influenced by the accuracy and calibration of the instruments].**

Table 4.1. LM3475 regulator input ripple current and efficiency, at 400 kHz switching frequency, with inductors L1 and L2, and input filter inductors L7 and L8 bypassed

inductor	L1				L2			
	0.6		1.2		0.6		1.2	
I_{out} [A]								
V_{in} [V]	6	10	6	10	6	10	6	10
input current I_{in} [mA]	385	246	813	504	395	252	862	532
output voltage V_{out} [V]	3.36	3.37	3.36	3.37	3.36	3.37	3.36	3.37
efficiency η [%]	87.3	82.2	82.7	80.2	85.1	80.2	78.0	76.0
peak-peak input ripple current $\Delta i_{inpp,n}$ [mA]	28	34	56	65	28	33	57	65

Table 4.2. LM3475 regulator input ripple current and efficiency, at 400 kHz switching frequency, with inductors L1 and L₂, and input filter inductors L7 and L8 connected

inductor	L1				L2			
	0.6		1.2		0.6		1.2	
I_{out} [A]								
V_{in} [V]	6	10	6	10	6	10	6	10
input current I_{in} [A]	386	247	819	506	396	253	868	533
output voltage V_{out} [V]	3.36	3.37	3.36	3.37	3.36	3.37	3.36	3.37
efficiency η [%]	87.0	81.9	82.1	79.9	84.8	79.9	77.4	75.9
peak-peak input ripple current $\Delta i_{inpp,r}$ [mA]	0.7	0.9	1.1	1.4	0.8	0.9	2.0	2.6
input ripple current attenuation [dB]	-32.0	-31.5	-34.1	-33.3	-30.9	-31.3	-29.1	-28.0



Tables of measurements (2)

The tables shown in this section are filled with values obtained by performing measurements on the TI-PMLK BUCK-WE board according to the previous test instructions. **[WARNING. The values reported in the tables are purely indicative. The results of your measurements on the TI-PMLK BUCK-WE board can be different due to tolerances and thermal effects of power components, and can be influenced by the accuracy and calibration of the instruments].**

Table 4.3. TPS54160 regulator input ripple current and efficiency, at 400 kHz switching frequency, with inductor L4 and L5, and input filter inductors L9 and L10 bypassed

inductor	L4				L5			
	0.6		1.2		0.6		1.2	
I_{out} [A]								
V_{in} [V]	6	10	6	10	6	10	6	10
input current I_{in} [mA]	377	237	805	491	374	234	793	480
output voltage V_{out} [V]	3.34	3.34	3.34	3.34	3.34	3.34	3.34	3.34
efficiency η [%]	88.6	84.6	83.0	81.6	89.3	85.6	84.2	83.5
peak-peak input ripple current $\Delta i_{inpp,n}$ [mA]	26	37	47	67	24	34	35	65

Table 4.4. TPS54160 regulator input ripple current and efficiency, at 400 kHz switching frequency, with inductor L4 and L5, and input filter inductors L9 and L10 connected.

inductor	L4				L5			
	0.6		1.2		0.6		1.2	
I_{out} [A]								
V_{in} [V]	6	10	6	10	6	10	6	10
input current I_{in} [mA]	378	238	810	492	376	235	798	482
output voltage V_{out} [V]	3.34	3.34	3.34	3.34	3.34	3.34	3.34	3.34
efficiency η [%]	88.4	84.2	82.5	81.5	88.8	85.3	83.7	83.2
peak-peak input ripple current $\Delta i_{inpp,f}$ [mA]	1.0	1.5	1.4	2.0	0.8	1.1	1.2	1.8
input ripple current attenuation [dB]	-28.3	-27.8	-30.5	-30.5	-29.5	-29.8	-29.3	-31.2

Experiment 5

The goal of this experiment is to analyze the impact of inductors on continuous and discontinuous mode operation of DC-DC switching converters. The impact of the inductance on inductor ripple current and converter efficiency is investigated.

The TPS54160 buck regulator is used for this experiment.

Theory Background (1)

Figure 5.1 shows a simplified schematic of a buck regulator power stage.

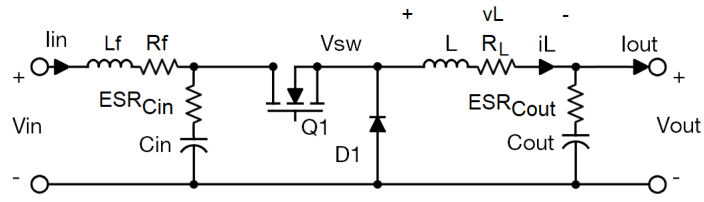


Figure 5.1. Buck converter simplified schematic

When the MOSFET Q1 is ON and the diode D1 is OFF (ON-OFF state), the inductor L withstands a positive voltage given by (1):

$$(1) \quad V_{L+} = V_{in} - (R_f + R_{dson} + R_L) i_L - V_{out} \approx V_{in} - (R_f + R_{dson} + R_L) I_{out} - V_{out}$$

When the MOSFET Q1 is OFF and the diode D1 is ON (OFF-ON state), the inductor L withstands a negative voltage given by (2):

$$(2) \quad V_{L-} = -V_{D1} - R_L i_L - V_{out} \approx -V_{D1} - R_L I_{out} - V_{out}$$

When both the MOSFET Q1 and the diode D1 are OFF (OFF-OFF state), the inductor L is floating, and its current and voltage are theoretically zero. The buck converter enters the OFF-OFF state when the current flowing through the diode D1 during the OFF-ON state crosses zero. The MOSFET Q1 and the diode D1 cannot ever be simultaneously ON (ON-ON state), as when the MOSFET Q1 turns ON the diode automatically turns OFF. There are two different operation modes a buck converter can undergo: the Continuous Conduction Mode (CCM) and the Discontinuous Conduction Mode (DCM). In CCM, the current flowing through the diode D1 during the OFF-ON state keeps positive until the transition to the next ON-OFF state is commanded by the MOSFET gate drive. Figure 5.2 shows the theoretical plots of the inductor voltage and current waveforms of a buck converter in open-loop CCM operation. In DCM operation, the current

flowing through the diode D1 during the OFF-ON state drops to zero before the transition to the next ON-OFF state is commanded by the MOSFET gate drive. Figure 5.3 shows the theoretical plots of the inductor voltage and current waveforms of a buck converter in open-loop DCM operation.

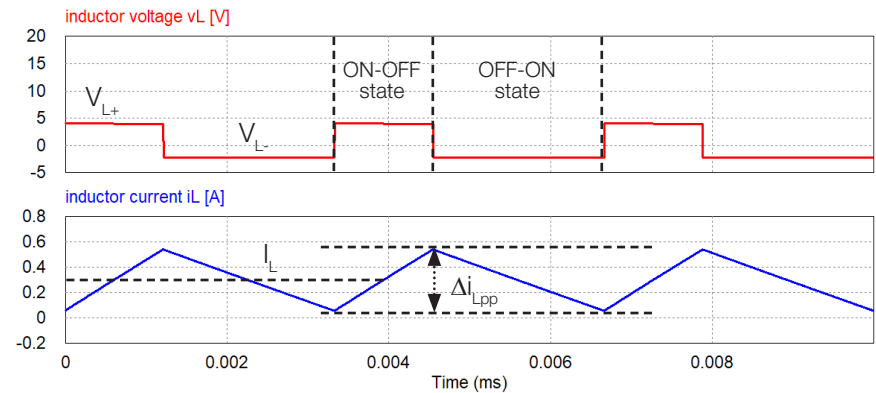


Figure 5.2. Inductor voltage and current waveforms in CCM

$$(V_{in}=6 \text{ V}, I_{out}=0.3 \text{ A}, f_{sw}=300 \text{ kHz}, D=36.5 \%, L=10 \mu\text{H})$$

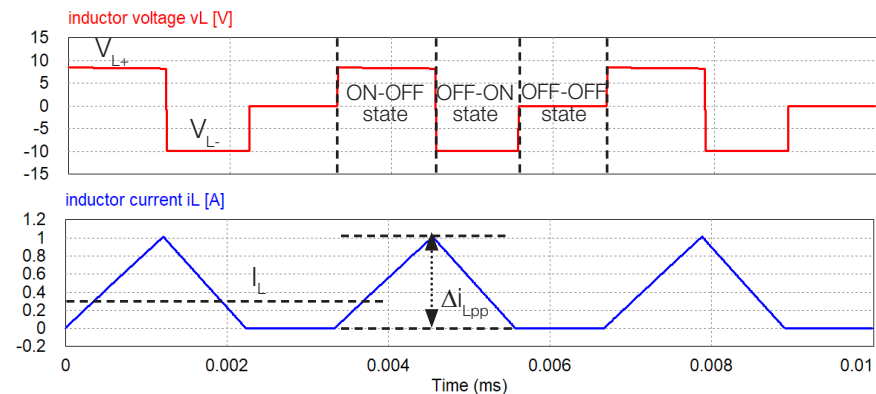


Figure 5.3. Theoretical inductor voltage and current waveforms in DCM

$$(V_{in}=18 \text{ V}, I_{out}=0.3 \text{ A}, f_{sw}=300 \text{ kHz}, D=36.5 \%, L=10 \mu\text{H})$$



Theory Background (2)

In a real buck converter, the voltage and current waveforms in DCM operation likely look as shown in Figure 5.4.

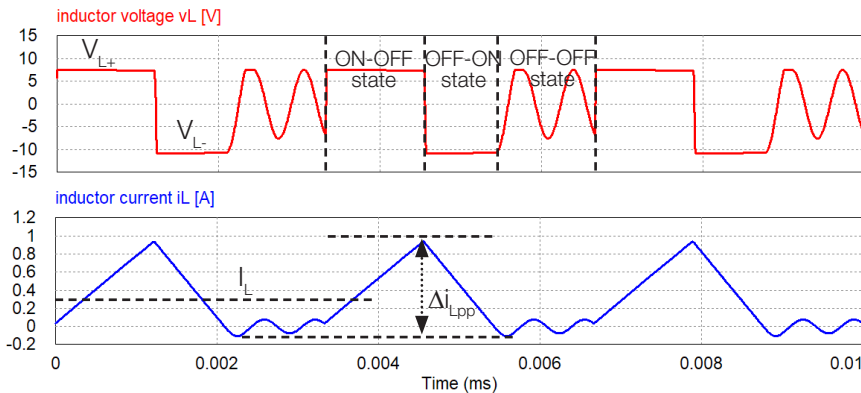


Figure 5.4. Real inductor voltage and current waveforms in DCM
 $(V_{in}=18\text{ V}, I_{out}=0.3\text{ A}, f_{sw}=300\text{ kHz}, D=36.5\%, L=10\text{ }\mu\text{H})$

The ringing observed in the OFF-OFF state interval is caused by the parasitic capacitances of the MOSFET Q1 and diode D1, which resonate with the inductor L . Figure 5.5 shows a simplified circuit model of the buck converter including the equivalent parasitic capacitance C_p of the MOSFET Q1 and diode D1.

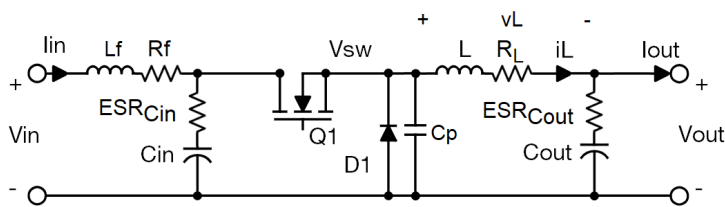


Figure 5.5. Buck converter schematic with parasitic capacitance C_p

The buck converter enters DCM operation when the peak-peak amplitude of the inductor ripple current is greater than two times the average inductor current:

$$(3) \quad \Delta i_{Lpp} > 2 I_L$$

where

$$(4) \quad \Delta i_{Lpp} = V_{L+} D / (f_{sw} L)$$

$$(5) \quad I_L = I_{out}$$

and V_{L+} is given by (1). Neglecting the effects of parasitic resistances R_f , R_{dson} , and R_L in (1), allows simplifying the condition (3) as shown in (6):

$$(6) \quad 1 - V_{out} / V_{in} > 2 I_{out} f_{sw} L / V_{out}$$

Equation (6) highlights that, for a given output voltage V_{out} , the conditions facilitating the DCM operation are:

- a high input voltage V_{in} ;
- a low load current I_{out} ;
- a low switching frequency f_{sw} ;
- a small inductance L .

According to (6), the inductor impacts the CCM/DCM operation with its inductance L . In particular, if the inductor is selected with small inductance, it can determine the DCM operation at light load. The DCM operation modifies the characteristics and the static and dynamic performances of the buck converter, with respect to CCM operation. A first difference between DCM and CCM can be found in the relationship between the input voltage, the output voltage, and the duty cycle. Neglecting the effects of parasitic resistances, in CCM the theoretical input-output voltage conversion ratio is given by (7):

$$(7) \quad V_{out} / V_{in} = D \quad \text{CCM}$$

whereas in DCM it becomes:

$$(8) \quad V_{out} / V_{in} = 2 / [1 + \sqrt{(1 + 4 K / D^2)}] \quad \text{DCM}$$

where $K = 2 I_{out} f_{sw} L / V_{out}$.



Return to previous page by:

Windows:



Mac:





Theory Background (3)

Equations (7) and (8) provide the theoretical value of the duty cycle required to achieve a desired output voltage in CCM and DCM:

$$(9) \quad D = V_{out} / V_{in} \quad CCM$$

$$(10) \quad D = V_{out} / V_{in} \sqrt{[K / (1 - V_{out} / V_{in})]} \quad DCM$$

Equations (9) and (10) highlight that the value of the duty cycle required to achieve a given output voltage in DCM is lower than in CCM. In fact, based on (6), the factor $\sqrt{[K / (1 - V_{out} / V_{in})]}$ is smaller than one. Moreover, as the factor K is proportional to the load current I_{out} , the duty cycle in DCM decreases at lower load current, whereas in CCM it is theoretically independent of the load current (in reality, in CCM, there is also a small dependence caused by the power losses, which is negligible if the efficiency of the converter is high).

A second effect of DCM operation is the modification of the power components losses. The increase of the peak-peak amplitude of inductor ripple current Δi_{Lpp} is expected to determine an overall increase of AC losses. However, the MOSFET turns ON at zero current at the beginning of the switching period, whereas in CCM it turns ON withstanding a positive current. This means that, in DCM, the MOSFET is not affected by turn ON switching losses, whereas in CCM it is. Turn OFF switching losses can also decrease as a higher turn OFF current reduces the MOSFET turn OFF switching time. Therefore, the operation in DCM may have a limited impact of the efficiency, as the reduction of MOSFET switching losses may balance the higher AC losses.

DCM can involve some issues in high-frequency operation. In fact, the integrated circuits implementing the control circuitry needed to regulate the voltage in switching converters can reliably generate PWM pulse trains with ON-time greater than a minimum time, t_{ONmin} , whose value depends on the chip technology. Typical values of minimum ON-time are from few tens up to few hundreds of nanoseconds. Supposing that the minimum ON-time of the chip t_{ONmin} is given, the resulting minimum allowed duty cycle is given by (11):

$$(11) \quad D_{min} = t_{ONmin} \times f_{sw}$$

If the converter has to supply a low current load, high switching frequency operation is allowed, thanks to low losses. However, if the inductor is selected with small inductance to operate in DCM, the value of duty cycle required to regulate the output voltage given by (10) could not fulfill the constraint (11). The resulting effect is that the controller will provide a duty cycle greater than the required value, and the output voltage will be higher than the required value.

Low load current operation is of great interest in real world applications, as low power consumption features in stand-by conditions are widely required. Normally, power converters for applications with load current varying over large ranges are designed to accept the transition to DCM below a certain load current threshold and above a certain input voltage threshold. Indeed, ensuring CCM operation at low load current and high input voltage may require a very high inductance (see the equations provided in the [Theory Background](#) section of the [Experiment 1](#)).

Certain controllers (like TPS54160) implement frequency folding and burst mode features (also known as hiccup mode) to limit power losses, which automatically reduce the switching frequency at low load, or perform a stop-and-go operation. According to (6), reducing the switching frequency facilitates the transition to DCM, but mitigates the possible conflicts between small duty cycle required in DCM, according to (10), and minimum duty cycle restrictions given by (11).

DCM impacts also the dynamic characteristics of the buck converter. In CCM, the buck converter has a second order response, with two complex conjugated poles. In DCM, instead, the buck converter exhibits a first order response, determined by a dominant low frequency real pole. The resulting transient response of the buck converter in DCM is typically slower than in CCM. The transition to DCM has to be taken into account in the control design, to ensure closed loop transient performance fitting the specifications in all load conditions.



Return to previous page by:

Windows:



Mac:





Case Study

The goal of this experiment is to analyze the impact of inductors on the CCM and DCM operation of the TPS54160 buck regulator, in low load operating conditions, under different input voltage and switching frequency operating conditions. The inductor peak-peak ripple current and average current are observed to detect the operation mode, and verify the prediction of theoretical formulae. Inductors L4, L5, and L6 are compared, to analyze the effects of inductors with different values of the inductance on CCM/DCM operation, and the impact of different inductors with the same value of the inductance on the efficiency of the buck converter in DCM.

The following test points of the TPS54160 regulator will be used:

- **TP₂'** to measure the input voltage V_{in}
- **TP₄₁'** to measure the peak-peak amplitude of input current ripple $\Delta i_{Lpp,in}$
- **TP₄₂'** to measure the switching period T_{sw} and the duty cycle D
- **TP₂₂'** to measure the peak-peak amplitude of inductor current ripple Δi_{Lpp}
- **TP₂₆'** to measure the output voltage V_{out}

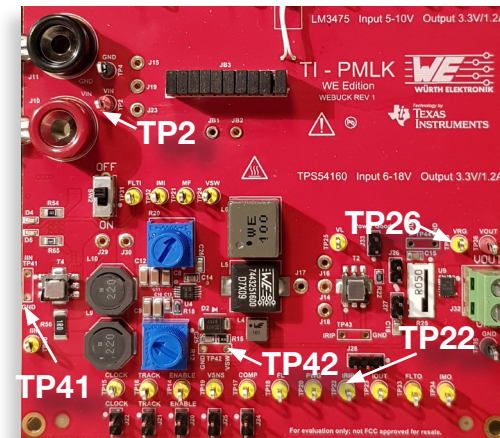


Figure 5.6. Test points used to analyze the CCM and DCM operation in the TPS54160 regulator



Experiment set-up: configuration

The instruments needed for this experiment are: a DC POWER SUPPLY, four MULTIMETERS, an OSCILLOSCOPE, and a DC ELECTRONIC LOAD. Figure 5.7 shows the instruments connections for measurements on TPS54160 regulator. Follow the instructions provided in next page to set-up the **connections**.

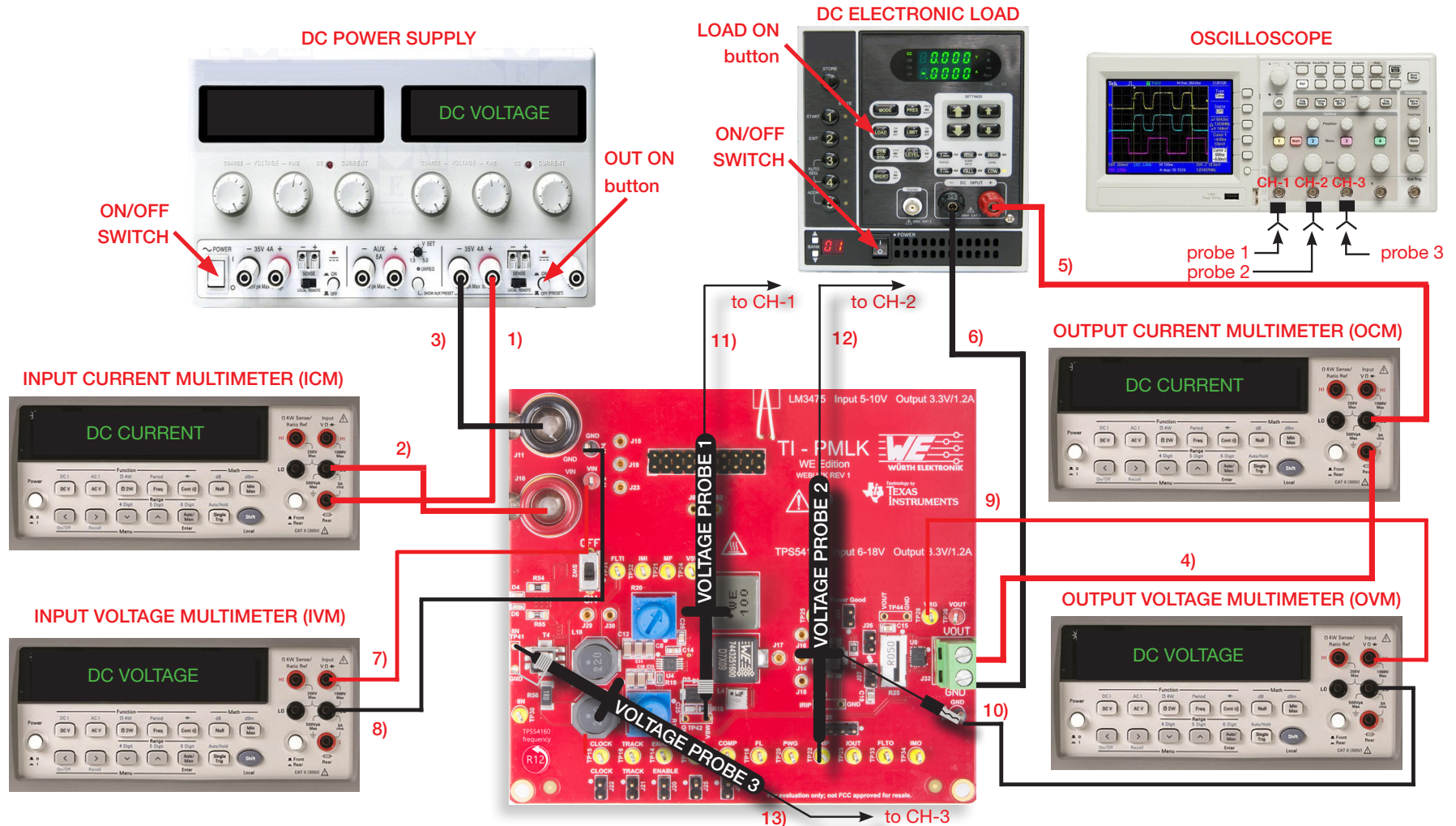


Figure 5.7. Experiment set-up for measurements on TPS54160 regulator



Experiment set-up: instructions

With all the instruments turned off, make the following **connections** [**WARNING: DO NOT INVERT THE POSITIVE AND GROUND PROBE CONNECTIONS**]:

1. Connect the POSITIVE (RED) OUTPUT of the DC POWER SUPPLY to the POSITIVE (RED) CURRENT INPUT of the INPUT CURRENT MULTIMETER (ICM) [**WARNING: THE POSITIVE INPUT OF THE MULTIMETER FOR CURRENT MEASUREMENT IS DIFFERENT FROM THE POSITIVE INPUT FOR VOLTAGE MEASUREMENT**]
2. Connect the NEGATIVE (BLACK) CURRENT INPUT of the INPUT CURRENT MULTIMETER (ICM) to the POSITIVE INPUT (VIN) banana connector J_{10} of the TI-PMLK BUCK-WE board
3. Connect the NEGATIVE (BLACK) OUTPUT of the DC POWER SUPPLY to the GROUND (GND) banana connector J_{11} of the TI-PMLK BUCK-WE board
4. Connect the POSITIVE OUTPUT (VOUT) of the screw terminal J_{32} of the TPS54160 regulator to the POSITIVE (RED) CURRENT INPUT of the OUTPUT CURRENT MULTIMETER (OCM) [**WARNING: THE POSITIVE INPUT OF THE MULTIMETER FOR CURRENT MEASUREMENT IS DIFFERENT FROM THE POSITIVE INPUT FOR VOLTAGE MEASUREMENT**]
5. Connect the NEGATIVE (BLACK) CURRENT INPUT of the OUTPUT CURRENT MULTIMETER (OCM) to the POSITIVE (RED) INPUT of the ELECTRONIC LOAD.
6. Connect the NEGATIVE (BLACK) INPUT of the ELECTRONIC LOAD to the GROUND (GND) of the screw terminal J_{22} of the TPS54160 regulator
7. Connect the POSITIVE (RED) VOLTAGE INPUT of the INPUT VOLTAGE MULTIMETER (IVM) to the test point TP_2 of the TI-PMLK BUCK-WE board
8. Connect the NEGATIVE (BLACK) VOLTAGE INPUT of the INPUT VOLTAGE MULTIMETER (IVM) to the test point TP_4 of the TI-PMLK BUCK-WE board
9. Connect the POSITIVE (RED) VOLTAGE INPUT of the OUTPUT VOLTAGE MULTIMETER (OVM) to the test point TP_{26} of the TPS54160 regulator
10. Connect the NEGATIVE (BLACK) VOLTAGE INPUT of the OUTPUT VOLTAGE MULTIMETER (OVM) to the test point TP_{35} of the TPS54160 regulator
11. Connect a voltage probe with ground spring to channel 1 of the OSCILLOSCOPE, insert its positive tip into the hole of test point TP_{42} labeled "VSW" and its ground spring tip into the hole of test point TP_{42} labeled "GND".
12. Connect a standard voltage probe to channel 2 of the OSCILLOSCOPE, hang its positive tip to the test point TP_{22} and its ground to the test point TP_{35} .
13. Connect a voltage probe with ground spring to channel 3 of the OSCILLOSCOPE, insert its positive tip into the hole of test point TP_{41} labeled "IIN" and its ground spring tip into the hole of test point TP_{41} labeled "GND".



Test#1: instructions (1)

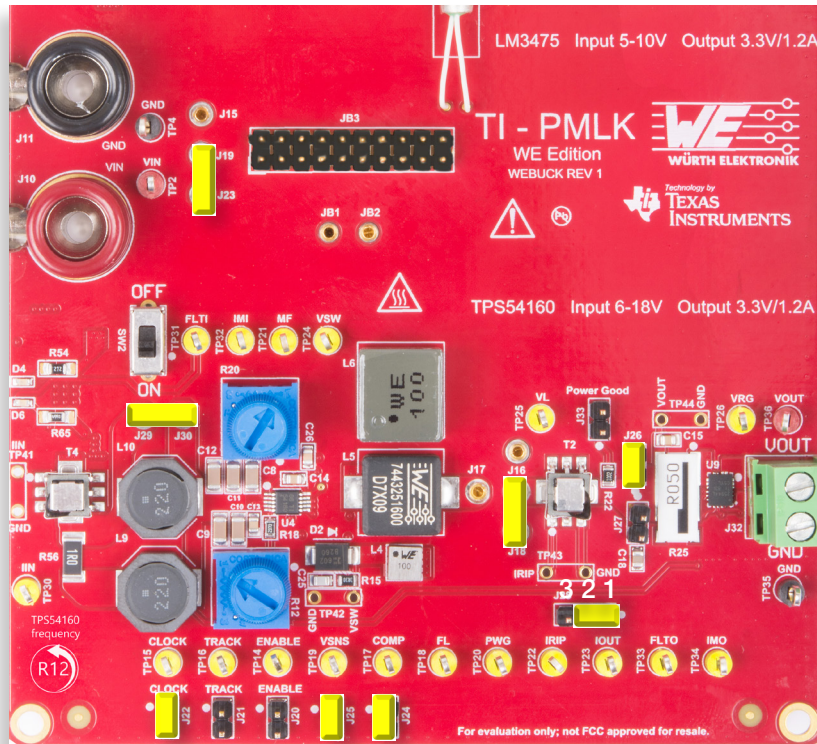


Figure 5.8. TPS54160 jumpers set-up for Test#1

Initial set-up (see Figure 5.8, jumpers not mentioned are open):

- short J_{19} - J_{23} , TPS54160 regulator connected to power input
- short J_{14} - J_{18} , inductor L4 connected
- short J_{22} , switching frequency adjust enabled
- short J_{26} , tantalum output capacitor C17 connected
- short J_{24} and J_{25} , compensation for high voltage
- short J_{29} - J_{30} , input filter inductors L9 and L10 bypassed
- short pins 1-2 of J_{28} , sum AC and DC inductor currents
- turn R_{12} left until it stops

Test Procedure:

1. Switch ON the SCOPE, set CH-1, CH-2 and CH-3 in DC 1 M Ω coupling mode with 20 MHz BW limit, the time base to 1 μ s/div, the trigger on CH-1 rising edge, the vertical scale to 5 V/div on CH-1, 500 mV/div on CH-2 and 20 mV/div on CH-3.
2. Switch ON the MULTIMETERS, select DC voltage measurement on IVM and OVM, and DC current measurement on ICM and OCM (see Figure 5.7).
3. Switch ON the POWER SUPPLY, set the "OUT ON" button OFF, output voltage at 6.0 V, and CURRENT LIMIT to 1.5 A.
4. Switch ON the ELECTRONIC LOAD, set the "OUT ON" button OFF, CONSTANT CURRENT MODE, and input current at 0.0 A.
5. Switch the POWER SUPPLY "OUT ON" button ON and the ELECTRONIC LOAD "LOAD ON" button ON. Under these conditions, you should see about 3.34 V on OVM display.
6. Rise slowly the ELECTRONIC LOAD current until you read 0.3 A on the OCM. Adjust the DC POWER SUPPLY fine regulation knob, if needed, until you read $V_{in} = 6.0$ V on the IVM.
7. Watch the switching frequency f_{sw} of the waveform on SCOPE CH-1 (switching node voltage V_{sw}), while turning the knob of trimmer R12, until you get $f_{sw} = 300$ kHz. Under these conditions, you should see the inductor current waveform on the SCOPE CH-2, with about 300 mA average and 500 mA peak-peak amplitude (the voltage reading provides directly the current). Set 4 or 8 sweeps average acquisition mode on the SCOPE CH-2, to get a less noisy waveform, if needed.

[WARNING. If the measurements do not look as described above, switch OFF the "OUT ON" button of the ELECTRONIC LOAD and POWER SUPPLY, check the connections, the jumpers setup, the instruments setup, and repeat the procedure]



Test#1: instructions (2)

8. Read the measurements of input voltage on the IVM, input current on the ICM, output voltage on the OVM, output current on the OCM, and record the results in Table 5.1.
9. Measure the amplitude of the peak-peak inductor ripple current Δi_{Lpp} on the SCOPE CH-2, and record the results in Table 5.1.
10. Measure the amplitude of the peak-peak input ripple current Δi_{inpp} on the SCOPE CH-3, and record the results in Table 5.1.
11. Set the POWER SUPPLY voltage to 18.0 V.
12. Repeat the steps 8 to 10.
13. Watch the switching frequency f_{sw} of the waveform on the SCOPE CH-1, while turning the knob of trimmer R12, until you get $f_{sw} = 450$ kHz, and adjust the DC POWER SUPPLY fine regulation knob, if needed, until you read $V_{in} = 6.0$ V on the IVM.
14. Repeat the steps 8 to 12, and record the results in Table 5.2.
15. Reduce the current of the ELECTRONIC LOAD to 0.0 A, switch its "LOAD ON" button OFF, and switch the POWER SUPPLY "OUT ON" button OFF.
16. Set the "OUT ON" button OFF, output voltage at 6.0 V
17. Short $J_{14}-J_{17}$ to connect inductor L5, and repeat the steps 5 to 15.
18. Short $J_{14}-J_{16}$ to connect inductor L6, and repeat the steps 5 to 15.
19. Switch OFF the ELECTRONIC LOAD, the POWER SUPPLY, the MULTIMETERS and the SCOPE.

Figures 5.9 and 5.10 show the waveforms of the TPS54160 switching node voltage (yellow), inductor current (green), and input ripple current (violet), at 18 V input voltage, 300 kHz switching frequency, with inductors L4 and L5, respectively.

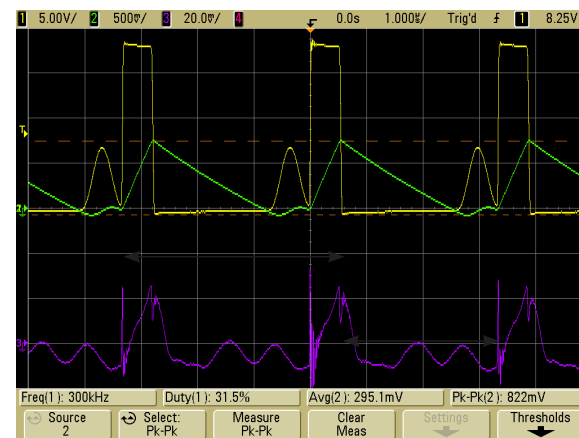


Figure 5.9. Measured TPS54160 regulator waveforms with inductor L4 at:
 $V_{in} = 18$ V, $I_{out} = 0.3$ A and $f_{sw} = 300$ kHz

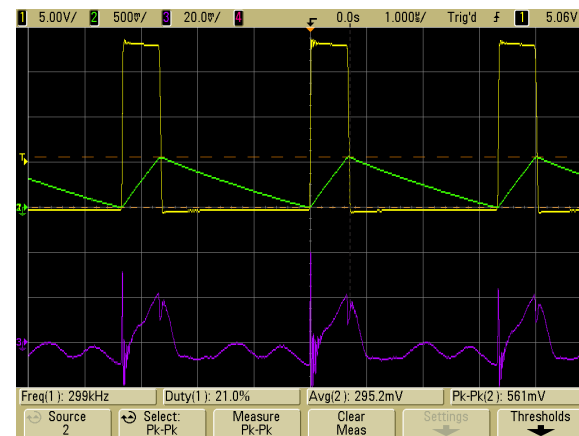


Figure 5.10. Measured TPS54160 regulator waveforms with inductor L5 at:
 $V_{in} = 18$ V, $I_{out} = 0.3$ A and $f_{sw} = 300$ kHz



Test#1: measure and calculate

Collect in Tables 5.1 and 5.2 the measured values of the DC input current I_{in} , DC output voltage V_{out} , amplitude of peak-peak inductor ripple current Δi_{Lpp} , average inductor current I_L , and amplitude of peak-peak input ripple current Δi_{inpp} , check the CCM/DCM box corresponding to the operation mode you have detected, evaluate the percent efficiency of the regulator η [%] = $V_{out} I_{out} / (V_{in} I_{in}) \times 100$, and report the results in Table 5.1 and 5.2.

Table 5.1. Peak-peak ripple and average inductor current and TPS54160 regulator efficiency, at $f_s = 300$ kHz and $I_{out} = 0.3$ A, with inductors L4, L5, and L6

Inductor	L4 (10 μ H)		L5 (16 μ H)		L6 (10 μ H)	
V_{in} [V]	6	18	6	18	6	18
CCM/DCM operation mode	<input type="checkbox"/> CCM <input type="checkbox"/> DCM					
DC input current I_{in} [mA]						
DC output voltage V_{out} [V]						
efficiency η [%]						
peak-peak inductor ripple current Δi_{Lpp} [mA]						
inductor average current I_L [mA]						
peak-peak input ripple current Δi_{inpp} [mA]						

Table 5.2. Peak-peak ripple and average inductor current and TPS54160 regulator efficiency, at $f_s = 450$ kHz and $I_{out} = 0.3$ A, with inductors L4, L5, and L6

Inductor	L4 (10 μ H)		L5 (16 μ H)		L6 (10 μ H)	
V_{in} [V]	6	18	6	18	6	18
CCM/DCM operation mode	<input type="checkbox"/> CCM <input type="checkbox"/> DCM					
DC input current I_{in} [mA]						
DC output voltage V_{out} [V]						
efficiency η [%]						
peak-peak inductor ripple current Δi_{Lpp} [mA]						
inductor average current I_L [mA]						
peak-peak input ripple current Δi_{inpp} [mA]						



Observe and Answer

1 Which inductor does determine DCM operation in the TPS54160 regulator?

- L4
 L5
 L6
 none

Please comment your answer: _____

2 For which input voltage and switching frequency setup do you detect DCM operation?

- $V_{in} = 6\text{ V}, f_{sw} = 300\text{ kHz}$
 $V_{in} = 6\text{ V}, f_{sw} = 450\text{ kHz}$
 $V_{in} = 18\text{ V}, f_{sw} = 300\text{ kHz}$
 $V_{in} = 18\text{ V}, f_{sw} = 450\text{ kHz}$

Please comment your answer: _____

3 What is the ratio between the inductor peak-peak ripple current and average current in DCM operation?

- greater than 2
 lower than 2
 other: _____

Please comment your answer: _____

4 How does the DCM operation influence the peak-peak amplitude of input ripple current?

- peak-peak input current ripple increases in DCM
 peak-peak input ripple current does not change in DCM
 other: _____

Please comment your answer: _____



Discussion (1)

Figure 5.11 shows the **REDEXPERT** simulation results of the TPS54160 buck regulator with three inductors L_4 , L_5 , and L_6 , at 300 kHz switching frequency, 0.3 A load current, and input voltage variable in the [6,18] V range.

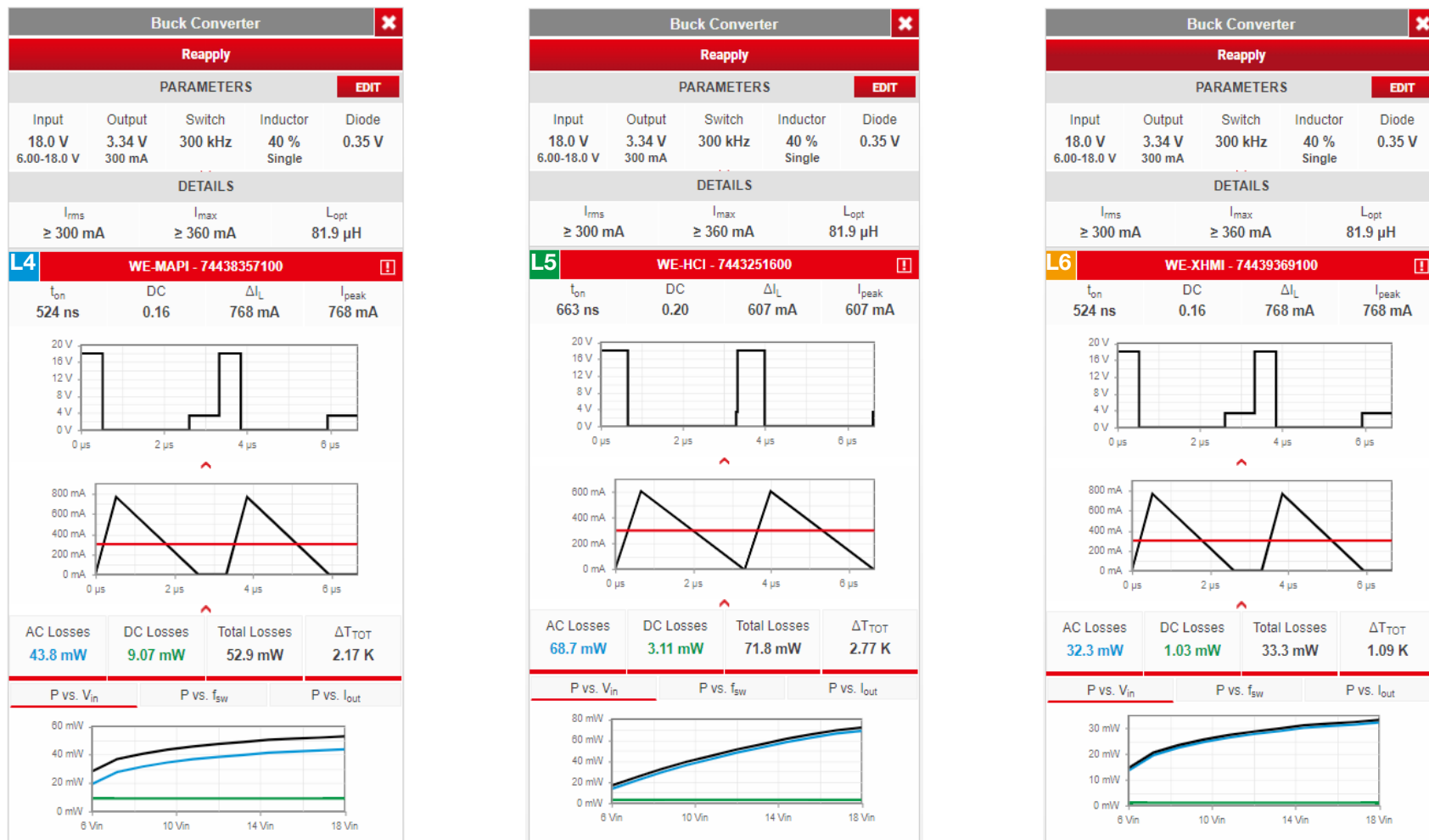


Figure 5.11. REDEXPERT simulation results of the TPS54160 buck regulator



Discussion (2)

Figure 5.12 shows the **REDEXPERT** simulation results of the TPS54160 buck regulator with three inductors L_4 , L_5 , and L_6 , at 450 kHz switching frequency, 0.3 A load current, and input voltage variable in the [6,18] V range.

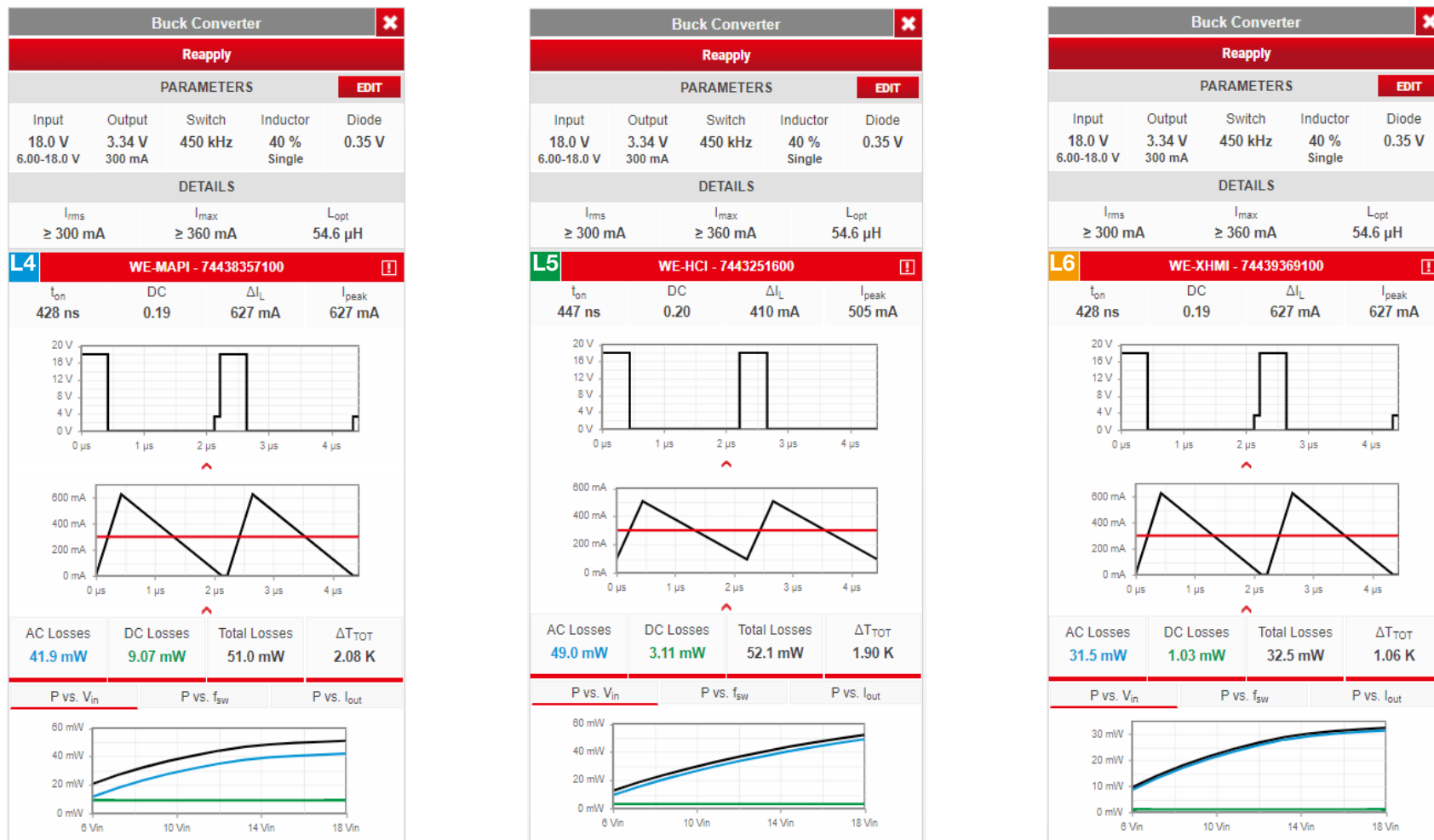


Figure 5.12. **REDEXPERT** simulation results of the TPS54160 buck regulator



Discussion (3)

The results of experimental measurements are in agreement with the **REDEXPERT** simulation results. In fact, at 3.34 V output voltage, 0.3 A load current, 300 kHz switching frequency, and 18 V input voltage, we observe that the 10 μH inductors L4 and L6 determine TPS54160 regulator DCM operation, whereas the 16 μH inductor L5 determines CCM operation. This is also in agreement with the prediction of theoretical Equation (6), provided in the **Theory Background** section, rewritten hereafter:

$$(13) \quad 1 - V_{out} / V_{in} > 2 I_{out} f_{sw} L / V_{out}$$

Putting the values of V_{in} , V_{out} , f_{sw} and I_{out} adopted for the tests into Equation (13) yields the inductance threshold values for DCM operation collected in Table 3.

Table 5.3. DCM inductance constraint.

	$f_{sw} = 300 \text{ kHz}$	$f_{sw} = 450 \text{ kHz}$
$V_{in} = 6 \text{ V}$	8.2 μH	5.5 μH
$V_{in} = 18 \text{ V}$	15.1 μH	10.1 μH

The results of Table 5.3 are in agreement with the experimental observations. Indeed, at 6 V input voltage operation we obtain inductor current waveforms whose valley current, $I_{vl} = I_L - \Delta I_{Lpp} / 2$, at the end of the OFF-ON state interval, is well above zero, with all the inductors. Experimental measurements show that we have CCM at 6 V input voltage with all the inductors. At 18 V input voltage, instead, the inductance threshold determining the DCM operation is higher, and we have DCM operation with the 10 μH inductors L4 and L6 at 300 kHz, which are below the 15.1 μH threshold. At 450 kHz, the valley current I_{vl} of the inductors L4 and L6 is slightly negative, as their inductance is slightly below the threshold. In these conditions, the buck regulator operates on the boundary between CCM and DCM. The **REDEXPERT** simulations predict barely DCM operation. Figures 5.13 and 5.14 show the current waveforms of the inductors L4 and L6, respectively, at 18 V input voltage and 450 kHz switching frequency operation, confirming the barely DCM operation (the valley current is slightly below zero).

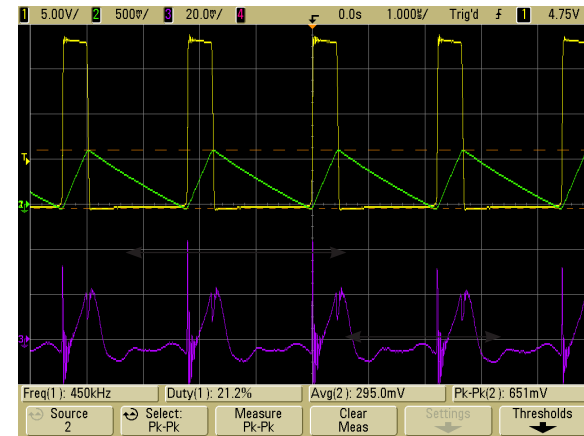


Figure 5.13. Measured TPS54160 regulator waveforms with inductor L4 at: $V_{in} = 18 \text{ V}$, $I_{out} = 0.3 \text{ A}$ and $f_{sw} = 450 \text{ kHz}$



Figure 5.14. Measured TPS54160 regulator waveforms with inductor L6 at: $V_{in} = 18 \text{ V}$, $I_{out} = 0.3 \text{ A}$ and $f_{sw} = 450 \text{ kHz}$



Discussion (4)

The results of experimental measurements show a weak impact of the DCM operation, determined by the 10 μH inductors L4 and L6, on the regulator efficiency.

In fact, the efficiency with the inductor L5, determining CCM operation, is slightly higher than with the inductors L4 and L6. The **REDEXPERT** simulation results show that, at 300 kHz switching frequency, the inductor L5 is affected by higher losses compared to the inductors L4 and L6. This means that the higher efficiency of the regulator is determined by a beneficial effect of the smaller peak-peak amplitude of inductor ripple current, ensured by the inductor L5, on the other power components. This is connected to the specific characteristics of the MOSFET and diode of the TPS54160 regulator implemented in the TI-PMLKBUCK-WE board. Power components with different characteristics may lead to different results.

It is interesting to note that the very small 10 μH inductor L4 (52 mm^3) and the much bigger 10 μH inductor L6 (1100 mm^3) provide similar efficiency performance.

The measurements have been performed with the input filter inductors bypassed, to allow a better observation of the influence of DCM operation on input current noise.

The experimental measurements show that, in DCM, the impact of the peak-peak amplitude of the inductor ripple current on the input ripple current is not negligible. In fact, the increase of the peak-peak inductor ripple current directly results in an increase of the peak-peak input ripple current. Indeed, in CCM operation, the current of the MOSFET Q1 is a trapezoid, comprised of a large amplitude square-wave component determined by the high load current and by a small amplitude triangle component determined by the inductor ripple current (see the **Theory Background** section of the **Experiment 4**). In DCM operation, instead, the current of the MOSFET Q1 is a triangle waveform whose peak-peak amplitude corresponds to the peak-peak amplitude of the inductor ripple current, as shown in Figure 5.15. So that, in DCM the peak-peak amplitude of the inductor ripple current directly influences the peak-peak amplitude of input ripple current.

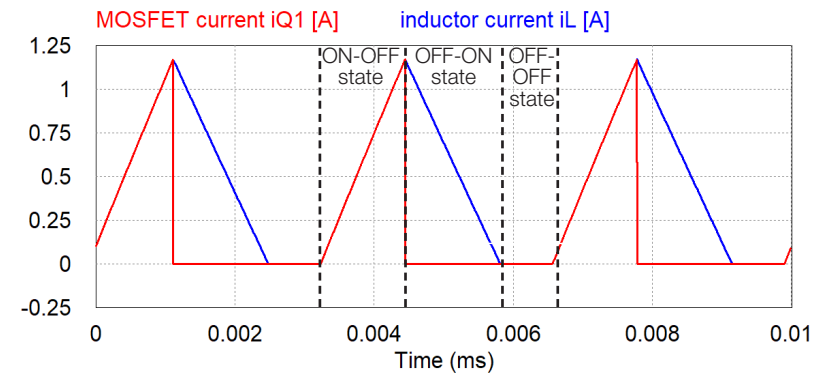


Figure 5.15. Inductor and MOSFET current in DCM operation

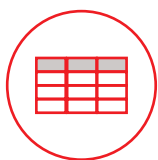


Expansion Activities

- Repeat the experiment with different switching frequency, input voltage and load current.

[Note. 1] The TPS54160 regulator features a skip-cycle mode, determining an automatic reduction of switching frequency at low load current. For more information see <http://www.ti.com/lit/ds/slvsb56c/slvsb56c.pdf> .

- Use [REDEXPERT](#)  to analyze the behaviour of different inductors in CCM and DCM operation.



Tables of measurements

The tables shown in this section are filled with values obtained by performing measurements on the TI-PMLK BUCK-WE board according to the previous test instructions. **[WARNING. The values reported in the tables are purely indicative. The results of your measurements on the TI-PMLK BUCK-WE board can be different due to tolerances and thermal effects of power components, and can be influenced by the accuracy and calibration of the instruments].**

Table 5.1. Peak-peak ripple and average inductor current and TPS54160 regulator efficiency, at $f_s = 300$ kHz and $I_{out} = 0.3$ A, with inductors L4, L5, and L6

Inductor	L4 (10 μ H)		L5 (16 μ H)		L6 (10 μ H)	
	6	18	6	18	6	18
V_{in} [V]						
CCM/DCM operation mode	<input type="checkbox"/> CCM <input type="checkbox"/> DCM					
DC input current I_{in} [mA]	187.1	76.5	184.9	75.8	186.6	76.8
DC output voltage V_{out} [V]	3.337	3.337	3.337	3.337	3.337	3.337
efficiency η [%]	87.7	71.5	88.7	72.2	87.9	71.2
peak-peak inductor ripple current Δi_{Lpp} [mA]	505	825	295	560	520	830
inductor average current I_L [mA]	295	295	295	295	295	295
peak-peak input ripple current Δi_{inpp} [mA]	21	38	20	31	22	44

Table 5.2. Peak-peak ripple and average inductor current and TPS54160 regulator efficiency, at $f_s = 450$ kHz and $I_{out} = 0.3$ A, with inductors L4, L5, and L6

Inductor	L4 (10 μ H)		L5 (16 μ H)		L6 (10 μ H)	
	6	18	6	18	6	18
V_{in} [V]						
CCM/DCM operation mode	<input type="checkbox"/> CCM <input type="checkbox"/> DCM					
DC input current I_{in} [mA]	186.9	77.7	185.4	77.5	186.2	77.9
DC output voltage V_{out} [V]	3.337	3.337	3.337	3.337	3.337	3.337
efficiency η [%]	87.8	70.4	88.5	70.6	88.1	70.2
peak-peak inductor ripple current Δi_{Lpp} [mA]	340	650	200	380	350	665
inductor average current I_L [mA]	295	295	295	295	295	295
peak-peak input ripple current Δi_{inpp} [mA]	19	33	17	28	23	38

Experiment 6

The goal of this experiment is to analyze the impact of the inductor on the closed loop load-transient response of a peak-current mode controlled buck regulator. The TPS54160 buck regulator is used for this experiment.

Theory Background (1)

Figure 6.1 shows a simplified schematic of a buck regulator with peak-current mode control.

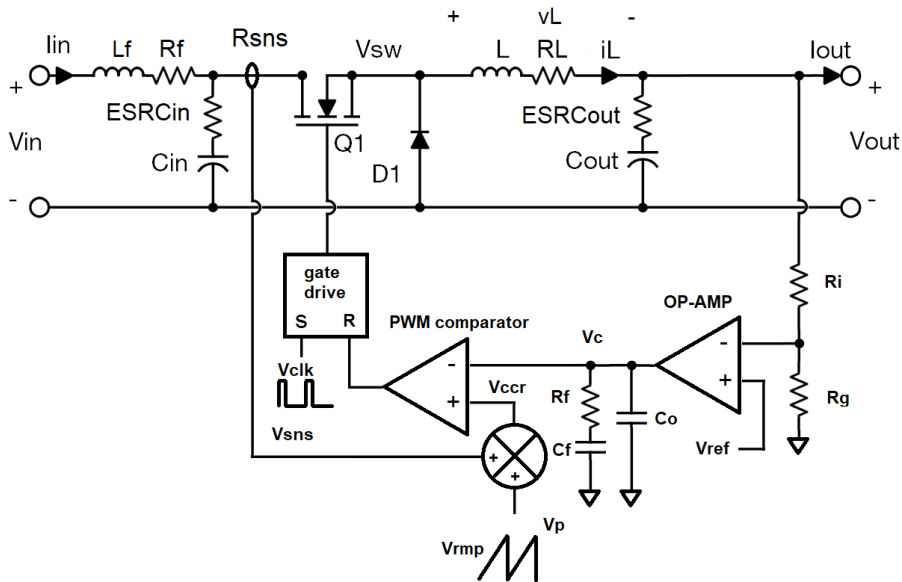


Figure 6.1. Simplified schematic of peak-current mode controlled buck regulator

Figure 6.2 shows the main signals characterizing the peak-current mode control operation. The MOSFET Q1 is turned ON at the beginning of each switching period, by the clock signal V_{clk} . The MOSFET current is sensed by means of a sensing device, characterized by a resistance R_{sns} . The sensing device can be a resistor, or the MOSFET itself (as in the TPS54160 regulator). The MOSFET current sensing signal V_{sns} is summed to a ramp signal V_{rmp} , resulting in the signal V_{ccr} , which is compared to the control signal V_c generated by the error amplifier OP-AMP. When the signal V_{ccr} reaches the signal V_c , the PWM comparator output sets high, and the gate drive turns OFF the MOSFET Q1.

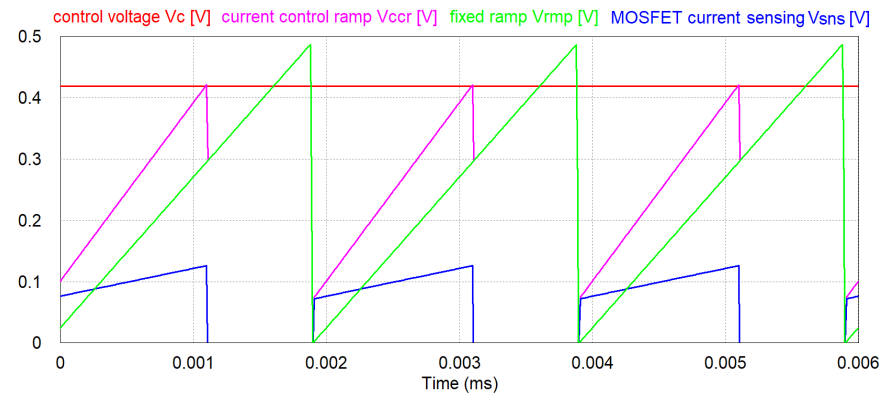


Figure 6.2. Peak-current mode control signals

Equation (1) provides the relationship among the signals V_{sns} , V_{rmp} , and V_c at the MOSFET turn OFF instant:

$$(1) \quad R_{sns} [I_{out} + (V_{in} - V_{out}) D / (2 f_{sw} L)] = V_c - D V_p$$

where I_{out} is the DC load current, V_p is the peak value of the ramp signal V_{rmp} , f_{sw} is the switching frequency, and D is the duty cycle. The control signal V_c is adjusted by the transconductance OP-AMP until the duty cycle D provides an output voltage V_{out} equal to the desired regulated voltage, which is set by the voltage divider R_i - R_g according to Equation (2):

$$(2) \quad V_{out} = V_{ref} (1 + R_i / R_g)$$

where V_{ref} is the reference voltage of the error amplifier OP-AMP.

The feedback compensation circuitry, comprised of capacitors C_f and C_o and of resistors R_f and R_p , is configured to ensure the stability of the regulator and to achieve dynamic performances fulfilling the design specifications, including output voltage regulation against input voltage and load current transient.



Theory Background (2)



Return to previous page by:

Windows:



Mac:



Equation (1) can be rewritten as shown in Equation (3):

$$(3) \quad D = (V_c - R_{sns} I_{out}) / [V_p + R_{sns} (V_{in} - V_{out}) / (2 f_{sw} L)]$$

Equation (3) shows that, given the output voltage and load current, the duty cycle of a peak-current controlled buck regulator is instantly determined by the input voltage. If the input voltage increases, the duty cycle decreases, and viceversa. This is the well known *feedforward* feature characterizing the peak-current mode control, which makes such kind of control suitable for power supplies applications affected by large and fast input voltage variations, like in automotive power electronics. Equation (3) suggests that a higher value of the current sensing resistance R_{sns} improves the sensitivity of the duty cycle with respect to the input voltage.

The peak-current controlled buck regulator can be affected by a current-loop instability in operating conditions requiring a duty cycle greater than 0.5, that happens when the output voltage V_{out} is higher than half the input voltage V_{in} . The fixed ramp signal V_{rmp} helps preventing such instability. The stability is ensured at whatever duty cycle if the following constraint is fulfilled:

$$(4) \quad r = \frac{\text{fixed ramp slope}}{R_{sns} \times \text{inductor current slope in the OFF-ON state}} > 0.5$$

Replacing the expressions of the fixed ramp and inductor current slope in the Equation (4) yields:

$$(5) \quad r = V_p f_{sw} L / (R_{sns} V_{out}) > 0.5$$

The value of the slope ratio r influences the transient response performance of the peak-current controlled buck regulator. A value of r closer to 0.5 involves better transient performance, but it increases the risk of instability caused by possible derating of the inductance L , connected to tolerance or determined by aging or saturation. A value of r much greater than 0.5 involves a degradation

of the inherent input voltage noise rejection capability of peak-current controlled buck regulator. A good setup range for the factor r is between 1 and 5.

Equations (3) and (5) highlight the manifold impact of the inductor on the peak-current controlled buck regulator. In particular, from (3) we see that a smaller inductance L increases the feedforward sensitivity of the peak-current mode control, whereas from (5) we see that a decrease of the inductance reduces the stability margin and requires higher V_p or lower R_{sns} . Moreover, according to (5), for a given inductance L , a lower switching frequency involves a decrease of the stability margin. Therefore, the condition (5) must be fulfilled in the worst case of minimum inductance and minimum switching frequency.

The closed loop transient performance of a peak-current mode controlled buck converter is determined by the voltage feedback compensation, implemented by means of the OP-AMP error amplifier. In particular, the voltage-loop gain of a peak-current controlled buck regulator is given by the simplified Equation (6):

$$(6) \quad T(s) = \frac{R_{out}}{R_{sns}} \frac{(1 + s/\omega_z)}{(1 + s/\omega_p)} \frac{\omega_o}{s} \frac{(1 + s/\omega_{z1})}{(1 + s/\omega_{p1})} \frac{1}{H_s}$$

where:

$$\begin{aligned} R_{out} &= V_{out} / I_{out} & \omega_z &= 1 / (ESR C_{out}) & \omega_p &= 1 / (R_o C_{out}) \\ \omega_o &= gm_{OTA} H / C_f & \omega_{z1} &= 1 / (R_f C_f) & \omega_{p1} &= 1 / (R_f C_o) \\ H_s &= 1 + s / (Q_s \pi f_{sw}) + s^2 / (\pi f_{sw})^2 & Q_s &= 1 / [\pi (2 D' - 0.5)] \\ D' &= 1 - V_{out} / V_{in} & H &= R_g / (R_g + R_i) = V_{ref} / V_{out} \end{aligned}$$

The factor H_s accounts for the effects of the current sampling which characterizes the peak-current mode control. Equation (6) is valid at frequency much lower than the switching frequency f_{sw} . In these conditions, if r is small, the current i_L of the inductor is almost proportional to the control signal v_c generated by the error amplifier, according to Equation (7):

$$(7) \quad i_L = v_c / R_{sns}$$



Theory Background (3)

The impact of the inductance L on the load transient response of the buck regulator can be better understood by considering Figures 6.3 and 6.4, which show an example of the output voltage perturbations of a buck regulator caused by load current step-down and step-up.

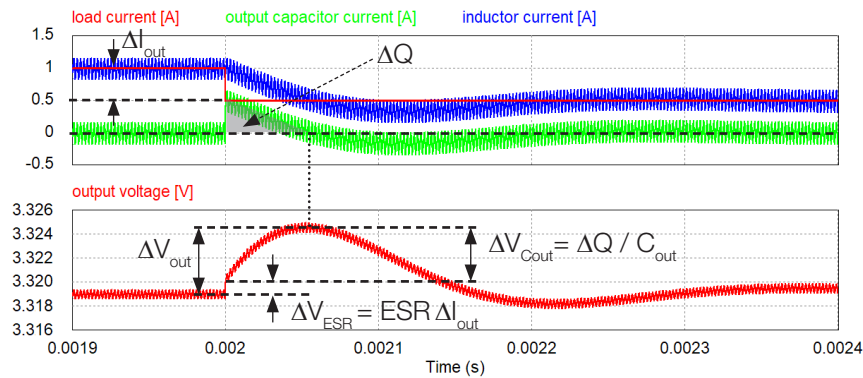


Figure 6.3. Output voltage overshoot caused by a load current step-down

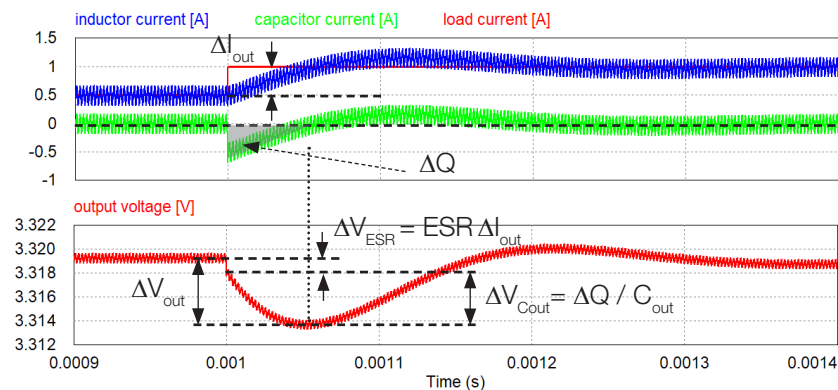


Figure 6.4. Output voltage undershoot caused by a load current step-up

The output voltage overshoot and undershoot ΔV_{out} are comprised of a step of amplitude $\Delta V_{ESR} = ESR \Delta I_{out}$, caused by the ESR of the output capacitor, and a



Return to previous page by:

Windows: + Mac: +

voltage surge of amplitude $\Delta V_{Cout} = \Delta Q / C_{out}$, caused by the capacitance C_{out} of the output capacitor, where ΔQ is the charge injected into the capacitor during the interval where the inductor current mismatches the load current. ΔQ is the area of the shaded grey triangle in Figures 6.3 and 6.4, and can be calculated, for load step down transient, as shown in Figure 6.5, where T_L is the time required by the inductor current to reach the load current, after the step-down transient.

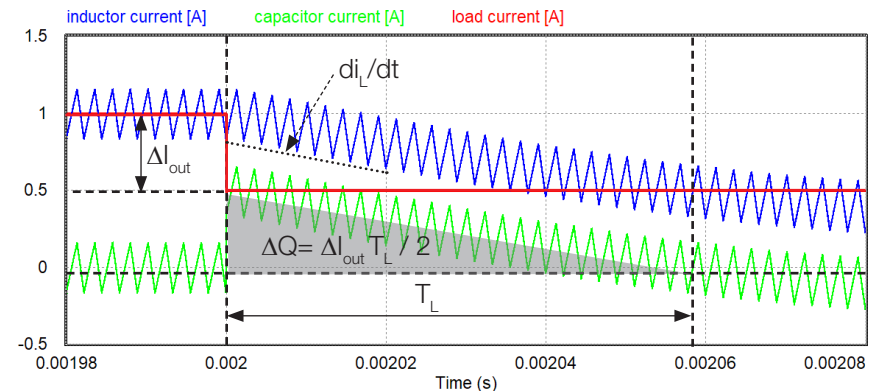


Figure 6.5. Inductor, load and capacitor current after a load current step-down

Defined D_L as the average value of the duty cycle during the interval T_L (D_L depends on the voltage feedback controller setup), the average slope of the inductor current can be approximated as shown in Equation (8):

$$(8) \quad di_L/dt \approx -\Delta I_{out} / T_L = [V_{in} D_L - V_{out} - ESR \Delta I_{out} - \Delta I_{out} T_L / (4 C_{out})] / L$$

Solving Equation (8) with respect to T_L yields Equation (9):

$$(9) \quad T_L \approx 2 C_{out} [\sqrt{(V_{\Delta}^2 + \Delta I_{out}^2 L / C_{out})} - V_{\Delta}] / \Delta I_{out}$$

where $V_{\Delta} = V_{in} D_L - V_{out} - ESR \Delta I_{out}$. Equation (9) highlights that a larger inductance L determines a longer time T_L , which in turn involves a larger charge ΔQ and ultimately a larger output voltage overshoot. Conversely, a larger inductance helps reducing the peak-peak amplitude of the output ripple voltage and increasing the converter efficiency (see [Experiment 2](#) and [Experiment 3](#)).



Case Study

The goal of this experiment is to analyze the impact of inductors on the load transient response of the TPS54160 buck regulator, under different input voltage and switching frequency operating conditions.

The transient waveforms of the inductor current and output voltage obtained with inductors L4 and L5 are compared, to analyze the effect of the inductance on the amplitude of the output voltage overshoot and undershoot of the TPS54160 buck regulator.

The following test points of the TPS54160 regulator will be used:

- **TP₂'** to measure the input voltage V_{in}
- **TP₄₂'** to measure the switching frequency f_{sw}
- **TP₂₂'** to measure the inductor current i_L
- **TP₂₆'** to measure the output voltage V_{out}

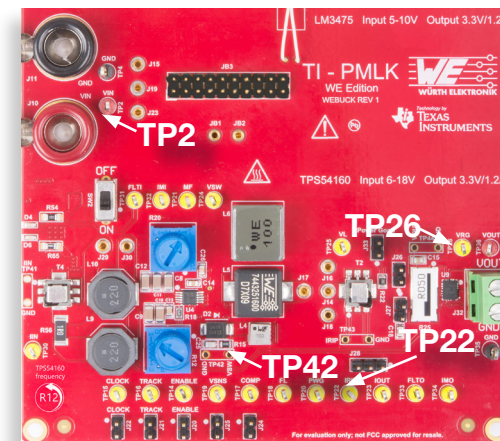


Figure 6.6. Test points used to analyze load transients in the TPS54160 regulator



Experiment set-up: configuration

The instruments needed for this experiment are: a DC POWER SUPPLY, an OSCILLOSCOPE and a DC ELECTRONIC LOAD. Figure 6.7 shows the instruments connections. Follow the instructions provided in next page to set-up the **connections**.

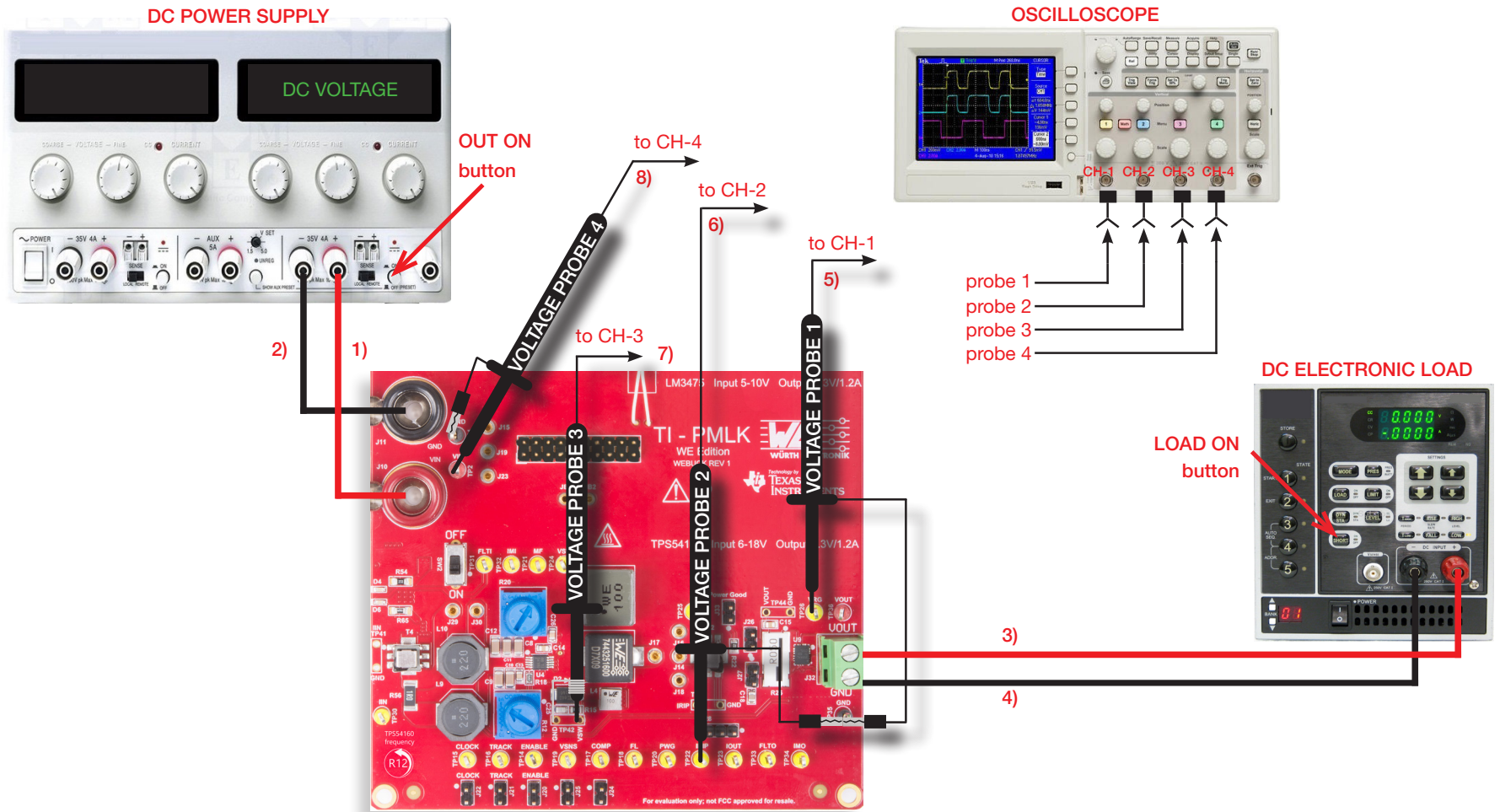


Figure 6.7. Experiment set-up



Experiment set-up: instructions

With all the instruments turned off, make the following **connections**:

1. Connect the POSITIVE (RED) OUTPUT of the DC POWER SUPPLY to the POSITIVE INPUT (VIN) banana connector J_{10} of the TI-PMLK BUCK-WE board
2. Connect the NEGATIVE (BLACK) OUTPUT of the DC POWER SUPPLY to the GROUND (GND) banana connector J_{11} of the TI-PMLK BUCK-WE board
3. Connect the POSITIVE OUTPUT (VOUT) of the screw terminal J_{32} of the TPS54160 regulator to the POSITIVE (RED) INPUT of the ELECTRONIC LOAD.
4. Connect the NEGATIVE (BLACK) INPUT of the ELECTRONIC LOAD to the GROUND (GND) of the screw terminal J_{32} of the TPS54160 regulator
5. Connect a standard voltage probe to channel 1 of the OSCILLOSCOPE, hang its tip to the test point TP_{26} and its ground clamp to test point TP_{35}
6. Connect a standard voltage probe to channel 2 of the OSCILLOSCOPE, hang its tip to the test point TP_{22} and its ground clamp to test point TP_{35}
7. Connect a voltage probe with ground spring to channel 3 of the OSCILLOSCOPE, insert its positive tip into the hole of test point TP_{42} labeled "VSW" and its ground spring tip into the hole of test point TP_{42} labeled "GND". **[WARNING: DO NOT INVERT THE POSITIVE AND GROUND CONNECTIONS OF THE VOLTAGE PROBE]**
8. Connect a standard voltage probe to channel 4 of the OSCILLOSCOPE, hang its tip to the test point TP_2 and its ground clamp to test point TP_4



Test#1: instructions (1)

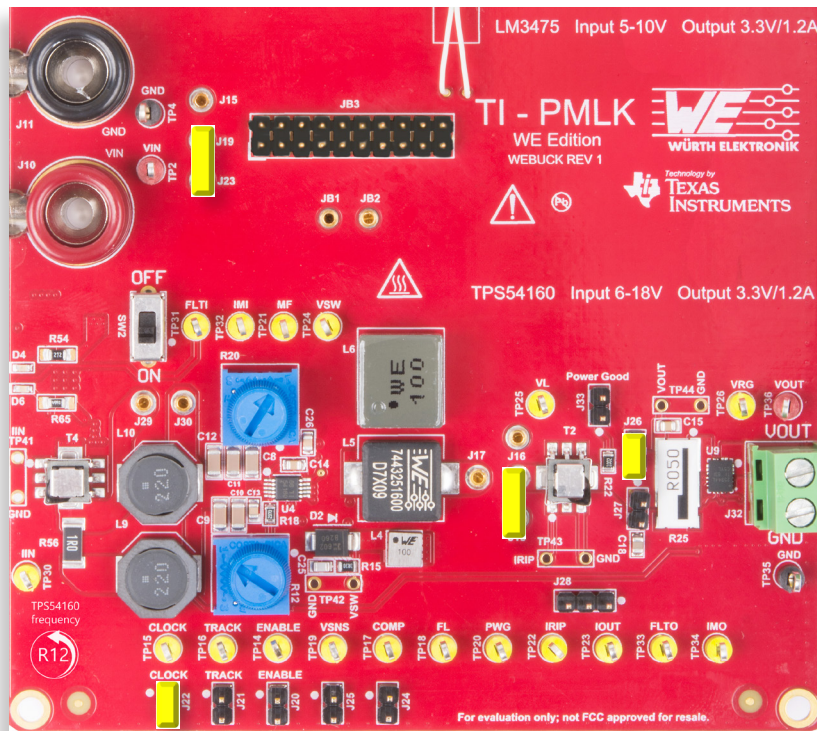


Figure 6.8. TPS54160 jumpers set-up for Test#1

Initial set-up (see Figure 6.8, jumpers not mentioned are open):

- short J_{19} - J_{23} , TPS54160 regulator connected to power input
- short J_{14} - J_{18} , inductor L4 connected
- short pins 1-2 of J_{28} , sum AC and DC inductor currents
- short J_{22} , switching frequency adjust enabled
- short J_{26} , tantalum output capacitor C17 connected
- turn R_{12} left until it stops

Test Procedure:

1. Switch ON the SCOPE, set all channels in DC 1 M Ω coupling mode with 20 MHz BW limit, the time base to 1 μ s/div, the trigger on CH-3 rising edge, the vertical offset to -3.34 V on CH-1, the vertical scale to 20 mV/div on CH-1, 500 mV/div on CH-2, and 5 V/div on CH-3 and CH-4.
2. Switch ON the POWER SUPPLY and the ELECTRONIC LOAD.
3. Set the POWER SUPPLY output voltage to 6 V and CURRENT LIMIT to 1.5 A.
4. Set the ELECTRONIC LOAD in CONSTANT CURRENT MODE to 0.5 A.
5. Switch the POWER SUPPLY and ELECTRONIC LOAD "OUT ON" buttons ON.
6. Under these conditions, you should see the flat 6 V voltage V_{in} on the SCOPE CH-4, the 20 mVpp output ripple voltage on CH-1, and the triangle inductor current ripple on CH-2. [**WARNING.** If the measurements do not look as described above, switch OFF the "OUT ON" button of the ELECTRONIC LOAD and POWER SUPPLY, check the connections, the jumpers setup, the instruments setup and repeat the procedure].
7. Watch the switching frequency f_{sw} of the waveform on the SCOPE CH-3 (switching node voltage V_{sw}), while turning the knob of trimmer R12, until you get $f_{sw} = 300$ kHz, adjust the DC POWER SUPPLY to 6 V using fine regulation knob (if needed), set the ELECTRONIC LOAD in DYNAMIC CURRENT MODE, with 1.0 A HIGH VALUE, 0.5 A LOW VALUE, 200 μ s HIGH TIME, 200 μ s LOW TIME, 0.25 A/ μ s CURRENT SLEW RATE, and activate the DYNAMIC MODE.
8. Set the SCOPE time base to 50 μ s/div, and set the trigger on CH-2 rise edge in high frequency noise rejection mode. Under these conditions, you should see the output voltage on the SCOPE CH-1 comprised of the 20 mVpp ripple component and rising and falling surges of 25 mV amplitude, and the inductor current the SCOPE CH-2 characterized by a 500 mApp square-wave waveform with small surges after rising and falling edges.



Test#1: instructions (2)

9. Measure output voltage average V_{out} , peak-peak ripple amplitude $\Delta V_{out,pp}$, peak value $V_{out,pk}$, valley value $V_{out,vl}$, and record the measured values in Table 6.1.
10. Repeat the step 9, at input voltage values 9 and 12.
11. Set the ELECTRONIC LOAD in CONSTANT CURRENT MODE at 0.5 A.
12. Set the POWER SUPPLY voltage at 6.0 V.
13. Set the SCOPE time base at 1 μ s/div, and set the trigger on CH-3 rise edge.
14. Watch the switching frequency f_{sw} of the waveform on the SCOPE CH-3, while turning the knob of trimmer R12, until you get $f_{sw} = 450$ kHz, activate the DYNAMIC MODE, and repeat the steps 8 to 10.
15. Reduce the current of the ELECTRONIC LOAD to 0.0 A, switch its "LOAD ON" button OFF, and switch the POWER SUPPLY "OUT ON" button OFF.
16. Short J_{14} - J_{17} to connect the inductor L5, repeat the steps 3 to 14, and record the measurement results in Table 6.2.
17. Reduce the current of the ELECTRONIC LOAD to 0.0 A, switch its "LOAD ON" button OFF, and switch the POWER SUPPLY "OUT ON" button OFF.
18. Switch the ELECTRONIC LOAD and the POWER SUPPLY OFF.

Figure 6.9 and 6.10 show the expected output voltage and inductor current waveforms at $f_{sw} = 300$ kHz and $V_{in} = 6$ V, with the inductors L4 and L5, respectively.

Comparing the output voltage waveforms highlights a larger amplitude overshoot and undershoot with the inductor L5 compared to the inductor L4, and a larger peak-peak amplitude of the output ripple voltage with the inductor L4 compared to the inductor L5.

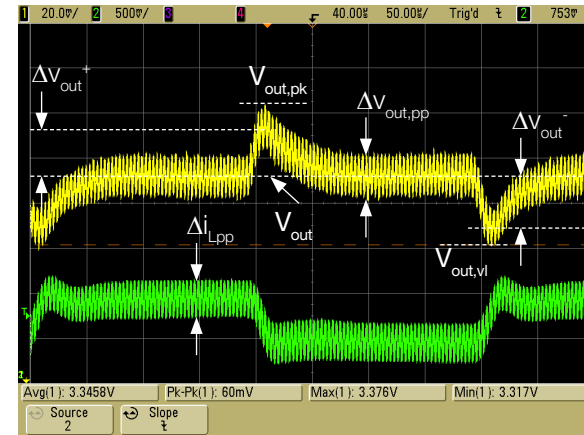


Figure 6.9. Measured waveforms with inductor L4 at $V_{in} = 6$ V and $f_{sw} = 300$ kHz

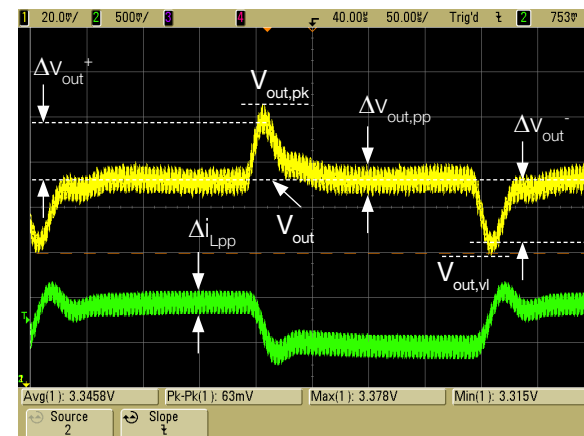


Figure 6.10. Measured waveforms with inductor L5 at $V_{in} = 6$ V and $f_{sw} = 300$ kHz



Test#1: instructions (3)

Figures 6.11, 6.12 and 6.13 show the expected output voltage and inductor current with inductor L4, at $f_{sw} = 450$ kHz and $V_{in} = 6$ V, 9 V, and 12 V, respectively. Comparing Figure 6.11 to Figure 6.9 highlights that the higher switching frequency reduces the peak-peak amplitude of output ripple voltage but does not visibly influence the amplitude of load transient overshoot and undershoot. Comparing Figure 6.13 to Figure 6.12 highlights a difference between waveforms of voltage and current at $V_{in} = 9$ V and $V_{in} = 12$ V when the regulator enters low load operating condition. In particular, the waveforms show much larger ripple and look non periodic. This behavior could be confused with instability, but it is determined instead by the skip-cycle feature of the TPS54160 regulator, which is activated in low load current and high input voltage operating conditions.

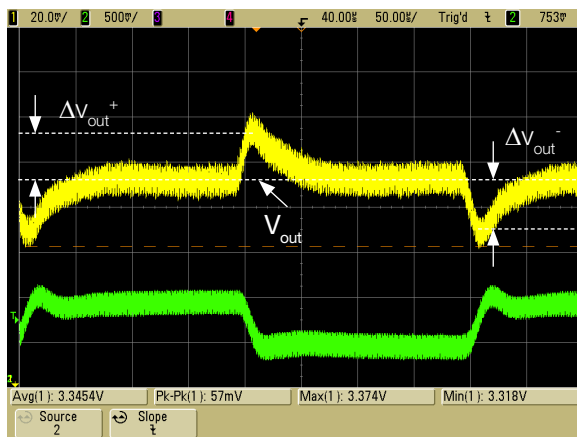


Figure 6.11. Measured waveforms with inductor L4 at:
 $V_{in} = 6$ V and $f_{sw} = 450$ kHz nominal

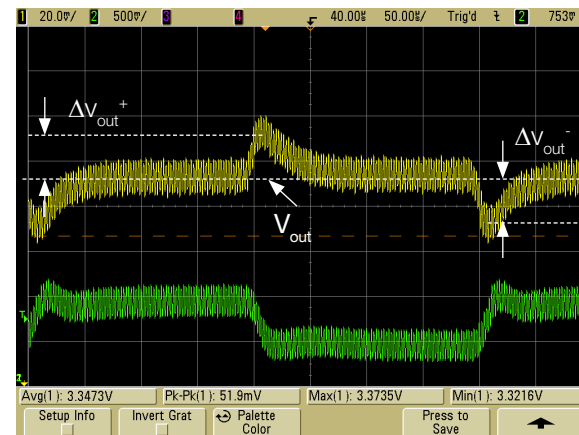


Figure 6.12. Measured waveforms with inductor L4 at:
 $V_{in} = 9$ V and $f_{sw} = 450$ kHz nominal

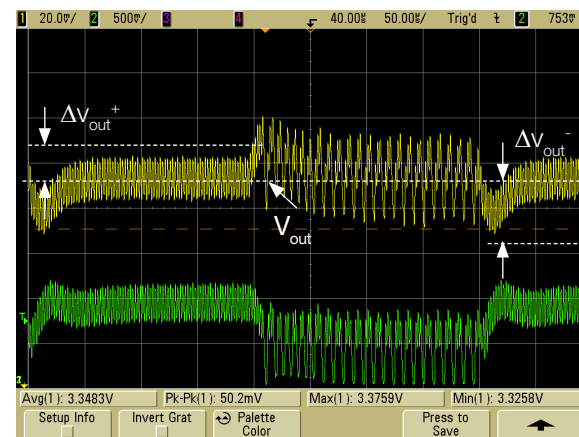


Figure 6.13. Measured waveforms with inductor L4 at:
 $V_{in} = 12$ V and $f_{sw} = 450$ kHz nominal



Test#1: instructions (4)

Figures 6.14 to 6.16 show the output voltage (yellow trace), switching node voltage (violet trace) and inductor current (green trace) waveforms with inductor L4, at 300 kHz nominal switching frequency, 0.5 A load current and 12.5 V, 13.5 V and 15.5 V input voltage, respectively. Figure 6.14 shows that at 12.5 V the controller skips one in four switching cycles. Consequently, the regulator operates alternately with one in three cycles at 150 kHz and two in three cycles at 300 kHz switching frequency. Figure 6.15 shows that at 13.5 V the controller skips one in three switching cycles. Consequently, the regulator operates alternately with one in two cycles at 150 kHz and one in two cycles at 300 kHz switching frequency. Figure 6.16 shows that at 16.5 V the regulator operates at 150 kHz switching frequency. The regulator undergoes discontinuous conduction mode operation during each 150 kHz switching frequency cycle, as evidenced by the ringing visible on the switching node voltage and inductor current waveforms (see [Experiment 5](#) to insight discontinuous conduction mode)

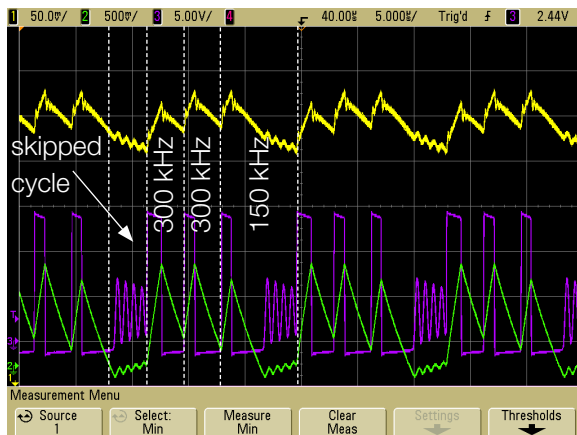


Figure 6.14. Measured waveforms with inductor L4 at:
 $V_{in} = 12.5 \text{ V}$, $I_{out} = 0.5 \text{ A}$, $f_{sw} = 300 \text{ kHz}$ nominal

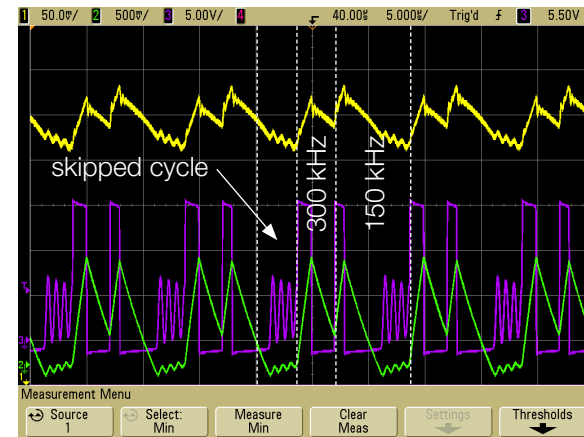


Figure 6.15. Measured waveforms with inductor L4 at:
 $V_{in} = 13.5 \text{ V}$, $I_{out} = 0.5 \text{ A}$, $f_{sw} = 300 \text{ kHz}$ nominal

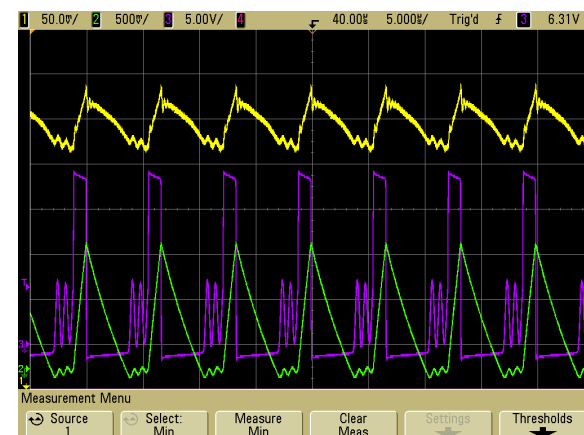


Figure 6.16. Measured waveforms with inductor L4 at:
 $V_{in} = 16.5 \text{ V}$, $I_{out} = 0.5 \text{ A}$, $f_{sw} = 300 \text{ kHz}$ nominal /150kHz real



Test#1: measure and calculate

Collect in Tables 6.1 and 6.2 the measured values of the output voltage average V_{out} , peak-peak ripple amplitude $\Delta V_{out,pp}$, peak value $V_{out,pk}$, valley value $V_{out,vl}$, calculate the amplitudes of the overshoot $\Delta v_{out}^+ = V_{outpk} - V_{out} - \Delta V_{out,pp}/2$ and undershoot $\Delta v_{out}^- = V_{out} - V_{outvl} - \Delta V_{out,pp}/2$, and report the results in Tables 6.1 and 6.2.

Table 6.1. Load transient output voltage overshoot and undershoot of TPS54160 regulator with inductor L_4

switching frequency [kHz]	300			450		
V_{in} [V]	6	9	12	6	9	12
DC voltage V_{out} [V]						
peak voltage V_{outpk} [V]						
valley voltage V_{outvl} [V]						
peak-peak ripple voltage Δv_{outpp} [mV]						
overshoot voltage Δv_{out}^+ [mV]						
undershoot voltage Δv_{out}^- [mV]						
peak - valley voltage $V_{outpk} - V_{outvl}$ [mV]						

Table 6.2. Load transient output voltage overshoot and undershoot of TPS54160 regulator with inductor L_5

switching frequency [kHz]	300			450		
V_{in} [V]	6	9	12	6	9	12
DC voltage V_{out} [V]						
peak voltage V_{outpk} [V]						
valley voltage V_{outvl} [V]						
peak-peak ripple voltage Δv_{outpp} [mV]						
overshoot voltage Δv_{out}^+ [mV]						
undershoot voltage Δv_{out}^- [mV]						
peak - valley voltage $V_{outpk} - V_{outvl}$ [mV]						



Observe and Answer

1 Which inductor does determine the largest load transient overshoot and undershoot?

L4 L5 no difference it depends on the input voltage it depends on the switching frequency other: _____

Please comment your answer: _____

2 How does the input voltage influence the amplitude of load transient overshoot and undershoot?

no influence larger overshoot/undershoot at higher voltage larger overshoot/undershoot at lower voltage other: _____

Please comment your answer: _____

3 How does the switching frequency influence the amplitude of load transient overshoot and undershoot?

no influence larger overshoot/undershoot at higher frequency larger overshoot/undershoot at lower frequency other: _____

Please comment your answer: _____

4 Which inductor does determine the largest load transient peak voltage to valley voltage amplitude?

L4 L5 no difference it depends on the input voltage it depends on the switching frequency other: _____

Please comment your answer: _____



Discussion (1)

The measurement results show that the 16 μH inductor L5 determines larger output voltage load transient overshoot and undershoot, compared to the 10 μH inductor L4. This is in agreement with the predictions based on the simplified load transient model discussed in the **Theory Background** section. The output voltage overshoot peak value and undershoot valley value determined by inductors L4 and L5 are only slightly different at 6 V input voltage, as shown in Figures 6.9 and 6.10. This is the effect of the reduced peak-peak amplitude of inductor ripple current determined by the larger inductance of the inductor L5, which compensates the larger amplitude overshoot and undershoot. As the input voltage increases, we have a different effect between the two inductors. In particular, we observe an increase of the peak-peak amplitude of ripple voltage and a decrease of the overshoot and undershoot amplitude with both inductors L4 and L5. However, the resulting overshoot peak to undershoot valley amplitude with inductor L4 increases whereas it decreases with inductor L5. Indeed, the higher inductance of the inductor L5 limits the ripple increase at higher input voltage more than the inductance of the inductor L4, and this compensates the worse overshoot and undershoot caused by the inductor L5. The reason why the amplitude of the overshoot and undershoot decreases as the input voltage increases can be understood by considering that a variation ΔV_c of the control voltage V_c results in a change of the inductor current load transient slope given by Equation (10):

$$(10) \quad \Delta (di_L/dt) = f_{sw} \Delta V_c (m_1 - m_2) / (R_{sns} m_1 + m_p)$$

where $m_1 = (V_{in} - V_{out}) / L$, $m_2 = -V_{out} / L$, and $m_p = V_p f_{sw}$. According to the **Theory Background**, a higher inductor current load transient slope reduces the overshoot and undershoot amplitude. Analyzing Equation (10) reveals that an increase of the input voltage causes an increase of the inductor current load transient slope if:

$$(11) \quad m_p > -R_{sns} m_2$$

that means if the slope ratio r is greater than 1.

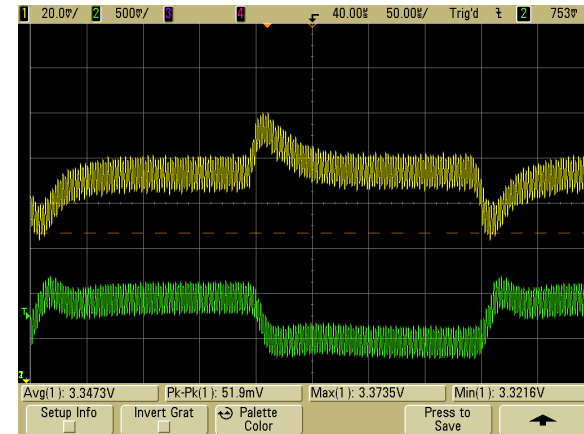


Figure 6.17. Measured waveforms with inductor L4 at:
 $V_{in} = 9 \text{ V}$ and $f_{sw} = 300 \text{ kHz}$

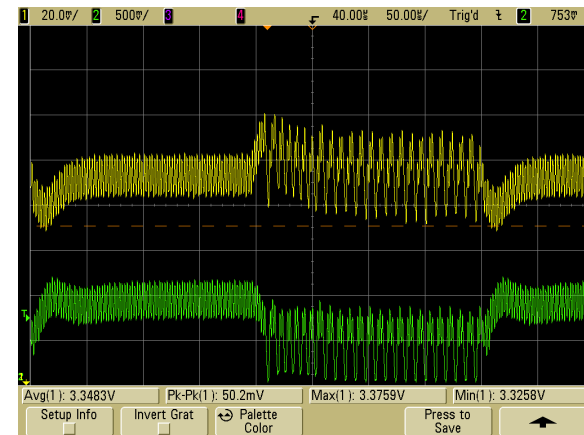


Figure 6.18. Measured waveforms with inductor L5 at:
 $V_{in} = 18 \text{ V}$ and $f_{sw} = 300 \text{ kHz}$



Discussion (2)

The slope ratio r , defined in Equations (4) and (5) in the [Theory Background](#) section, is rewritten hereafter:

$$(12) \quad r = V_p f_{sw} L / (R_{sns} V_{out})$$

In the TPS54160 test we have: $f_{sw} = 300 \text{ kHz}/450 \text{ kHz}$, $L = 10 \text{ }\mu\text{H}$ (L4)/ $16 \text{ }\mu\text{H}$ (L5), $R_{sns} = 180 \text{ m}\Omega$, $V_p = 487 \text{ mV}$, $V_{out} = 3.34 \text{ V}$. Putting the values of R_{sns} , V_p , V_{out} , f_{sw} and L into Equation (10) yields the slope ratio values collected in Table 6.3.

Table 6.3. Slope ratio r .

	$f_{sw} = 300 \text{ kHz}$	$f_{sw} = 450 \text{ kHz}$
$L = L4 = 10 \text{ }\mu\text{H}$	2.43	3.64
$L = L5 = 16 \text{ }\mu\text{H}$	3.89	5.83

The resulting slope ratio values are all greater than 1, which is consistent with the decrease of the overshoot and undershoot amplitude observed in the test results at higher input voltage.

An increase of the switching frequency impacts the peak and valley values of the output voltage load transient overshoot and undershoot mainly thanks to its beneficial effect on the amplitude of the peak-peak output ripple voltage, while it has only a marginal impact on the overshoot and undershoot amplitude.

Figures 6.19 and 6.20 show the expected load transient waveforms, at $V_{in} = 6 \text{ V}$ and $f_{sw} = 450 \text{ kHz}$, with inductors L4 and L5, respectively.

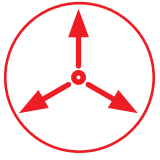
Overall, the test results show that an appropriate setting of the slope ratio r makes the peak-current controlled buck regulator tolerant to changes of inductance and input voltage, thanks to the balancing between the effects determined on the amplitude of the output voltage load transient overshoot and undershoot and of the peak-peak ripple.



Figure 6.19. Measured waveforms with inductor L4 at:
 $V_{in} = 6 \text{ V}$ and $f_{sw} = 450 \text{ kHz}$

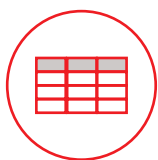


Figure 6.20. Measured waveforms with inductor L5 at:
 $V_{in} = 6 \text{ V}$ and $f_{sw} = 450 \text{ kHz}$



Expansion Activities

- Repeat the experiment with different amplitude of load current step.



Tables of measurements

The tables shown in this section are filled with values obtained by performing measurements on the TI-PMLK BUCK-WE board according to the previous test instructions. **[WARNING. The values reported in the tables are purely indicative. The results of your measurements on the TI-PMLK BUCK-WE board can be different due to tolerances and thermal effects of power components, and can be influenced by the accuracy and calibration of the instruments].**

Table 6.1. Load transient output voltage overshoot and undershoot of TPS54160 regulator with inductor L4

switching frequency [kHz]	300			450		
V_{in} [V]	6	9	12	6	9	12
DC voltage V_{out} [V]	3.337	3.337	3.337	3.337	3.337	3.337
peak voltage V_{outpk} [V]	3.367	3.388	3.371	3.365	3.365	3.369
valley voltage V_{outvl} [V]	3.307	3.302	3.303	3.310	3.308	3.310
peak-peak ripple voltage Δv_{outpp} [mV]	26.0	41.0	49.0	19.0	30.0	37.0
overshoot voltage Δv_{out}^+ [mV]	17.0	10.5	9.5	18.5	13.0	13.5
undershoot voltage Δv_{out}^- [mV]	17.0	14.5	9.5	17.5	14.0	8.5
peak - valley voltage $V_{outpk} - V_{outvl}$ [mV]	60.0	66.0	68.0	55.0	57.0	59.0

Table 6.2. Load transient output voltage overshoot and undershoot of TPS54160 regulator with inductor L5

switching frequency [kHz]	300			450		
V_{in} [V]	6	9	12	6	9	12
DC voltage V_{out} [V]	3.337	3.337	3.337	3.337	3.337	3.337
peak voltage V_{outpk} [V]	3.368	3.366	3.365	3.367	3.365	3.359
valley voltage V_{outvl} [V]	3.305	3.306	3.306	3.307	3.308	3.310
peak-peak ripple voltage Δv_{outpp} [mV]	15.0	25.0	29.0	12.0	19.0	22.0
overshoot voltage Δv_{out}^+ [mV]	23.5	16.5	13.5	24.0	18.5	11.0
undershoot voltage Δv_{out}^- [mV]	24.5	18.5	16.5	24.0	19.5	16.0
peak - valley voltage $V_{outpk} - V_{outvl}$ [mV]	63.0	60.0	59.0	60.0	57.0	49.0